1-1-2005

Cationic facially amphiphilic phenylene ethynylenes as host defense peptide mimics.

Lachelle, Arnt
University of Massachusetts Amherst

CATIONIC FACIALLY AMPHIPHILIC PHENYLENE ETHYNYLENES AS HOST DEFENSE PEPTIDE MIMICS

A Dissertation Presented

by

LACHELLE ARNT

Submitted to the Graduate School of the
University of Massachusetts Amherst in partial fulfillment
of the requirements for the degree of

DOCTOR OF PHILOSOPHY

May 2005

Polymer Science and Engineering

CATIONIC FACIALLY AMPHIPHILIC PHENYLENE ETHYNYLENES AS HOST DEFENSE PEPTIDE MIMICS

A Dissertation Presented

by

LACHELLE ARNT

Approved as to style and content by:

Gregory N. Tew, Chair

David Hoagland, Member

Vincent Rotello, Member

Shaw Ling Hsu, Department Head
Polymer Science and Engineering

To Andy

ACKNOWLEDGMENTS

Many people supported me through the completion of this thesis with helpful discussions and guidance as well as stress relief. Without them, this thesis would have never been possible. First off, I would like to thank my advisor, Gregory Tew, for his direction and support. I had the pleasure (and occasionally pain) of being his first student. This gave me the opportunity to set up the laboratory and take part in getting the research group up and running. This has helped me grow as an individual and see how a research group develops. I have also witnessed Greg grow as a professor and advisor throughout the past several years.

I would also like to thank my other committee members, Dave Hoagland and Vince Rotello. Dave and I have had many insightful discussions about science among other things. He has been a wonderful mentor throughout graduate school and has many times given me motivation. He has helped me with career decisions and wrote endless amounts of recommendations. Vince has helped me see my research in a different light and taught me to think about science from multiple angles.

Besides my committee, there have been several other professors at UMass whom have helped me with my endeavors. Bryan Coughlin took me on as one of his own students before Greg arrived in the department. Tom Russell gave me encouragement when I had a relatively slow start to the cumulative exams. Al Crosby acted as a mentor when it came to making career decisions and also offered a fantastic class on scientific management. Both Klaus Nüsslein and Kathleen Arcaro generously helped me with the biological testing of my molecules by allowing me to explore and play with living cells in their laboratories.

Outside of UMass, there have been a few notable professors who have taken time to become mentors and friends. At SUNY Buffalo, Joe Gardella was my advisor and mentor throughout my undergraduate years and serves as a role model. He helped me see how much fun chemistry and polymer science can be by being a wonderful teacher both in the classroom and lab. He also helped me obtain many of the research experiences I have had during my undergraduate years. Mike Young, the department head at Westfield State College, is also a role model for me. He had faith in my teaching abilities and allowed me to design and teach a polymer science course during the spring of 2004. Throughout that semester, we had several helpful discussions about teaching, science, and career choices. Since then, he has written several recommendation letters and been a huge supporter of my job search. Rich Blatchly (Keene State College) and Pat O'hara (Amherst College) have given me advice on science as well as my career. Rich particularly took interest in my thesis while he spent time working in our research group.

The staff of the PSE department has also been a great help over the last several years. Greg Dabkowski does a amazing job running the K-12 Outreach Program, which helped me become interested in teaching. I would also like to thank Steve Eyles for running the mass spec facility as well as fascinating and amusing discussions. Charlie Dickenson runs a wonderful NMR facility. Without the administrative staff (Eileen, Joann, Anita, Sophi, and Ann) the department would not still be running as they provide the backbone for the department.

Thanks to all the members of the Tew Group. In particular, Ticora Jones has been a faithful and supportive officemate. Without her, my time in graduate school

would have been much lonelier. Thanks for the many unsolicited hugs and stress relief talks. And by the way, you will never find Eeyore now! Naomi DeLong has provided numerous hours of discussions, fun, and synchronized swimming. The undergraduates, Dannon Stigers and Katelyn Spillane, kept me on my toes about many things while trying to teach them laboratory skills. I am especially indebted to Jason Rennie for all the microbiology knowledge that he has provided. Most of all I would like to thank Fred, the honorary Tew group member. Without Fred, this thesis would not have been possible.

Friendships that I have made at UMass will last a long time. Julie Belanger has been especially supportive (in many ways) over the past several years as a graduate student. She is always willing to listen and find solutions to problems. She is also an inspiring swim buddy. Jen Craymer has also been really wonderful during my time here and is definitely the best cume buddy anyone could ask for. We survived the first year, the cumes, and the sixth floor together. Ken, Carrie, and Hayden Ellzey are great friends through the good times and the bad. Ken particularly helped with the science while Carrie and Hayden provided a lot of needed stress relief. Liz Glogowski always has fresh perspectives on everything. Thanks to Melissa Light for moral support, dinners, and for being who she is. Jessica McCoy is my food buddy (both healthy and non-healthy) and always will lend an ear and a sensible perspective on things. She is very hard working and willing to do what needs to be done to make sure things are satisfactory. Gabi Menges was full of ideas and willing to escape when necessary and continues now to be a fantastic friend. Joanna Pool should be an inspiration to everyone: she is smart, supportive, and outgoing. She has really pushed me to pursue

what I want to do and gives me the encouragement to keep trying. Kevin Wier is a wonderful guy who took me ice fishing and fishing in his canoe, both things I did not think I would ever experience. Donna Wrublewski made graduate school much more bearable and never fails to lend an ear, or hand, when necessary.

There are three friends from other walks of life that I would like to thank: Sarah Dowdell, Devin Militello, and Brian Gilmartin. Sarah was my chemistry partner in high school where this whole chemistry thing started. We helped each other to survive college and we continue to support each other. Devin was my lab partner in biology and she dissected most of the animals I did not want to touch. Throughout college, she and I had endless hours of fun and excitement ranging from amusing classes to fun socializing experiences. Now she and her husband, Kevin, continue to be very supportive and encouraging with all aspects of life. I met Brian in college and he continues to be one of my best friends. It took some convincing that he wanted to sit with me in physics class and ultimately be my lab partner, but after that we spent a lot of time together. We studied, did many projects together, and watched the Penguins beat the Sabres multiple times. I know that these three people will continue to be amazing friends wherever life takes us.

Last, but certainly not least, I would like to express my thanks to my family. Without them, I would definitely not be where I am today. My parents, Mike and Jill Sussman, have always supported my endeavors and been two of my biggest cheerleaders. They have always been there for me through the good and the bad times with hugs and love and encouragement. I owe part of this thesis to them. My sister, Evelyn, has also helped me in more ways than she knows. She is the best sister I could

ever ask for. I really have to acknowledge my grandparents, Ruth and Ted Jacobs. They have always pushed me to do my best. Through college and graduate school, I looked forward to visiting with them and their weekly calls. I know if my grandma was still around, she would be really proud of me. I owe part of this thesis to her. My aunt, Gail Smith, is also worthy of recognition for always being interested in my latest life experiences and providing care packages for all major life events.

My cats, Maxwell and Maple, also deserve praise. They give me purrs, kitty-love, snuggles, (and sometimes slobber), and of course, much warmth. And saving the best for last, I express my deepest thanks to my husband, Andy. He has provided me with the strength I needed to start and finish this thesis. He is always there when I need him and has given me love, encouragement, and vision. Andy, I love you and this thesis is dedicated to you!

ABSTRACT

CATIONIC FACIALLY AMPHIPHILIC PHENYLENE ETHYNYLENES AS HOST DEFENSE PEPTIDE MIMICS

MAY 2005

LACHELLE ARNT, B.S., STATE UNIVERSITY OF NEW YORK AT BUFFALO

M.S., UNIVERSITY OF MASSACHUSETTS AMHERST

Ph.D., UNIVERSITY OF MASSACHUSETTS AMHERST

Directed by: Professor Gregory N. Tew

The goal of this research is to design molecules that capture the essential elements and biological properties of host defense peptides without the use of amino acids or peptide-like backbones. This is accomplished via a *meta*-phenylene ethynylene backbone with polar amine and nonpolar alkyl groups as side chains. These molecules are shown to form stable monolayers at the air-water interface with the polymer chains assuming an edge-on structure with the aromatic rings perpendicular to the water surface and the polar amines groups below the water surface. Furthermore, these molecules aggregate in solution with the addition of a non-solvent, as expected with facially amphiphilic molecules. When tested against biological systems, the result is promising: growth inhibition against a wide variety of bacteria at relatively low concentrations with minimal disruption towards red blood cells. The average minimal concentration needed to disrupt bacterial growth is 2 μg/mL and occurs in less than 5 minutes. Furthermore, tests indicate negligible evolution of bacterial resistance over a month-long experiment. Incorporation of these compounds into polymeric substrates

proves to be an effective way of preventing bacterial growth on surfaces. Further probing the mode of action of these molecules shows results similar to many host defense peptides.

TABLE OF CONTENTS

LIST OF TABLES

Table

Page

LIST OF FIGURES

Figure Page

CHAPTER 1

HOST DEFENSE PEPTIDES: AN OVERVIEW

1.1 Introduction

The extensive over-use of antibiotics to treat non-bacterial infections is causing a rapid increase in bacterial resistance. As this trend continues, society heads towards an era where today's antibiotics will be rendered useless. The Center for Disease Control and Prevention (CDC) estimates that more than 50 million unnecessary antibiotic prescriptions are written each year.(1) This translates into antibiotics being prescribed for up to 80% of the patients seen in a clinic while only 20% of the patients require antibiotic treatment.(2) For example, 100% of the 18 million prescriptions written each year for the common cold and 80% of the 16 million prescriptions for bronchitis are unwarranted.(1)

The occurrence of bacterial resistance from antibiotic overuse is shared by patients and doctors. This evolution of resistance can be reduced or even eliminated in two ways: doctors need to require more patient information before prescribing an antibiotic coupled with the patient not demanding antibiotics from health-care providers when prescribed treatment is deemed unnecessary. Ultimately, this continued antibiotic abuse will render today's antibiotics useless. The prevalence of antibiotic resistance could result in more trips to the doctor's office, longer recovery times, or the use of more toxic drugs, or, potentially, death. The CDC estimates that nearly 2 million people in the United States each year that acquire a bacterial infection while in the hospital and 90,000 of them die due to bacterial resistance towards antibiotics.(3) Thus, there is an

enormous need to find new antibiotics and antimicrobial agents to replace the ones that are becoming ineffective.

1.2 Evolution of Bacterial Resistance toward Common Antibiotics

Bacterial resistance is an outcome of forced evolution by society's demands. Most organisms contain a few prevalent genomic mutations that give them the ability to withstand attack from antibiotics. Resistance occurs because the antibiotic successfully kills the weak, defenseless bacteria, while selecting the strong, mutated bacteria to survive. These mutated, now resistant, bacteria grow and multiply becoming the predominant microorganism. In this case, antibiotics do not cause the resistance in the microbes, but rather select the stronger, resistant bacteria to flourish. It is estimated that virtually all bacteria are resistant to one or more of the drugs required to treating an infection.(4) Unfortunately the amount of resistance is continually rising. Figure 1.1 shows the increase of bacterial resistance towards antibiotics from 1997-2001 (average) to 2002.

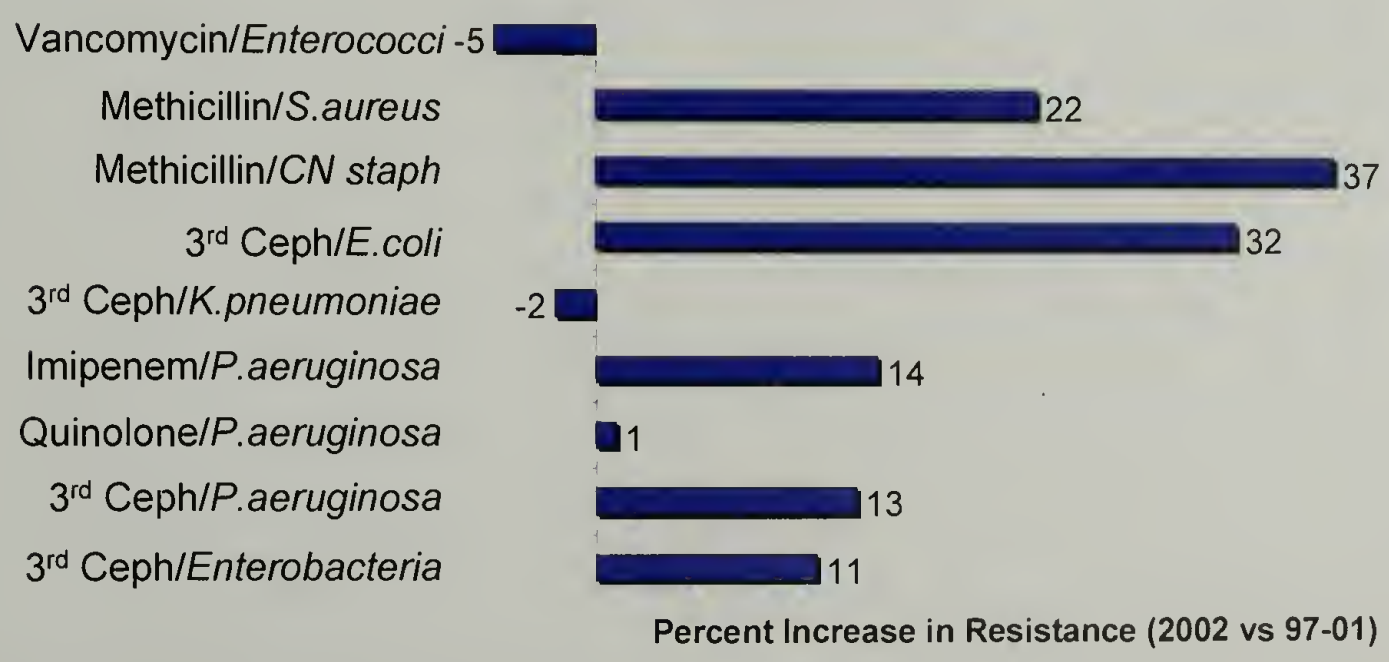

Figure 1.1: Increase in bacterial resistance over the past few years (adapted from NNIS 2003 report).

One pathway bacteria use to develop resistance is by interfering with the antibiotic's mechanism of action.(5) This can be easily accomplished by the production of hydrolyzing or modifying enzymes that either degrade the antibiotic or change the chemical structure rendering the antibiotic ineffective. For example, penicillin kills bacteria by inhibiting cell wall synthesis. Penicillin resistant bacteria produce enzymes, called Penicillinase, which hydrolyze the antibiotic rendering it useless. Production of hydrolyzing enzymes, like Penicillinases, is a common pathway of antibiotic resistance in many bacteria.

Another mode of resistance is accomplished through altering the antibiotic's target, such as modifying the cellular structure.(2, 5) This can be achieved by modification of the cell wall making it thicker and less permeable or by varying an internal cellular component. Erythromycin, a frequently prescribed antibiotic, attacks bacterial ribosomes and prevents protein production. By slightly altering ribosomal structure, bacteria can prevent the antibiotic from binding to the ribosome. This route is also taken by other bacteria to become resistant to streptomycin and gentamicin.

A third mechanism of resistance commonly used by bacteria is through the production of efflux pumps.(2) This pathway is enabled by the production of enzymes that actively remove the antibiotic from the interior of the cell. Many cells can increase the number of efflux pumps present in a bacterial strain resulting in an increase in antibiotic resistance. This is a common route taken to develop resistance to tetracyclines and chloramphenicol.

1.3 The New Wave of Antibiotics

Antibiotics with specific protein targets or receptors allow microbes to mutate and become resistant to the administered drugs. Ideally, antibiotics that will not succumb to the mechanisms of bacterial resistance should be developed. A general membrane disruption pathway without specific targets can significantly reduce or eliminate the evolution of resistance. Nature provides an excellent starting point for insight into broad-spectrum antibiotics which are effective against multiple microorganisms. Multicellular organisms successfully live and flourish in the presence of microbes (including bacteria, fungi, and viruses) due to their ability to produce antimicrobial, or host defense peptides (HDPs), which fend off microbial attack.(6) Since HDPs have broad-spectrum activity, they can provide a model system for the generation of novel antibiotics.

HDPs are natural peptides that provide the first line of defense against bacterial infection and are widespread throughout several eukaryotic systems. Due to their prevalence, it is thought that they played a fundamental role in the evolution of complex multicellular organisms.(6) Despite their long-term existence, they have retained their effectiveness as antimicrobial agents. This makes HDPs an attractive source for understanding how to effectively prepare antibiotics which induce negligible bacterial resistance.

There is widespread diversity in the sequence, structure, and size of HDPs, but they can be separated into two general categories; anionic and cationic molecules. There are a limited number of anionic HDPs which are mostly found in sheep, goats and most recently in cattle.(7) The class of cationic HDPs is much larger and includes

several hundred peptides which are common in all types of organisms ranging from insects to fish to humans.(7, 8) Table 1.1 lists several cationic HDPs as well as their natural hosts and how many different variations of peptides are found in each family.(8)

Table 1.1: Brief list of cationic HDPs (adapted from reference 8).

Group	# of Peptides	Origin
Cecropins	33	Insect
Melittins	4	Insect
Pardaxins	4	Fish
Magainins	2	Frog
Dermaseptins	15	Frog
Cathelicidins	10	Mammal

1.4 Cationic HDPs

Cationic HDPs are a large class of natural peptides that continue to be discovered and isolated at a rapid rate from a variety of organisms including vertebrates, invertebrates, anthropoids, plants, insects, and mollusk species.(9, 10) These peptides can be synthesized on demand and stored in large amounts in the granules of neutrophils and secretions of the mucosal epithelia, so that the host is ready to defend against infection from a variety of microorganisms.(11) Since HDPs have retained their efficacy over the years, they are thought to work by a different pathway than conventional antibiotics. While conventional antibiotics have specific microbial targets, generally HDPs work through selective, non-receptor-based, interactions with microbial membranes.

Cationic HDPs can be categorized into five families of peptides based on structural features: α-helices, β- sheets, looped structures (connected by a single

disulfide bond), extended structures, and cyclic structures (connected by a peptide bond)(11) of which the first two classes are the most common.(10) Examples of peptides from the first two categories are shown in Figure 1.2: Magainin (α-helical) and Defensin (β-sheet). The majority of the known cationic HDPs have been studied by circular dichroism to elucidate the structural class they belong and some peptides have been investigated by two-dimensional nuclear magnetic resonance (NMR) to determine their three dimensional structures.(10)

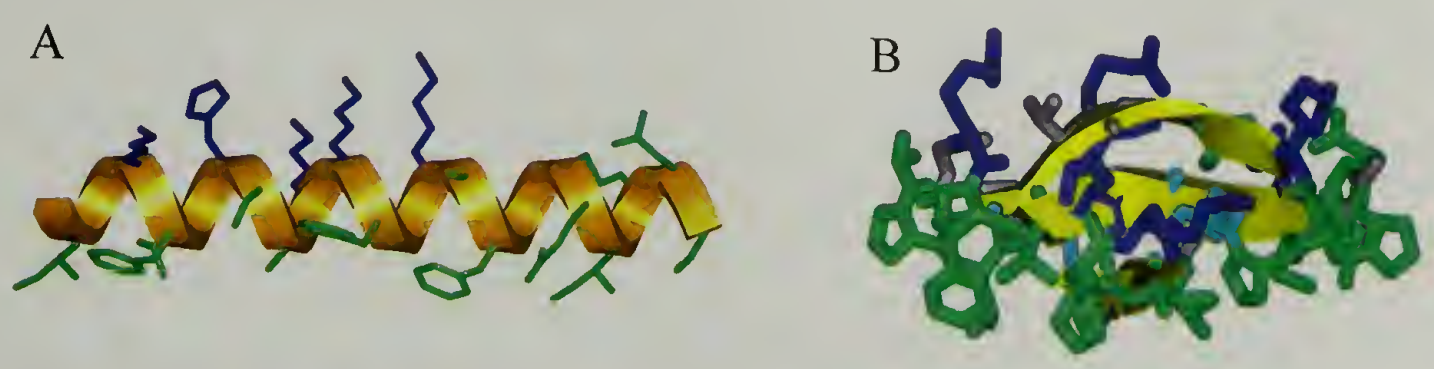

Figure 1.2: Examples of two host defense peptides a) α-helical Magainin and b) β-sheet Defensin.

Even though HDPs have very different structural features, they have three characteristic properties: they are relatively small (less than 50 amino acids), basic (arginine- and lysine-rich), and amphiphilic (containing hydrophobic and hydrophilic moieties).(8, 11, 12) After these common characteristics of HDPs were determined, the correlation to potency was investigated. Tossi and coworkers indicated that there are at least six parameters that influence the potency and spectrum of activity of HDPs: size, sequence, degree of structuring, charge, overall hydrophobicity, and amphipathicity.(8) The degree of structuring relates to the general structure adopted by the peptide: some peptide sequences have structured and unstructured portions. The overall hydrophobicity is related to the ratio of hydrophobic to hydrophilic moieties within the peptide sequence. In general, these parameters are interrelated, thereby altering one can

highly influence one or more of the others. For example, a modification to the charge of a peptide affects the overall hydrophobicity which could in turn affect the degree of structuring.

1.4.1 Parameters that Influence Biological Activity

The interrelationships of the parameters discussed in the previous section make it challenging to choose a specific parameter to investigate. Some researchers have narrowed all the above parameters down to one fundamental underlying structure, the amphipathic design.(6) Amphipathicity is the ability of a molecule to segregate hydrophobic and hydrophilic segments to opposite sides of the structure. This is commonly referred to as a facially amphiphilic (FA) structure and can be seen in Figure 1.2 with the segregation of the hydrophobic (shown in green) and hydrophilic (shown in blue) moieties of Magainin and Defensin.

The classic example of the importance of a FA structure for antibacterial activity was demonstrated by Houghten and coworkers in 1992 with the synthesis of peptides composed of lysine and leucine.(13) In the study, they systematically varied the sequence of the amino acids to give different degrees of amphiphilicity and determined that the peptides with the highest degree of amphiphilicity were the most biologically active. Before this study, Degrado and coworkers made similar α-peptides composed of lysine and leucine but only reported the peptide secondary structures and not the antibacterial activity.(14) The same principle of the necessity of FA for antimicrobial activity was shown with β-peptides by Gellman and coworkers.(15, 16) The difference between α- and β-peptides comes from the presence of a carbon between the carboxyl

and the amine group, as shown in Figure 1.3, however, the backbone still has amide bonds present.

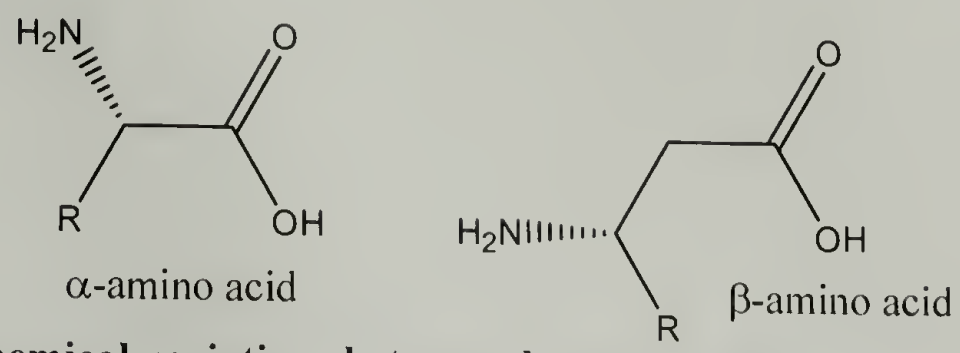

Figure 1.3: Chemical variations between the structures of α- and β-amino acids.

While the importance of a FA structure has been illustrated, the several other parameters need to be considered as well. Many research groups focus on determining the effect of the degree of structuring of peptides, however, it should be noted that it is very complicated to experiment with this parameter without affecting other parameters such as sequence and charge. Houghton and coworkers investigated the antimicrobial effect in relation to the FA structure and the degree of structuring.(13) They found that peptides with alternating lysine and leucine amino acids had more of a β-sheet like structure while the FA peptides (lysine and leucine segregated to opposite sides of the helix) were α-helical. Hancock and coworkers used two methods to examine the effect of increasing the helicity of a peptide. In this first study, they introduced a preformed helix, as opposed to an unstructured peptide in solution,(17) while in the second study they made specific amino acid substitutions that increased the helix forming potential.(18) In the first case, the increase in the degree of structuring with a preformed helix reduced antibacterial activity, but on the other hand, increasing the helix potential by amino acid substitutions increased the activity. Sitaram and coworkers also found that disrupting the secondary structure by introducing diastereo amino acid analogs resulted in loss of biological activity.(19) Overall, the effect of secondary structure on

antibacterial activity seems contradictory, but the available data suggests that a specific secondary structure is not important for antibacterial activity.

The influence of peptide charge, hydrophobicity, and length have also been closely examined.(20-22) Some research groups have found that alterations in these three categories do not significantly affect the antimicrobial activity,(20) while others find that there are major changes, both improvements and deteriorations, in activity.(21, 22) Table 1.2 shows some of the results from Hancock and coworkers showing that length, degree of charge, and hydrophobicity do not affect antibacterial activity.(20) In comparing the structures with similar lengths and overall hydrophobicity while varing the charge (CM3 and CP29), illustrates no significant change in the MIC against *E. coli*. CP29 and CM5 show that increasing the hydrophobicity slightly changes the antibacterial activity but it is not significant. CPα2 and CPα3 represent a change in peptide length without greatly affecting charge and hydrophobicity but again results in no significant change in activity.

Table 1.2: Effect from peptide alterations of charge, hydrophobicity, and length on bacterial activity (adapted from reference 20).

Peptide	# of residues	Overall charge	Percent hydrophobicity	$MIC_{E.coli}$ (μgmL)
CM3	26	+9	52	1
CP29	26	+6	50	2
CM5	26	+6	65	5
CPa2	30	+9	60	2
CPa3	23	+8	57	4

In contrast to the results suggesting these parameters do not affect the antibacterial activity, Nicolas and coworkers performed an elegant study using

Dermaseptin as a HDP modcl.(22) By signifieantly shortening the scquencc from 34 amino acids to 18, they found a peptide which rctained the antibacterial activity of the parent eompound. Sitaram and eoworkers did a similar study using Mclittin and showed that by decreasing the peptide size from 26 to 15 residues, the antibaetcrial aetivity is deereased; however the 15 rcsiduc compound is also 300 times less hemolytic than the parent eompound.(23) In both these models, not only was the size of the active compound deereased, but the sequenee ehosen encompassed most of the amphiphilic segment, thus, resulting in a mueh less hydrophobie compound.

Between the eontradieting results about size, hydrophobicity, and eharge as well as those diseussed above for degree of strueturing, the literature ean beeome confusing. Attempting to compile results from a broad speetrum of HDPs and pathogens has proven diffieult.(6, 8, 24) However, some generalizations ean be made: amphipathicity is neeessary, smaller peptides retain biological aetivity with the optimal size between 12 and 46 residues, the hydrophobie to eharged residue ratio is optimal between 1:1 and 2:1, and there is a direct eorrelation between eationieity and poteney (net positive charge of at least 2, usually 4-6) since the initial eleetrostatic interaction is very important.(8, 12, 24-26) Controlling the antimierobial aetivity using many of the aforementioned parameters provides a good starting point for researeh, but HDPs must also show selectivity to be sueeessful host defense agents.

1.5 Selectivity

Selectivity of these host defense peptides demands that they must be able to differentiate between host and invader eells. This feature is most likely derived from

the fundamental differences between bacterial and mammalian cell membranes. Figure 1.4 shows diagrams of the two membranes, bacterial and mammalian, and an immediate difference can be observed. Both the inner and the outer leaflets of the bacterial membrane (Figure 1.4a) contain negatively charged phospholipids, while only the inner leaflet of the mammalian membrane (Figure 1.4b) contains negatively charged phospholipids. The additional negative charges aid in electrostatic interactions between the cationic peptide and the bacterial membrane. This driving force for association is in addition to any hydrophobic interactions the peptide has with the membrane. The combination of the electrostatic and the hydrophobic interactions allows HDPs to have the unique characteristic of being highly water soluble but also have favorable interactions with phospholipid bilayers.(8) Water solubility is not a requirement with HDP mimics since they are not stored within the host for extended periods of time, although some degree of water solubility is necessary for antimicrobial activity.

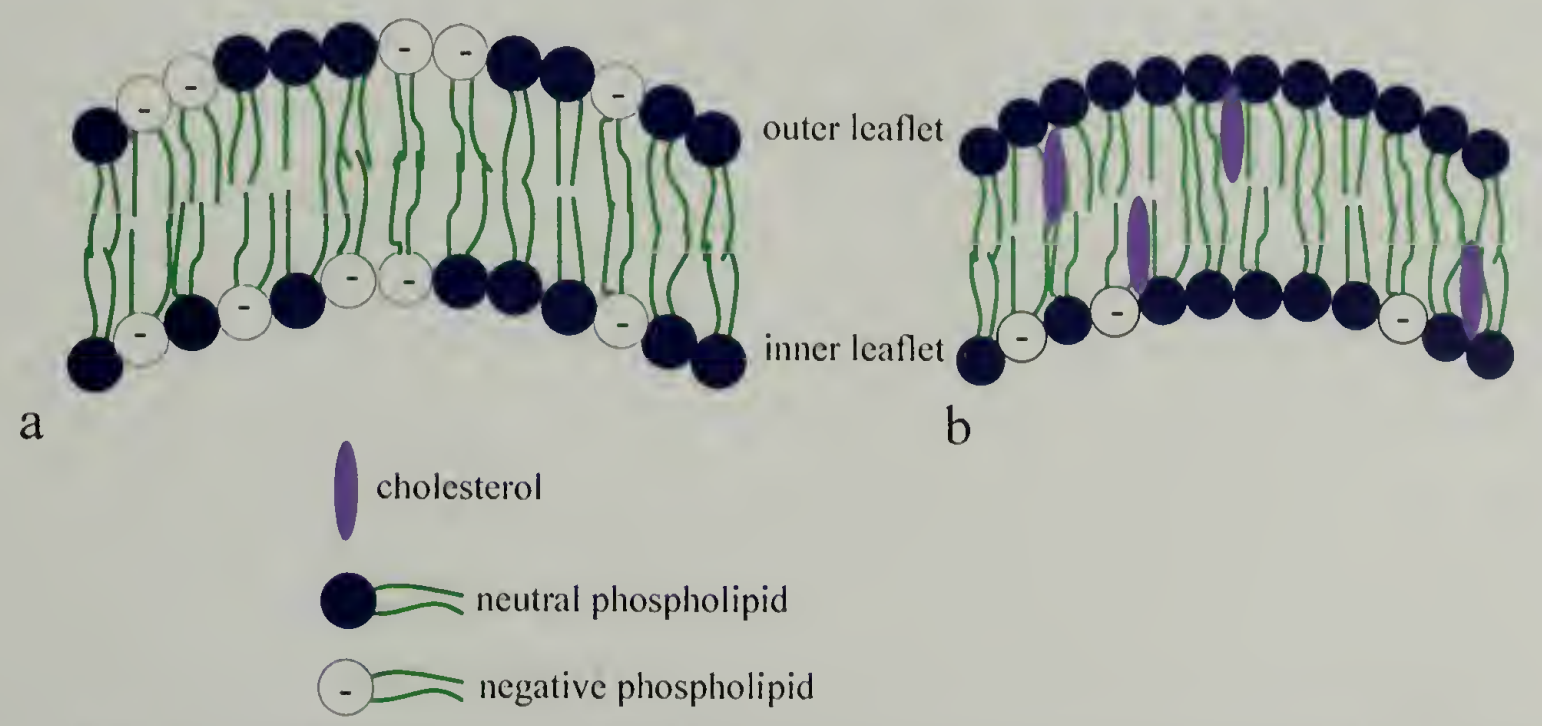

Figure 1.4: Diagrams of a) bacterial membranes and b) mammalian membranes.

Aside from the absence of negatively charged phospholipids in the outer leaflet of untransformed mammalian cells, there are other properties that determine selectivity

towards bacteria. These properties include the lower transmembrane potential and presence of cholesterol in the animal cell membrane.(8, 27) Also, unlike bacteria, the respiratory and macromolecule synthesis in mammalian cells is not coupled to the cytoplasmic membrane.(8) These properties not only make animal cells much more rigid than bacterial cells, but it also means that if HDPs have secondary interactions that inhibit cellular mechanisms through the membrane, then they should have less of an effect on mammalian cells.

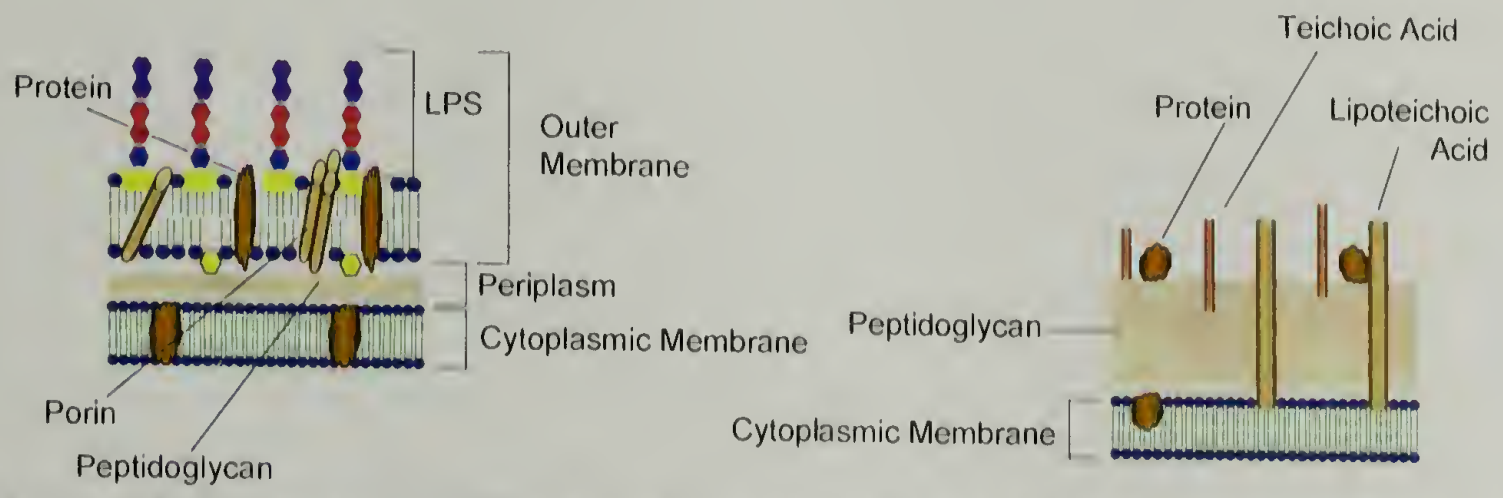

Figure 1.5: Schematic of differences in gram-negative and gram-positive bacterial cell walls.

Even though many HDPs have broad spectrum activity against both gram positive and negative bacteria, fungi, viruses, protozoa, and yeast cells,(6, 9, 11, 28, 29) some peptides are specific to one type of microorganism. This selective activity can be accounted for by the specifics of the microbe cytoplasmic membranes. For example, there is wide variation in gram-negative and -positive cytoplasmic membranes of bacteria, as seen in Figure 1.5.(2) In gram-negative bacteria there are two cell membranes, the outer and the cytoplasmic membrane, while in gram-positive bacteria there is only a cytoplasmic membrane. Another major difference is the presence of lipopolysaccharides (LPS) on the external leaflet of the outer membrane of gram-negative bacteria. These molecules are known to be negatively charged, however, it is

also speculated that they also repel hydrophobic molecules.(30) Figure 1.6a shows a general schematic of Lipid A,(2) while 1.6b shows a chemical structure of a synthetic *E. coli* Lipid A.(31) Lipid A structures vary significantly depending on bacterial strain, but the sequence of major components is generally uniform and the fatty acid tails are connected to the glucose group by ester amine linkages.(2, 31-33) The surface of gram-positive bacteria is also negatively charged due to the presence of teichoic and teichuronic acids. The negative charges from both gram-negative and -positive membrane features add to the overall negative charges of the lipids in the outer leaflet of the membranes thus allowing electrostatic interactions with cationic molecules. Cytoplasmic membrane composition will be further discussed in Chapter 5.

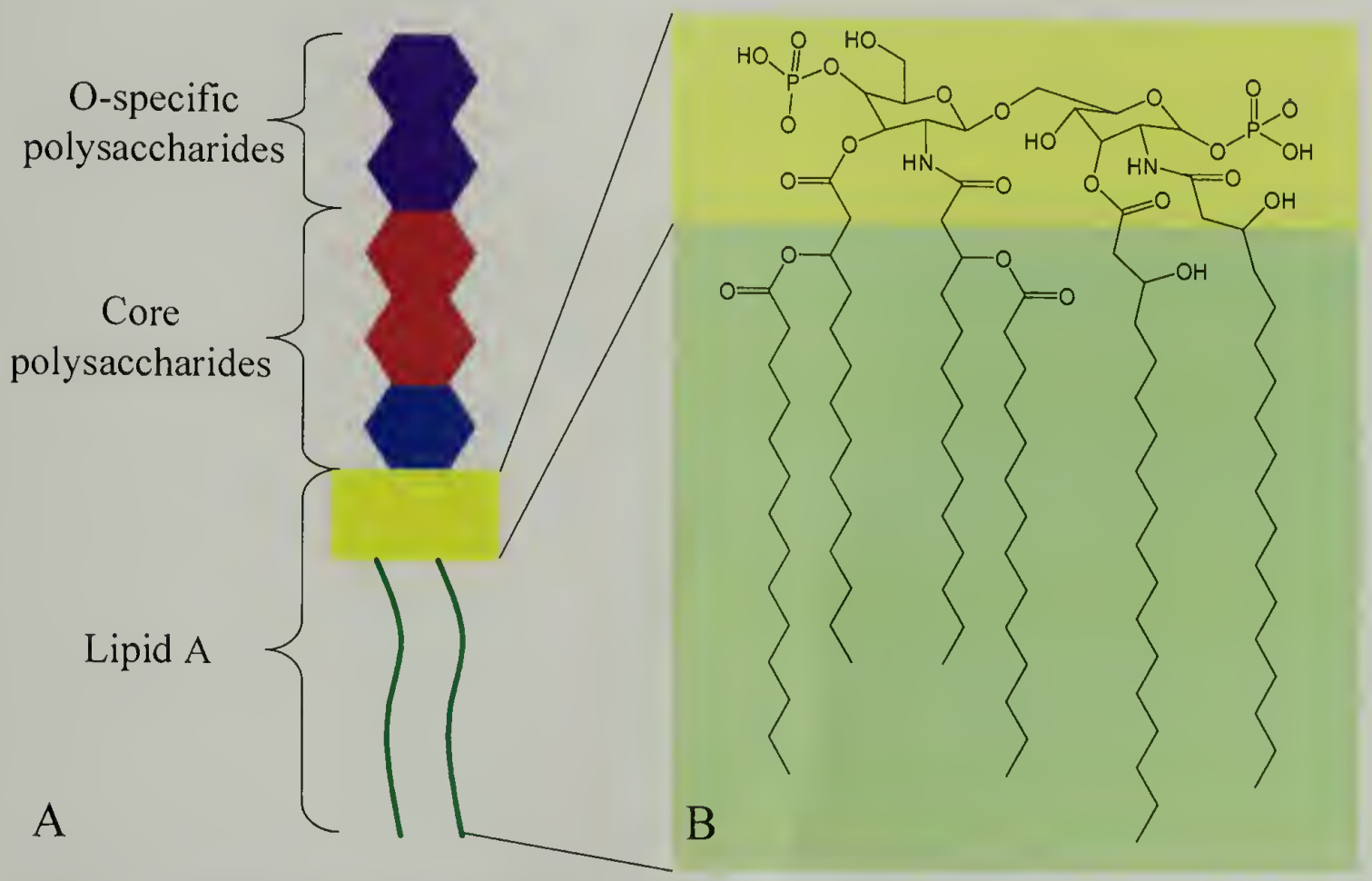

Figure 1.6: a) Schematic of LPS b) chemical structure of Lipid A from *E. coli*.

HDPs are also known to be selective towards cancerous, or transformed cells over non-cancerous, or untransformed mammalian cells.(9, 34-37) This selectivity comes from the differences in the membranes of transformed and untransformed cells.

Typieally, eaneerous eells have a small amount (3 to 6%) of negatively eharged phospholipids in the outer leaflet of the cell membrane whieh induee favorable eleetrostatie interaetions between HDPs and those membranes, similar to that of baeterial eells. Reeently the use of HDPs for antieaneer drugs have been investigated and show promising initial results.(34, 36)

1.5.1 Factors that Influence Selectivity

All the eharaeteristie parameters of eationie HDPs discussed in Seetion 1.4 ean affeet seleetivity towards baeterial over untransformed mammalian eells. A signifieant amount of work has been done to determine exaetly how to eontrol and inerease HDP seleetivity, sinee natural HDPs are often toxie, limiting their therapeutie use. While the literature is filled with seemingly eontradietory results from a wide variety of HDPs and pathogens, it is generally aeeepted that three parameters highly affeet the seleetivity: hydrophobieity, eharge density, and size.(8, 21)

Hydrophobieity is a eomplex parameter: there is a delieate balanee between having too mueh and too little hydrophobieity.(21) If the peptide is too hydrophobie then it is not suffieiently soluble in water to be stored at the eoneentrations needed for host defense and eannot be rapidly transported to the invaded site. Yet, if the peptide is not hydrophobie enough, then there is no driving foree for interaetions with the hydrophobie region of the membrane bilayer and the moleeule will not be membrane permeable. This is problematie beeause both electrostatie and hydrophobic interaetions with eell membranes are required for membrane disruption.

Tweaking the hydrophobicity of a peptide is often accomplished through single residue substitution. It has been reported that changing the hydrophobicity of a single amino acid will significantly change the selectivity of that peptide.(38) Changing a single residue will also effect the hydrophobic moment of a peptide, since the hydrophobicity is not equally spread out over an entire peptide sequence.(21) Most naturally occurring peptides have 40-60% hydrophobic amino acids and, in general, the selectivity for bacterial membranes is decreased as the peptide hydrophobicity is increased.(8, 21)

Initially, charge density appears to be inversely related to hydrophobicity when relating to amphiphilic peptides, but this is not always the case. Some peptides have a reduced amount of charged residues, but a large number of polar residues, while others have a balance between positively and negatively charged residues. Extensive work has been done to optimize the amount of charge in a peptide, often by single residue substitutions(18, 39) or changing the terminal amino acids of the peptide.(40, 41) From these experiments, it has been determined that increasing the net cationic charge improves the selectivity. Unfortunately, charge density can only be effective up to a certain point as too much charge interferes with secondary structuring.(8)

The size of a peptide also plays an important role in determining the selectivity towards bacterial cells. Several studies have shown that it is possible to reduce the size of HDPs and retain or even improve their activity.(8, 22, 23, 42) Some researchers have shown that the optimal length for the highest selectivity is 14 residues.(13, 43) Table 1.3 shows results from a study done on the influence of peptide length on biological activity. From this data, it can be seen that there is a huge effect on antibacterial

activity: there is inactivity at both extremely short and long peptide lengths. This data also suggests that longer peptides are more hemolytic. The 14-residue peptide had the lowest MIC as well as minimal hemolysis at more than 6 times the MIC. In general, the first 20 residues in a peptide sequence provide sufficient antimicrobial activity and a reasonable basis for the design of new antimicrobial peptides or improvement of natural peptides.(8)

Table 1.3: Study on the influence of peptide length on activity (adapted from reference 13).

Peptide Length	$MIC_{E.coli}$ (μg/mL)	% hemolysis (at 100 μg/mL)
8	128	0
10	128	0
12	32	4
14	16	1
16	64	16
18	64	19
20	256	27
22	256	33

1.6 The Development of Resistance to HDPs

There are three generalized pathways for bacterial resistance to develop towards HDPs: 1) the production of more proteases, 2) thickening of the cell wall, and 3) change in the electrostatics of the cell wall. If the cell starts to produce more proteases, these enzymes can recognize peptide sequences, degrade them, and render the HDPs ineffective. This would be similar to penicillin resistance from the production of Penicillinase. If the bacterial cell wall thickens, antibacterial peptides relying on spanning the membrane for cell disruption could be rendered ineffective. Most of the

reeently reported HDP rcsistanee falls within the third categ0ry resulting in a reduetion of the net negative surface charge.(44-48) In gram-negative bacteria, this oecurs through modification of the LPS layer, specifieally acylation of Lipid A, on the cytoplasmic outer membrane (Figure 1.6).(44, 46-48) Conversely, gram-positive bacteria can incorporate teichoic aeids which lack D-alanine, resulting in a reduetion of negative surface charge.(45) In both eases, the decreased net negative surface charge results in decreased binding efficiency of positively eharged moleeules, including HDPs. Currently, resistance reported against HDPs is minimal compared to the widespread resistance towards common antibioties.

1.7 The Future Potential of HDPs as Antimicrobials

HDPs have several advantages that will aid in their use as future antimicrobial agents. Most HDPs kill bacteria rapidly, with a three or more logarithmic decrease of viable cells in 5 minutes at four times the minimal inhibitory concentration (MIC).(37, 49) They are broad spectrum and work well against many clinically resistant mutant bacterial strains with low MICs (between 0.25 and 4 μg/mL).(10, 37) They are proven to be good topical therapeutic agents against microbial infeetions.(50) Due to the encouraging characteristics of HDPs, several peptides have been commercialized for use as antibiotics;(11, 37) both Agennix (Houston, TX) and AM Pharma (Bilthoven, the Netherlands) have developed anti-infective peptides based on natural HDP sequences, while Helix BioMedix, Inc. (Bothell, WA) and Dermegen, Inc. (Pittsburgh, PA) have both introduced topical therapeutics that are active against many infeetive agents.

Despite all these seemingly optimistic results from HDPs, there are some negative characteristics. First, peptides are very complex structures that require time and cost intensive programs to generate. This has been addressed by some companies and researchers trying to find smaller analogs of HDPs that are still as biologically active and selective. However, it is not realistic to use high cost materials for antimicrobial agents, either topical or as systemic therapeutic agents because this high cost is conveyed to the consumer. If the cost of such medications can be reduced significantly, then more realistic applications and commercialization can be explored.

Another issue with the use of HDPs as antimicrobial agents is their toxicity. It is true that some peptides show selectivity towards invader cells over host cells, but there are also peptides that are not selective, or are selective only to their natural hosts and not transferable to other hosts. Many of the commercialized peptides seem to have applications in topical therapies where there is less stringent regulation with regard to toxicity since the medication is not ingested. However, the use of these agents as systemic therapeutics requires more definitive understanding of toxicity and selectivity towards invader cells.

The use of HDPs as antimicrobials is also hampered by their susceptibility to proteolytic degradation. All cells can produce enzymes which can recognize these peptides and degrade the sequence, destroying the effectiveness of HDPs. The production of more proteases is a plausible way that bacteria can exhibit resistance to HDPs as discussed in Section 1.6. With the production of proteases, the bacteria can account for the presence of unknown peptides before the antimicrobial peptides exert their action.

1.8 Mimicking HDPs

The strategy investigated here is to design materials that will mimic the biological activity of HDPs. Many researchers have reported structures to be used as HDP mimics, however all of them include amide bonds and several of them do not show the desired selectivity.(15, 16, 51-56) We extend and change the status quo to mimic HDPs by capturing the essential design elements without limiting the chemical structure to a peptide-based molecular composition. The abiotic, conformationally flexible, *meta*-phenylene ethynylene (*meta*-PE) backbone will be used as a scaffold for the production of cationic facially amphiphilic molecules. This fully hydrocarbon backbone will allow us to begin to probe whether simple, truly abiotic molecules containing no chirality can have similar antimicrobial properties to HDPs. Furthermore, with the addition of polar and nonpolar groups, these molecules should assume the desired amphiphilic structure. The work reported here showcases the first facially amphiphilic polymers based on a *meta*-PE backbone.

Through variation of the side chain structures on the *meta*-PE molecules, we will probe to determine the effect of charge, degree of hydrophobicity, and overall amphipathicity needed to effectively mimic HDPs. Tuning the chemical structure will provide the first polymeric and oligomeric structures without amide bonds to show selectivity towards bacteria over red blood cells. Limiting the size of the molecules will provide compounds that show selectivity that is significantly higher than many natural HDP analogs.

1.9 Thesis Overview

This dissertation describes the preparation, eharaeterization, and biological activity of several novel *meta*-phenylene ethynylene molecules to be used as HDP mimies and antimierobial agents. Chapter 2 diseusses the synthesis of novel molecules based on *meta*-phenylene ethynylene backbones. Both diserete oligomers and polymers were synthesized to be tested as antimierobial agents. In Chapter 3, the eharaeterization at the air-water interface and in solution of these moleeules is presented. The polymers form stable monolayers at the air-water interface as seen by Langmuir experiments, revealing conformational and paeking properties of the polymers. Solution aggregation of these molceules was studied by fluorescenee and turbidity measurements. Chapter 4 discusses the biological activity of these moleeules, indieating that the polymers and diserete oligomers show scleetivity towards bacterial cells over human red blood ecells. The bacterial activity is broad spectrum (20 baeteria studied) and the MIC was found to average 2 μg/mL and be as low as 0.4 μg/mL. These discrete moleeules are also incorporated into polymer plugs and were found to prevent biofilm formation. Chapter 5 attempts to probe the mode of the antimicrobial action of these moleeules. It has been shown that these molecules are membrane active but whether this is the lethal event or if further cellular interactions cause cell death is still under investigation. Chapter 6 contains all the experimental data, such as NMR, GPC, MS, and elemental analysis, and parameters that are not found in the other chapters. The appendix deseribes a side project investigated with these materials which was published in Maeromoleeules in 2004. This involved solution studies with several different polymers to probe whether these molecules ean form a helix.(57) Overall, it will be shown that *meta*-PE moleeules

can be used as HDP mimics, providing a viable route to creating effective antimicrobial agents.

1.10 References

1. Nordenberg, T. (1998) *FDA Consumer Magazine*.
2. Madigan, M. T., Martinko, J. M. & Parker, J. (2003) *Brock Biology of Microorganisms* (Pearson Education, Inc., Upper Saddle River).
3. Bren, L. (2002) *FDA Consumer Magazine* **July-August**.
4. (1999) (Center for Disease Control and Prevention, Atlanta).
5. Lewis, R. (1995) *FDA Consumer Magazine*.
6. Zasloff, M. (2002) *Nature (London)* **415,** 389-395.
7. Brogden, K. A., Ackermann, M., McCray Jr., P. B. & Tack, B. F. (2003) *Int. J. of Antimicrobial Agents* **22,** 465-478.
8. Tossi, A., Sandri, L. & Giangaspero, A. (2000) *Biopolymers* **55,** 4-30.
9. Marshall, S. H. & Arenas, G. (2003) *Electronic J. of Biotech* **6,** 271-284.
10. Powers, J.-P. S. & Hancock, R. E. (2003) *Peptides* **24,** 1681-1691.
11. Zhang, L. & Falla, T. J. (2004) *Expert Opin. Investig. Drugs* **13,** 97-106.
12. Devine, D. A. & Hancock, R. E. (2002) *Current Pharmaceutical Design* **8,** 703-714.
13. Blondelle, S. E. & Houghten, R. A. (1992) *Biochemistry* **31,** 12688-12694.
14. DeGrado, W. F. & Lear, J. D. (1985) *J. Am. Chem. Soc.* **107,** 7684-7689.
15. Porter, E. A., Weisblum, B. & Gellman, S. H. (2002) *J. Am. Chem. Soc.* **124,** 7324-7330.
16. Raguse, T. L., Porter, E. A., Weisblum, B. & Gellman, S. H. (2002) *J. Am. Chem. Soc.* **124,** 12774-12785.
17. Houston Jr., M. E., Kondejewski, L. H., Karunaratne, D. N., Gough, M., Fidai, S., Hodges, R. S. & Hancock, R. E. W. (1998) *J. Peptide Res.* **52,** 81-88.
18. Friedrich, C. L., Rozek, A., Patrzykat, A. & Hancock, R. E. (2001) *J. Biol. Chem.* **276,** 24015-24022.
19. Subbalakshmi, C., Nagaraj, R. & Sitaram, N. (2001) *J. Peptide Res.* **57,** 59-67.
20. Scott, M. G., Yan, H. & Hancock, R. E. (1999) *Infection and Immunity* **67,** 2005-2009.
21. Dathe, M. & Wieprecht, T. (1999) *Biochim. Biophys. Acta* **1462,** 71-87.
22. Mor, A. & Nicolas, P. (1994) *J. Biol. Chem.* **269,** 1934-1939.
23. Subbalakshmi, C., Nagaraj, R. & Sitaram, N. (1999) *FEBS Letters* **448,** 62-66.
24. Hancock, R. E. & Scott, M. G. (2000) *Proc. Natl. Acad. Sci.* **97,** 8856-8861.
25. Hancock, R. E. (1997) *Lancet* **349,** 418-422.
26. Hancock, R. E. & Lehrer, R. (1998) *Trends Biotechnol.* **16,** 82-88.
27. Alberts, B., Bray, D., Lewis, J., Raff, M., Roberts, K. & Watson, J. D. (1994) *Molecular Biology of the Cell* (Garland Publishing, Inc., New York).
28. Hancock, R. E. & Rozek, A. (2002) *FEMS Microbio. Lett.* **206,** 143-149.
29. Oren, Z. & Shai, Y. (1998) *Biopolymers* **47,** 451-463.
30. Rivas, B. L., Pereira, E. D., Mondaca, M. A., Rivas, R. J. & Saavedra, M. A. (2003) *J. Appl. Polym. Sci.* **87,** 452-457.
31. Brade, L., Bessler, W. G. & Brade, H. (1988) *Infection and Immunity* **56,** 1382-1384.

32. Kato, H., Haishima, Y., Iida, T., Tanaka, A. & Ken-Ichi, T. (1998) *J Bacteriol* **180,** 3891-3899.
33. Broady, K. W., Rietschel, E. T. & Luderitz, O. (1981) *Eur. J. Biochem.* **115,** 463-468.
34. Papo, N. & Shai, Y. (2003) *Biochem. J.* **42,** 9346-9354.
35. Papo, N., Braunstein, A., Eshhar, Z. & Shai, Y. (2004) *Cancer Research* **64,** 5779-5786.
36. Kim, S. K., Kim, S. S., Bang, Y. J., Kim, S. J. & Lee, B. J. (2003) *Peptides* **24,** 945-953.
37. Hancock, R. E. (2000) *Expert Opin. Investig. Drugs* **9,** 1723-1729.
38. Juvvadi, P., Vunnam, S., Merrifield, E. L., Boman, H. G. & Merrifield, R. B. (1996) *J. Peptide Res.* **49,** 89-102.
39. Wu, M. & Hancock, R. E. (1999) *Antimicrob. Agents Chemother.* **43,** 1274-1276.
40. Fink, J., Merrifield, R. B., Boman, A. & Boman, H. (1989) *J. Biol. Chem.* **264,** 6260-6267.
41. Bessalle, R., Haas, H., Goria, A., Shalit, I. & Fridkin, M. (1992) *Antimicrob. Agents Chemother.* **36,** 313-317.
42. Tossi, A., Scocchi, M., Skerlavaj, B. & Gennaro, R. (1994) *FEBS Letters* **339,** 108-112.
43. Lee, S., Mihara, H., Aoyagi, H., Kato, T., Izumuya, N. & Yamasaki, N. (1986) *Biochim. Biophys. Acta* **862,** 211-219.
44. Shi, Y. X., Cromie, M. J., Hsu, F. F., Turk, J. & Groisman, E. A. (2004) *Molecular Microbiology* **53,** 229-241.
45. Peschel, A., Otto, M., Jack, R. W., Kalbacher, H., Jung, G. & Gotz, F. (1999) *Journal of Biological Chemistry* **274,** 8405-8410.
46. Guo, L., Lim, K. B., Poduje, C. M., Daniel, M., Gunn, J. S., Hackett, M. & Miller, S. I. (1998) *Cell* **95,** 189-198.
47. Gunn, J. S., Lim, K. B., Krueger, J., Kim, K., Guo, L., Hackett, M. & Miller, S. I. (1998) *Molecular Microbiology* **27,** 1171-1182.
48. Nummila, K., Kilpelainen, I., Zahringer, U., Vaara, M. & Helander, I. M. (1995) *Mol Microbiol* **16,** 271-278.
49. Friedrich, C. L., Scott, M. G., Karunaratne, D. N., Yan, H. & Hancock, R. E. (1999) *Antimicrob. Agents Chemother.* **43,** 1274-1276.
50. Hancock, R. E. (1999) *Drugs* **57,** 469-473.
51. Kirshenbaum, K., Barron, A. E., Goldsmith, R. A., Armand, P., Bradley, E. K., Truong, K. T. V., Dill, K. A., Cohen, F. E. & Zuckermann, R. N. (1998) *Proc. Natl. Acad. Sci.* **95,** 4303-4308.
52. Kirshenbaum, K., Zuckermann, R. N. & Dill, K. A. (1999) *Current Opinion in Structural Biology* **9,** 530-535.
53. Liu, D. & DeGrado, W. F. (2001) *J. Am. Chem. Soc.* **123,** 7553-7559.
54. Patch, J. A. & Barron, A. E. (2003) *J. Am. Chem. Soc.* **125,** 12092-12093.
55. Porter, E. A., Wang, X., Lee, H. S., Weisblum, B. & Gellman, S. H. (2000) *Nature (London)* **404,** 565.

56. Tew, G. N., Lui, D., Chen, B., Doerksen, R. J., Kaplan, J., Corroll, P. J., Klein, M. L. & DeGrado, W. F. (2002) *Proc. Natl. Acad. Sci. U.S.A.* **99,** 5110-5114.
57. Arnt, L. & Tew, G. N. (2004) *Macromolecules* **37,** 1283-1288.

CHAPTER 2

THE SYNTHESIS OF *META*-PHENYLENE ETHYNYLENE MOLECULES

2.1 Introduction

Phenylene ethynylene (PE) polymeric backbones have beeome more prevalent due to the discovery of effieient ways to eouple aromatie halogens and terminal alkynes.(1-13) A very effeetive eoupling reaetion is the Sonogashira reaetion whieh utilizes a eombination of a palladium eatalyst, eopper iodide, base, and metal ligand. The palladium souree ranges from Pd(II) to Pd(0), ineluding $Pd(PPh_3)_4$, $Pd(PPh_3)_2Cl$, and $Pd(dba)_2$. All the reported reaetion conditions ean be utilized to synthesize either *para*, *ortho*, or *meta* polymers depending on the monomer substitution. The literature has numerous papers that use the Sonogashira reaetion to synthesize *para*-PE baekbones(14-24), most of whieh explore these moleeules for eleetronie devices. Sonogashira reaetion conditions are just as useful for making m*eta*-PE moleeules, a backbone that is mueh less studied.(25-28)

The driving foree for synthesizing *meta*-derived moleeules is to produce novel PE molecules with defined substitution patterns that under eertain conditions assume facially amphiphilie (FA) structures where the hydrophobie and hydrophilie moieties segregate to opposite sides of the moleeule as shown in Figure 2.1. These moleeules will not only add to the meta-PE literature, but will provide a seaffold for building FA struetures on a eonformationally flexible baekbone.

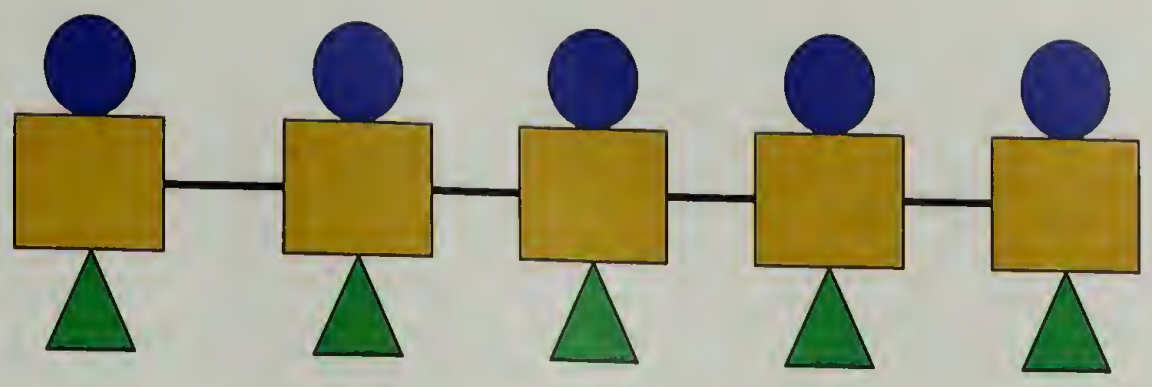

Figure 2.1: Facially amphiphilic structure where hydrophilic (blue circles) and hydrophobic (green triangles) moieties segregate to opposite sides of the molecule.

Para-PE molecules have been studied extensively for their fluorescent properties(1, 12, 29-31) and potential uses as molecular wires.(32-36) Our group has studied the *para* substituted polymers shown in Figure 2.2 for the stabilization of oil droplets in acidic aqueous solution.(37) Depending on the solvent conditions, droplet size can be controlled. At this time, it is unknown what other factors may contribute to the changes in droplet size.

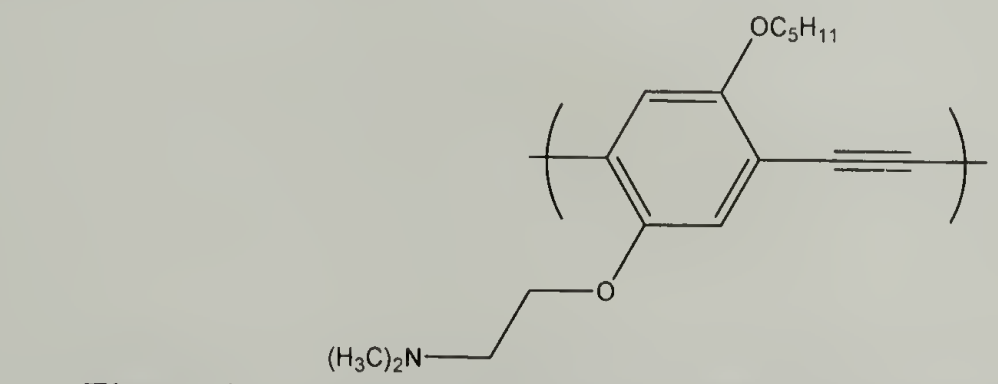

Figure 2.2: Example of facially amphiphilic para-PE molecule.

Ortho-PE(11, 38) and *meta*-PE(4, 5, 26, 28, 39, 40) molecules have been investigated for folding properties. Moore and coworkers have made stable helical structures by varying the side chains of a *meta*-PE backbone and controlling the solvent composition.(28) Our group is currently working on understanding the solvophobic folding properties of several *ortho*-PE derivatives by using different side group substituents. This is shown schematically in Figure 2.3. The stability of the helix varies

depending on the substituents used, such as ethers or esters.(11) Being able to design a helix where one-third of the helix has hydrophilic side chains while the other two-thirds is hydrophobic can lead to some very interesting facially amphiphilic helices which under specific solvent conditions can form multi-helix bundles.

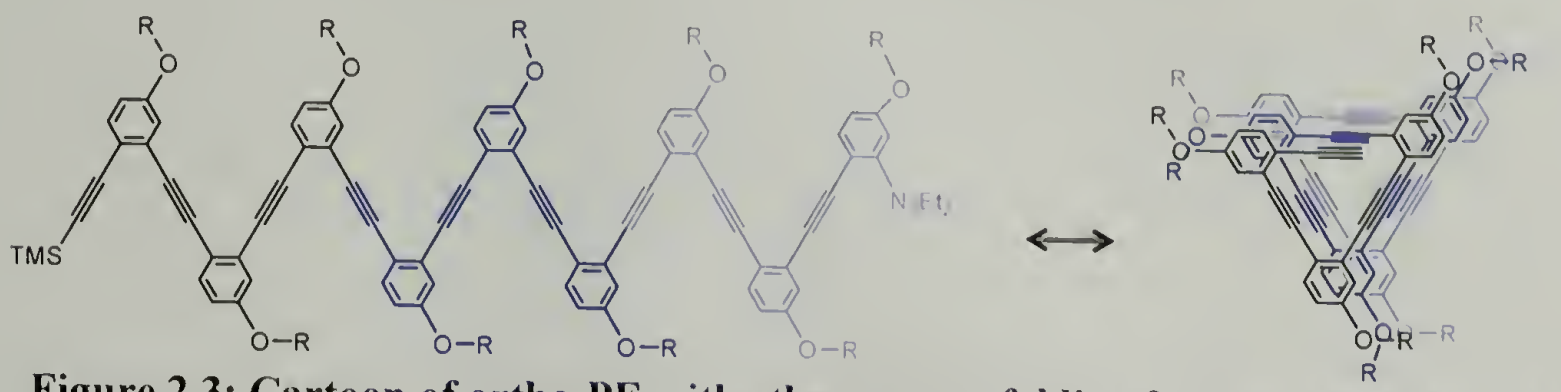

Figure 2.3: Cartoon of ortho-PE with ether groups folding from an extended to a helical structure.

There are many goals of the isomers of PE molecules studied in our group, antimierobials, foldamers, and self-assembly; however, the unifying property is the design of a facially amphiphilic (FA) structure. In all these molecules, the hydrophobic nature of the molecule comes from a combination of side chains and backbone and the hydrophilic moieties are generally side chains of either ethylene glycol or amine substituents. These molecules fit into the literature, not only for their applications, but also their FA structure. There are only a few papers in the literature, other than those published by our group, that market phenylene ethynylene molecules as being amphiphilic(28, 41-43) so there is definite room for expansion in this field.

This chapter demonstrates that by using functionalized dihalogenated monomers and the eommercially available *meta*-diethynyl benzene, it is possible to synthesize a series of *meta*-PE polymers and oligomers with various non-polar (NP) and polar (P) groups. The *meta*-PE backbone is flexible and can adopt different structures, including

an extended or helical conformation, as shown in Figure 2.4. When the backbone has large enough NP groups, the molecule will prefer an extended FA structure rather than a helical structure in solution where the P and NP groups on opposite sides of the molecule as shown in the top structure of Figure 2.4. At the air-water interface, all the *meta*-PE polymers designed with a FA structure should assume an extended conformation. All the characterization data that is not presented in this chapter is in Chapter 6.

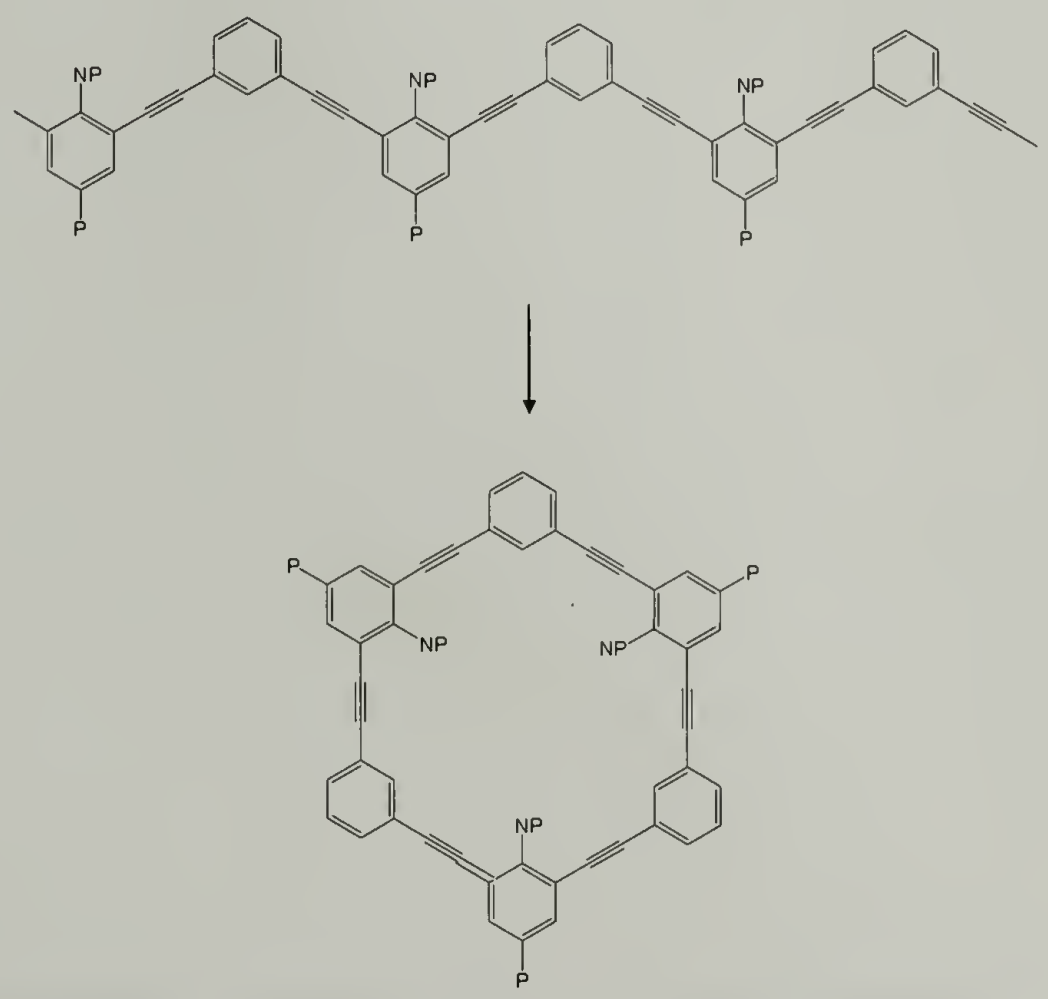

Figure 2.4: Extended and helical structures of *meta*-substituted PE molecules.

2.2 Monomer Synthesis

2.2.1 Alkoxy Substituted Monomer

In order to build the proposed FA structures, monomers with appropriate functionality must first be synthesized (Figure 2.5). The commercially available 3,5-diiodo-4-hydroxy-benzonitrile, **1**, was reacted under Mitsunobu conditions to

incorporate an alkoxy group. Several different alkyl chain lengths were prepared ranging from C5 to C12. Next, the nitrile functionality was successfully reduced with Borane-THF to yield the benzyl amine, which was protected right away as the *tert*-butyl carbamate (Boc) since concentration and storage of the primary amine often lead to multiple degradation products. Borane-THF gave good yields of the primary amine with limited dehalogenation, which often occurs with aryl iodides and bromines under reducing conditions. The final compounds, **8**, **9**, and **10**, were pure, functionalized monomers ready for use in Sonogashira coupling.

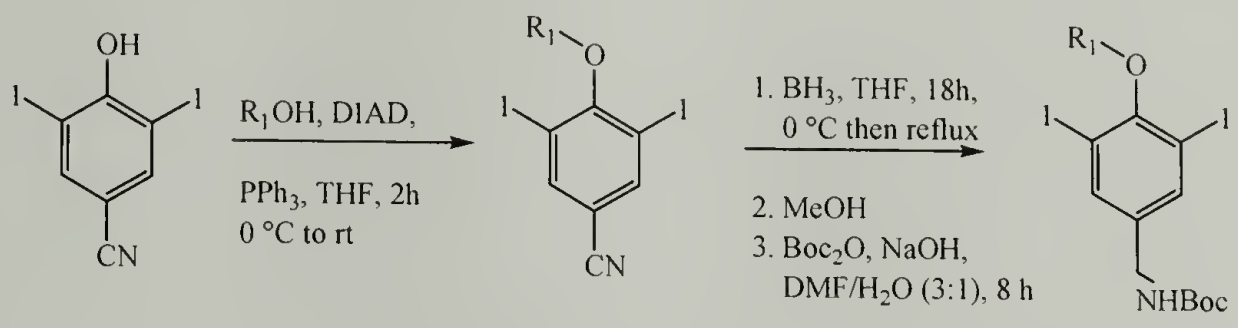

1

2, $R_1 = C_5H_{11}$, 92 %
3, $R_1 = C_8H_{17}$, 90%
4, $R_1 = C_{12}H_{25}$, 90%

8, $R_1 = C_5H_{11}$, 62%
9, $R_1 = C_8H_{17}$, 63%
10, $R_1 = C_{12}H_{25}$, 64%

Figure 2.5: Synthesis of alkoxy substituted molecules.

The monomer transformations were followed by ^{1}H NMR, ^{13}C NMR, and GC-MS. The final monomer composition was confirmed by elemental analysis. As an illustration, Figure 2.6 shows the ^{1}H NMR for the pentoxy side chain monomer synthesis.(44) Figure 2.6a shows the resulting NMR from the introduction of the pentoxy side chain, **2**. The triplet, at 4.0 ppm is from the methylene next to the oxygen, with the following peaks accounting for the rest of the methylene groups in the alkoxy chain progressively becoming further away from the aromatic ring. With the reduction of the nitrile group, Figure 2.6b shows a new singlet in the NMR accounting for the

methylene group at 3.9 ppm. Finally protection of the free amine, **8**, introduces a singlet at 1.4 ppm accounting for the nine protons of the Boc group, shown in Figure 2.6c. The amine proton can be seen as a broad peak at 4.8 ppm while the methyl amine is now a doublet at 4.2 ppm. The trends of the other monomers with longer alkoxy chains are similar, suggesting that the proton environments and structural transformations are comparable.

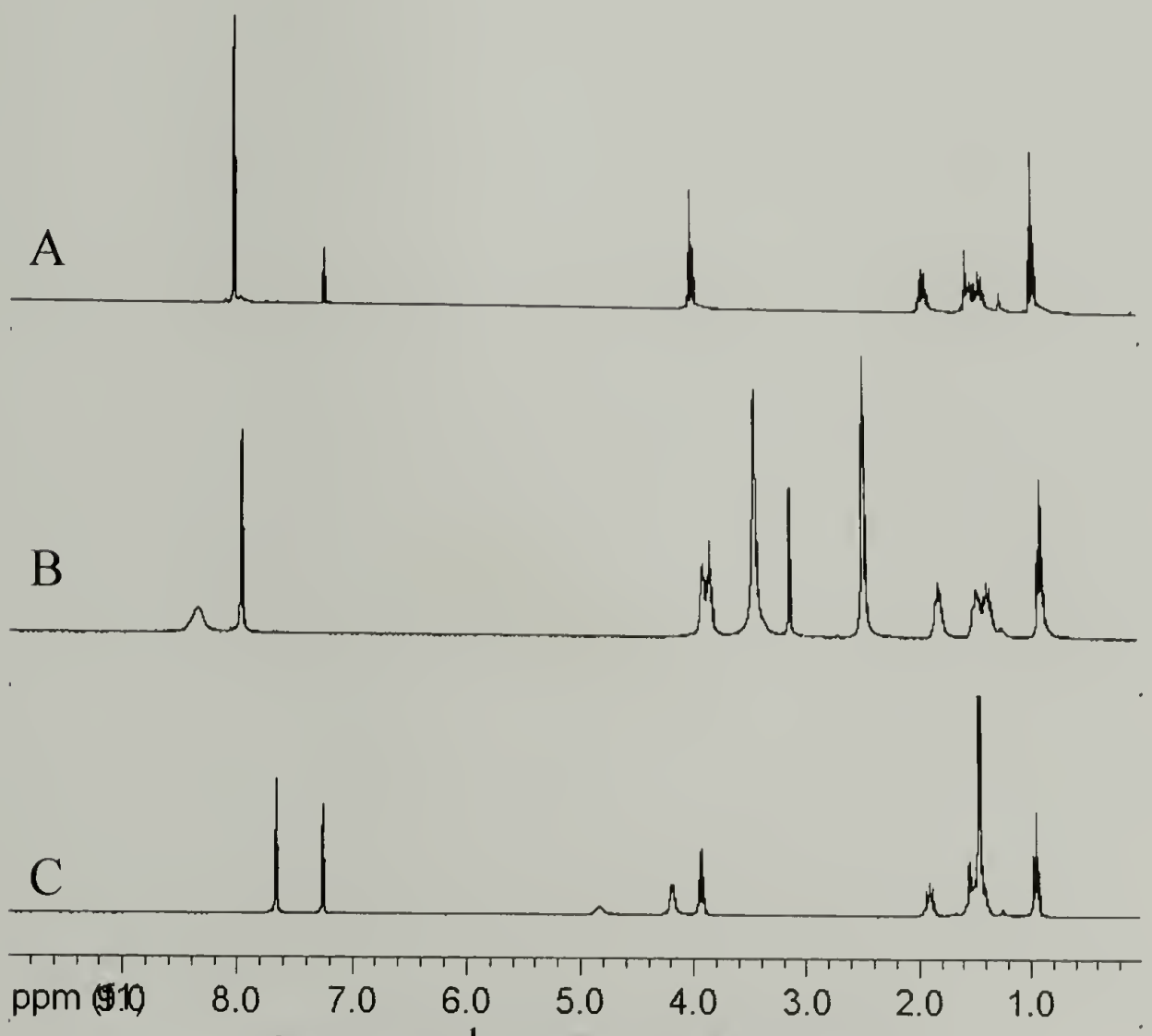

Figure 2.6: ^{1}H NMR of C5 synthesis.

2.2.2 Synthesis of C0 Monomers

A series of molecules without the alkoxy substituents or any substituents *para* to the amine (denoted as C0) were synthesized as shown in Figure 2.7. Dibromobenzoic acid, **11**, was purchased as the starting material and the acid group was reduced in good

yield using lithium aluminum hydride in ether without the loss of bromide. The benzyl alcohol, **12**, was reacted with N-bromosuccinimide and triphenylphosphine to yield the benzyl bromide, **13**. This was followed by reaction with sodium cyanide to yield the benzyl nitrile, **14**. Reduction with Borane-THF gave the free amine which was subsequently protected with the Boc group yielding a white crystalline solid, **16**. This compound, **16**, was then used in coupling reactions to produce discrete oligomers and polymers.

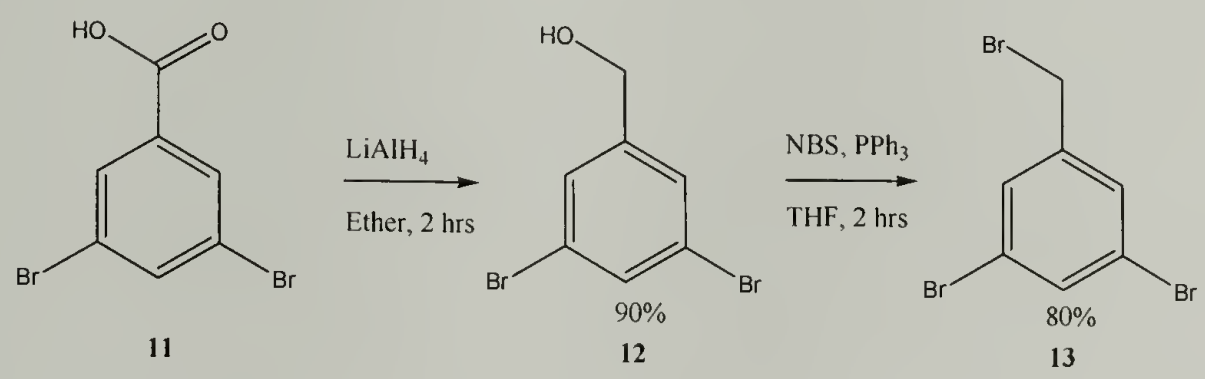

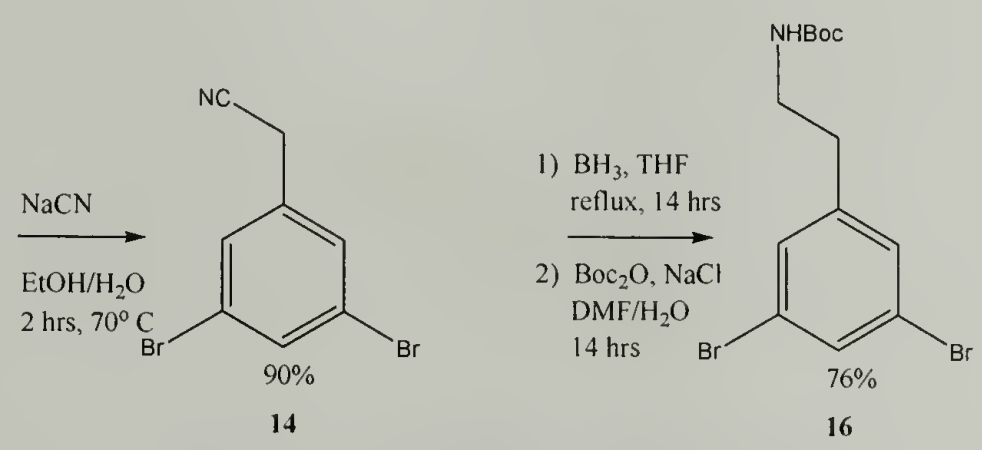

Figure 2.7: Synthesis of C0 molecules.

The monomer transformations were followed by ^{1}H NMR, ^{13}C NMR, and GC-MS. The final monomer, **16**, was confirmed by elemental analysis. Figure 2.8 shows the progression by ^{1}H NMR. The benzyl alcohol, **12**, results in a triplet at 7.6 ppm accounting for one proton and a doublet a 7.5 ppm accounting for two protons in the aromatic region. The simplicity of the aromatic region is expected due to the 1,3,5-substitution which eliminates *ortho* proton coupling resulting in singlet peaks. The benzyl protons are a singlet at 4.7 ppm. Throughout the rest of the transformations, the

aromatic peaks do not shift significantly, but the benzyl protons shift upfield to 4.4 and 3.7 ppm for the benzyl bromide, **13**, and benzyl nitrile, **14**, respectively. Upon reduction to the free amine and protection with the Boc group, **16**, the ethyl protons produce peaks at 3.4 and 2.7 ppm while the amine and Boc protons are at 4.5 and 1.4 ppm, respectively.

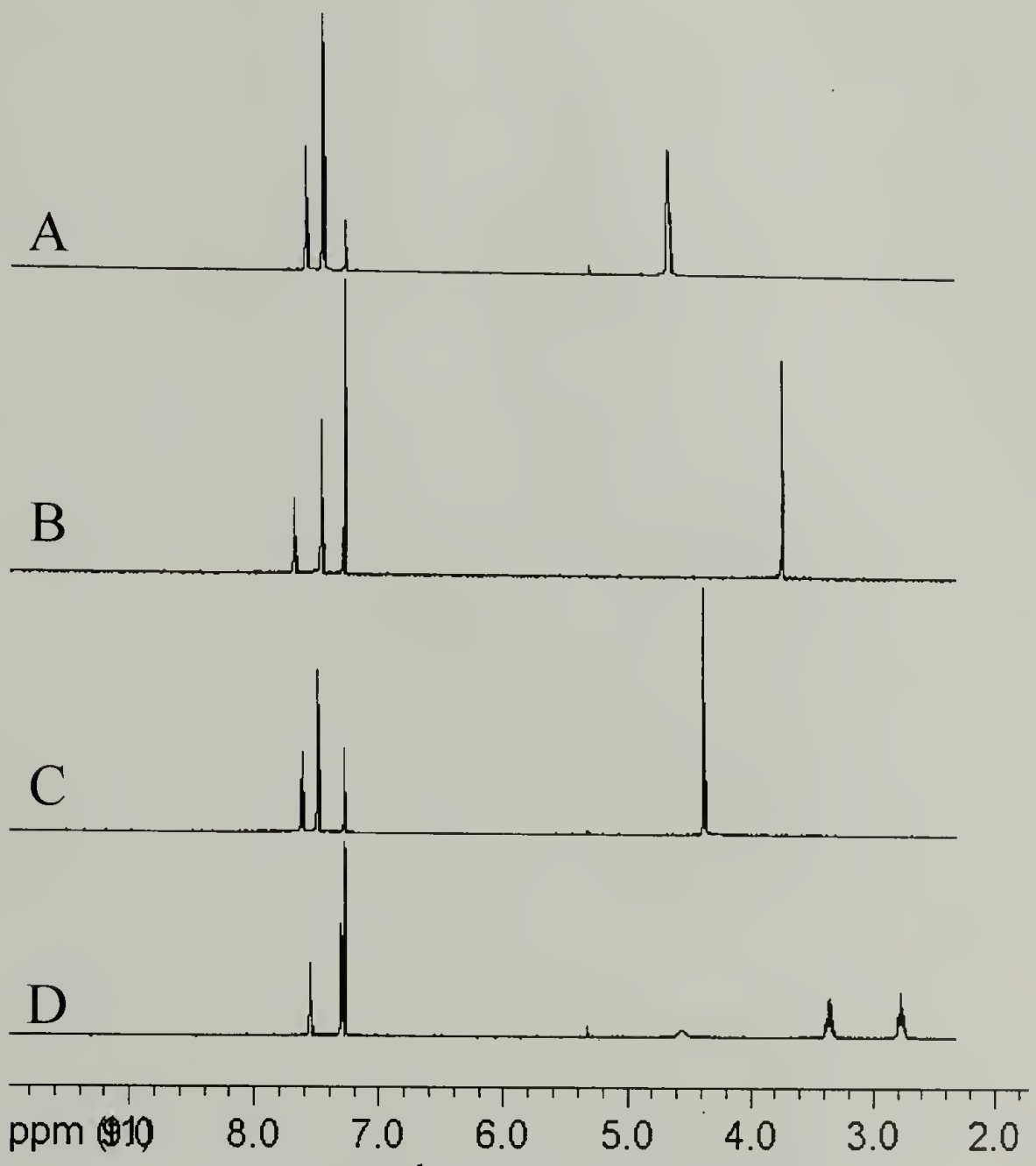

Figure 2.8: ^{1}H NMR of C0 synthesis.

2.2.3 Synthesis of Other Monomers

Various iterations of similar monomers were synthesized to develop structure-property relationships. Figure 2.9 shows several other monomer synthetic schemes used

to make dihalogenated monomers for polymerization. Scheme A shows a reaction introducing an ether substituent with a nonpolar pentyl group. In this reaction, potassium hydride removes the proton from the pentanol and displaces the bromide of **13**. This reaction was also used in scheme D to introduce a triethylene glycol P group, **23**. In scheme B, the Mitsonobu reaction was utilized to introduce an ethyl amine group to the methyl functionalized molecule, **18**, resulting in monomer **19** with both P and NP substituents. Scheme C utilizes an esterification reaction to introduce a methyl ester group in place of the carboxylic acid yielding **21**. Next a transesterification reaction was done using potassium carbonate and triethylene glycol monomethyl ether to make the Peg-ester monomer **22**. These monomers were all characterized by ^{1}H NMR and GC-MS before being used for polymerization as described in the following section.

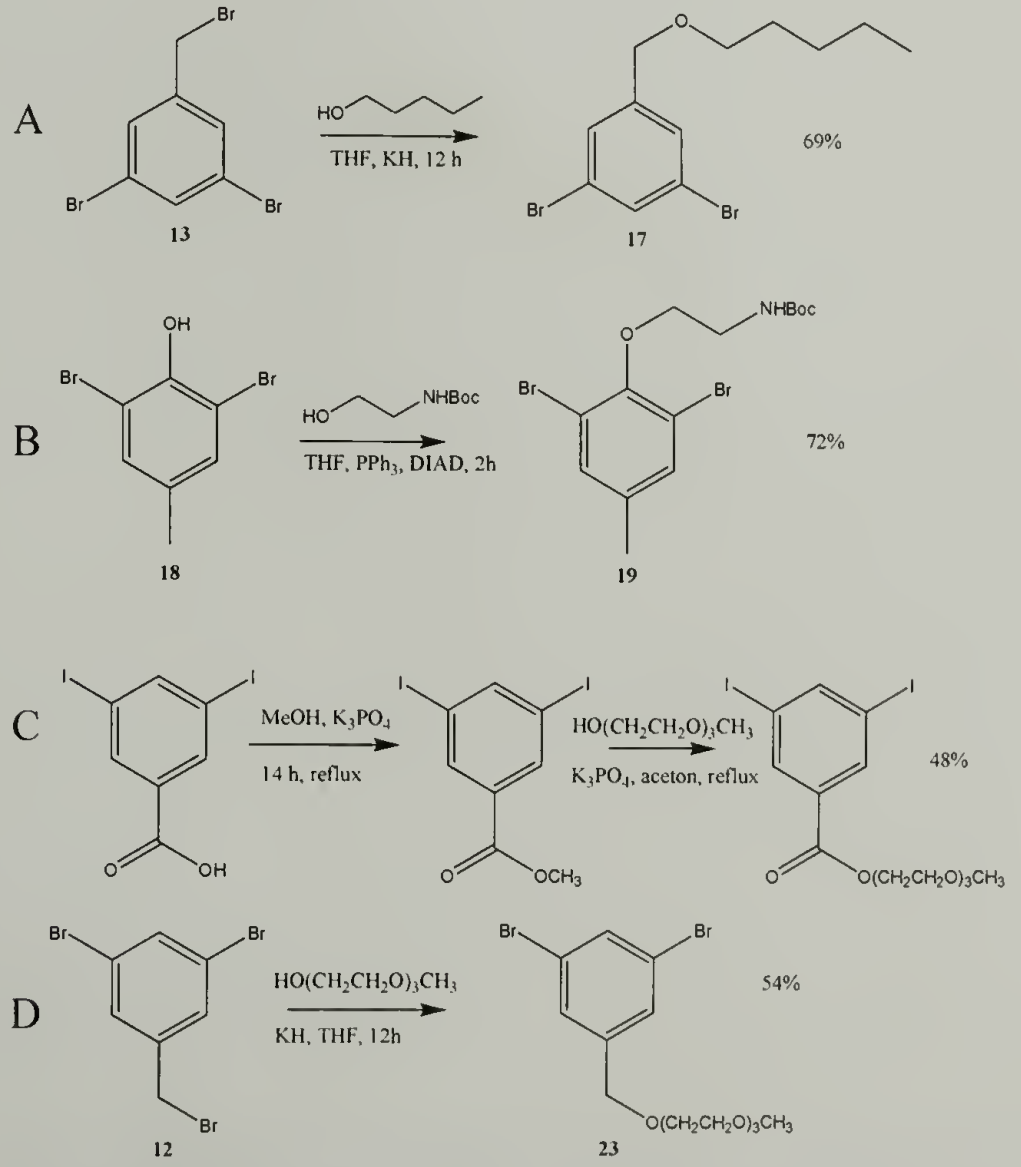

Figure 2.9: Dihalogenated monomer synthetic schemes.

2.3 General Polymer Synthesis

A general polymerization scheme is shown in Figure 2.10 for the dihalogenated monomer series. The polymerization utilizes Sonogashira coupling between the halogen and the terminal acetylene of *meta*-diethynyl benzene. This is carried out in an air-free Schlenk flask under a nitrogen atmosphere. The diethynyl benzene was weighed directly into the flask followed by the addition of reagents, solvent, and purging with nitrogen before being sealed. A ratio of 1.03:1 diacetylene:dihalogen was used to account for acetylene-acetylene coupling.(45) The reaction was allowed to stir at room temperature for 30 minutes, until a homogeneous solution was formed, before submerging in a 65°C oil bath overnight. The formation of salt precipitate was observed after a couple of hours while the reaction solution remained clear. For the alkoxy-substituted monomers, the solution remained a yellowish-orange color, while for the monomers without the alkoxy moiety, the solution often turned dark. After the completion of the reaction, the polymer, as a yellow solid, was recovered by precipitation from methanol and fully characterized by NMR, fluorescence, and GPC. The amine was deprotected using 4M HCl in dioxane with quantitative yield. These harsh conditions do not affect the polymer backbone or substituents as evidenced by NMR and fluorescence.

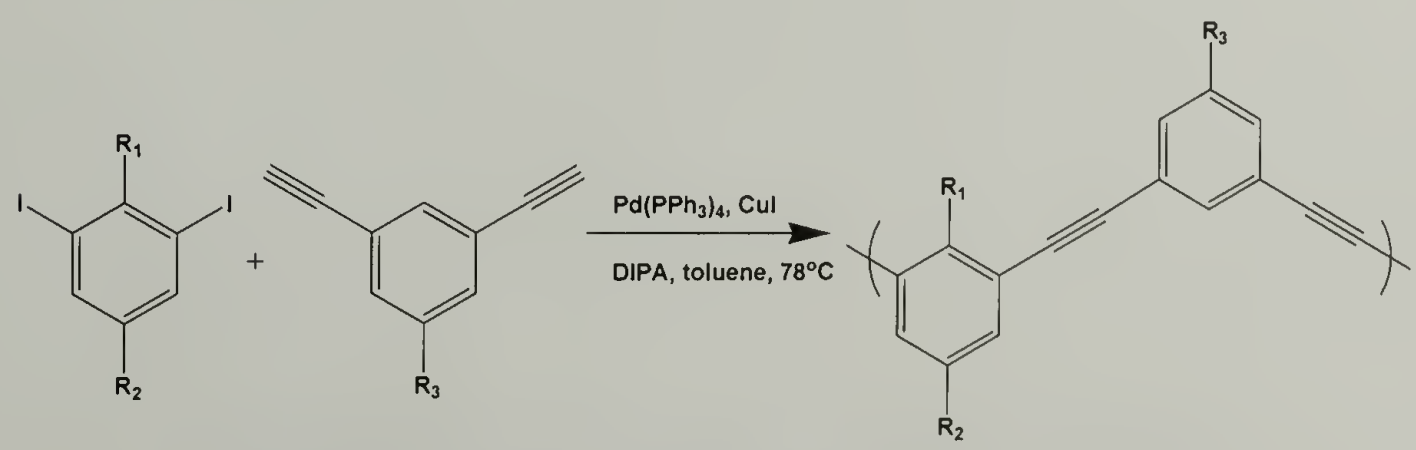

Figure 2.10: Representative polymerization conditions.

The ^{1}H NMR for both the protected, **24p**, and deprotected, **24d**, pentoxy polymers can be seen in Figure 2.11. Polymer **24p**, with the amine still Boc protected, is shown in the top spectrum. Coupling between the aromatic protons makes the aromatic region between 7.0 and 8.0 ppm very complicated. The peak from the amine proton is present at 4.9 ppm and the two methylene groups give rise to the peak at 4.3 ppm with the peaks from the rest of the alkoxy chain between 2.0 and 0.7 ppm. There is no evidence of terminal acetylene protons suggesting that the end groups are most likely halogens. The most notable differences upon deprotection of the polymer to **24d** are the presence of the amine protons at 8.5 ppm and the absence of the Boc group at 1.4 ppm. Peaks from the alkoxy protons and the backbone aromatic protons remain unaffected during the deprotection. Minimal shifting of these protons is due to the solvent change from chloroform to dimethylsulfoxide.

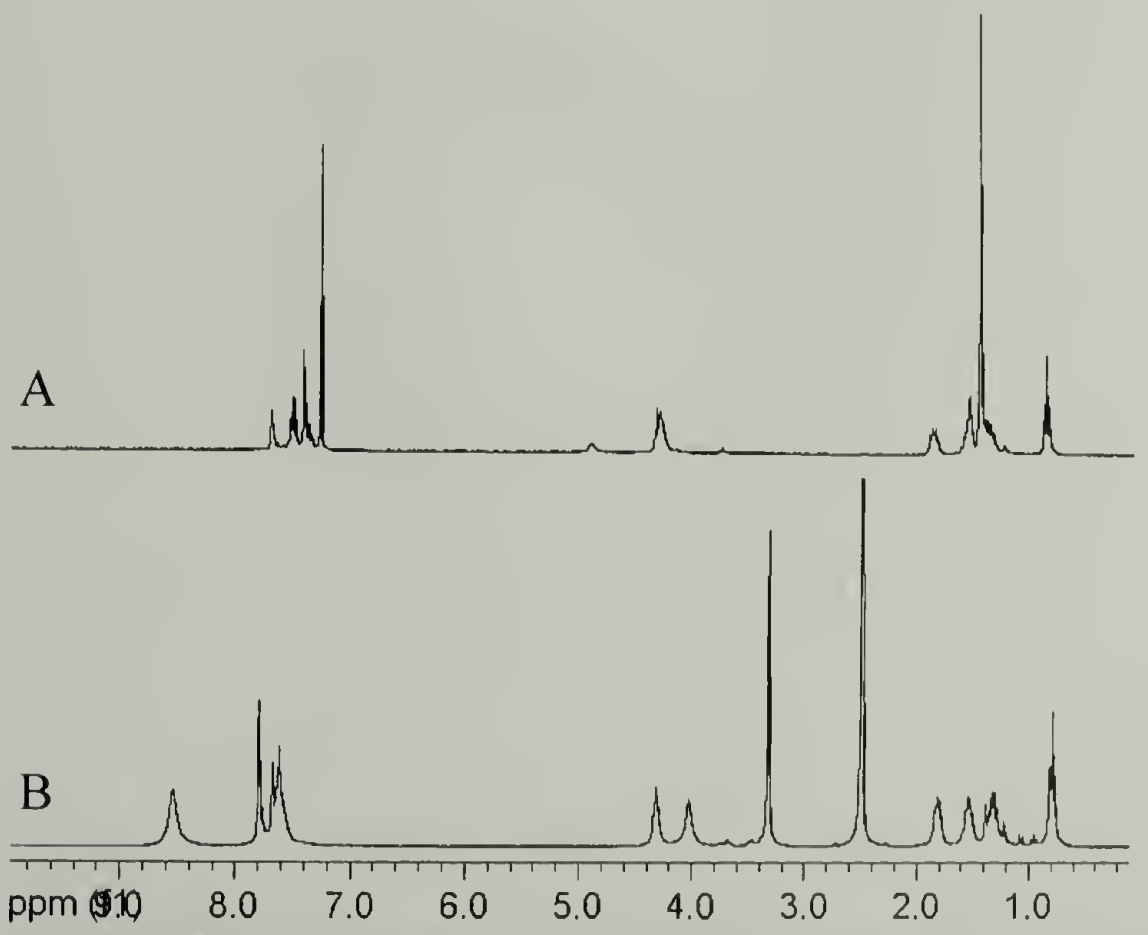

Figure 2.11: NMR of protected (24p) and deprotected (24d) polymers with alkoxy side chains

Representative polymer structures and their molecular weight characterization data is shown in Table 2.1. The data is taken from gel permeation chromatography (GPC) in THF calibrated versus polystyrene standards. GPC is known to overestimate the molecular weight of rigid polymers. In fact, fractionation and collection of a polymer sample analyzed by MALDI-ToF verified that the GPC does overestimate the molecular weight of these polymers by a factor of two. Even still, the corrected molecular weight of the resulting polymers ranged from about 2000 g/mol to 15,000 g/mol with polydispersities between 1.3 and 4. The high polydispersity values are expected since this is a step-polymerization; however, they can be kept below 2.0 if the reaction time is less than 14 hours.

Table 2.1: Summary of Polymers synthesized.

Number	R_1	R_2	R_3	Mn^* ($x10^{-3}$)	PDI
24p	$O(CH_2)_4CH_3$	CH_2NHBoc	H	17.8	2.3
25p	$O(CH_2)_7CH_3$	CH_2NHBoc	H	7.7	1.3
26p	$O(CH_2)_{11}CH_3$	CH_2NHBoc	H	10.1	1.4
27p	$O(CH_2)_2CH_3CH_2CH_3$	CH_2NHBoc	H	10.1	1.6
28p	H	$(CH_2)_2NHBoc$	H	5.3	1.5
29p	$(CH_2)_2NHBoc$	H	$O(CH_2)_4CH_3$	4.6	1.8
30p	H	$O(CH_2CH_2O)_3CH_3$	H	4.8	2.3
31p	CH_2NHBoc	$O(CH_2)_4CH_3$	$O(CH_2)_2NHBoc$	23.5	2.3
32	H	$O(CH_2CH_2O)_3CH_3$	$O(CH_2CH_2O)_3CH_3$	10.0	1.5
33	H	$COO(CH_2CH_2O)_3CH_3$	$COO(CH_2CH_2O)_3CH_3$	5.1	3.8

* Representative Mn values from GPC in THF against PS standards

2.4 Synthesis of Discrete Oligomers

Discrete oligomers **34p** and **35p**, shown in Figure 2.12 were also synthesized from the above monomers (**16**, section 2.2b, and **8**, section 2.2a) using similar conditions as the polymerization but changing the stoichiometry from 1.03:1 to 0.4:1 diacetylene:dihalogen. The reaction resulted in several spots that could be monitored by TLC under both long and short wave UV illumination. Since both the monomers used were difunctional, there were several longer oligomers formed during the reaction in addition to the structure of interest with three aromatic rings. Flash column chromatography was used to separate **34p** and **35p** from the crude reaction mixtures to yield white solids (30% and 35% respectively). Quantitative deprotection was achieved with the same conditions used for the polymeric analogs in Section 2.3.

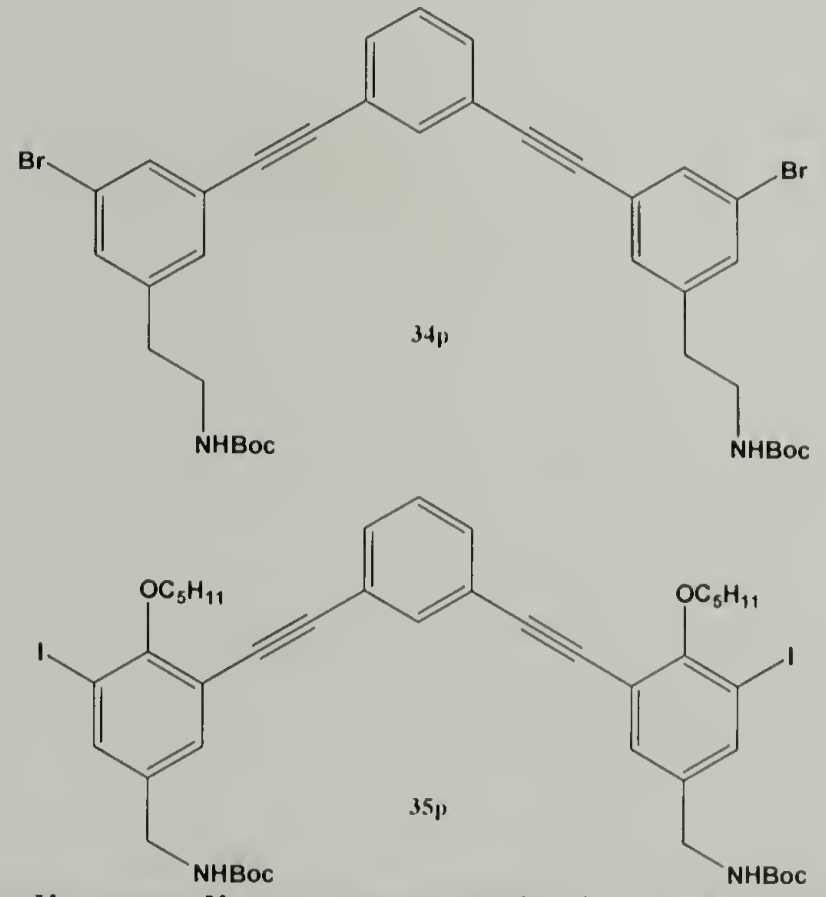

Figure 2.12: Two discrete oligomers synthesized. In general, they represent two classes of oligomers: with and without alkyl side chains.

The ^{1}H NMR spectrum for **34p** is shown in Figure 2.13. The NMR splitting patterns for the discrete compounds are much narrower than those of the polymers and

the molecule is C2 symmetric, so the *ortho*, *meta*, and *para* splitting can be assigned. The triplet in the aromatic region of the ^{1}H NMR accounting for one proton at 7.7 ppm is assigned as H_d. This proton is the furthest downfield because of its proximity to the ethylene groups, allowing for easy identification. The triplet centered around 7.6 ppm is assigned as H_c and H_h while the doublet of doublets at 7.5 ppm account for H_e and H_g. There is triplet centered around 7.4 ppm accounting for H_f. The signals between 7.4 and 7.3 ppm account for H_a, H_b, H_i, and H_j. The discrete oligomer was also characterized by high resolution electrospray ionization to confirm the molecular structure. Both the loss of the Boc groups and the bromine end groups can be seen in the fragmentation of the molecule.

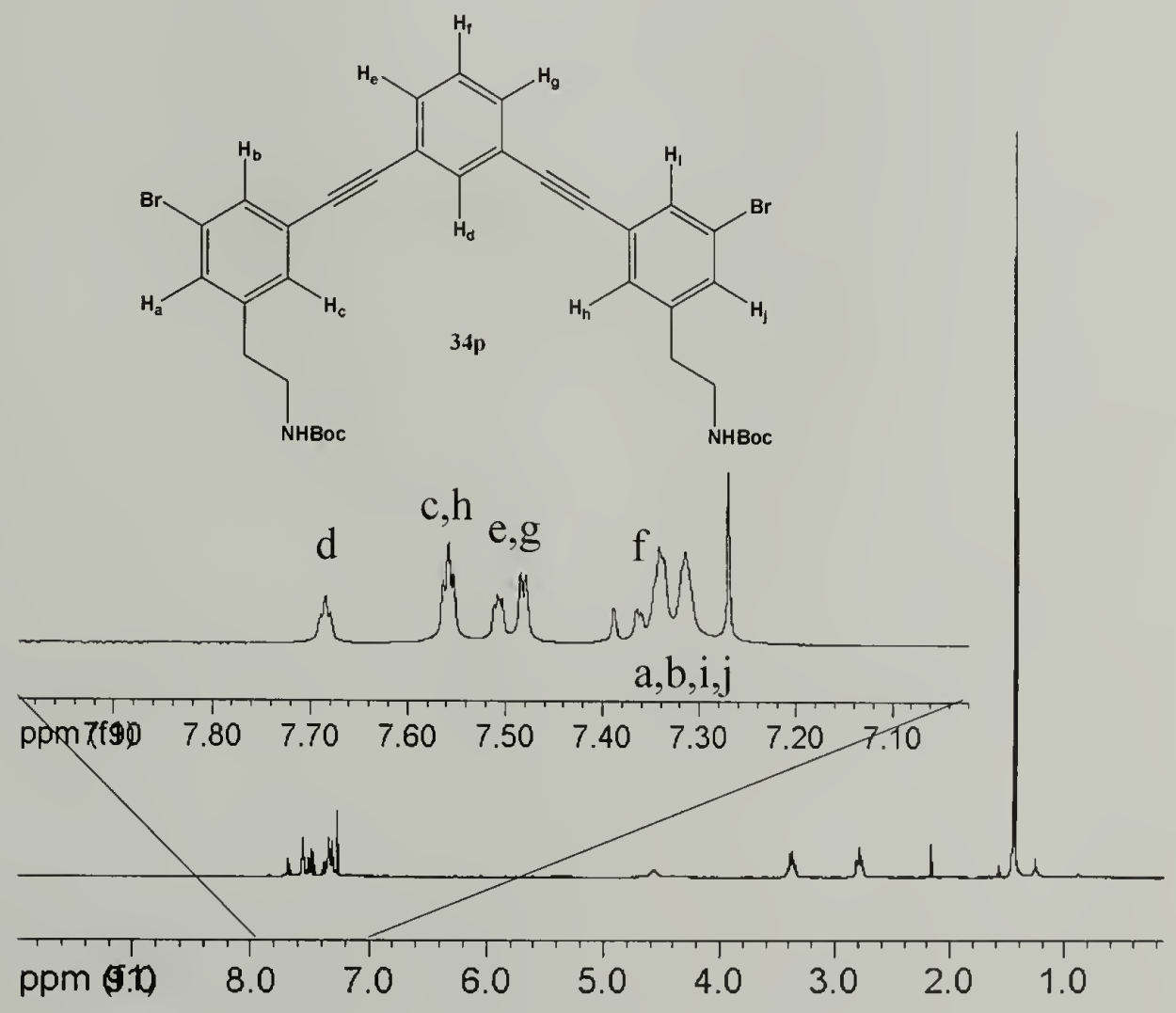

Figure 2.13: ^{1}H NMR of C0 oligomer, 34p.

2.4.1 Structure-Activity Relationship of Oligomers

In an attempt to investigate the structure-activity relationship (SAR) of these discrete oligomers, several modifications to the original structures were made, including modifications of the bromine end groups, the amine side chain, and the alkoxy side chain. Most of the modifications were performed on the dihalogenated monomer before coupling with diethynyl benzene since reaction and purification of the monomer gave higher yields than post-oligomerization reactions.

Table 2.2: SAR study on discrete oligomers varying end groups, where R_1 and R_2 were initially bromine.

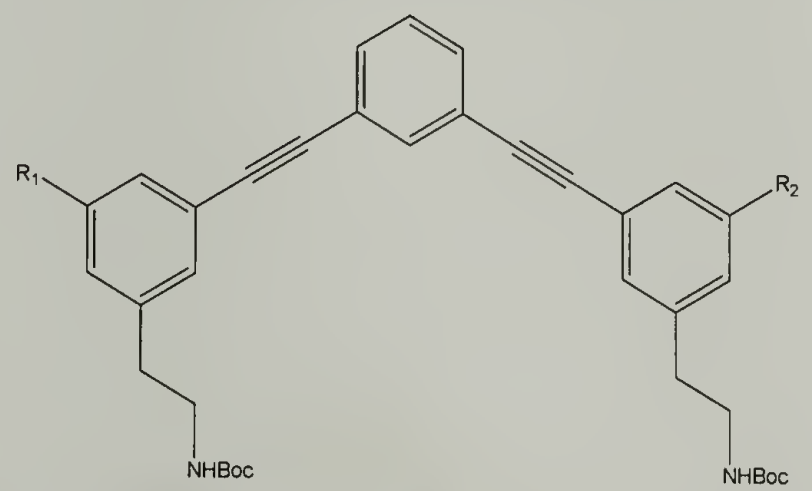

Number	R_1	R_2
36p	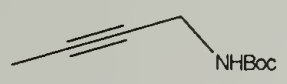	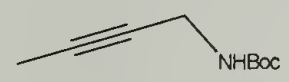
37p	Br	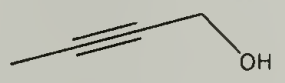
38p	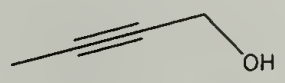	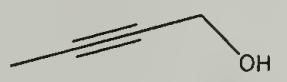
39p	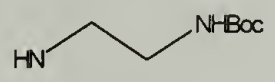	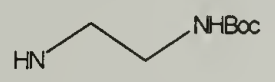
40p	H	H

The bromine moieties provide a convenient handle with which to perform reactions, resulting in modification of the oligomer end groups, as shown in Table 2.2. The Sonogashira reaction was utilized to introduce new carbon-carbon bonds for the end groups; entries **36p**, **37p**, and **38p** in Table 2.2. The general reaction scheme is

shown in Figure 2.14. Various end groups with propargyl moieties, amines (**42**) and alcohols (**41**), were introduced by mono-substitution of **16** to yield **43** and **44**. The mono-substituted monomer could be purified by column chromatography and then coupled with diethynyl benzene yielding the new oligomers **36p** and **38p**. This reaction had significantly lower yields than the original reaction even with only one halogenated site to react with the acetylene. This is most likely due to a change in electrophilicity of the substituted monomer, but monomer purity could also be a factor. When the Sonogashira reaction to introduce propargyl alcohol moieties was done directly on **34p** (in an attempt to make **38p**), the yield was very poor (~8%), although both the mono- and di-substituted oligomers could be isolated from the crude reaction mixture (entry **37p** and **38p**). Even with the drop in yield of the oligomerization reaction, the two-step reaction using the pre-functionalized monomer had a higher yield than one-step reaction trying to disubstitute the oligomer.

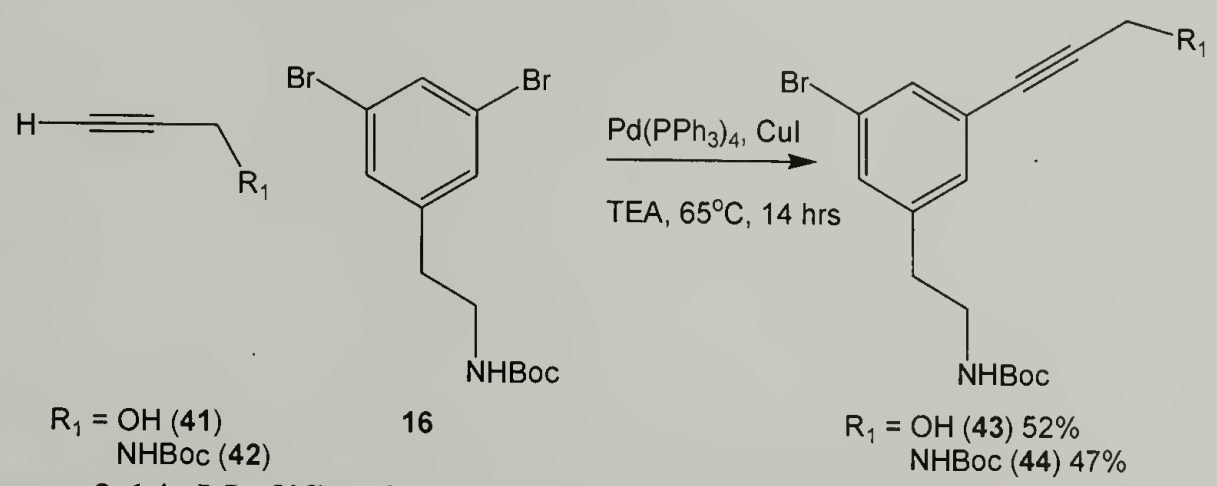

Figure 2.14: Modification through the bromine end group with alkynes.

Recently, Buchwald and coworkers published a series of papers on the substitution of arylbromides with amines.(46-48) Entry **39p** in Table 2.2 utilizes the chemistry shown in Figure 2.15, to introduce P end groups onto the oligomers. In this case, ethylene diamine, with one amine protected, was reacted with **16** using copper (I)

iodide as the catalyst, potassium phosphate as the base, and N,N-Diethyl-2-hydroxy-benzamide as the ligand in anhydrous DMF at 90°C overnight to yield **45**. This reaction is not exceedingly air sensitive but it is moisture sensitive so care was taken to make sure the reaction was anhydrous and kept under a nitrogen atmosphere at all times. The yield of this reaction was greater than 50%, similar to yields reported in the literature.

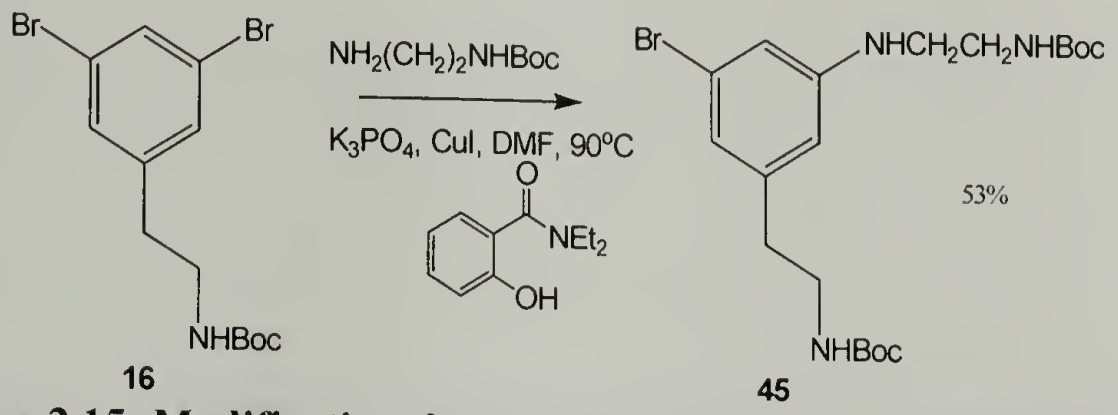

Figure 2.15: Modification through the bromine end groups with amines.

The last entry, **40p**, in Table 2.2 is similar to **34p**, however there are no halogen end groups. This molecule has a similar synthetic scheme to that of the C0 monomer, **16**, Figure 2.8, but the starting material is 3-bromobenzoic acid rather than 3,5-dibromobenzoic acid. The reactions have the same general work up and yields; however the R_f of the products via Thin Layer Chromatography (TLC) did change significantly from the dibrominated versions and the products were all viscous oils rather than solid. The overall yield of the five step reaction scheme was 52%, similar to that of the dihalogenated monomer; however, coupling of the monomer with diethynyl benzene provided a great synthetic challenge. The recovered yield of that reaction was 8%, unexpectedly low since there was only one possible reaction site on the halogenated monomer. This significant drop in yield is most likely due to impurities within the monomer which change the stoichiometry and increase potential side reactions. By ^1H

NMR and GC-MS, the purity was >95% but this does not account for impurities that are either inorganic or non-volatile. All the products within this synthetic scheme are viscous oils which often cause purification to be more challenging. The low yield was not a problem since the goal was to make a few milligrams, enough for characterization and bacterial studies.

Table 2.3: SAR study on discrete oligomers varying amine groups

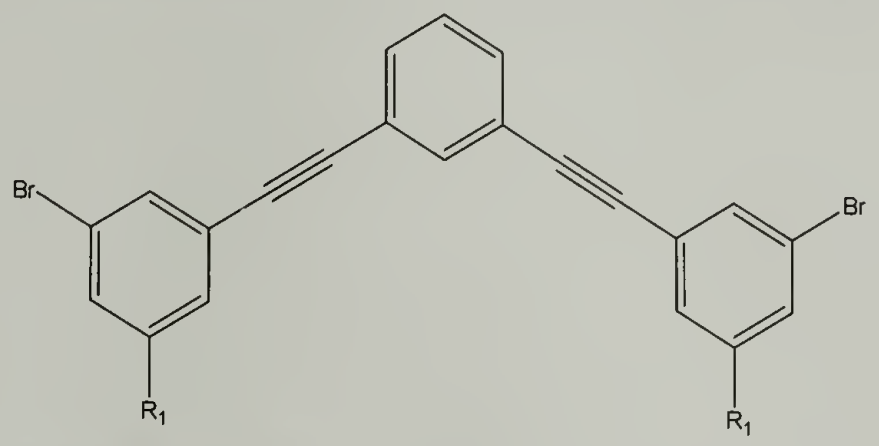

Number	R_1
46p	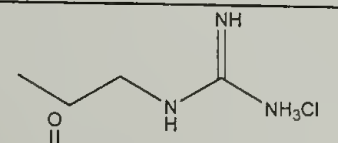
47p	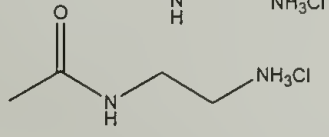
48p	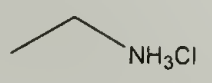
49p	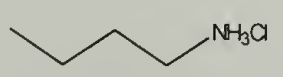

The amine side chain of the oligomer also provides a good handle for modification. Table 2.3 shows the variations of the side chains while keeping the P nature. The original C0 oligomer, **34p**, has an primary ethyl amine P group which can react with 1,3-Bis(*tert*-butoxycarbonyl)-2-methyl-2-thiopseudourea and mercury (II) chloride in dimethylsulfoxide to introduce a guanidine group, entry **46p**, increasing the

hydrophilicity of the resulting structure. This reaction, shown in Figure 2.16, is quantitative and requires little purification during the work-up.

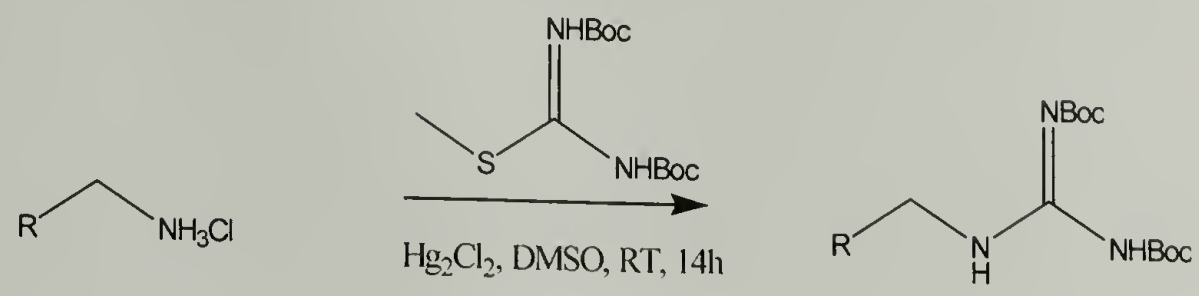

Figure 2.16: General scheme for modification of amine with guanidine groups.

Another modification at the amine side chain is the introduction of an amide bond, entry **47p**. This amide bond is introduced by coupling 3,5-dibromobenzoic acid, **11**, and (2-Amino-ethyl)-carbamic acid tert-butyl ester with EDC and HOBt to form **52**, as shown in Figure 2.17. This coupling yields 63% product and the by-products of EDC and HOBt are water soluble and easily removed by extraction. This is an advantage over other coupling reactants such as DCC that require extensive precipitation and crystallization for quantitative removal. This monomer was reacted with diethynyl benzene to form **47p** in 47% recovered yield. Presumably the yield is higher than **34p** due to the difference in electrophilicity of the ring with the addition of an ester group. Since the ester group is electron withdrawing, the insertion of the palladium between the halogen and the ring is more favorable, furthering the extent of reaction.

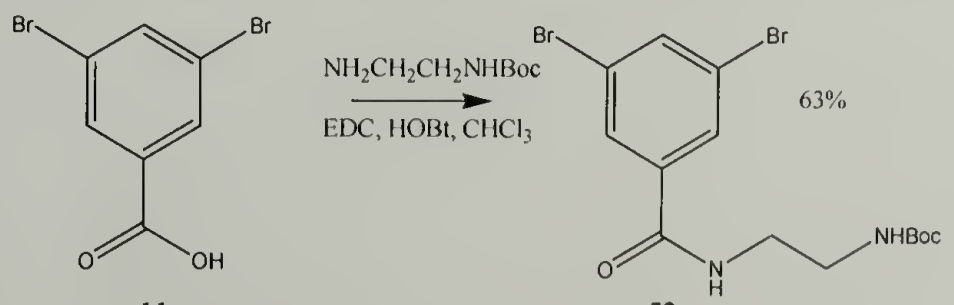

11 52

Figure 2.17: Amidation reaction.

The last two modifications in Table 2.3, **48p** and **49p**, show changes to the carbon chain between the aromatic backbone and the amine P group. The changes in length of the amine side chain provide a set of molecules that have only slight differences in structure while keeping the same net charge. Figure 2.18 and 2.19 shows the monomer synthesis for entries **48p** and **49p**, respectively.[1] In both schemes, the starting material was 3,5-dibromobenzoic acid, **11**, which can be reduced using lithium aluminum hydride. For **54**, the benzyl alcohol, **12**, was reacted with sodium azide and triphenyl phosphine in DMF at 90°C to produce **47** which was then protected with the Boc group resulting in the dihalogenated monomer **54**. For **55**, the bromide of **13** was displaced with an acetonitrile anion using N-butyl lithium. The nitrile was reduced with borane and protected with the Boc group in the same way as **54** to yield **57**.

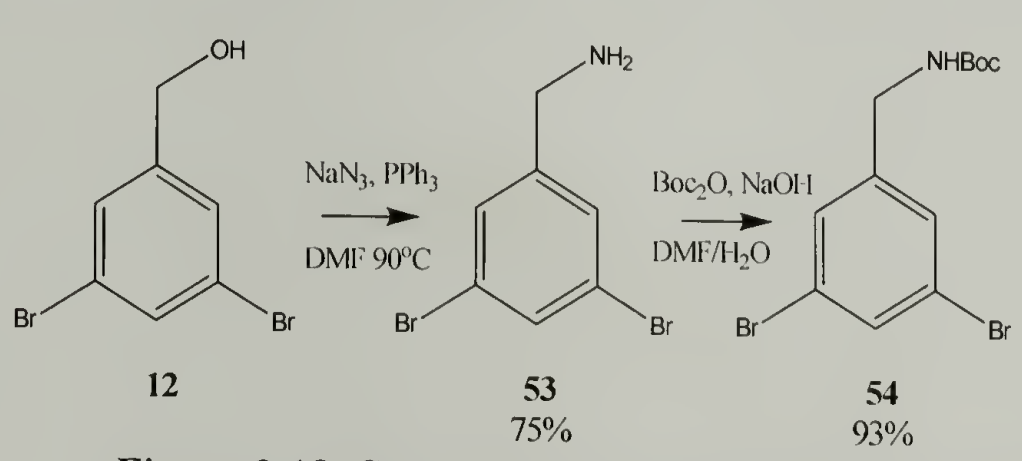

Figure 2.18: Synthesis of methyl amine monomer.

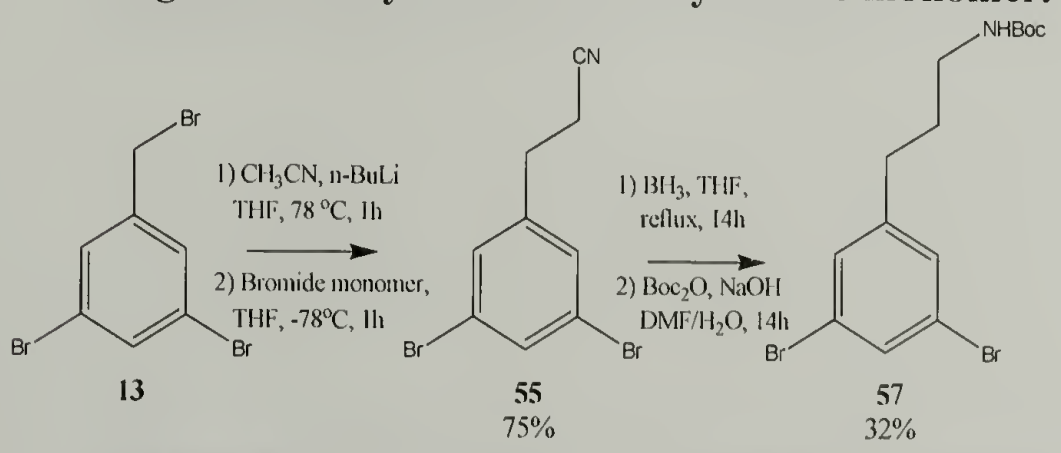

Figure 2.19: Synthesis of propyl amine monomer.

[1] When purifying **49p**, it was possible to separate longer oligomers **50p** and **51p** which had 5 and 7 aromatic rings, respectively.

The presence or absence of alkoxy side chains also acts as a handle for synthetic modification. Table 2.4 shows the modifications done with the alkoxy side chain. Entry **35p** shows the first oligomer made with an alkoxy side chain. This molecule utilizes monomer **8** made in Figure 2.5. The same schematic can be followed using methanol in the first step to produce a methoxy side chain, as shown in entry **58p** of Table 2.4. The last entry, **59p**, shows the modification of **8** with a guanidine group using the same reaction as in Figure 2.16.

Table 2.4: SAR study on discrete oligomers with alkoxy side chains.

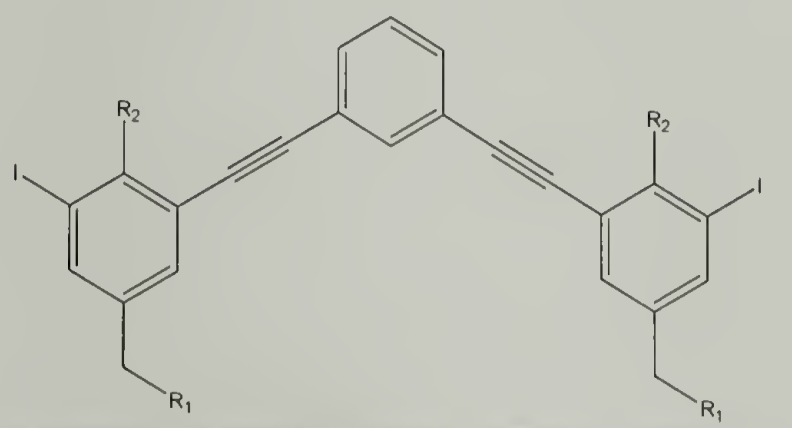

Number	R_1	R_2
35p	NHBoc	OC_5H_{11}
58p	NHBoc	OCH_3
59p	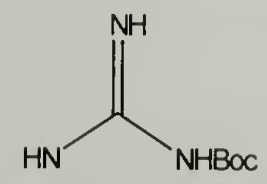	OC_5H_{11}

2.5 Conclusions

A series of *meta*-PE molecules ranging from discrete oligomers to polymers have been successfully synthesized. The use of Sonogashira conditions proved to be very versatile in the synthesis of monomers as well as oligomers and polymers. Flash column chromatography was utilized extensively to purify products ranging from small

molecules with one aromatic ring up to discrete oligomers with seven aromatic rings in the *meta*-PE backbone. Fifteen different discrete oligomers were synthesized to investigate the structure-activity relationship in regards to the biological activity of these compounds. The molecules discussed here are the first reported in the literature that have free amine side chains on phenylene ethynylene backbones.(4, 44, 49, 50) This was accomplished by deprotection of the Boc group from these molecules with 4M HCl, which did not affect the backbone structure as evidenced by fluorescence and NMR. The majority of these molecules have both P and NP side chains on the backbone which will aid the formation of FA structures under specific conditions. These structures are further characterized for the FA structure and biological activity in the following chapters.

2.6 References

1. Hittinger, E., Kokil, A. & Weder, C. (2004) *Macromolecular Rapid Communications* **25,** 710-715.
2. Nielsen, M., Thomsen, A. H., Clo, E., Kirpekar, F. & Gothelf, K. V. (2004) *Journal of Organic Chemistry* **69,** 2240-2250.
3. Lu, S. L., Yang, M. J., Luo, J. & Cao, Y. (2004) *Synthetic Metals* **140,** 199-202.
4. Arnt, L. & Tew, G. N. (2004) *Macromolecules* **37,** 1283-1288.
5. Stone, M. T. & Moore, J. S. (2004) *Organic Letters* **6,** 469-472.
6. Wosnick, J. H. & Swager, T. M. (2003) *Abstracts of Papers of the American Chemical Society* **226,** U171-U171.
7. Breitenkamp, R. B. & Tew, G. N. (2004) *Macromolecules* **37,** 1163-1165.
8. Percec, S., Getty, R., Marshall, W., Skidd, G. & French, R. (2004) *Journal of Polymer Science Part a-Polymer Chemistry* **42,** 541-550.
9. Wang, L. & Li, P. H. (2003) *Chinese Journal of Chemistry* **21,** 474-476.
10. Sanford, A. R. & Gong, B. (2003) *Current Organic Chemistry* **7,** 1649-1659.
11. Jones, T. V., Blatchly, R. A. & Tew, G. N. (2003) *Organic Letters* **5,** 3297-3299.
12. Pinto, M. R., Kristal, B. M. & Schanze, K. S. (2003) *Langmuir* **19,** 6523-6533.
13. Zhao, D. H. & Moore, J. S. (2003) *Macromolecules* **36,** 2712-2720.
14. Kim, I. B., Erdogan, B., Wilson, J. N. & Bunz, U. H. F. (2004) *Chemistry-a European Journal* **10,** 6247-6254.
15. Zheng, J. & Swager, T. M. (2004) *Chemical Communications*, 2798-2799.
16. Wosnick, J. H. & Swager, T. M. (2004) *Chemical Communications*, 2744-2745.
17. Xue, C. H. & Luo, F. T. (2004) *Tetrahedron* **60,** 6285-6294.
18. Wilson, J. N., Josowicz, M., Wang, Y. Q. & Bunz, U. H. F. (2003) *Chemical Communications*, 2962-2963.
19. Kuroda, K. & Swager, T. M. (2003) *Macromolecular Symposia* **201,** 127-134.
20. Breen, C. A., Deng, T., Breiner, T., Thomas, E. L. & Swager, T. M. (2003) *Journal of the American Chemical Society* **125,** 9942-9943.
21. Kim, J. & Swager, T. M. (2001) *Nature* **411,** 1030-1034.
22. Brizius, G., Pschirer, N. G., Steffen, W., Stitzer, K., zur Loye, H. C. & Bunz, U. H. F. (2000) *Journal of the American Chemical Society* **122,** 12435-12440.
23. Hwang, J. J. & Tour, J. M. (2002) *Tetrahedron* **58,** 10387-10405.
24. Schiedel, M. S., Briehn, C. A. & Bauerle, P. (2002) *Journal of Organometallic Chemistry* **653,** 200-208.
25. Nelson, J. C., Saven, J. G., Moore, J. S. & Wolynes, P. G. (1997) *Science* **277,** 1793-1796.
26. Prince, R. B., Saven, J. G., Wolynes, P. G. & Moore, J. S. (1999) *J. Am. Chem. Soc.* **121,** 3114-3121.
27. Tan, C. Y., Pinto, M. R., Kose, M. E., Ghiviriga, I. & Schanze, K. S. (2004) *Advanced Materials* **16,** 1208.
28. Hill, D. J. & Moore, J. S. (2002) *Proc. Natl. Acad. Sci. U.S.A.* **99,** 5053-5057.
29. Ho, S. W., Kwei, T. K., Vyprachticky, D. & Okamoto, Y. (2003) *Macromolecules* **36,** 6894-6897.

30. DiCesare, N., Pinto, M. R., Schanze, K. S. & Lakowicz, J. R. (2002) *Langmuir* **18,** 7785-7787.
31. Pinto, M. R. & Schanze, K. S. (2002) *Synthesis-Stuttgart*, 1293-1309.
32. Cai, L. T., Skulason, H., Kushmerick, J. G., Pollack, S. K., Naciri, J., Shashidhar, R., Allara, D. L., Mallouk, T. E. & Mayer, T. S. (2004) *Journal of Physical Chemistry B* **108,** 2827-2832.
33. Taylor, P. N., Hagan, A. J. & Anderson, H. L. (2003) *Organic & Biomolecular Chemistry* **1,** 3851-3856.
34. Huang, H. M., Wang, K. M., Xiao, Y., Zhai, Q. G., An, D. L., Huang, S. S. & Li, D. (2003) *Chinese Science Bulletin* **48,** 1947-1951.
35. Dholakia, G. R., Fan, W., Koehne, J., Han, J. & Meyyappan, M. (2003) *Journal of Nanoscience and Nanotechnology* **3,** 231-234.
36. Bumm, L. A., Arnold, J. J., Cygan, M. T., Dunbar, T. D., Burgin, T. P., Jones, L., Allara, D. L., Tour, J. M. & Weiss, P. S. (1996) *Science* **271,** 1705-1707.
37. Arnt, L., Breitenkamp, R. B. & Tew, G. N. (2005) *Polymers for Advanced Technologies*, accepted.
38. Shotwell, S., Windscheif, P. M., Smith, M. D. & Bunz, U. H. F. (2004) *Organic Letters* **6,** 4151-4154.
39. Lahiri, S., Thompson, J. L. & Moore, J. S. (2000) *J. Am. Chem. Soc.* **122,** 11315-11319.
40. Moore, J. S. (1997) *Acc. Chem. Res.* **30,** 402-413.
41. Prince, R. B., Barnes, S. A. & Moore, J. S. (2000) *J. Am. Chem. Soc.* **122,** 2758-2762.
42. Arias-Martin, E., Arnault, J. C., Guillon, D., Mailou, T., Le Moigne, J., Geffroy, B. & Nunzi, J. M. (2000) *Langmuir* **16,** 4309-4318.
43. Arias, E., Maillou, T., Moggio, I., Guillon, D., Le Moigne, J. & Geffroy, B. (2002) *Synthetic Metals* **127,** 229-231.
44. Arnt, L. & Tew, G. N. (2002) *J. Am. Chem. Soc.* **124,** 7664-7665.
45. Kim, G., Hong, H. W. & Lee, S. H. (1999) *Bull. Korean Chem. Soc.* **20,** 321-324.
46. Klapars, A., Huang, X. & Buchwald, S. L. (2002) *J. Am. Chem. Soc.* **124,** 7421-7428.
47. Kwong, F. Y. & Buchwald, S. L. (2003) *Organic Letters* **5,** 793-796.
48. Kwong, F. Y., Klapars, A. & Buchwald, S. L. (2002) *Organic Letters* **4,** 581-584.
49. Arnt, L. & Tew, G. N. (2003) *Langmuir* **19,** 2404-2408.
50. Arnt, L., Nusslein, K. & Tew, G. N. (2004) *J. Polym. Sci. Part A* **42,** 3860-3864.

CHAPTER 3

THE FACIAL AMPHIPHILICITY AND AGGREGATION OF *META*-POLY(PHENYLENE ETHYNYLENE)S

3.1 Introduction

It is well known that many biopolymers, such as proteins and RNA, adopt specific structures in solution.(1, 2) In proteins, segregation of hydrophobic and hydrophilic domains is routinely used to direct tertiary structure formation or perform other functions like membrane-activity.(3) One example is amphiphilic β-sheets which are formed by patterning polar (P) and non-polar (NP) amino acids with a repeat of two so that the P and NP groups segregate onto opposite faces of the extended structure. This forms amphiphilic two-dimensional planes, where the individual strands of the sheet are held together by multiple hydrogen bonds. In addition, the majority of the P amino acid groups are charged, giving these structures the potential to exhibit polyelectrolyte-like behavior. Transferring these facially amphiphilic (FA) structures into polymeric backbones result in attractive molecules that assume discrete conformations. They are remarkably different than random or block amphiphilic polymers which typically adopt random coil configurations in solution.

The study of synthetic facially amphiphilic polymers include rigid rod polymers based on thiophene, phenylene, and *para*-phenylene ethynylene, as shown in Figure 3.1. Polythiophenes were prepared with perfectly alternating hydrophobic and hydrophilic side groups and investigated using Langmuir and scattering techniques.(4, 5) X-ray

diffraction of the films showed peaks corresponding to π-stacking of molecules and disordered alkyl chains above the water surface.(4) Diffraction studies of the film at different surface pressures showed that even in the uncompressed state (zero pressure) a π-π stacking distance of ~3.9 Å between chains was present, which upon compression to 35 mN/m decreased only to ~3.85 Å. This observation suggests pre-association or self-assembly of the system before compression which would be expected from rigid rod molecules.

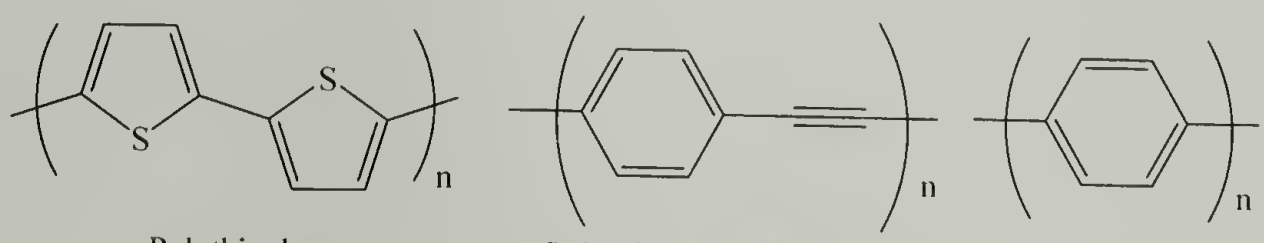

Polythiophene Poly(phenylene ethynylene) Polyphenylene

Figure 3.1: Examples of extended polymeric backbones.

Poly(*p*-phenylenes) have recently been reported with P or NP groups attached as pendant generation 2 or 3 dendrons.(6) By controlling the architecture of the side chains, stable monolayers were observed with hydrophilic dendrons and hydrophobic linear chains, but not in the opposite case when hydrophobic dendrons and hydrophilic linear chains were studied.(6, 7) Presumably, in the latter case, the size difference between the hydrophobic dendrons and the hydrophilic linear chains caused the molecules to be asymmetric and "top-heavy," resulting in an unstable monolayer.

Swager and co-workers studied the effect different substituents had on the orientation of the backbone aromatic rings to the air-water interface for a series of poly(*para*-phenylene ethynylenes).(8, 9) Examples of the molecules studied are shown in Figure 3.2 with the P side chains shown in blue and the NP shown in green. Most of these polymers are not FA but this study provided very unique insight on the interplay

between chain conformation, stacking area occupied for each conformation, and optical properties. Langmuir films were investigated by UV-Vis and fluorescence at a variety of surface pressures to determine whether both aromatic rings were parallel (face-on, Figure 3.3a), perpendicular (edge-on, Figure 3.3b), or one parallel and the other perpendicular (zipper structure, Figure 3.3c) to the interface.

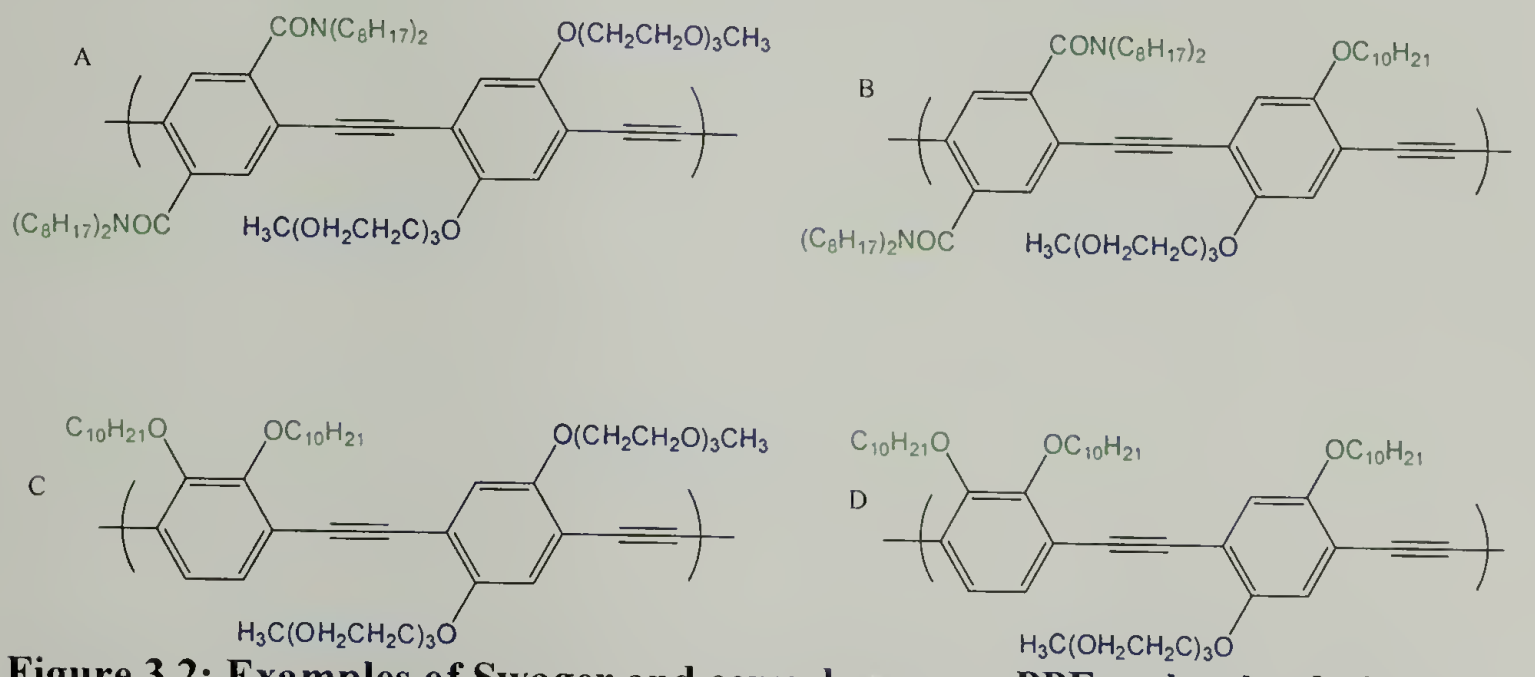

Figure 3.2: Examples of Swager and coworkers para-PPE molecules designed to have varying structures at the air-water interface (P groups blue, NP green).

By changing the chemistry of the attached side chains, the orientation of the aromatic rings relative to the air-water interface was controlled and correlations to UV-Vis and fluorescence spectra were made. For instance, molecule A in Figure 3.2 prefers to obtain a face-on orientation to the air-water interface while molecule D prefers an edge-on structure due to the locations of the hydrophobic and hydrophilic substituents. The other two structures in Figure 3.2, B and C, are more complicated. Due to the varying side chains, the conformation at the air-water interface is dictated by the surface pressure of the system. Under low surface pressures, B will assume a face-on structure like that shown in Figure 3.3a, but as the pressure increases, the second ring will take on an edge-on structure making the overall polymer assume a zipper structure. Molecule C

starts out in a zipper structure with the second ring in a face-on configuration, but as the pressure increases, the polymer is forced to an edge-on structure like that shown in Figure 3.3b. As these changes in conformation occur, there is a change in slope of the surface pressure-area isotherm.

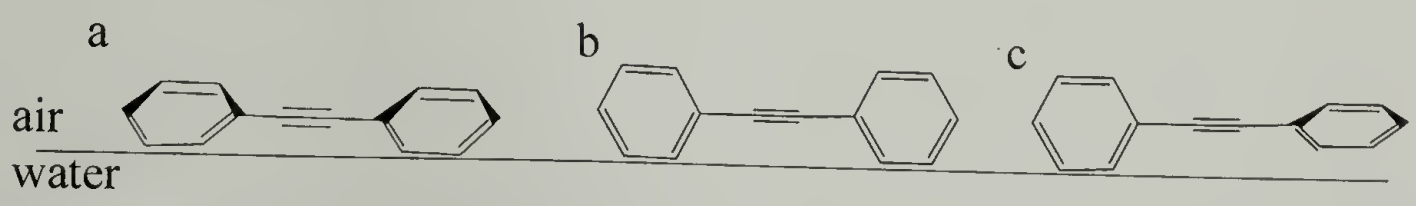

Figure 3.3: Different conformations assumed by facially amphiphilic PE polymers at the air-water interface a) face-on, b) edge-on, and c) zipper.

The experiments described above were all performed at the air-water interface but molecules with phenylene ethynylene (PE) backbones have also been studied in solution and the solid state. Figure 3.4 shows *meta*-PE discrete oligomers with ester side chains that Moore and coworkers have synthesized. When changing the solvent to one with a higher dielectric constant, these molecules show cooperative transitions between the extended and helical structure.(10) This change was monitored by measuring the intensities of the UV absorption maxima at 290 and 303 nm as well as NMR titrations changing from chloroform to acetonitrile. The ultimate result was that the molecular conformation was mostly helical in acetonitrile. When the same molecules are studied in the solid state, an extended structure with lamellar packing is favorable.(11) The lamellar packing in the solid state was determined from annealed samples in glass capillaries using small- and wide-angle X-ray diffraction studies. Increasing the oligomer chain length caused an increase in the spacing, verifying the lamellar structure rather than helical packing of the chains. With the addition of a methyl group in the *para* position to the ester substituent, the helical structure can be

stabilized in the solid state since there is a reduction in free volume of the helix interior.(12)

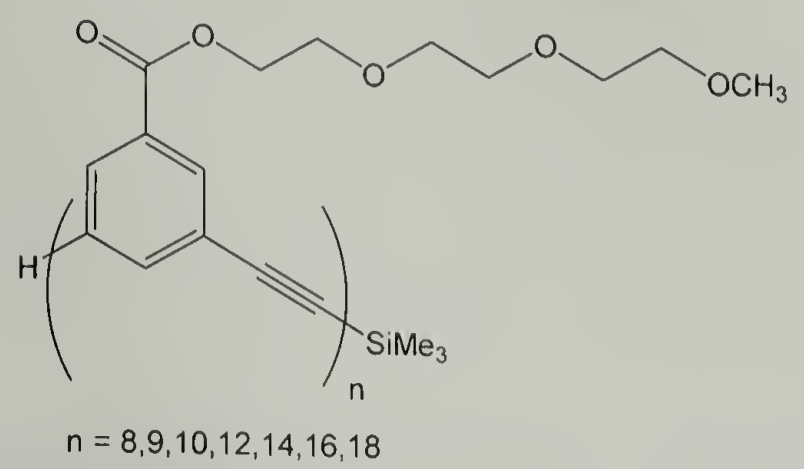

n = 8,9,10,12,14,16,18

Figure 3.4: *meta*-PE molecules made by Moore and coworkers for solvophobic helical structure studies.

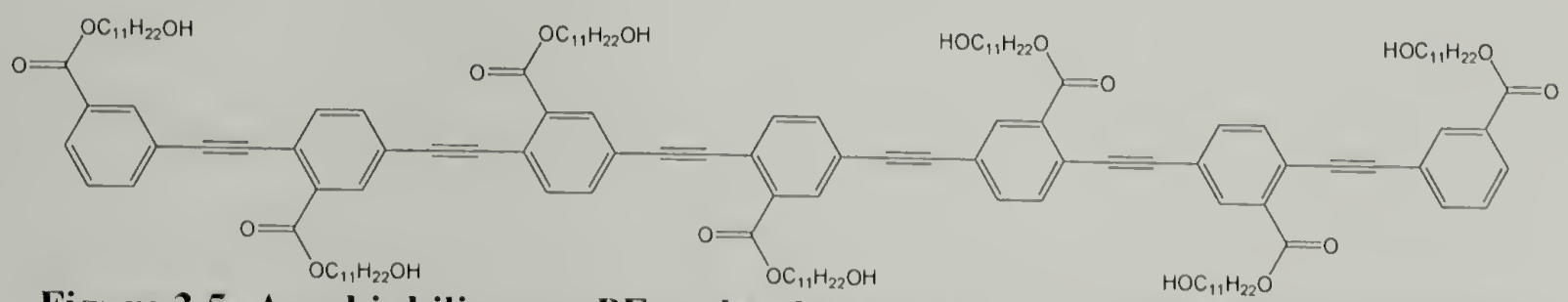

Figure 3.5: Amphiphilic *para*-PE molecules studied for blue-green light emitting diodes.

The moleeules studied by Moore and eoworkers are not FA, and the study of FA PE moleeules in the literature is mueh more limited.(13, 14) Amphiphilie *para*-PE diserete oligomers with hydrophilie alkyl hydroxyl ester side ehains were synthesized in a step-by-step method up to the heptamer, shown in Figure 3.5. The hydroxyl ester side ehain was chosen to ensure solubility and amphiphilie eharaeter of the moleeules. These moleeules were studied in the powder form as well as deposition of a Langmuir film onto a substrate. At low temperatures, powder X-ray diffraetion shows two sharp refleetions in the ratio of 1:2 eorresponding to a lamellar arrangement with a d-spaeing of 3.87 nm. As the temperature inereases, the peaks deerease in intensity and above 110°C the peaks are essentially non-existent. These moleeules also show lamellar

structures from deposition of Langmuir films onto surfaces. These well-defined structures were investigated as blue-green light emission devices due to the conjugation and molecular organization of the oligomers. While these molecules are FA, they are discrete compounds with a *para*-PE backbone. The molecules discussed throughout the rest of the chapter are polymeric and have *meta*-PE backbones.

3.2 Langmuir Studies

The ability of the polymers discussed in Chapter 2 to adopt FA conformations was studied at the air-water interface using a Langmuir trough.(15, 16) This technique entails spreading a dilute solution between a set of barriers at the air-water interface. After the molecules equilibrate on the water surface, the barriers are slowly compressed at a rate of 0.1648 cm/min until maximum compression. The surface pressure measurements were obtained by using a Wilhelmy plate attached to a Cahn

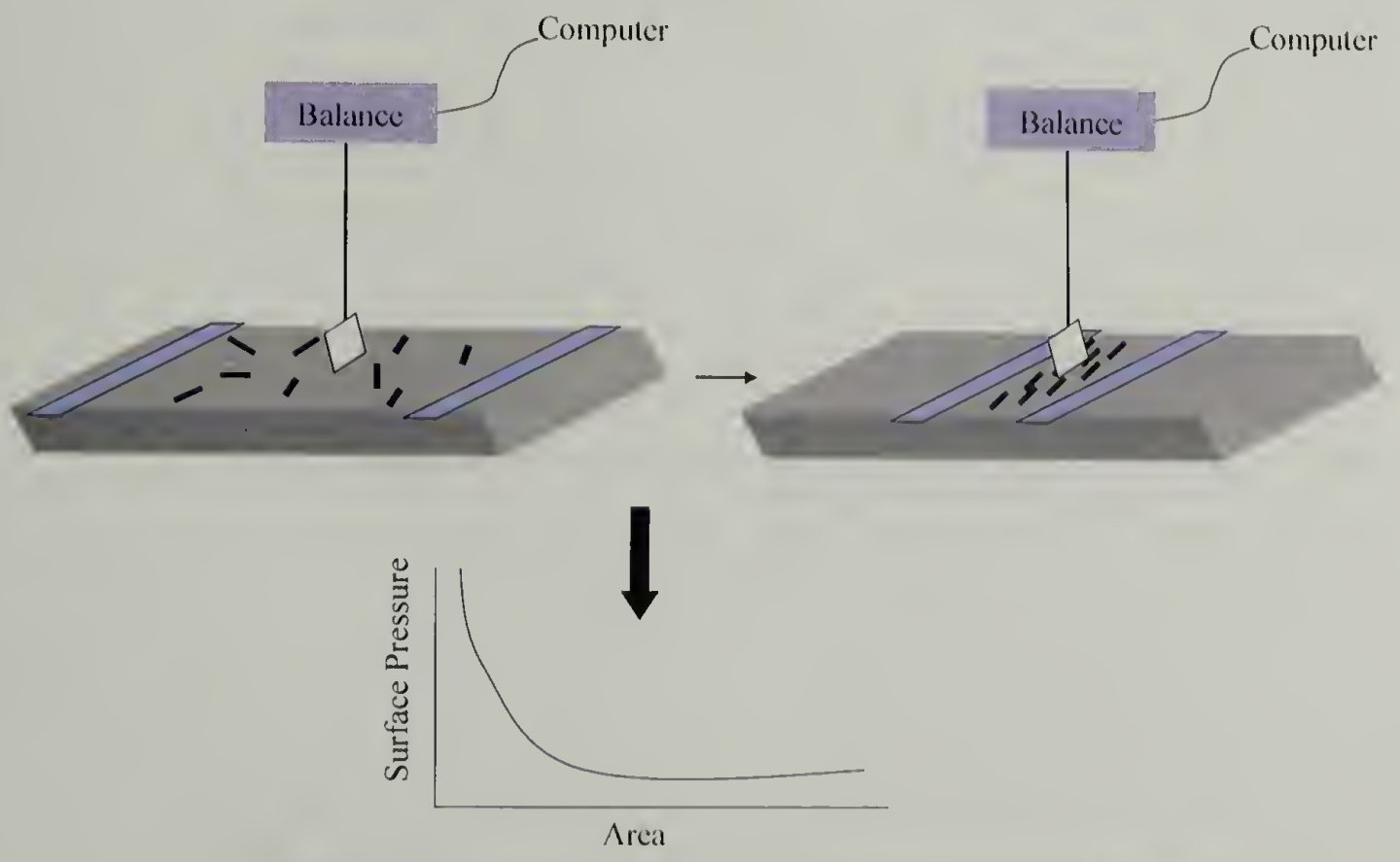

Figure 3.6: Schematic of Langmuir experiment set-up.

electrobalance. As the barriers compress reducing the available area per molecule, the molecules begin interacting with one another and the surface pressure increases. By obtaining the surface pressure-area isotherm, the steepest part of the curve can be extrapolated to zero surface pressure giving the area occupied per molecule, or in this case, the area per repeat unit of the polymer. The experimental set-up is shown schematically in Figure 3.6.

Table 3.1: Polymers used in the Langmuir study.

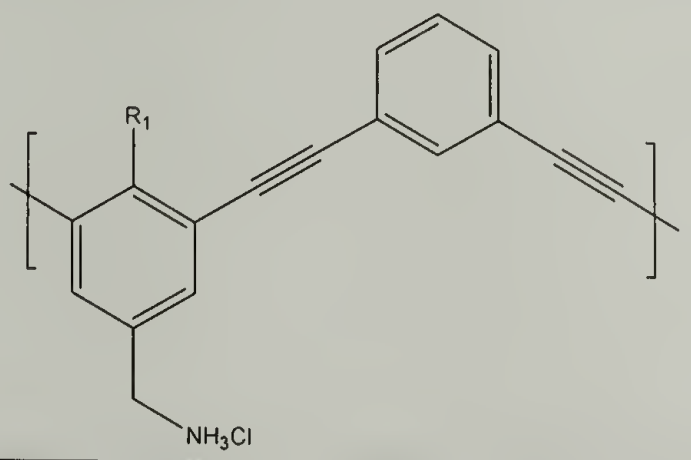

Number	R_1	M_n ($x10^3$) (g/mol)	PDI
60d	OC_5H_{11}	17.8	2.3
61d	OC_8H_{17}	7.73	1.3
62d	$OC_{12}H_{25}$	10.1	1.4

The polymers studied are listed in Table 3.1. While the polymers vary in molecular weight, the polymer length does not affect the results since the calculations take into account the number of repeats per polymer chain.[2] These three polymers were chosen to investigate the conformation at the air-water interface as well as the effect of alkoxy side chain length. As shown in Figure 3.3, there are three possible structures for these polymers at the air-water interface; edge-on, face-on, and zipper structure. Two of

the polymer eonformations, edge-on and zipper, are more probable than the faee-on strueture sinee there is no driving foree for the unsubstituted ring to lay parallel on the water surfaee. Figure 3.7 shows the pentoxy-substituted polymer in the other two possible eonformations at the air-water interfaee.

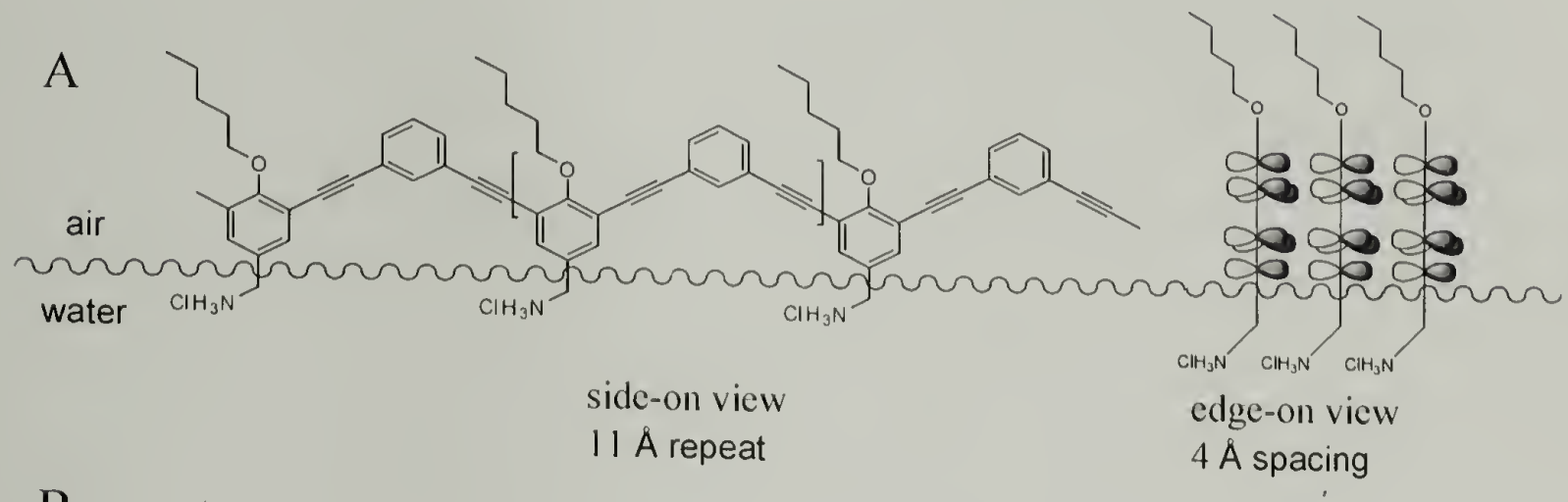

Figure 3.7: Conformation of *meta*-PE molecules as an a) edge on structure and b)zipper structure.

The pressure-area isotherms for these three moleeules are shown in Figure 3.8. Extrapolation of the steepest part of the eurve to zero pressure yields the area per repeat unit of 41, 42, and 45 Å^2 for polymer **60d**, **61d**, and **62d**, respeetively. At a surfaee pressure of 38 mN/m, the slope of **60d** ehanges sharply suggesting eollapse of the monolayer into multilayers.(8, 17) Films of polymers **61d** and **62d** do not eollapse at pressures up to ~48 mN/m whieh likely results from the inereased length of the alkyl side ehain.(4, 5, 9) Intuitively, upon paeking, there is more contaet area between

---

[2] These caleulations are further explained in Seetion 6.9.1.

polymer chains as the side chain lengthens, thus, increasing the stability of the monolayer. These areas per repeat unit are comparable to that of **60d**, suggesting all three amphiphilic polymers adopt edge-on structures similar to that presented in Figure 3.7a as opposed to a structure where the rings assume a zipper structure, shown in Figure 3.7b. If the polymers assume a zipper structure at the interface, the areas per repeat units would be much larger, on the order of 100 to 200 Å^2. The slope of all three curves is less steep than observed for many rigid amphiphilic polymers(4-6) but similar to those observed by Swager and co-workers in systems with conformational flexibility.(8, 9)

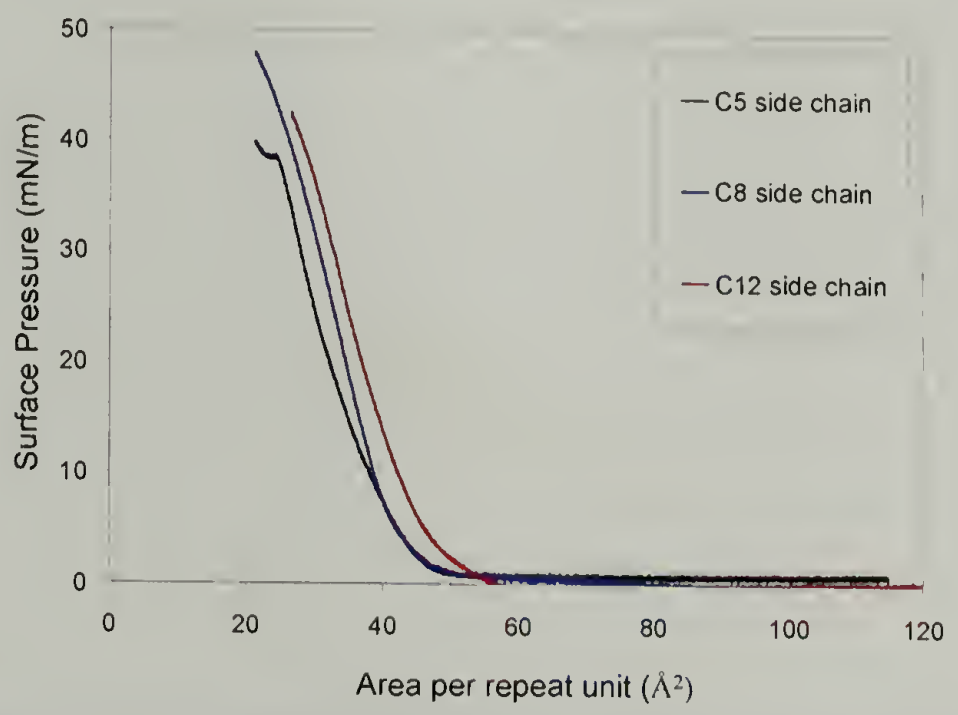

Figure 3.8: Langmuir data for polymers 60d, 61d, and 62d.

Another experiment was performed at the air-water interface to investigate the reversibility and stability of the monolayer of **60d**. The initial set-up of the experiment was similar to that shown in Figure 3.6, only after the initial compression, the barriers were slowly uncompressed to their original state and recompressed a second time. Throughout this experiment, the surface pressure was monitored and the results are

shown in Figure 3.9. At high surface pressures during the first compression, there is a change in slope due to folding of the monolayer into multilayers. As the barriers are relaxed, there is an initial sharp drop in surface pressure slope due to the increase in molecular area. At an area of about 20 $Å^2$, there is a change in slope most likely related to multilayer unfolding as the molecules have sufficient room and experience decreased pressure so they can relax back into a FA structure at the air-water interface. The polymer chains can then return to the initial uncompressed state as the area per repeat unit increases and the barriers fully relax. Upon the second compression, the isotherm follows a very similar path with limited hysteresis. This small amount of hysteresis is most likely due to the polymer chains already being somewhat oriented. There is still a change in slope at very high surface pressures accounting for multilayer formation; however, it is not as pronounced as the first compression. This could be due to the organization of the alkoxy chains above the plane of the rings. During the first compression, the alkyl chains were most likely unordered until full compression after

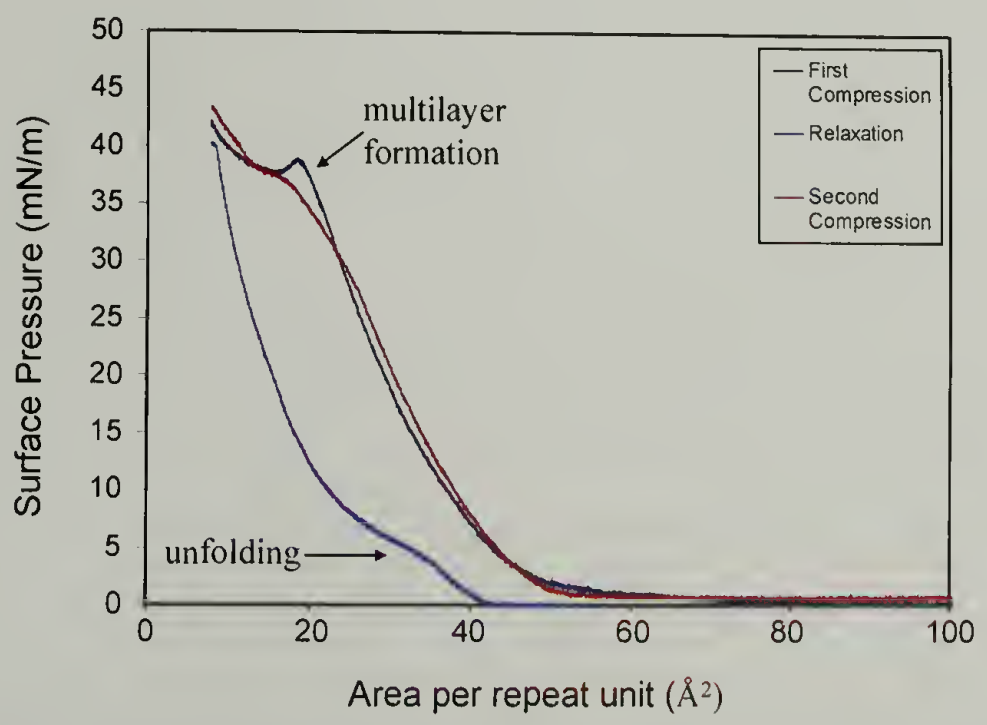

Figure 3.9: Reversible stable monolayer formation of 60d.

whieh they start to eontaet eaeh other and have less room. This forees the side ehains to obtain a more ordered extended eonfiguration whieh was then retained upon relaxation. Thus, during the multilayer formation of the seeond eompression, there probably was redueed entropy loss, whieh resulted in a less dramatie ehange in slope.

Fitting the data to an equation of state ean provide insight into the limiting moleeular area as well as the degree of polymer assoeiation before eompression. Rigid rod polymers, as diseussed in Seetion 3.1, tend to have some pre-assoeiation due to the extended nature of the baekbone and favorable interaetions between polymer chains. Table 3.2 shows the analysis of the polymer monolayers aeeording to the equation $\Pi(A-A_0)= kT/n(DP)$ where Π is the observed surfaee pressure for a given area per repeat unit (A), DP is the average number of repeat units per moleeule, k is Boltzmann's eonstant, and T is the temperature.(18) The data was analyzed between surfaee pressures of 1.4 mN/m and 3.0 mN/m.(18) Linear regression gives A_0, the limiting moleeular area, and n, the degree of association, whieh should be near unity for an ideal gas.

Table 3.2: Equation of state used to determine the limiting molecular area and the degree of association.

structure	DP	A_{exp}	A_o	n	R^2
60d	53.8	41	42	1.01	0.93
61d	27.9	42	42	1.78	0.96
62d	24.2	45	46	1.72	0.95

Two interesting observations are found from the analysis. First, the values of A_o in Table 3.2 show good agreement with those obtained by simple extrapolation of the pressure-area isotherms to zero pressure. Second, the degree of polymer chain aggregation is very small or non-existent before compression which suggests the polymers form a two dimensional gas-like state at high dilution. Typically, a degree of association near unity represents a gaseous state while higher values indicate there is association. Peptides have been shown to have degrees of association near 30.(18) The degree of association for **60d** was determined to be unity, in excellent agreement with a gaseous state, while that of **61d** and **62d** are closer to two. This is consistent with **61d** and **62d** containing larger hydrophobic alkyl chains that make the polymers more hydrophobic, increasing the preassociation. Similarly, the increase in alkyl chain length from pentyl to octyl does affect the maximum stable surface pressure of the film. From Figure 3.8, it is observed that monolayers of **61d** are stable beyond 48 mN/m while monolayers of **60d** collapse at 38 mN/m. In addition, monolayers of **62d**, like those formed by **61d**, are stable above 40 mN/m. Therefore, it appears that a transition in monolayer stability and pre-association occurs in these polymers between an alkyl length of five and eight carbons.

Fitting the second compression data in Figure 3.9 to the equation of state determines the degree of association of the polymer after the first compression and relaxation, during recompression. Using the equation the same way as above, the degree of association is again near unity, 1.05, suggesting little or no polymer association in the uncompressed state. This is surprising since the polymer chains are in contact with each other during the first compression and collapse of the monolayer into

multilayers. Upon relaxation, the multilayer does unfold but one would assume there could still be interaction between individual polymer chains due to the favorable π interactions of the backbone. The lack of polymer association before the first compression is not as surprising since the molecules most likely do not assume a FA structure in the solution used to spread the polymer onto the air-water interface. This result suggests that not only is the monolayer stable, but it is fully reversible allowing the polymer chains to relax into a two dimensional gaseous state at high dilution.

The extrapolated area per repeat unit at zero pressure and A_o for the three polymers is consistent with an edge-on orientation as shown in Figure 3.7a. Both geometric and molecular dynamics calculations were used to verify this proposed structure. The length of the repeat unit in an all-*trans* conformation is between 10.8 and 12.1 Å and the π-π distance between chains was assumed to be 4 Å(19, 20) resulting in an area per repeat between 43 and 48 $Å^2$. Dynamics calculations were performed with Materials Studio on two oligomers of four polymeric repeat units each. In these calculations, the two oligomers were placed in a frame and the energy allowed to minimize. The only constraint put on the system was the planar structure of the molecules. These calculations provided an area of 44.7 $Å^2$ for **60d**, agreeing with the geometric calculations. The geometric and molecular dynamics calculations are consistent with the adoption of the edge-on structure shown in Figure 3.7a. Other orientations with one or both aromatic rings parallel to the interface would produce areas on the order of ~140 and 200 $Å^2$, respectively.(8, 9)

The experimental and calculated data suggests that the aromatic rings have a separation distance of 4 Å at the air-water interface. It is known that *para*-PE molecules

prefer to pack at a slightly off-set angle as opposed to directly on top of each other.(21-23) At the air-water interface, this slip stacked orientation can occur through two different mechanisms. Either the aromatic rings can adopt a slightly non-perpendicular angle with the air-water interface (Figure 3.10a) or by adopting a right angle but sliding one chain along the water surface, with respect to the neighboring chain, into or out of the plane of the page (Figure 3.10b). The latter orientation is most likely since it occupies the smallest area(4, 8) although no direct experimental evidence relating to these details for either orientation has been obtained.

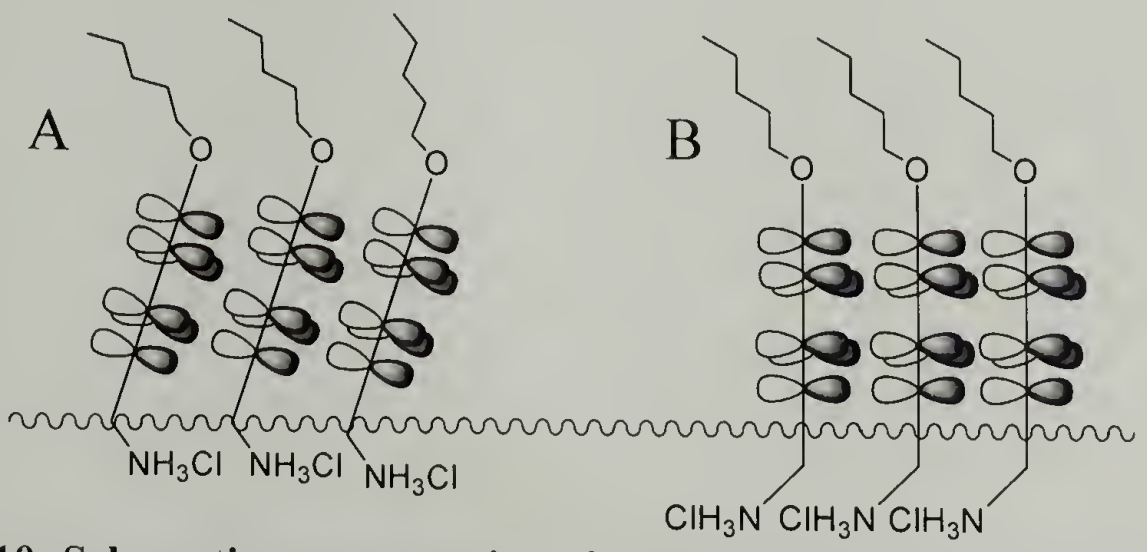

Figure 3.10: Schematic representation of aromatic rings at the air-water interface either a) a non-perpendicular angle or b) slip-stacked.

The structure of this monolayer draws comparison to β-sheet peptides as a result of the patterning of P and NP groups onto opposite faces of the structure to produce amphiphilic plates. Both these polymers and β-sheet peptides have P and NP groups repeating with a pattern of two along the backbone; however, β-sheets are held together by hydrogen bonds oriented parallel to the air-water interface which are replaced in these systems with π-π interactions between adjacent polymer backbones (Figure 3.7). The typical distance between backbones in β-sheets is 4.7 Å(24-26) compared to approximately 4.0 Å for these polymers.

3.3 Emission Studies in Solution

Emission studies were used to monitor the fluorescence of the polymer systems in dilute solution as the solvent was changed. Figure 3.11 shows polymers **60** (Figure

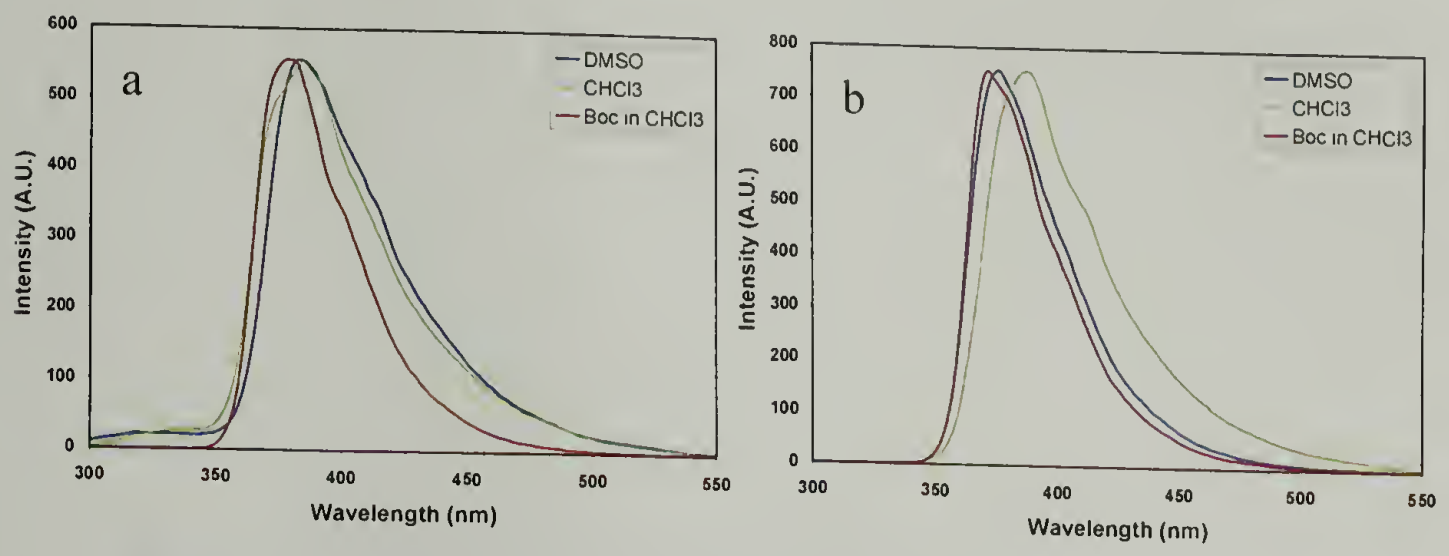

Figure 3.11: Emission studies of a) 60d and b) 61d in varying solvents.

3.11a) and **62** (Figure 3.11b) in different solvents. Both protected polymers (**60p** and **62p**) have somewhat narrow peaks in chloroform (red curves), indicating that this is a good solvent for the system. This is not surprising since the polymer before deprotection is not facially amphiphilic, so an organic solvent can solvate both the backbone and the side chains. Upon deprotection (**60d** and **62d**), the polymers are no longer soluble in neat chloroform, but they are soluble in DMSO. The spectra taken for the polymers in DMSO are shown in green. The peak from **60d** seems to be red shifted with the change in solvent, unlike **62d**, but both are the same shape as that of the protected polymer in chloroform, indicating that the chemical structures of the protected and deprotected polymers are similar and that there are no structural changes upon deprotection of the amine by acid treatment. The spectra for the deprotected polymers in 90% chloroform are shown in blue. For **60d**, the spectrum seems to be a combination

of the protected polymer in chloroform and the deprotected polymer in neat DMSO. The spectra in the same solvent system for **62d**, is also slightly broader than the previous spectra and the peak is shifted by about 10 nm. The broadening and shifting of these peaks highly suggests the presence of multiple conformations as well as some aggregation in the system. This is expected since the chloroform is not particularly a good solvent for the amine side chains but is a good solvent for the alkoxy side chains and the backbone structure. It is preferable for the amine moieties to minimize their interactions with the increasingly poor solvent through aggregation with other polymer chain segments.

After determining the initial fluorescence in the system, studies were done to monitor the association of polymer chains in dilute solution as the percentage of a nonsolvent was increased. Because Figure 3.11 shows that DMSO is a relatively good solvent for the polymer system, the experiment was begun using neat DMSO. The emission spectrum was monitored as the amount of water, a poor solvent for the polymer backbone and alkyl groups, was increased. Figure 3.12 shows the change

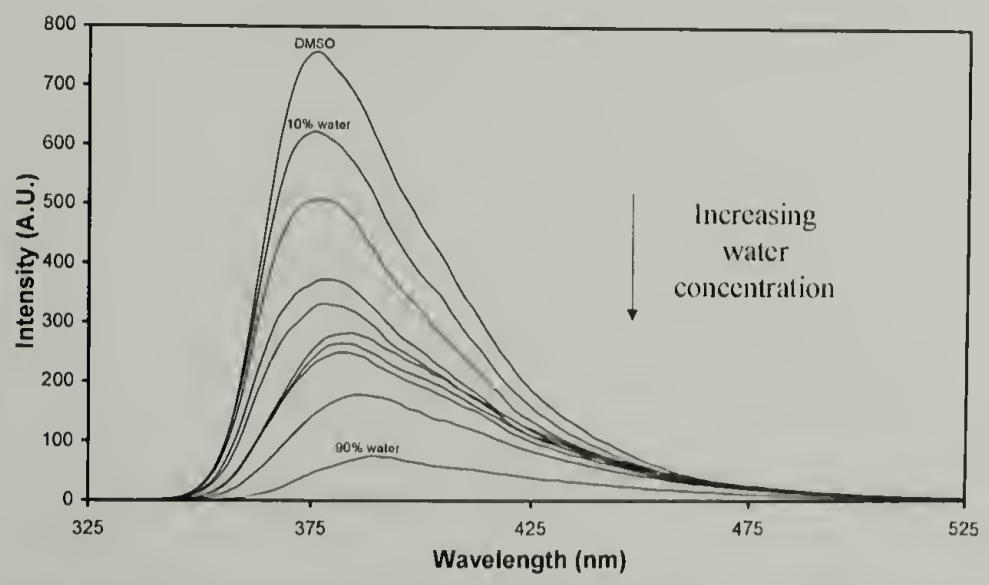

Figure 3.12: Fluorescence of 62d with increasing water concentration.

observed in the emission spectra of **62d** as the percentage of water is increased. The concentration of the sample was kept constant in order to directly observe the effect on quantum yield. It can be seen that the intensity of the emission decreases with increasing water concentration and the band is broadened and red-shifted.

Figure 3.13 shows a comparison between **60d** and **62d** for DMSO, 50% water/DMSO, and 90% water/DMSO, which show the same trends as observed for **60d** as discussed above for **62d**. These observations suggest intermolecular aggregation of polymer chains in an extended conformation as the water content is increased and not the formation of a helix where NP groups fold in the interior while P side chains are solvated.(27) This is supported by the data in Figure 3.11 showing that it is unlikely that the observed changes are related to a change in the dielectric constant since spectra in $CHCl_3$ and DMSO are essentially identical. In addition, calculations for the inner helix dimensions of *meta*-PE molecules support that the dodecoxy side chains will definitely not fit into the center of the helix, particularly since three side chains would be present in each turn of the helix. The pentoxy side chains might be able to fit in the center of the helix, however is very improbable. Since the emission data for both **60d**

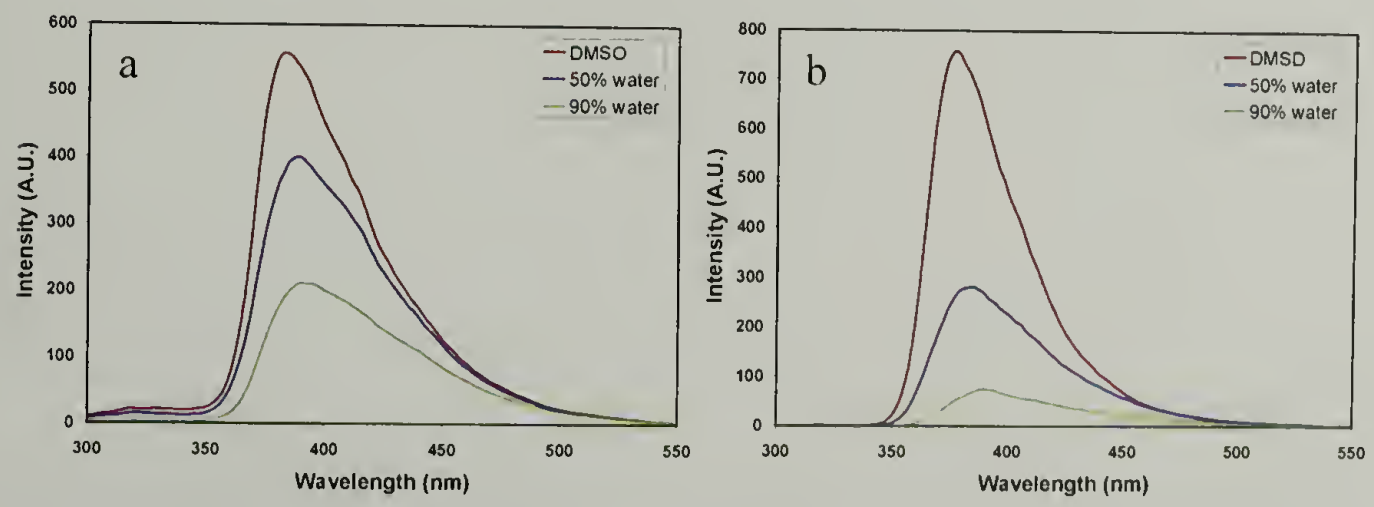

Figure 3.13: Comparison of fluorescence in varying solvents for a) 60d and b) 62d.

and **62d** are very similar, these two polymers are most likely adopting similar structures. Therefore, it is concluded that supramolecular aggregation of the polymer chains occurs as the solvent is changed from DMSO to water.

3.4 Turbidity Studies

After observing aggregation in solution using fluorescence, the aggregates were studied for size. Light scattering lead to multiple problems since the aggregates were constantly changing with time and the overall molecular weights of the polymers were relatively small to study this way. However, the onset of aggregation could be studied by taking scattering measurements with a UV-Vis spectrometer at 500 nm (OD_{500}). These optical densities could then be converted to percent transmittance and plotted versus concentration. Since there is no absorbance of the polymer or solvent system,

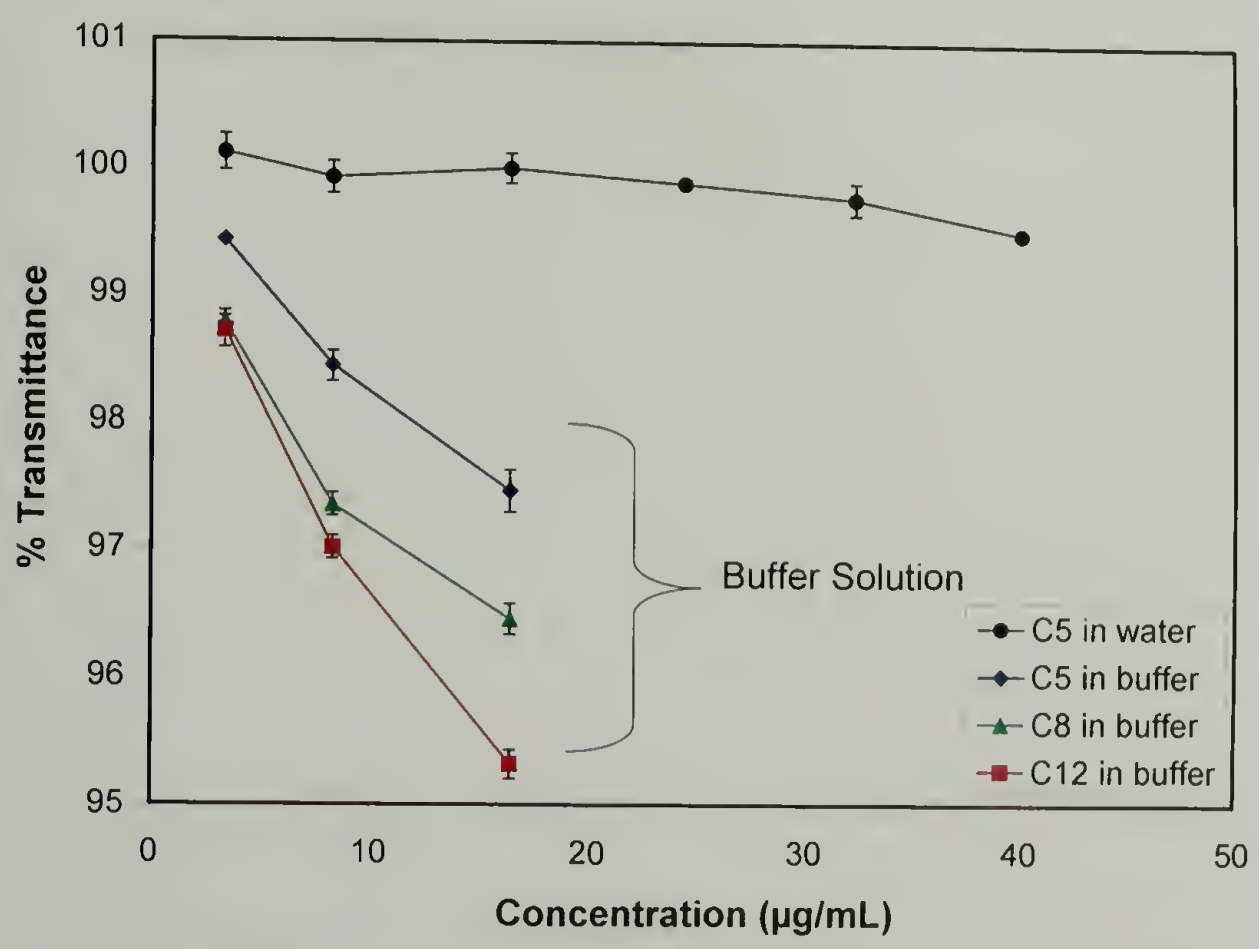

Figure 3.14: Solution turbidity of polymers at varying concentrations.

this technique only looks at the scattering from the polymer in solution. In this experiment, the polymer was first dissolved in DMSO and added to the aqueous solutions so the final concentration of DMSO was <5%. The resulting solutions were allowed to equilibrate until the optical density was steady and data was taken until three consecutive readings had deviations in the absorbance of less than 0.001.

Figure 3.14 compares not only the effect of alkyl chain length but also the effect of a buffered salt solution, similar to the media used in antibacterial experiments. Scattering was not observed in water until the onset of aggregation at 40 μg/mL for **60d**, while in buffer there is visual precipitation at 16 μg/mL. This is expected since buffered solutions have high salt concentrations, which is known to have an effect on the solubility of organic compounds. Similar trends were seen for the **61d** and **62d** polymers (not shown). As the alkyl length of the side chain is increased, the turbidity of the solution is amplified from a transmittance of 97.5% for **60d** to 95.3% for **62d** at concentrations of 16 μg/mL. This suggests that lengthening the alkyl chain enhances the hydrophobicity of the polymer, causing a decrease in the solubility and an increase in the turbidity of the solution. This concept of turbidity is important particularly for understanding the behavior of the polymers in the buffered solutions used to study the antimicrobial activity of the compounds discussed in Chapter 4.

3.5 Conclusions

Cationic *meta*-PE polymers were characterized at the air-water interface using a Langmuir trough and the results show it is possible to design cationic, facially amphiphilic polymers by appropriately decorating the backbone with P and NP groups.

This further suggests that there is no need to design a backbone structure with conformational control to create molecules that assume facially amphiphilic structures at the air-water interface. The organization at the interface draws direct comparison with β-sheet peptides due to the patterning of P and NP groups with a repeat of two and π-π stacking between polymer chains as opposed to hydrogen bonds found between β-strands. The solution behavior was also investigated and the results are consistent with aggregation of the polymer chains and not helix formation.

3.6 References

1. Baltzer, L., Nilsson, H. & Nilsson, J. (2001) *Chem. Rev.* **101,** 3153-3163.
2. Branden, C. & Tooze, J. (1999) *Introduction to Protein Structure* (Garland Publishing, New York).
3. Eisenberg, D., Weiss, R. M. & Terwillinger, T. C. (1984) *Proc. Natl. Acad. Sci. U.S.A.* **81,** 140-144.
4. Reitzel, N., Greve, D. R., Kjaer, K., Howes, P. B., Jayaraman, M., Savoy, S., McCullough, R. D., McDevitt, J. T. & Bjørnholm, T. (2000) *J. Am. Chem. Soc.* **122,** 5788-5800.
5. Bjørnholm, T., Greve, D. R., Reitzel, N., Hassenkam, T., Kjaer, K., Howes, P. B., Larsen, N. B., Bøgelund, J., Jayaraman, M., Ewbank, P. C. & McCullough, R. D. (1998) *J. Am. Chem. Soc.* **120,** 7634-7644.
6. Bo, Z., Zhang, C., Severin, N., Rabe, J. P. & Schulter, A. D. (2000) *Macromolecules* **33,** 2688-2694.
7. Bo, Z., Rabe, J. P. & Sehulter, A. D. (1999) *Angew. Chem., Int. Ed.* **38,** 2370-2372.
8. Kim, J. & Swager, T. M. (2001) *Nature* **411,** 1030-1034.
9. Kim, J., Levitsky, I. A., McQuade, T. & Swager, T. M. (2002) *J. Am. Chem. Soc.* **124,** 7710-7718.
10. Nelson, J. C., Saven, J. G., Moore, J. S. & Wolynes, P. G. (1997) *Science* **277,** 1793-1796.
11. Prest, P.-J., Prinee, R. B. & Moore, J. S. (1999) *J. Am. Chem. Soc.* **121,** 5933-5939.
12. Kubel, C., Mio, M. J., Moore, J. S. & Martin, D. C. (2002) *J. Am. Chem. Soc.* **124,** 8605-8610.
13. Arias-Martin, E., Arnault, J. C., Guillon, D., Mailou, T., Le Moigne, J., Geffroy, B. & Nunzi, J. M. (2000) *Langmuir* **16,** 4309-4318.
14. Arias, E., Maillou, T., Moggio, I., Guillon, D., Le Moigne, J. & Geffroy, B. (2002) *Synthetic Metals* **127,** 229-231.
15. Arnt, L. & Tew, G. N. (2002) *J. Am. Chem. Soc.* **124,** 7664-7665.
16. Arnt, L. & Tew, G. N. (2003) *Langmuir* **19,** 2404-2408.
17. Birdi, K. S. (1989) *Lipid and Biopolymer Monolayers at Liquid Interfaces* (Plenum Press, New York, NY).
18. DeGrado, W. F. & Lear, J. D. (1985) *J. Am. Chem. Soc.* **107,** 7684-7689.
19. MeQuade, T., Kim, J. & Swager, T. M. (2000) *J. Am. Chem. Soc.* **122,** 5885-5886.
20. Prosa, T. J., Winokur, M. J. & MeCullough, R. D. (1996) *Macromolecules* **29,** 3654-3656.
21. Venkataraman, D., Lee, S., Zhang, J. & Moore, J. S. (1994) *Nature* **371,** 591-593.
22. Hunter, C. A. (1994) *Chem. Soc. Rev.* **23,** 101-109.
23. Shetty, A. S., Zhang, J. & Moore, J. S. (1996) *J. Am. Chem. Soc.* **118,** 1019-1027.

24. Rappaport, H., Kjaer, K., Jensen, T. R., Leiserowitz, L. & Tirrell, D. A. (2000) *J. Am. Chem. Soc.* **122,** 12523-12529.
25. Choo, D. W., Schneider, J. P., Graciani, N. R. & Kelly, J. W. (1996) *Macromolecules* **29,** 355-366.
26. Krejchi, M. T., Atkins, E. D. T., Waddon, A. J., Fournier, M. J., Mason, T. J. & Tirrell, D. A. (1994) *Science* **265,** 1427-1432.
27. Arnt, L. & Tew, G. N. (2004) *Macromolecules* **37,** 1283-1288.

CHAPTER 4

ANTIMICROBIAL ACTIVITY OF CATIONIC FACIALLY AMPHIPHILIC PHENYLENE ETHYNYLENE MOLECULES

4.1 Introduction

The antibacterial activity of host defense peptides is due to the disruption of bacterial phospholipid cytoplasmic membranes as discussed in Chapter 1. The literature supports that this activity is not due to a precise chemical makeup but rather the overall physiochemical properties such as hydrophobic balance, charge, and facial amphiphilicity. The previous three chapters showed the design, synthesis, and characterization of new facially amphiphilic molecules. The following discussion focuses on the antimicrobial activity of these compounds.

Novel approaches to the development of new antimicrobial compounds and materials remain an important area of research. Many advances in this research area report using polymeric backbones and tethering known antibiotics, like ciprofloxacin or vancomycin, with hydrolyzable groups.(1-3) Another approach is to synthesize novel inherently antimicrobial compounds. For instance, cationic polymers have been developed as bioactive compounds,(4) including those containing ammonium(5-7) or phosphonium salts,(8) polylysine,(9) pyridinium salts,(10, 11) or polyguanidines and polybiguanidines.(12) The cationic nature of these molecules is important due to the electrostatic interaction of the positive charges of the antimicrobial agents with negatively charged groups present in microbial cytoplasmic membranes.(13) Polymers typically have an advantage over conventional small molecule antimicrobial agents

since they are essentially non-volatile and chemically stable.(13) However, a critical limitation is that the exact polymer composition is hard to define due to the polydispersity of the sample. For this reason, it is very hard to obtain FDA approval for polymers as antimicrobial agents. Many of the compounds synthesized to date do not show selectivity towards bacteria over mammalian cells, rather they are biocidal towards all types of cells.[3]

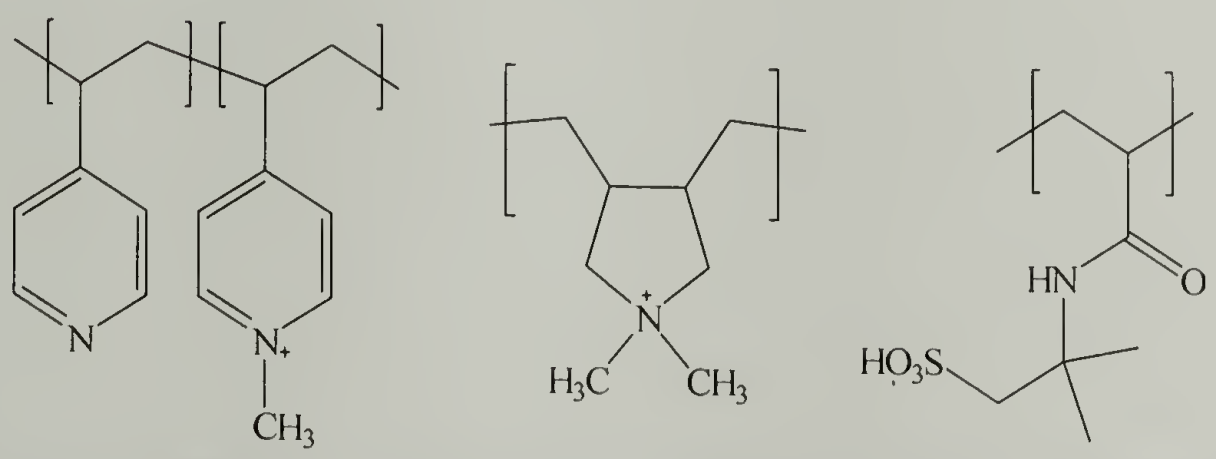

Figure 4.1: Series of water soluble polymers synthesized by Rivas et al.

Rivas and coworkers synthesized a series of water-soluble cationic polymers along with a anionic polymer, shown in Figure 4.1.(13) They investigated the antibacterial activity against *Eschericia coli* and *Staphylococcus aureus* and found that the anionic polymer did not show any bacteriocidal activity while the polycations were moderately active against gram-negative bacteria. This corroborated the idea that electrostatic interactions are important and cationic charges can impart antibacterial activity. They went on to suggest that the decreased efficiency against gram-positive bacteria was due to differences in membrane composition; specifically the dense lipopolysaccharides (LPS) of gram-negative bacteria, as shown in Figure 4.2. LPS are negatively charged and could potentially attract positively charged macromolecules;

---

[3] A biocide is a chemical agent, such as a pesticide, that is capable of destroying living organisms.

however, they are known to repel hydrophobic molecules. These authors also investigated the kinetics of bacterial death and determined that within the first 60 minutes, the bacterial count was reduced by 90%. Tests also concluded that the molecules did not show genotoxic activity.[4]

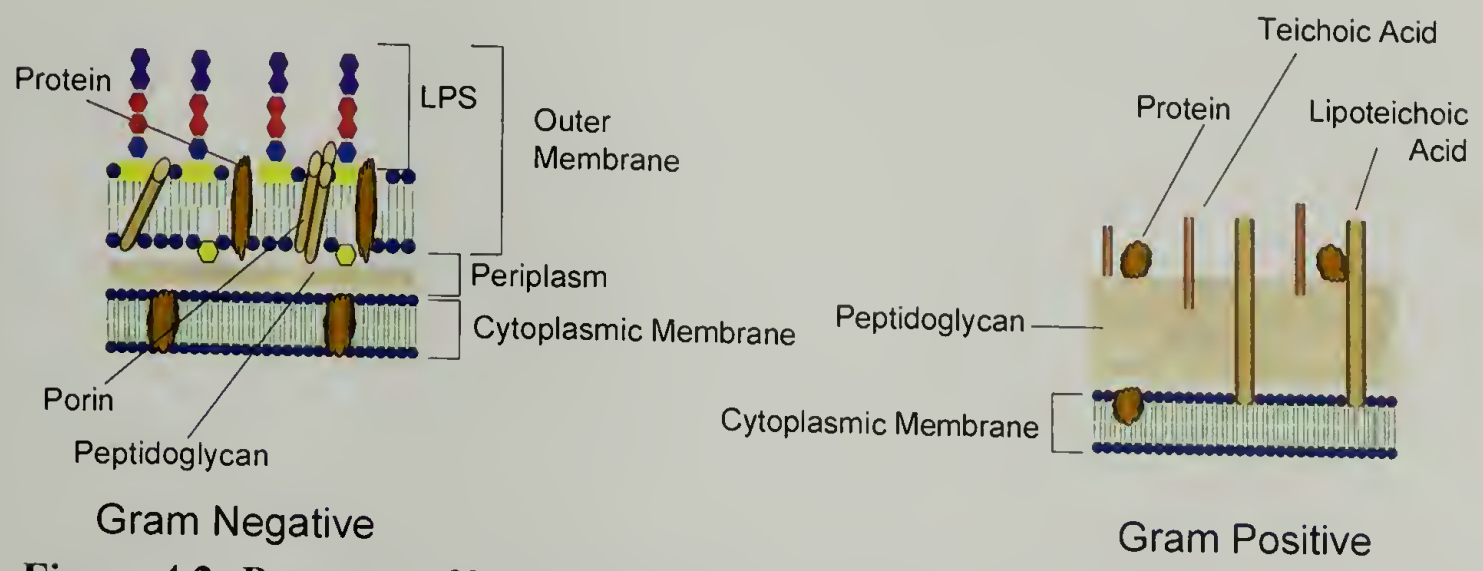

Figure 4.2: Presence of LPS on gram-negative but not on gram-positive bacterial cell membranes.

Conventional polymers, such as functionalized polystyrene, have also been synthesized for potential biocidal activity.(7) Gellman and coworkers synthesized polystyrene molecules from monomers that were either cationic by virtue of protonation of a dimethylaminomethyl group or contain a quaternary ammonium moiety (Figure 4.3). The polymer obtained from monomer A (polyA) showed significant biocidal activity against the four bacteria tested as well as human erythrocytes while the polymer of B (polyB) showed essentially no activity against bacteria or erythrocytes. These authors suggested that reversible N-protonation leads to greater biocidal activity than does irreversible N-quaternization since polyA is much more biocidal than polyB. However, they also mentioned that polyB displayed antimicrobial activity in an agar-

[4] A genotoxin is a chemical or other agent that damages cellular DNA, resulting in mutations or cancer.

plate assay but not in the liquid-medium assay which insinuates that polyB is most likely not soluble at the concentrations needed to induce biocidal activity.

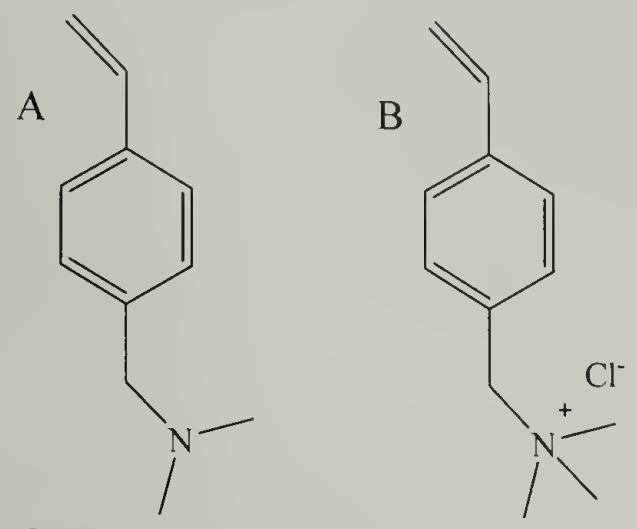

Figure 4.3: Monomers Gellman et al. used to synthesize a series of functionalized polystyrene molecules.

Biocidal cationic polymers can be useful for situations where selectivity towards bacterial cells over mammalian cells is not required such as in many material applications. However, in many instances, such as for ingestible or injectable antibiotic use, selectivity is extremely necessary. Host defense peptides represent a large class of natural compounds with broad spectrum antimicrobial activity that also show selectivity for bacterial over mammalian red blood cells (RBC).(9, 14) They have captured the attention of many researchers because of this selectivity towards bacteria, and now there is a significant body of knowledge of their essential physiochemical properties.(15-18)

The ability of host defense peptides to disrupt phospholipid membranes, ultimately killing the cell, is thought to come from the adoption of a facially amphiphilic (FA) structure.(9, 14, 19, 20) Gellman and coworkers demonstrated this concept by synthesizing a series of amphiphilic helical structures based on synthetic β-peptides (Figure 4.4) which mimic the overall structure and activity of Magainin.(21-23) The

series of β-peptides had the same net charge while varying the substitution patterns.(21-23) The most active peptides were those whose substitution pattern leads to the highest degree of FA. Therefore, they concluded the FA architecture is important for antibacterial activity and selectivity, consistent with previous findings from synthetic α-peptides.(22, 23)

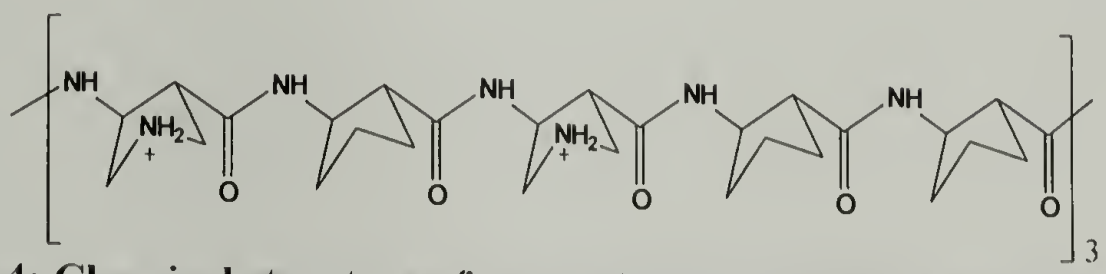

Figure 4.4: Chemical structure of an amphiphilic helical peptide that mimics the structure and activity of magainin.

DeGrado and coworkers have patterned β-peptide helices to contain charged lysine and nonpolar side chains on opposite sides of the helix.(24) This patterning leads to stable amphiphilic structures, which showed antibacterial activity with selectivity values up to 2. Following further purification of the compound, they report an increased selectivity value of 15.(25) In the same study, a selectivity of 180 was obtained by substituting the more hydrophobic β-valine for β-alanine. From this study, they suggested that the highly flexible compounds were able to show selectivity values equal to or better than natural host defense peptide analogs.

Another route to mimicking host defense peptides is the use of a peptoid backbone. Peptoids are similar to peptide backbones; however the traditional α-side chain is positioned at the nitrogen, creating a tertiary amide. Due to this altered chemical structure, all of the hydrogen bonding seen both intra- and inter-molecularly in natural peptides is eliminated. Peptoids were recently shown to adopt stable helical

structures with bulky α-chiral side chains (Figure 4.5).(26-28) When these helical molecules were patterned to adopt FA helices, they demonstrated antibacterial properties.(29) Similar molecules have shown resistance to proteolytic degradation(30) and this stability makes this backbone attractive for use in many biological applications.

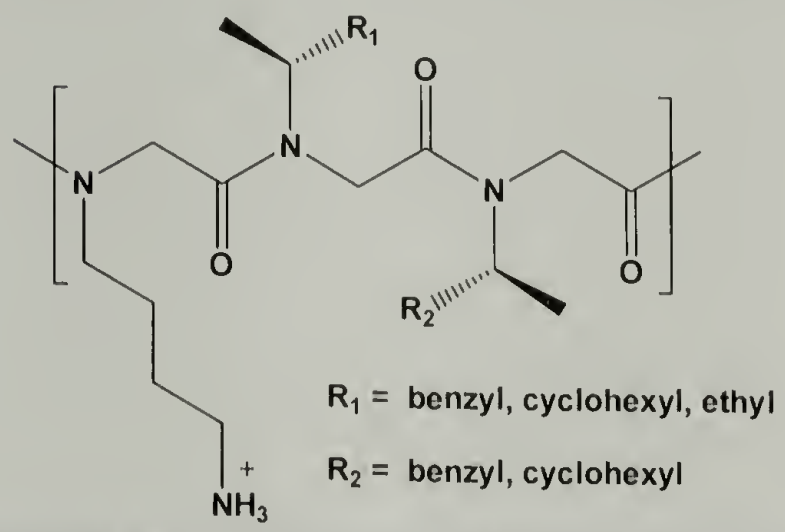

Figure 4.5: Peptoids with bulky chiral side chains that form FA helical structures.

The β-peptides and peptoids demonstrate the power of coupling design with function but remain structurally similar to natural α-peptides and mimic the helical nature of host defense peptides. These peptides also require costly and time intensive synthetic methods. The extension of design principles to simpler oligomers and polymers will provide fundamental understanding of structure-activity relationships and lead to new biologically active materials.

4.2 Polymer Antibacterial Activity

Early work on polymeric systems as abiotic host defense peptide mimics used arylamide backbones, shown in Figure 4.6.(31) These systems were designed to mimic the FA architecture and physiochemical properties of host defense peptides without necessarily providing a helical structure. They demonstrated broad spectrum activity

against several bacterial strains, however, these polymers were found to be hemolytic[5] at or near their minimum inhibitory concentration (MIC)[6] values.(31) Additionally, these arylamide polymers contain amide bonds, lending susceptibility toward proteolytic degradation. The ability to transfer the essential physiochemical properties to simple entirely abiotic polymers would provide access to fast, inexpensive antimicrobial materials for various applications including coatings, medical tubing, and consumer products.

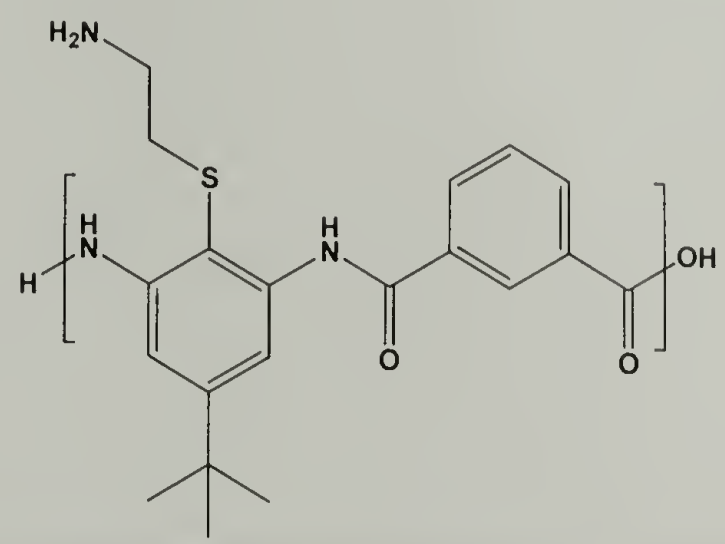

Figure 4.6: Initial peptide mimics based on arylamide backbones.

Due to the FA nature of the polymers discussed in the previous chapters, these molecules were tested for biological activity. The polymers shown in Figure 4.7 were the first set of molecules tested for antibacterial activity. In these polymers, the facially amphiphilic nature comes from the hydrophobic backbone and alkoxy groups coupled with the hydrophilic amine side chains. The FA extended conformation is strongly favored at the air-water interface as seen in Chapter 3. This interface is similar to the oil-water interface of the cytoplasmic membrane. Specifically, these polymers were chosen to look at the effect of different hydrophobic side chain substituents and varying

[5] Hemolytic agents lyse red blood cells.

molecular weights. As discussed in Chapter 1, both the degree of hydrophobicity and the size of the molecule play significant roles in antimicrobial activity. Polymers **63d** and **28d** provide a direct assessment at constant degree of polymerization of varying structure (the presence (**63d**) or absence (**28d**) of the pentoxy side chain). Since **63d** has an additional pentoxy side chain on each polymer repeat unit, this structure is considerably more hydrophobic than **28d**. Polymers **28d** and **64d**, on the other hand, allow us to examine the effect of varying the number of repeat units while keeping the molecular structure constant. Polymer **64d** is a significantly smaller polymer, with an average of 6 repeat units per chain as opposed to an average of 20 repeat units in **28d**.

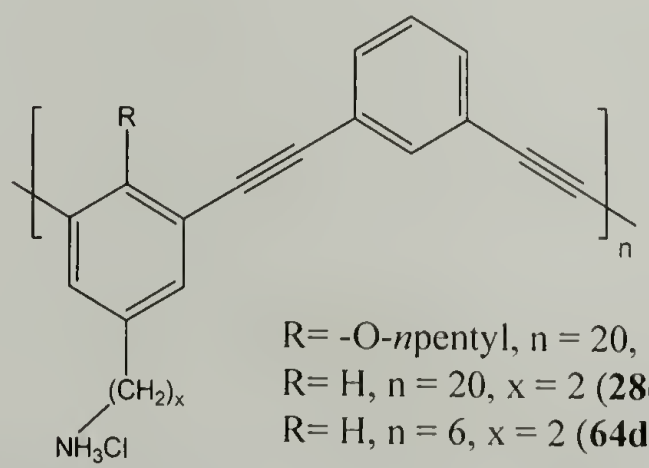

R= -O-*n*pentyl, n = 20, x = 1 (**63d**)
R= H, n = 20, x = 2 (**28d**)
R= H, n = 6, x = 2 (**64d**)

Figure 4.7: Polymers with amine side chains tested for antibacterial activity.

The antibacterial action of these polymers was measured against both gram-negative (*E. coli*) and gram-positive (*B. subtilis*) bacteria following standard protocols.(32) The bacteria were grown overnight into the stationary phase, diluted after 12 hours into the lag phase, and grown for three more hours back into the log phase. This procedure ensures the bacteria grew correctly and allows the experiment to be performed with cells already growing exponentially in the log phase. The bacteria

---

[6] MIC as defined here is the minimum concentration of a compound that is required to inhibit 90% of cell growth.

were rediluted to an optical density at 600 nm (OD_{600}) of 0.001 and seeded into 96 well plates. The compound of interest was introduced at various concentrations and the plate was incubated for six hours, as schematically shown in Figure 4.8. The OD_{600} was read and the minimum inhibitory concentration (MIC) was determined for each polymer.

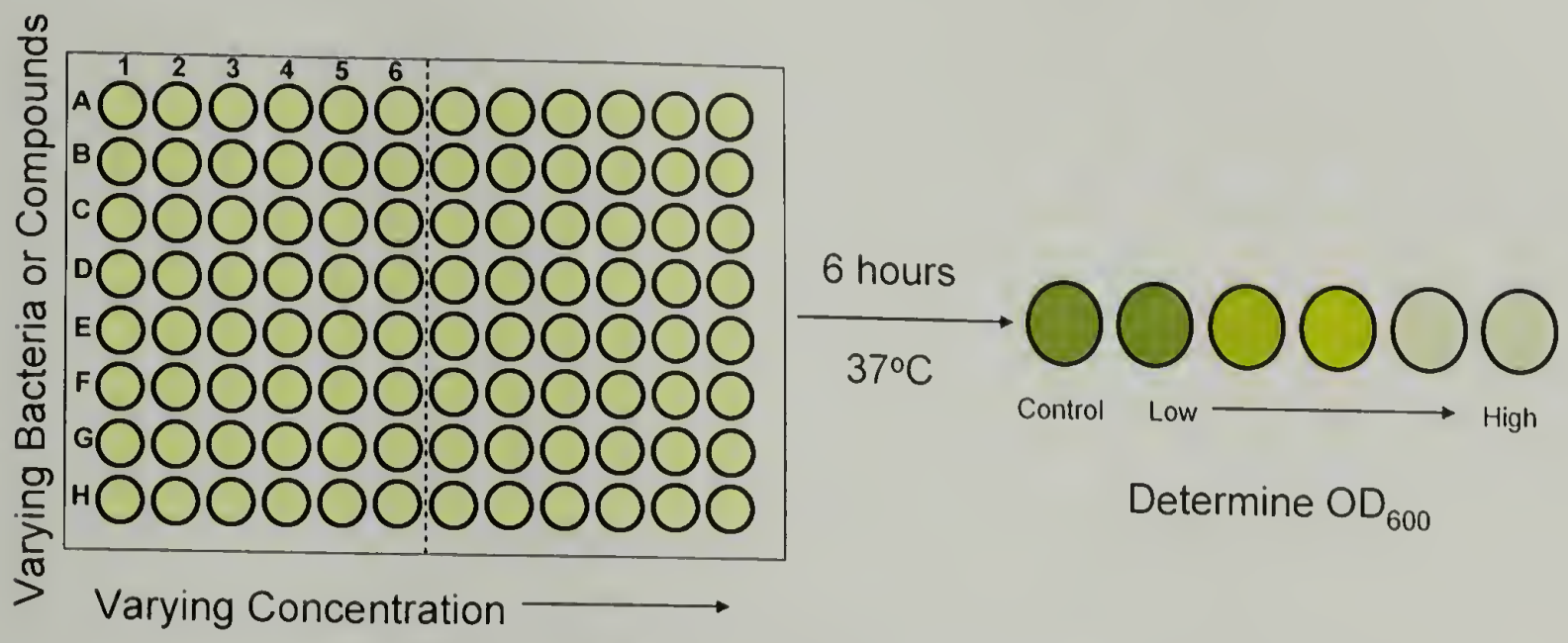

Figure 4.8: Schematic of the MIC test.

It is also important to determine the selectivity of each compound. Selectivity, measured as the ratio of the hemolytic concentration (HC_{50}) to MIC_{90}, indicates how active a compound is towards bacterial rather than red blood cells (RBCs). This value is useful when comparing the activities of different compounds. For instance, a compound that has a lower MIC than a second compound is not necessarily better since it could be very hemolytic (as designated by a low HC_{50} value). Typically, the desired target is a compound that has a low MIC value and a high selectivity value.

The HC_{50} is defined as the amount of compound needed to lyse 50% of RBCs. To determine HC_{50}, the compounds of interest were mixed with human blood for thirty minutes at 37°C. This incubation was relatively short compared to the six-hour incubation in the MIC test but is sufficient since the RBCs do not grow or reproduce.

After the incubation, the remaining intact RBCs were removed by centrifugation. This did not harm the RBCs as monitored by the hemoglobin release from control samples with no active compound. The amount of hemoglobin released due to RBC lysis was monitored in the supernatant by determining the absorbance at 414 nm. To determine the hemoglobin absorbance with 100% disruption of the RBCs, triton-X100 was added to the solution, acting as a surfactant and lysing all the RBCs. The HC_{50} was determined either directly from the experiment at the concentrations of active compound tested or by extrapolating the data to higher concentrations than those tested.

The results of the antibacterial and hemolytic tests are shown in Table 4.1. Polymer **63d**, the most hydrophobic sample, showed no antibacterial activity up to 100 μg/mL against either of the two strains, probably a result of low solubility. The lack of activity and solubility of **63d** most likely arises from the hydrophobicity of the pentoxy chain. Polymers **28d** and **64d**, which have decreased overall hydrophobicity due to the absence of pentoxy chains, demonstrated increased solubility and activity. A comparison of **63d** and **28d**, which are closest in molecular weight and have the same degree of polymerization (DP=20), finds that **28d** is visibly more soluble in the cell growth medium and has a MIC of 25 μg/mL (4.6 μM). After finding activity in **28d**, we prepared **64d** with smaller overall molecular weight based on the previous arylamide report suggesting that smaller molecules are more biologically active.(31)

Table 4.1 shows that polymer **64d**, with identical structure to **28d**, is less active than **28d** at 50 μg/mL (31.2 μM) but significantly more selective. The selectivity is determined to be 10.8 for polymer **64d**. This selectivity compares very well with the

Table 4.1: Summary of antibacterial activity of polymers with primary amines.

Molecule	Side Chain	M_n+	DP†	MIC_{90} (μg/mL)		HC_{50}	Selectivity
				E. coli	*B. subtilis*		$HC_{50}/MIC_{E.\ coli}$
63d	OC_5H_{11}	6800	20	-	-	N/A	N/A
28d	H	5400	20	25	25	12.5	0.5
64d	H	1600	6	50	100	540	10.8
15	Monomer	315*	N/A	>100	>100	3400	N/A
-	Magainin			12.5		120	9.6

+ Molecular weight was determined by THF GPC against PS standards.
* This is a discrete compound.
† Average degree of polymerization taken from Mn of GPC.

highly aetive magainin analog, MSI-78(33), whieh was determined to be 9.6 against the same *E. coli* strain used here. Although the overall antibaeterial aetivity of **64d** is not as potent as MSI-78, the selectivity is comparable and the first reported for polymerie analogs designed as host defense peptide mimies.(34) Finally, monomer **15**, whieh was used to prepare this polymer, was tested and found to be essentially inaetive. No bacterial activity was measured up to 100 μg/mL and extrapolation of the HC_{50} curve provided a value of 3400 μg/mL. Therefore, it is clear from the monomer inaetivity and polymer aetivity, that the FA design is important for aetivity.

After determining a relationship between aetivity and the hydrophobieity of the polymer, several polymerie derivatives utilizing guanidine groups were synthesized. The addition of this group was utilized to increase the polymer hydrophilieity. The resulting polymers (Figure 4.9) have three amine groups per repeat unit in eomparison to one in the previous set of polymers (Figure 4.7). This new set of moleeules provides three additional eomparisons. There is now a direet eomparison of the influenee from

the number of amine groups (**65d** vs. **63d**) while keeping the degree of polymerization constant. It also allows a comparison of varying the polymer molecular weight while keeping the structure the same (**65d**, **66d**, and **67d**). Finally, a comparison between the presence (**65d**, **66d**, and **67d**) and absence (**68d** and **69d**) of the hydrophobic alkoxy side chain.

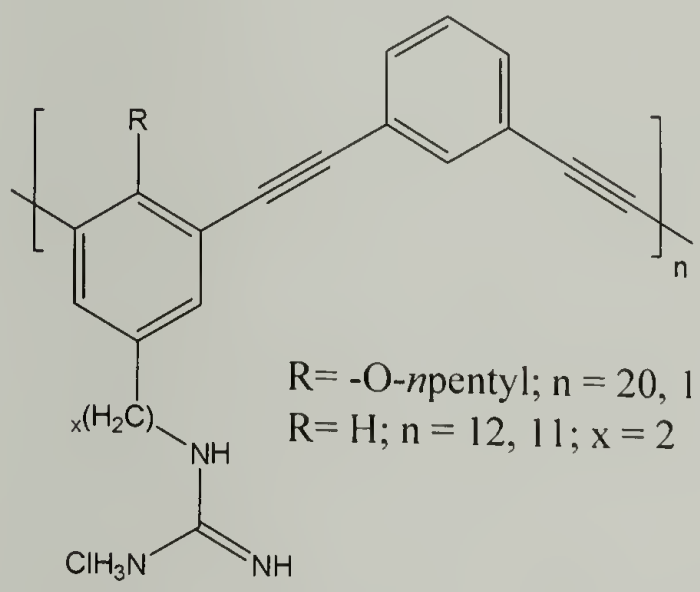

R= -O-*n*pentyl; n = 20, 16, or 7; x = 1
R= H; n = 12, 11; x = 2

Figure 4.9: Polymers with guanidine side chains tested for antibacterial activity.

Table 4.2: Summary of polymer antibacterial activity with guanidine side chains. The biological activities of these polymers were determined with the same

Molecule	Side Chain	M_n	DP	MIC_{90} (μg/mL)	
				E. coli	*B. subtilis*
65d	OC_5H_{11}	11400	20	>100	>100
66d	OC_5H_{11}	9300	16	>100	>100
67d	OC_5H_{11}	4300	7	>100	>100
68d	H	6100	12	>100	50
69d	H	5600	11	>100	100

* Discrete monomers were active: $MIC_{E.\ coli}$=50 μg/mL and 6.6 μg/mL for H and OC_5H_{11} respectively.

method as described above and the results are shown in Table 4.2. The data indicates that none of these polymers are active against bacteria up to the highest concentration

tested, 100 μg/mL. Higher molecular weight polymers with the pentoxy side chains, **65d** and **66d**, were insoluble at the higher concentrations tested. Most likely, these polymers are too hydrophobic to display any antimicrobial activity. Polymers **67d**, **68d**, and **69d** did not have any solubility problems but still did not show significant antibacterial activity. The result from **67d** is somewhat surprising since it is a relatively short analog of **63d** with the additional hydrophilicity from the guanidine group so it was expected to show antibacterial activity. One probable reason for the inactivity is a favorable interaction between the guanidine group and the aromatic backbone rendering the molecule no longer FA which could also explain the inactivity of **68d** and **69d**. Therefore, introducing guanidine groups does increase the solubility of these polymers but does not improve their antibacterial activities. Interestingly, the monomeric versions were highly active at 6.6 μg/mL and 50 μg/mL for the presence and absence of the pentoxy side chain, respectively. In this case, the monomers are probably acting as surfactants which are known to be biocidal towards most living cells.

4.3 Discrete Oligomer Antibacterial Activity

After observing an increase in antibacterial activity as the molecular weight decreased, Table 4.1, two discrete oligomers, **35d** and **34d**, were synthesized and their antibacterial activity monitored, as summarized in Table 4.3. The oligomer with the pentoxy side chain, **35d**, shows no selectivity towards bacteria but rather selectivity toward human erythrocytes. Visual precipitation of this compound from solution can be seen in the cell growth medium, suggesting that the very hydrophobic nature of this compound can account for the lack of bacterial activity. As the pentoxy chain is

removed, the hydrophobicity is decreased and the desired selectivity is seen. The C0 oligomer, **34d**, shows activity against *E. coli* at 0.8 μg/mL and hemolysis at 75 μg/mL. This indicates a selectivity of almost 90, which is remarkable for a synthetic abiotic molecule.

The difference in both the bacterial and hemolytic activities between these two compounds is not surprising. **35d** is significantly more hydrophobic than **34d** due to the presence of two pentoxy side chains. The hemolytic activity of **35d** is very high (HC_{50} <12.5 μg/mL), suggesting that the overall hydrophobicity of the molecule leads to interactions with the zwitterionic RBC membrane in order to satisfy the hydrophobic needs of the molecule when exposed to an aqueous environment. The lack of activity

Table 4.3: Discrete oligomer antibacterial activity.

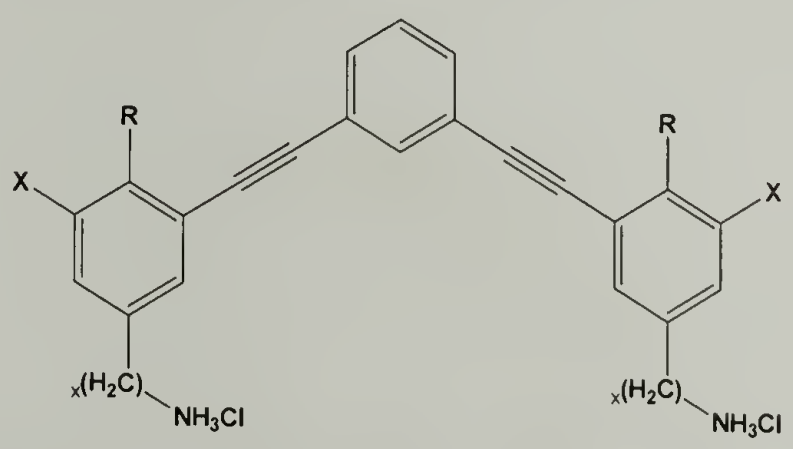

Molecule	x	X	R	MIC (μg/mL)		HC_{50}	Selectivity
				E. coli	*B. Subtilis*		$HC_{50}/MIC_{E. coli}$
35d	1	I	OC_5H_{11}	25	>100	<12.5	<0.5
34d	2	Br	H	0.8	1.7	75	88

toward bacterial cells is most likely due to a combination of insolubility and overwhelming hydrophobicity of **35d**. Once the pentoxy side chains are removed resulting in **34d**, the overall hydrophobicity is significantly decreased and the molecule

appears to have the proper hydrophobic balance to interact with the negatively charged head groups and the hydrophobic tails of the phospholipids of the bacterial membrane.

4.4 Structure-Activity Relationship of Discrete Oligomers

Since increased selectivity was seen with the small discrete oligomers, a structure-activity relationship was investigated around the *meta*-PE backbone using the bromine end groups, the polar amine groups, and the alkoxy chains as handles.

4.4.1 Modifications at the End Groups

The structures and biological activity of the derivatives with varying end groups are shown in Table 4.4. These molecules all have the same backbone structure and

Table 4.4: SAR relationship of discrete oligomers varying end group functionality.

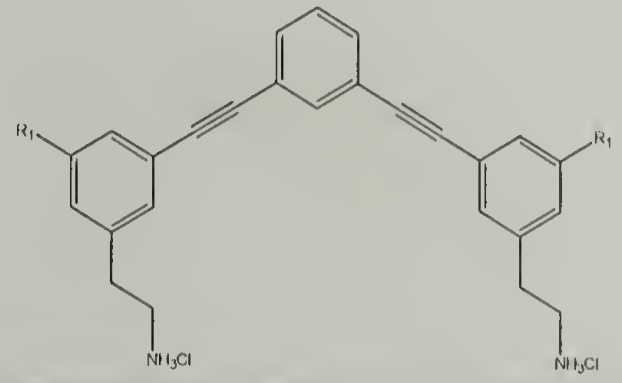

Molecule	R_1	MIC_{90} (μg/mL)		HC_{50}	Selectivity
		E. coli	*B. subtilis*		$HC_{50}/MIC_{E.\ Coli}$
36d		12	12	10	0.8
37d		1.6	1.6	<6	<3.8
38d		6.4	6.4	<6	<0.9
39d	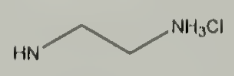	3.2	3.2	9	2.8
40d	H	3.2	3.2	4.5	1.4

ethylamine side chains as **34d**. Since the only structural difference is the end group moieties, the derivatives can be referenced back to **34d**.

The introduction of a propargyl amine group, **36d**, increases the charge density of the molecule and makes the overall molecule more hydrophilic than **34d**. This change decreases the biological activity by a factor of 15 and makes the compound significantly more toxic, rendering the molecule unselective. The introduction of the propargyl alcohol moiety, either mono- or di-substituted (**37d** and **38d**, respectively), decreases the charge density compared to **36d**, making it similar in charge to **34d**. These new molecules are more biologically active than **36d**, but they are also more hemolytic. The mono-substituted oligomer, **37d**, is more selective than the di-substituted counterpart, **38d**; however neither of these modifications results in the desired selectivity.

In the above modifications, a new alkyne bond is introduced to the end group. The addition of this alone would significantly increase the hydrophobicity of the molecule, however each of these modifications also introduce one or two additional heteroatoms to increase the hydrophilicity of these molecules. Changing both the hydrophobicity and hydrophilicity of the compounds at the same time complicates interpretation of the results. If only the additional heteroatoms were considered, the trend is as expected: namely as the polarity of the end group is increased, the molecules become increasingly more biologically active (MIC **37d**>**38d**>**36d**). However, since the alkyne adds hydrophobicity, all the molecules become too hydrophobic to show selectivity towards bacterial cells.

The introduction of ethylamine end groups, **39d**, provides an increase in charge compared to **34d** without the triple bond seen in **36d**. The resulting oligomer is more biologically active than **36d** (3.2 μg/mL as opposed to 12 μg/mL) with similar hemolytic concentrations. This difference could be due to the ethylamine group having greater conformational flexibility than the propargyl amine. **39d** retains selectivity towards bacterial cells, which is rare amongst the derivatives with end group modifications and attributed here to the flexibility of the cationic amine end groups.

The last modified oligomer in the set, **40d**, is absent of end groups. This derivative is 4 times less active than **34d** which has bromine end groups and about 20 times more hemolytic, resulting in a selectivity of 1.4. The bromine end groups do not account for the biological activity since the monomer with bromine groups, **15**, is not antibacterial; however, the size contribution and resulting hydrophobicity from the bromines as compared to the hydrogen analog might play a role in the activity. The length of **34d** is 17.6 Å while **40d** is 16.4 Å: this slight change in chemical structure results in a significant change in size.

4.4.2 Modifications at the Polar Amine Groups

The derivatives shown in Table 4.5 are modifications to the P amine group. The original oligomer, **34d**, has an ethyl amine group as the P side chain. The first modification, **46d**, shown in Table 4.5 has a guanidine group on the P side chain, increasing the overall hydrophilicity. This modification slightly decreases the antibacterial activity but makes the compound much more hemolytic; however **46d** is still selective towards bacteria over RBCs. The second derivative, **47d**, has an amide

group between the aromatic ring and the ethylamine P group, increasing the heteroatoms in the compound and the hydrophilicity. Surprisingly this modification makes the compound significantly less biologically active and very toxic to RBCs. However, this could be due to the close proximity of the hydrophilic amide moiety and the hydrophobic backbone, disrupting the overall FA structure.

Table 4.5: SAR relationship of discrete oligomers varying amine functionality.

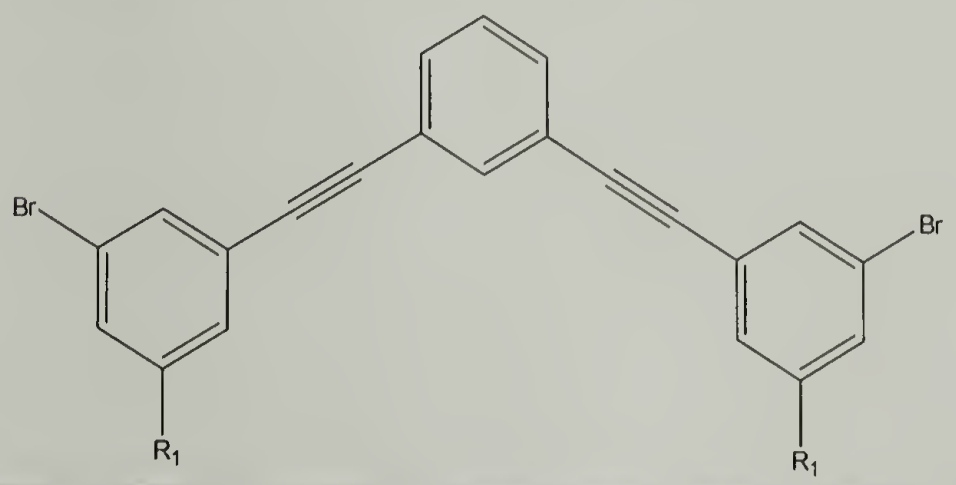

Molecule	R_1	MIC_{90} (μg/mL)		HC_{50}	Selectivity
		E. coli	*B. subtilis*		$HC_{50}/MIC_{E.\ Coli}$
46d	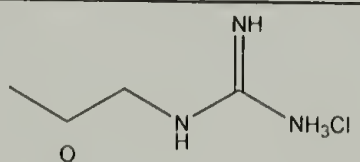	3.2	1.6	8	2.5
47d	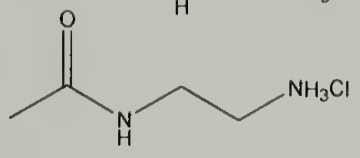	50	25	12.5	0.3
48d	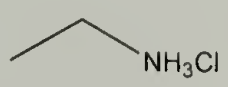	>100	>100	150	<1.5
49d	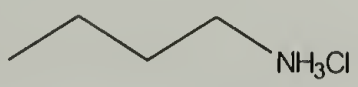	1.6	3.2	3.2	2

The last two derivatives, **48d** and **49d**, in Table 4.5 probe the effect of the number of carbons separating the amine from the aromatic backbone. The original oligomer, **34d**, has two, while **48d** and **49d** have one and three respectively. It is

apparent that the length of the P chain has a great effect on the biological activity. When the length of the carbon chain is decreased by one carbon, as in **48d**, the compound becomes completely inactive (up to 100 μg/mL) against bacteria and hemolytic at 150 μg/mL. When the length of the carbon chain is increased to three carbons, as in **49d**, the compound becomes highly toxic towards bacteria (1.6 μg/mL) and RBCs (3.2 μg/mL). It was unexpected that such a slight change in structure would have such a dramatic effect; however there are some explanations. In derivative **48d**, the cationic amine is much closer to the hydrophobic backbone, which could disrupt the FA structure and diminish any biological activity. With the charge closer to the backbone, the molecule would penetrate the lipid bilayer less in order for the charged amine group to retain interactions with the negatively charged lipid head groups in the outer leaflet of the bilayer. In the second derivative, **49d**, the carbon chain length is increased, potentially increasing the overall hydrophobicity which results in a biocidal derivative.

Table 4.6: Effect of molecule length on activity.

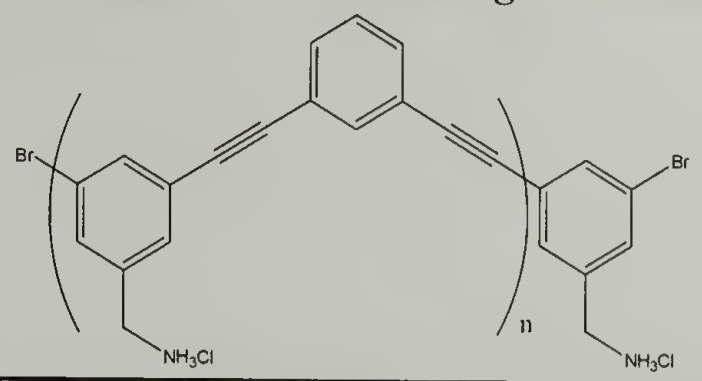

		MIC_{90} (μg/mL)			Selectivity
Molecule	n	*E. coli*	*B. subtilis*	HC_{50}	$HC_{50}/MIC_{E.\ Coli}$
48d	1	>100	>100	150	<1.5
50d	2	>100	>100	150	<1.5
51d	3	>100	>100	300	<3

While synthesizing **48d**, it was possible to separate the longer oligomers, **50d** and **51d** shown in Table 4.6, by column chromatography. These molecules provide insight into the effect of oligomer length on activity. None of these oligomers were active against bacteria up to the concentrations tested, but they did show variance in the hemolytic activity. The shorter oligomers, **48d** and **50d**, were hemolytic at 150 μg/mL while the longer oligomer, **51d**, was hemolytic at 300 μg/mL. This data suggests that there is a chain length dependence for biological activity: the longer molecule (n=3) is significantly less biologically (in this case hemolytically) active than the shorter analogs (n=1,2). Presumably, if the molecules were soluble at concentrations above 100 μg/mL, then they would show antibacterial activity with **48d** having the most activity and/or selectivity while **51d** would have the least activity and/or selectivity.

4.4.3 Modifications to the Alkoxy Side Chains

The set of derivatives with alkoxy side chains are shown in Table 4.7. The original oligomer, **35d**, had a pentoxy side chain. The first derivative, **58d**, has a methoxy derivative in place of the pentoxy chain. This modification makes the compound essentially inactive towards bacteria but highly hemolytic. At the higher concentrations tested, this molecule was not soluble, which could account for its inactivity. Another reason for inactivity could be due to the addition of the polar methoxy moiety disrupting the FA nature of the molecule. The second derivative, **59d**, has a guanidine group introduced to the P side of the molecule and the pentoxy chain as the NP substituent. The bacterial activity of **59d** (6.4 μg/mL) is increased compared to **35d** (25 μg/mL); however, **59d** is still toxic to RBCs, rendering it unselective. This

change in activity could be due to favorable interactions between the guanidine group and the aromatic backbone, disturbing the FA nature of the molecule.

Table 4.7: SAR relationship of discrete oligomers with alkoxy side chains.

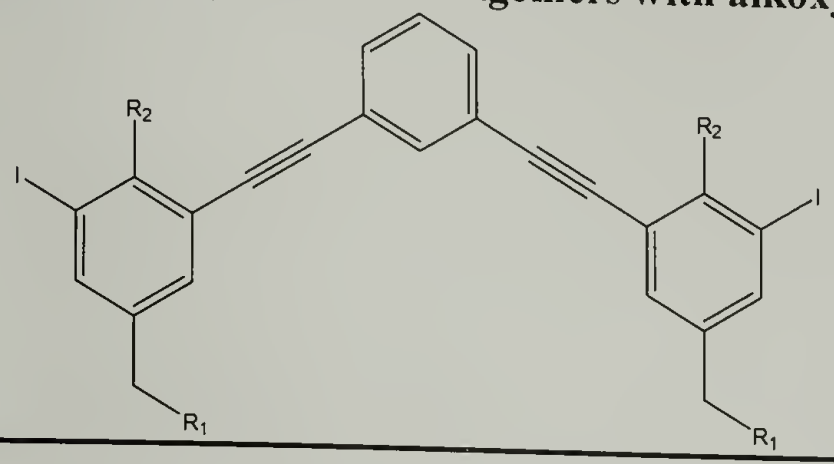

Molecule	R_1	R_2	MIC_{90} (μg/mL)		HC_{50}	Selectivity
			E. coli	*B. subtilis*		$HC_{50}/MIC_{E.\ Coli}$
35d	NH_3Cl	OC_5H_{11}	25	>100	<12.5	<0.5
58d	NH_3Cl	OCH_3	>100	>100	<6	N/A
59d	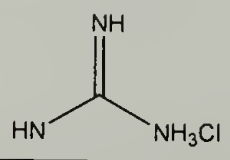	OC_5H_{11}	6.4	3.2	4.6	0.71

Of all the derivatives studied in the structure-activity relationship, the original oligomer, **34d**, remains the most selective compound synthesized and tested. This study has proven that with this *meta*-PE backbone, it is difficult to determine which modifications, if any, will be selective towards bacteria. At this time, the suggestions given for inactivity are only postulations and cannot be fully explained. In general, the compounds in which hydrophobicity is solely due to the aromatic backbone are more active than those with alkoxy side chains. This is most likely due to the alkoxy-substituted molecules being excessively hydrophobic. Also, the addition of guanidine groups onto the molecules seems to render the molecule inactive, possibly due to favorable interactions between the guanidine moieties and the aromatic backbone which

disrupt the FA nature. Lastly, the addition of alkyl end groups to the molecules increases the hemolytic activity of the derivatives. Most of the modifications introduced more heteroatoms to increase the polarity; however alkyl and alkyne substituents were also added in the process. Both the variations of the overall hydrophobic balance and the sizes of the molecules are two factors known to affect the biological activity and selectivity. Further work to determine the mechanism by which these compounds act on the membrane could potentially elucidate reasons for inactivity and are discussed in Chapter 5.

4.5 Probing the Bacterial Activity

Since **34d** is the most selective compound out of all the molecules prepared, several tests were run to probe further the antibacterial activity. These tests included screening for broad-spectrum activity, determining the minimum bactericidal concentration, probing the activity in the presence of whole blood, determining the rate at which the compounds kill cells, and investigating the development of bacterial resistance.

Table 4.8: Activity of 34d in comparison to Polymyxin B.

Bacterial Species	Gram	MIC_{90} (μg/mL)	
		34d	Polymyxin B
Eschericia coli D31	-	0.8	0.5
Klebsiella pneumoniae ATCC 13883	-	1.7	0.5
Bacillus subtilis ATCC 8037	+	1.7	0.5
Staphylococcus aureus ATCC 25923	+	1.7	13.3

After determining the activity and selectivity towards two strains of bacteria, *E. coli* and *B. subtilis*, the broad-spectrum activity was investigated. Table 4.8 shows the strains of bacteria tested against both **34d** and Polymyxin B. For comparison Polymyxin B, a natural bacterium-derived polycationic antimicrobial peptide with a

Table 4.9: Broad spectrum activity of 34d.

Bacterial Species	Gram	MIC_{90} (μg/mL)	Selectivity
Enterobacter cloacae ATCC 13047	-	1.7	44
Escherichia coli C1S	-	1.7	44
Escherichia coli D31	-	0.8	94
Klebsiella aerogenes ATCC 35150	-	3.4	22
Klebsiella pneumoniae ATCC 13883	-	1.7	44
Moraxella catarrhalis ATCC 25240	-	0.8	94
Neisseria sicca ATCC 29256	-	3.4	22
Proteus vulgaris ATCC 13315	-	3.4	22
Proteus mirabilis C20	-	12.1	6
Pseudomonas aeruginosa ATCC 10145	-	3.4	22
Pseudomonas stuartii C3S	-	12.1	6
Salmonella typhymurium ATCC 29631	-	3.4	22
Serratia marcescens ATCC 43861	-	3.4	22
Francisella tularensis ATCC 17135	-	1.0	75
Francisella tularensis ATCC 17137	-	1.0	75
Bacillus anthracis ATCC 1099	+	1.0	75
Bacillus cereus var. *mycoides*	+	1.7	44
Bacillus globigii ATCC 9372	+	3.4	22
Bacillus subtilis ATCC 8037	+	1.7	44
Enterococcus faecalis ATCC 19433	+	0.8	94
Listeria monocytogenes ATCC 35152	+	1.7	44
Staphylococcus aureus ATCC 25923	+	1.7	44
Staphylococcus epidemidis ATCC 155	+	0.8	94
Staphylococcus saprophyticus ATCC	+	0.8	94
Streptococcus agalactiae ATCC 13813	+	0.4	188
Streptococcus gordonii ATCC 33399	+	1.7	44

long hydrophobic tail, was added as a control antibiotic and the results corroborated those reported in the literature. Polymyxin B is derived from strains of soil bacteria *Bacillus polymyxa* and is usually used to treat infections of gram-negative bacteria. The activity of **34d** is comparable to that of Polymyxin B for several strains and even better against *S. aureus*, a gram-positive bacterium. **34d** has the advantage of being broad-spectrum against both gram-positive and -negative bacteria while polymyxin B is mainly used to treat gram-negative infection.

Table 4.9 shows results of further testing **34d** against several other strains of bacteria including both gram-positive and gram-negative bacteria as well as several antibiotic-resistant strains. With an average MIC of 2 μg/mL, this compound was bactericidal against most organisms tested. The highest effective concentration of **34d** tested was 12.1 μg/mL, with weakest activities against *Proteus mirabilis* and *Pseudomonas stuartii* while the lowest activity was 0.4 μg/mL against *Streptococcus agalactiae*. Compound **34d** potently inhibits the growth of several important human pathogens including *Listeria monocytogenes*[7], *Pseudomonas aeruginosa*[8] and *Staphylococcus aureus*.[9] It also inhibits the growth of the bacteria, *Enterococcus*

---

[7] *L. monocytogenes* is a food-born pathogen which causes flu-like symptoms which can lead to serious infections and even miscarriages in pregnant women.

[8] *P. aeruginosa* causes various systemic infections including urinary tract, respiratory, bone and joint, as well as dermatitis, especially in immunosuppressed people. It is a particular problem in hospitals where it accounts for more than 10% of all hospital-acquired infections.

[9] *S. aureus* causes a variety of pus-forming infections as well as toxinoses. These range from skin infections like boils and styes to more serious infections such as pneumonia and meningitis. It is also a problem in hospitals where it causes infections in surgical wounds and medical device implants such as catheters.

faecalis and *Salmonella typhymurium*, which are known to resist the action of antimicrobial peptides. Potent activity is also shown against the pathogens *Bacillus anthracis* and *Francisella tularensis* which are both known possible bioweapons and are currently monitored by the CDC.

With the broad-spectrum activity of **34d**, the minimal bactericidal concentration (MBC) was investigated. The MBC is defined as the concentration of the active agent needed to kill 99% of the bacteria as opposed to the MIC which is the concentration needed to inhibit bacterial growth. Commonly, the MBC of natural host defense peptides is between two and four times the MIC.(35) In order to determine the MBC, bacteria were grown in the presence of **34d** for six hours, diluted, and then plated on agar dishes and grown for 24 hours. A small aliquot of the bacteria growth media was removed after six hours and visualized with a microscope, shown in Figure 4.10. Figure 4.10a shows the control for normal bacteria growth without the addition of **34d**. Figure 4.10b shows an aliquot from the experiment with a concentration of twice the MIC. Qualitatively, it can be seen that there is significantly less bacteria when the active compound is present.

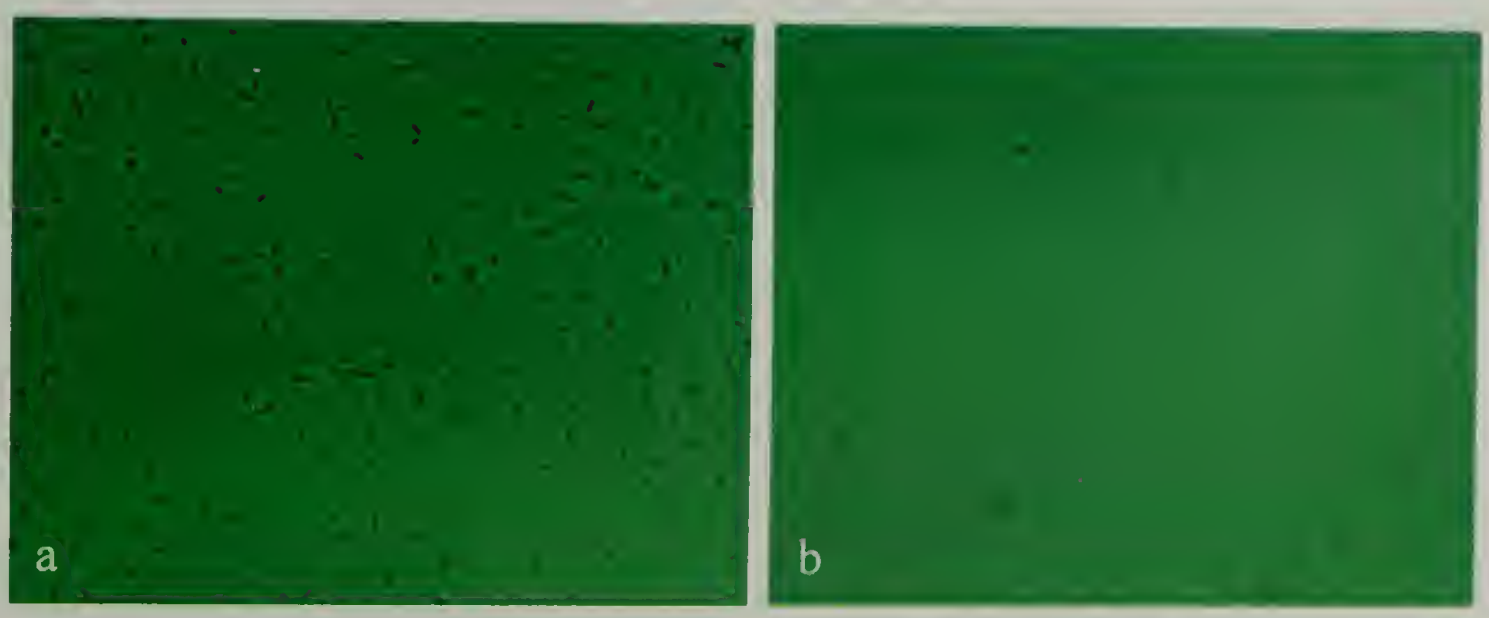

Figure 4.10: MBC test under the microscope after 24 hours. a) control b) 2MIC.

After diluting and plating the experiments on agar, bacterial colonies were grown overnight and quantified. Figure 4.11 shows pictures of the bacterial growth on the control plate and at two concentrations of **34d**, the MIC and twice the MIC. Full bacterial growth, Figure 4.11a, shows significant colony formation, as expected. The experiment performed at the MIC, Figure 4.11b, still shows bacterial growth, however there are 50% less colonies present when compared to the control plate.[10] This was expected since the bacteria have more time (24 hours) to grow than in a typical MIC experiment (6 hours). Regrowth of bacteria was also seen at the MIC if the experiment continued for a longer amount of time since the bacteria was only inhibited and not killed. At twice the MIC, Figure 4.11c, there were only a few colonies, representing more than 99% reduction in bacterial growth. This concentration, twice the MIC, can thus be designated as the MBC. These results highly suggest that at the MIC, **34d** is simply bacteriostatic, inhibiting bacterial growth, while the MBC is bacteriolytic, destroying and lysing the bacterial cells.

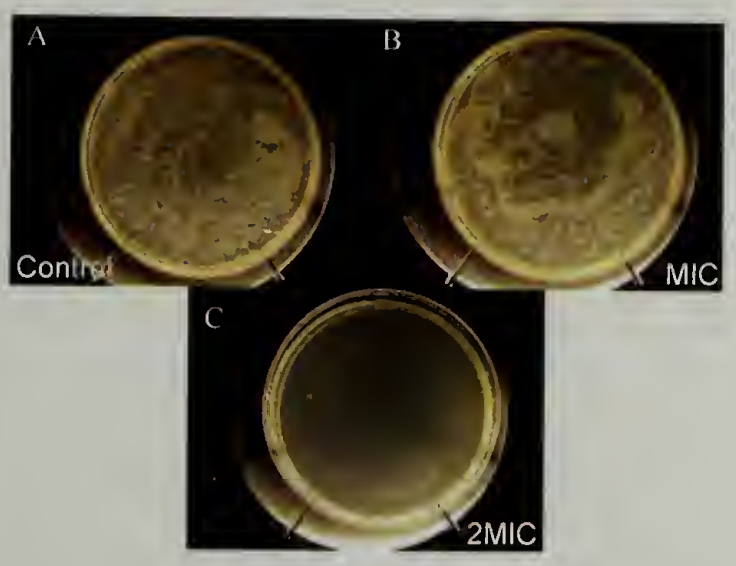

Figure 4.11: Pictures of the experiment confirming that MBC is twice the MIC. A) control, B) MIC, and C) 2MIC.

[10] Further diluted samples from the liquid experiments were plated on agar and allowed quantification of the number of colonies formed at each concentration of **34d**.

While hemolytic assays confirmed the selectivity of **34d**, the activity might decrease if it becomes unavailable for interactions with bacterial cytoplasmic membranes due to the presence of excess of mammalian cytoplasmic membranes or other compounds present in whole blood. Based on this assumption, the potential for saturation kinetics was tested by comparing preincubation versus coincubation variations of drug, bacterial target cells, and fresh human blood. Briefly, this experiment was set up in the same way as the MIC experiment, only with the addition of 1% final volume of whole blood. There were three experiments investigated. The first included mixing blood, bacteria, and **34d** together to give the active compound equal opportunity to act on either the RBC or bacterial membranes. The second experiment mixed blood and **34d** for 30 minutes before introducing bacteria, which allowing the active compound time to become inactivated by the presence of RBC membrane before introducing the bacteria. The third experiment mixed the bacteria and **34d** for 30 minutes to allow the active compound to interact with bacterial membranes before introduction of RBC membranes.

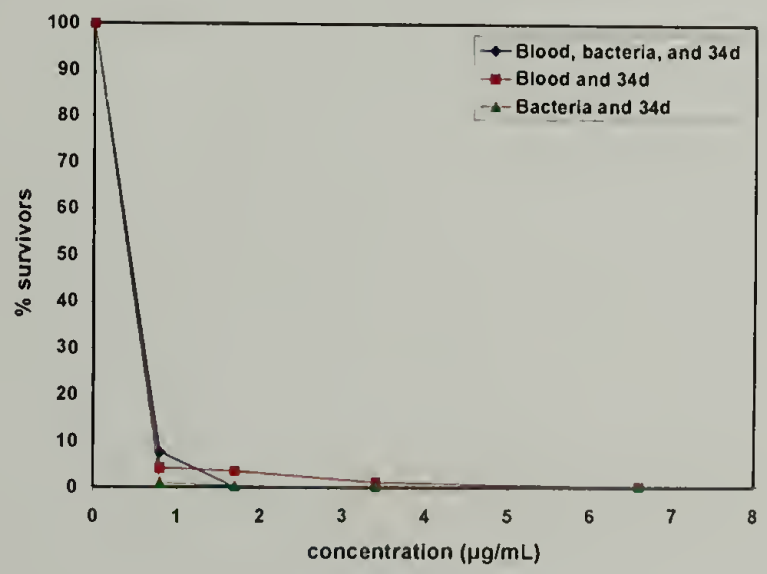

Figure 4.12: Whole blood experiment with *E. coli* showing that 34d is not inactivated in the presence of red blood cells.

Repeated experiments with both gram-negative (*E. coli*, Figure 4.12) and gram-positive (*B. subtilis*, data not shown) strains indicated that **34d** is not inactivated in the presence of excess eukaryotic cytoplasmic membrane or against the background of a rich biological matrix such a whole blood. All three experimental variations resulted in greater than 90% reduction of cell growth at the respective MIC concentrations (0.8 μg/mL for *E. coli* and 1.6 μg/mL for *B. subtilis*) for both bacterial strains. Thus, **34d** does not appear to be inactivated in the presence of whole blood during these experiments.

Time-kill experiments show bactericidal kinetics indicating that short exposure times are sufficient for complete activity, similar to host defense peptides, where at concentrations 4-fold higher than the MIC kill up to 99.999% of the bacteria within 5 minutes.(35) In this experiment, the bacteria were exposed to **34d** for the specified periods of time and the amount of bacteria remaining was quantified. Figure 4.13 shows the results for *B. subtilis*. This experiment was also done with *E. coli* to show that the kinetics are not strain specific. A concentration dependent susceptibility is obvious: both the MIC and twice the MIC producing a continuous decrease in the number of surviving cells within the first few minutes and continuing over the full thirty-minute experiment. At concentrations of half the MIC, the bacterial growth was significantly hindered compared to the control experiment but not inhibited. The rapid reduction in the viable count as observed here is a characteristic feature of membrane permeating agents.(9) This shows that even at low concentrations, **34d** still effects bacterial growth. Continuous incubation showed regrowth of these samples over 24

hours. This is not surprising since there is a limit to the quantity of bacteria exposed to **34d** before an increase in MIC is observed. Early experiments have shown that even a ten-fold increase in the initial amount of bacteria rendered the active compound "inactive" suggesting that there is a specific ratio of compound to bacteria needed for activity. The amount of bacteria used in this experiment is 100-fold more than the amount used in the traditional MIC experiment.

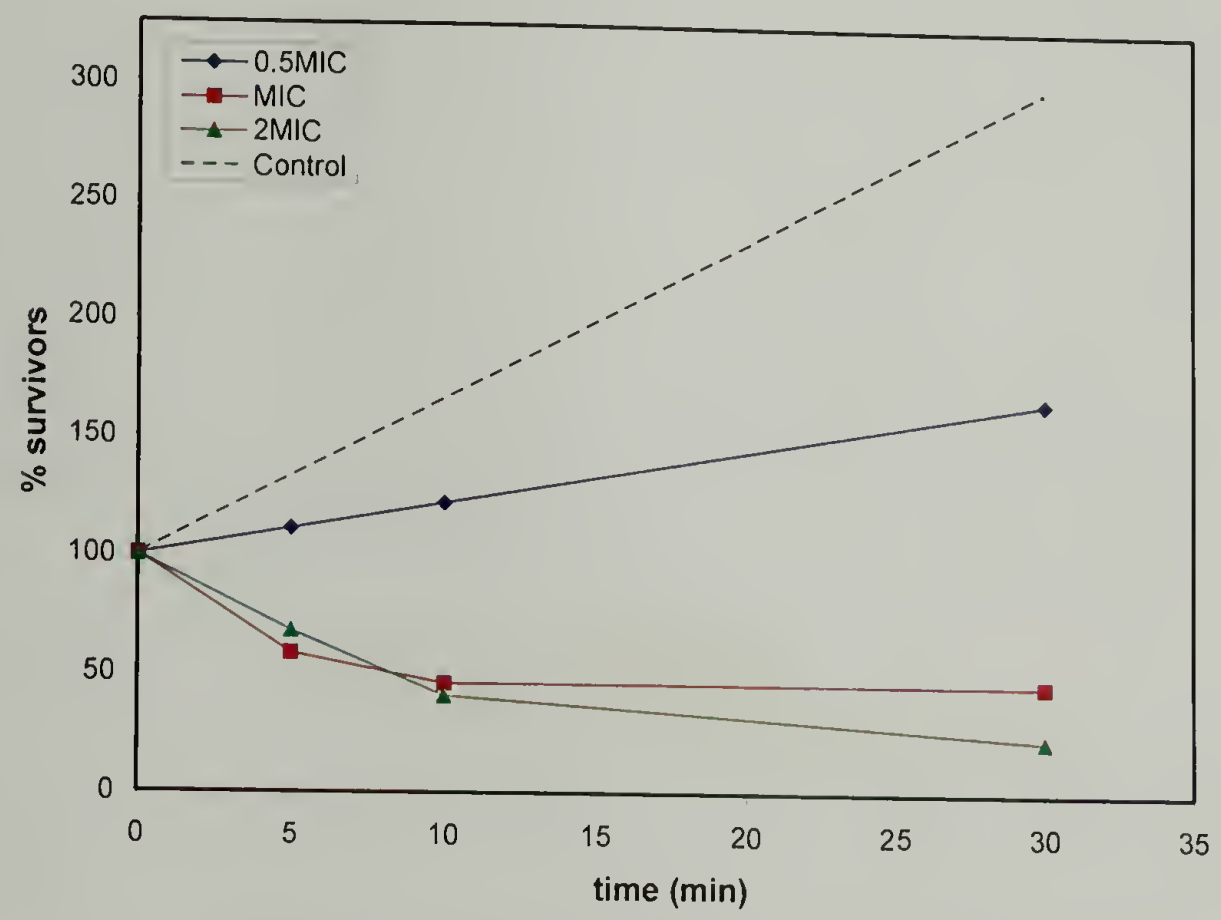

Figure 4.13:Kinetic Studies with *B. subtilis* and 34d.

To experimentally measure the ability of bacteria to develop resistance to **34d**, both *S. aureus* and *E. coli* were exposed to sublethal concentrations of **34d**. After exposure for 24 hours, the MIC was determined and any change in the value was noted. This process was continued for 26 days. This dilution method is commonly used in industrial settings and is the standard accepted in the literature.(36-38) The positive controls used in this experiment are ciprofloxacin for *E. coli* and penicillin for *S.*

aureus, two antibiotics towards which these bacteria readily develop resistance. The development of resistance is indicated by a progressive increase in the MIC value over time.

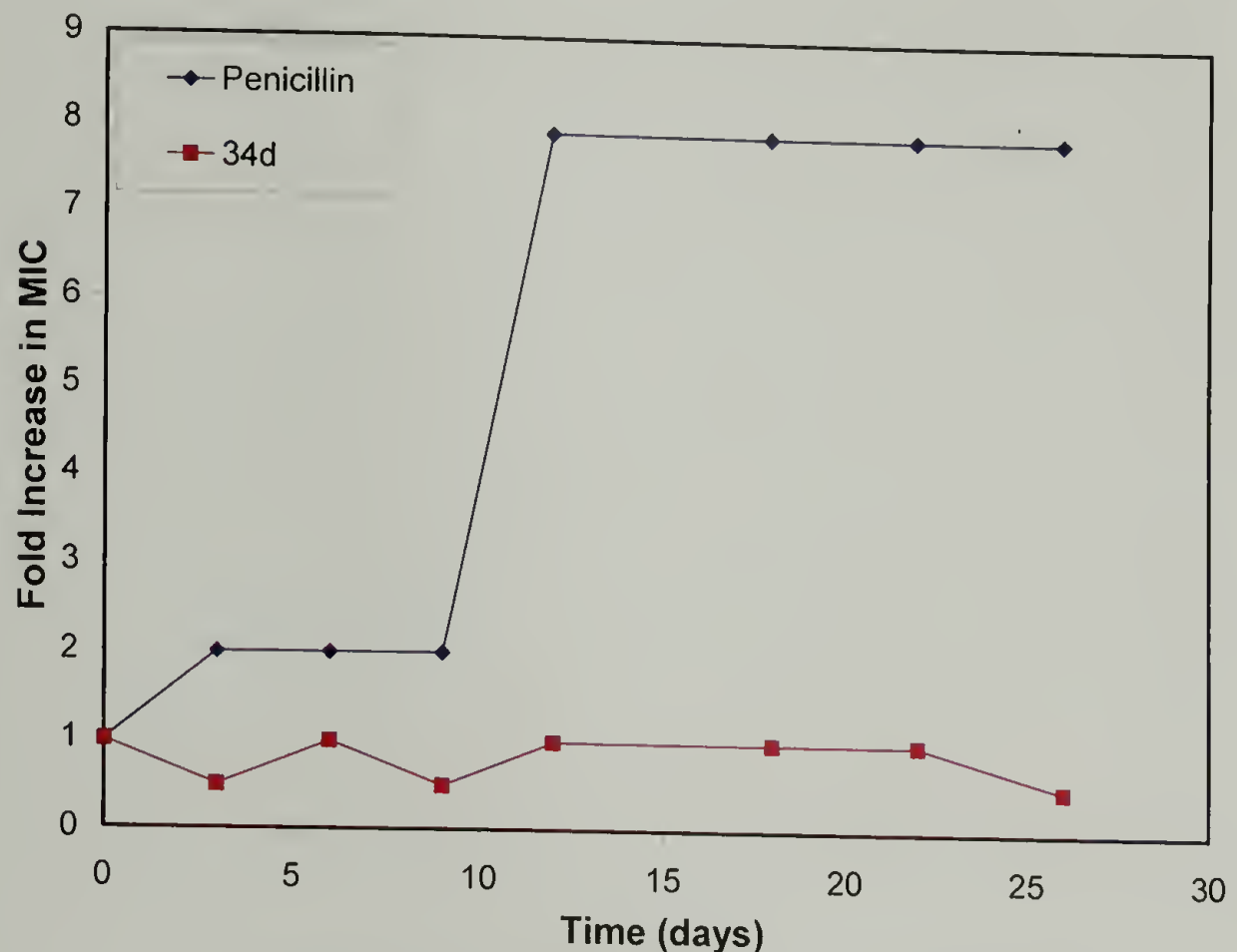

Figure 4.14: Resistance studies with *S. aureus*.

The results for *S. aureus* are shown in Figure 4.14 and similar results were obtained for *E. coli* (not shown). The MIC of the control, penicillin, increased over time. After three days of exposure, the MIC doubled as the bacteria started to develop resistance to the commercially available drug. At the end of the experiment, the bacteria developed significant resistance towards ciprofloxacin, as indicated by the 8-fold increase in MIC. When exposed to **34d**, the bacteria did not show any change in susceptibility. This is a very important and promising result, suggesting a very low likelihood of resistance developing upon longer exposures. Even though resistance to HDPs is not extensively reported, there is evidence that some resistance results from a reduction of the net negative surface charge on bacterial membranes.(39-43) This

decreased net negative charge could induce resistance against *meta*-PE molecules, but they will not be susceptible to other mechanisms of antibiotic resistance such as proteolytic degradation (see Section 1.6).

4.6 Prevention of Biofilm Growth

There has been several reports of antimicrobial agent incorporation into polymeric substrates(44-47), most of which discuss the prevention of biofilm growth on a substrate over a specified length of time while the active agent leaches out. In order to look at the prevention of bacterial growth on a surface, **34d** was incorporated into polymer plugs of either polyurethane (PU) or poly(vinyl chloride) (PVC). These samples were prepared by making polymer plugs at the bottom of glass vials. In the case of PU, the polymer was a viscous liquid and a solution of **34d** could easily be mixed with the polymer. Upon moisture curing, the mixture formed a hard plug. To make the PVC samples, catheter tubing was dissolved in THF and then mixed with **34d**. Upon evaporation of the solvent, an opaque plug was formed in the vial. In both cases, **34d** was introduced as 5% by volume; for every 1 mL of polymer solution 50 μL of **34d** (2 mg/mL in DMSO) was added.[11] This strategy incorportates 0.05 and 0.008 wt% **34d** into PVC and PU, respectively. The prepared vials were then inoculated with *S. aureus* and the bacterial growth on the surface was monitored.

---

[11] To make sure that **34d** was incorporated within the polymer plug, some surfaces were rinsed with DMSO to remove any adsorbed **34d**. The plugs that were rinsed compared to plugs that were not rinsed showed no difference in antibacterial activity, indicating that **34d** is most likely incorporated into the plug.

With the PU samples it was possible to determine the number of living cells by using a dye that becomes UV active (red) when metabolized by cells. The difference in absorption between solutions with and without living cells can be quantified. After incubation and before dye addition, the media was fully changed to monitor only the cell growth on the surface and not that in solution, since there was significant cell growth in the supernatant. One potential problem with this experiment is that it does not account for the bacteria adhered to the vial wall left behind during the media change.

Pictures of the bacterial growth in the supernatant can be seen in Figure 4.15a. The supernatant of both the control and the treated sample have similar turbidities. Pictures of the PU sample vials after media exchange are shown in Figure 4.15b. The control sample, a plug with no incorporation of **34d**, shows significant bacterial growth, as shown by the deep red color of the vial on the right of Figure 4.15b. The treated sample, far left sample in Figure 4.15b, still retains the yellow color of the media indicating a reduction in cell adhesion and growth on the PU surface in comparison to the control sample. This is a significant finding indicating that even with a bacteria-rich supernatant, attachment and growth on the PU surface is prevented.

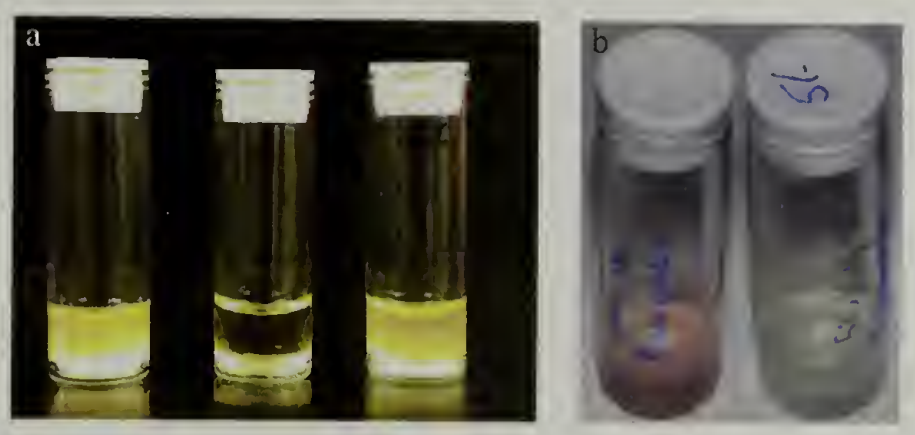

Figure 4.15: Biofilm growth experiment with PU. A) Sample vials before media exchange, B) Sample vials after media exchange. In both cases, the control sample is on the far right and the treated samples on the far left. In A) the middle sample is an uninoculated

Upon investigating the PU surfaces under a microscope, Figure 4.16, significant bacterial coverage is seen on the control sample (Figure 4.16a), while the bacterial growth on the treated sample (Figure 4.16b) is sparse. These samples were treated with a live-dead stain to increase the visualization of the cell colonies. The green dye is small so it can be taken up into both living and dead cells. However, the red dye is large and can only be taken into the dead cells, which have more permeable membranes. From these pictures, it is clear there is a reduction in bacterial film formation on the treated PU samples that corroborates the experiment discussed above with the metabolic dye: the incorporation of **34d** into a PU plug can prevent bacterial adhesion even when exposed to a bacteria-rich supernatant.

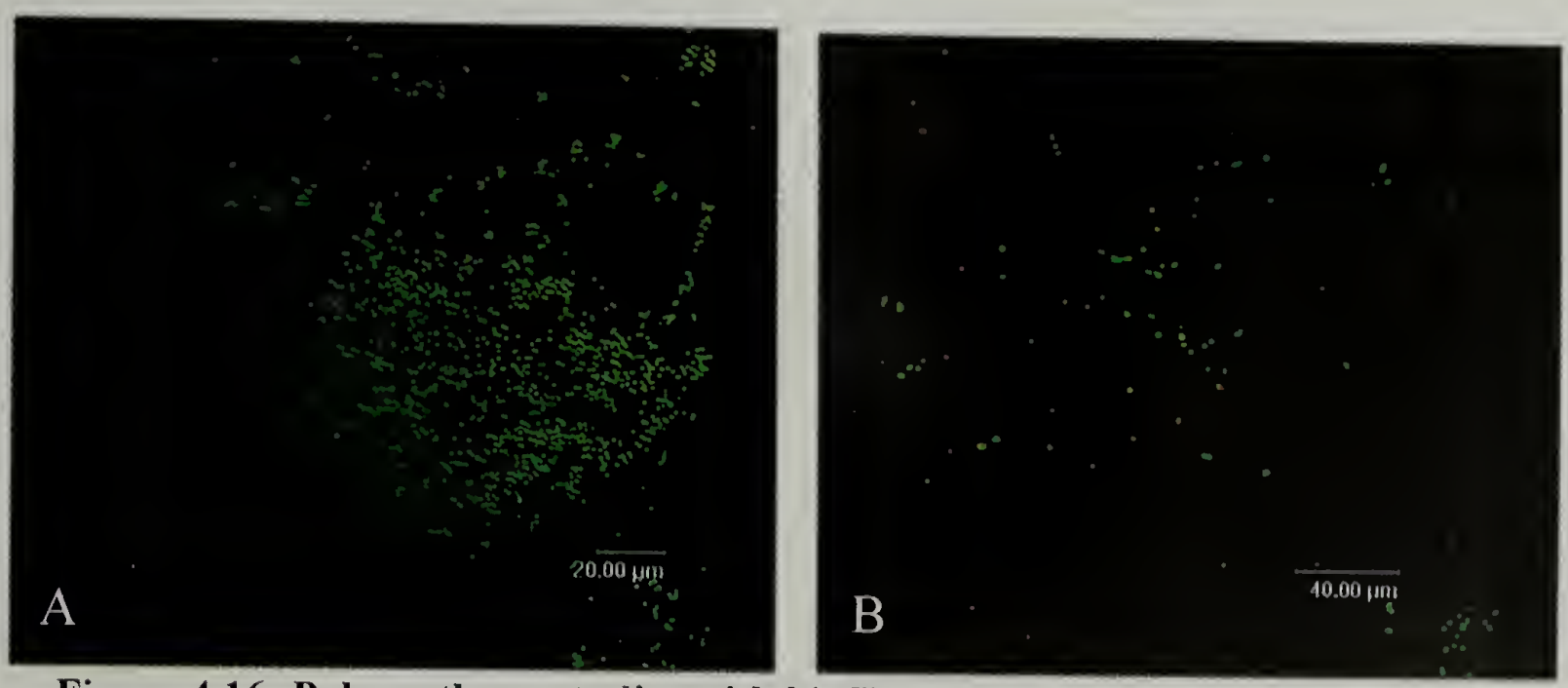

Figure 4.16: Polyurethane studies with biofilm growth A) Untreated (significant bacterial adhesion) B) Treated (minimal bacterial adhesion)

This experiment was also performed with PVC samples prepared as stated above. These samples were more challenging than the PU samples since the plugs often floated in the cell media making the use of the metabolic dye to determine cell surface adhesion very tricky. Pictures of these vials are shown in Figure 4.17. The untreated sample (Figure 4.17a) shows full bacterial growth as determined by the turbidity of the

cell growth media above the plug. The treated sample (Figure 4.17b) has an optically clear supernatant suggesting no bacterial growth. Examining the media under a microscope suggests there are no cells present and even with further incubation of the samples, no cell growth is observed. This result highly suggests full reduction in bacteria present in the media.

Figure 4.17: Catheter tubing with 34d incorporation a) untreated sample b) treated sample.

Table 4.10: Summary of prevention of bacterial adhesion to polymer plugs.

	Reduction in Cells (%)	
Substrate	Untreated	5% v/v **34d** (wt%)
PVC	0	99 (0.05)
PU	0	80 (0.008)

The data for the PU and PVC samples discussed above is summarized in Table 4.10. Incorporation of **34d** into both substrates tested prevented more than 80% of the bacterial growth when compared to the control samples. However, when probing the

long-term activity of these samples, the question of **34d** leaching from the plugs was raised. To investigate this, an experiment was done exposing the plugs to water for different periods of time at 37°C. Then HPLC was used to monitor the increase of **34d** in the water over time. This experiment was performed over 120 hours and the results are shown in Figure 4.18. It can be seen that significant leaching of **34d** occurs after 70 hours. This is not surprising since **34d** is a charged molecule and the PU plug offers a very non-favorable hydrophobic environment.

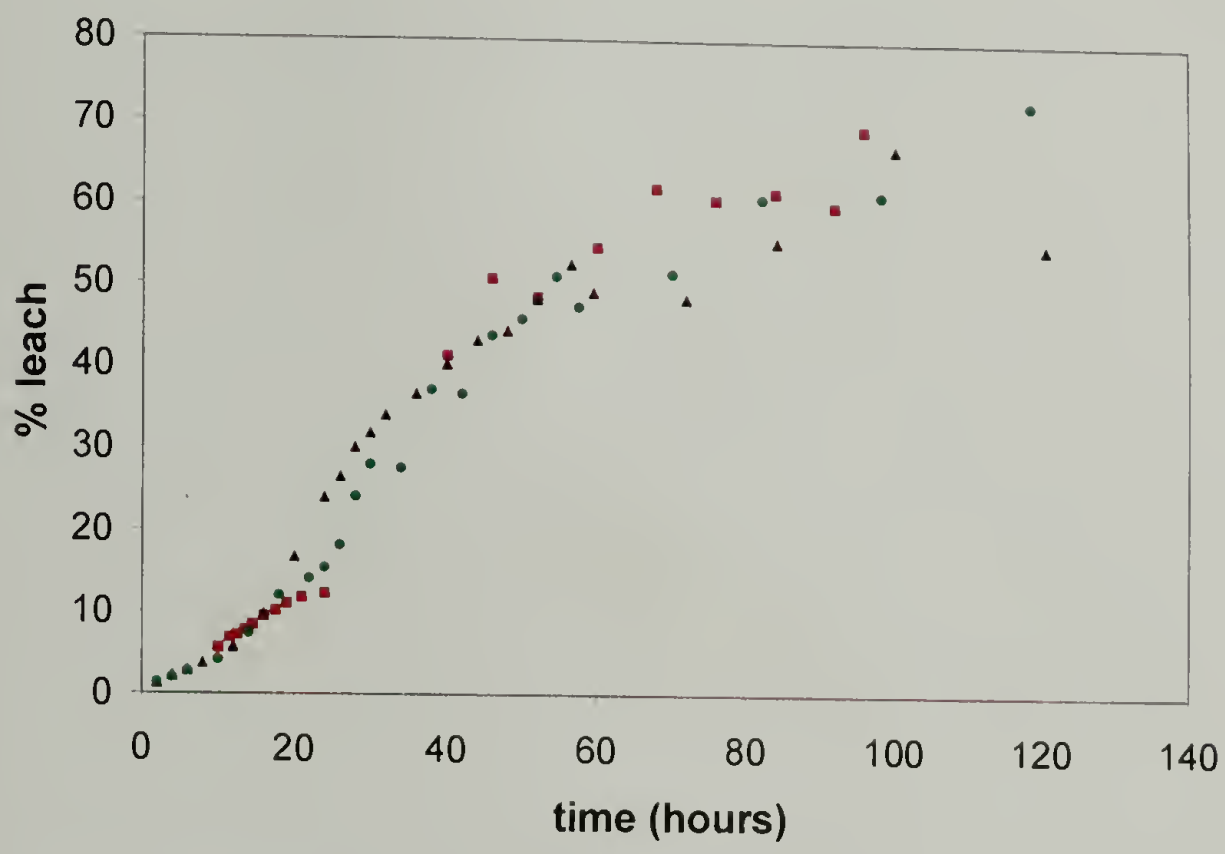

Figure 4.18: HPLC leaching experiment (three different polyurethane plugs).

The shape of the curve suggests that during the first several hours the active compound is leaching at an extremely slow rate, after which the rate significantly increases until it levels off after 70 hours. When analyzing this data as mass at time t (M(t)) versus the square root of time (Figure 4.19), the shape of the plot suggests that release at the initial time points is governed by something other than simple diffusion of the active compound. This is most likely due to the initial swelling by water of the PU

plug at early times. Initially, the plug is hard and glassy but at the end of the experiment it is soft and swollen. This behavior is characteristic of Case II diffusion, where there plug needs to be swollen by water initially to induce leakage of **34d**. The active compound is not initially solvated in the hydrophobic polymer plug so it cannot easily diffuse out. When the water begins to swell the plug, it also solvates the oligomer and promotes leaching. This swelling process most likely happens during the first several hours of the experiment, after which the oligomer can more easily diffuse out of the plug.

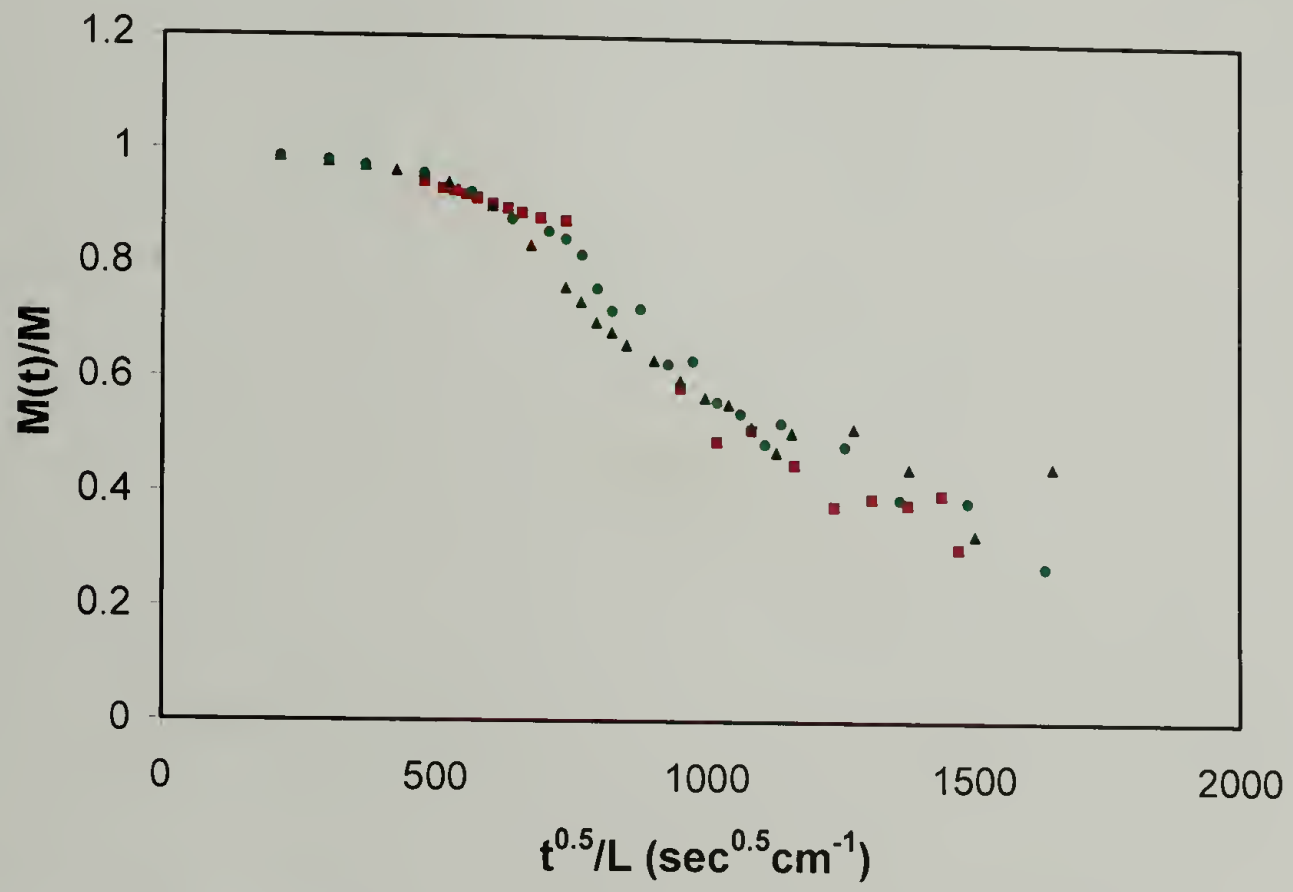

Figure 4.19: Leaching experiment data replotted. Notice the change in slope after the initial portion of the experiment.

Leaching of the active compound suggests that the bactericidal action may occur due to solubilization of the active compound. Leaching continued during the exposure time of 24 hours for the above experiments. Currently, we are investigating the reintroduction of an inoculated supernatant to see if there is still prevention of bacterial adhesion after full leaching of the active compound. The apparent leaching of the active

compound is not detrimental to the use in biomedical devices, such as catheters, because often the desired time period for antibacterial activity is between 24 and 48 hours.

4.7 Breast Cancer Cell Activity

The activity of **34d** against breast cancer cells was investigated, since the phospholipid composition of cell membranes of cancer cells has a slight excess of negatively charged molecules (3 to 6% as opposed to the 10% for bacterial cells).(48) This change in membrane composition was investigated as a handle to target cancerous cells over non-cancerous cells. In this set of experiments, the activity of **34d** against two human breast cancer cell lines, MCF-7 (ATCC HTB-22) and TMX2-28, and one non-cancerous breast cell line, MCF-10A (ATCC CRL-10317), was investigated. The cells were grown in media supplemented with 5% bovine growth serum using standard techniques. In short, the cells were seeded in flasks and allowed to incubate at 37°C with 5% CO_2. After growing to 50% confluence, the cells were removed from the flasks using trypsin. The trypsin was then removed from solution by centrifugation and the cells were resuspended into fresh medium. Sterile 96 well plates were seeded at a density of 10,000 cells/well and allowed to grow overnight yielding 50% confluence. The molecules were then added to solution and allowed to further incubate for 48 hours. A dye that becomes optically active upon being metabolized was used to determine the number of cells in each well.

Table 4.11 shows the activity of **34d** against the three cell lines. When tested against the cancerous cell lines, MCF-7 and TMX2-28, **34d** inhibits growth of 90% (IC_{90}) of the cells at 6.3 μg/mL but starts negatively affecting cell growth at

Table 4.11: Activity of 34d against three different eukaryotic cell lines. It can be seen that there is selectivity towards the cancerous cell lines over the non-cancerous cell lines.

Cell Line	Cell Type	IC_{90} (μg/mL)	IC_{90} (mM)	Selectivity (IC_X/IC_{MCF10A})
MCF-7	cancerous	6.3	10.5	2
TMX2-28	cancerous	6.3	10.5	2
MCF10A	non-cancerous	12.5	21.0	N/A

eoneentrations as low as 1.6 μg/mL. Against MCF-10A eells, the IC_{90} is 12.5 μg/mL. This shows that there is a seleetivity of 2 towards eaneerous breast eells over non-eaneerous breast eells. It ean be hypothesized that this seleetivity eomes from differenees in the phospholipid eomposition of the eell membrane between eancerous and non-eaneerous eells. This aetivity against normal breast cells is not dependent on eukaryotic cell origin beeause similar aetivity is seen against HEPG2 cells, a strain of normal liver cells. Though the seleetivity results for eukaryotic cells are not as promising as those for prokaryotie eells, these findings provide a nice starting point for developing novel anti-eancer drugs.

4.8 Conclusions

The biologieal aetivity of several *meta*-PE polymers and discrete oligomers was probed, and results showed that seleetivity towards bacteria eould be aeeomplished with

these simple structures. Several subtle modifications to the chemical structure resulted in dramatic biological differences. Small polymeric samples were as selective as the natural peptide analog, Magainin, with discrete oligomers proving to be most selective. The best discrete oligomer, **34d**, showed broad-spectrum antibacterial activity as well as activity towards breast cancer cells. Material incorporation of **34d** within PU and PVC showed promising results in preventing biofilm formation on these polymeric films.

4.9 References

1. Oh, S. T., Han, S. H., Ha, C. S. & Cho, W. J. (1996) *J. Appl. Polym. Sci.* **59,** 1871-1878.
2. Woo, G. L. Y., Mittelman, M. W. & Santerre, J. P. (2000) *Biomaterials* **21,** 1235-1246.
3. Patel, M. B., Patel, S. A., Ray, A. & Patel, R. M. (2003) *J Appl Polym Sci* **89,** 895-900.
4. Tiller, J. C., Liao, C. J., Lewis, K. & Klibanov, A. M. (2001) *Proc. Natl. Acad. Sci. U.S.A.* **98,** 5981-5985.
5. Sauvet, G., Fortuniak, W., Kazmierski, K. & Chojnowski, J. (2003) *J Polym Sci Part A: Polym Chem* **41,** 2939-2948.
6. Kenawy, E. R., Abdel-Hay, F. I., El-Shanshoury, A. & El-Newehy, M. H. (2002) *J Polym Sci Part A: Polym Chem* **40,** 2384-2393.
7. Gelman, M. A., Weisblum, B., Lynn, D. M. & Gellman, S. H. (2004) *Org. Lett.* **6,** 557-560.
8. Popa, A., Davidescu, C. M., Trif, R., Ilia, G., Iliescu, S. & Dehelean, G. (2003) *Reactive and Functional Polmyers* **55,** 151-158.
9. Haneock, R. E. & Chapple, D. S. (1999) *Antimicrob. Agents Chemother.* **43,** 1317-1323.
10. Tashiro, T. (2001) *Macromolecnlar Mater. Eng.* **286,** 63-87.
11. Worley, S. D. & Sun, G. (1996) *Trends Polym. Sci.* **4,** 364-370.
12. Albert, M., Feiertag, P., Hayn, G., Saf, R. & Honig, H. (2003) *Biomacromolecules* **4,** 1811-1817.
13. Rivas, B. L., Pereira, E. D., Mondaea, M. A., Rivas, R. J. & Saavedra, M. A. (2003) *J. Appl. Polym. Sci.* **87,** 452-457.
14. Tossi, A., Sandri, L. & Giangaspero, A. (2000) *Biopolymers* **55,** 4-30.
15. Zasloff, M. (2002) *Nature (London)* **415,** 389-395.
16. Zasloff, M. (1992) *Curr. Opin. Immmnol.* **4,** 3-7.
17. Boman, H. G. (2000) *Immmnol. Rev.* **173,** 5-16.
18. Hancoek, R. E. & Lehrer, R. (1998) *Trends Biotechnol.* **16,** 82-88.
19. DeGrado, W. F. (1988) *Adv. Protein Chem.*, 51-124.
20. Oren, Z. & Shai, Y. (1998) *Biopolymers* **47,** 451-463.
21. Porter, E. A., Wang, X., Lee, H. S., Weisblum, B. & Gellman, S. H. (2000) *Nature (London)* **404,** 565.
22. Raguse, T. L., Porter, E. A., Weisblum, B. & Gellman, S. H. (2002) *J. Am. Chem. Soc.* **124,** 12774-12785.
23. Porter, E. A., Weisblum, B. & Gellman, S. H. (2002) *J. Am. Chem. Soc.* **124,** 7324-7330.
24. Hamuro, Y., Schneider, J. P. & DeGrado, W. F. (1999) *J. Am. Chem. Soc.* **121,** 12200-12201.
25. Liu, D. & DeGrado, W. F. (2001) *J. Am. Chem. Soc.* **123,** 7553-7559.
26. Gellman, S. H. (1998) *Acc. Chem. Res.* **31,** 173-180.
27. Wu, C. W., Sanborn, T. J., Zuckerman, R. N. & Barron, A. E. (2001) *J. Am. Chem. Soc.* **123,** 2958-2963.

28. Wu, C. W., Sanborn, T. J., Huang, K., Zuckerman, R. N. & Barron, A. E. (2001) *J. Am. Chem. Soc.* **123,** 6778-6784.
29. Patch, J. A. & Barron, A. E. (2003) *J. Am. Chem. Soc.* **125,** 12092-12093.
30. Miller, S. M., Simon, R. J., Ng, S., Zuckerman, R. N., Kerr, J. M. & Moos, W. H. (1995) *Drug Dev. Res.* **35,** 20-32.
31. Tew, G. N., Lui, D., Chen, B., Doerksen, R. J., Kaplan, J., Corroll, P. J., Klein, M. L. & DeGrado, W. F. (2002) *Proc. Natl. Acad. Sci. U.S.A.* **99,** 5110-5114.
32. *National Committee for Clinical Laboratory Standards. 2002. Performance Standards for antimicrobial susceptibility testing; 12th informational supplement (aerobic dilution) M100-S12. National Committee for Clinical Laboratory Standards, Wayne, PA.*
33. Maloy, W. L. & Kari, U. P. (1995) *Biopolymers* **37,** 105-122.
34. Arnt, L., Nusslein, K. & Tew, G. N. (2004) *J. Polym. Sci. Part A* **42,** 3860-3864.
35. Hancock, R. E. & Rozek, A. (2002) *FEMS Microbio. Lett.* **206,** 143-149.
36. Shelburne, C. E., Coulter, W. A., Olguin, D., Lantz, M. S. & Lopatin, D. E. (2005) *Antimicrobial Agents and Chemotherapy* **49,** 183-187.
37. Cudic, M., Lockatell, C. V., Johnson, D. E. & Otvos, L. (2003) *Peptides* **24,** 807-820.
38. Lui, S. Y., Yeoh, K. G. & Ho, B. (2003) *Journal of Clinical Microbiology* **41,** 5011-5014.
39. Shi, Y. X., Cromie, M. J., Hsu, F. F., Turk, J. & Groisman, E. A. (2004) *Molecular Microbiology* **53,** 229-241.
40. Peschel, A., Otto, M., Jack, R. W., Kalbacher, H., Jung, G. & Gotz, F. (1999) *Journal of Biological Chemistry* **274,** 8405-8410.
41. Guo, L., Lim, K. B., Poduje, C. M., Daniel, M., Gunn, J. S., Hackett, M. & Miller, S. I. (1998) *Cell* **95,** 189-198.
42. Gunn, J. S., Lim, K. B., Krueger, J., Kim, K., Guo, L., Hackett, M. & Miller, S. I. (1998) *Molecular Microbiology* **27,** 1171-1182.
43. Nummila, K., Kilpelainen, I., Zahringer, U., Vaara, M. & Helander, I. M. (1995) *Mol Microbiol* **16,** 271-278.
44. Piozzi, A., Francolini, I., Occhiaperti, L., Di Rosa, R., Ruggeri, V. & Donelli, G. (2004) *Journal of Chemotherapy* **16,** 446-452.
45. Schierholz, J. M., Steinhauser, H., Rump, A. F. E., Berkels, R. & Pulverer, G. (1997) *Biomaterials* **18,** 839-844.
46. Schierholz, J. M., Rump, A. & Pulverer, G. (1997) *Arzneimittel-Forschung/Drug Research* **47,** 70-74.
47. Donelli, G., Francolini, I., Piozzi, A., Di Rosa, R. & Marconi, W. (2002) *Journal of Chemotherapy* **14,** 501-507.
48. Papo, N. & Shai, Y. (2003) *Biochem. J.* **42,** 9346-9354.

CHAPTER 5

PROBING THE MECHANISM OF ANTIBACTERIAL ACTION

5.1 Introduction

Many host defense peptides exert their antimicrobial action through permeabilization of cellular membranes. Antimicrobial agents can distinguish between host and invader cells because of the distinct nature of their cellular membranes. The exact mechanism of action for host defense peptides against invader cells remains debated in the literature. There are three general mechanisms of membrane disruption discussed: the carpet, barrel-stave, and binding mechanisms.

The carpet mechanism suggests that the antimicrobial agent aggregates onto the membrane, parallel to the surface, forming a "carpet" as the concentration increases.(1, 2) This aggregation ultimately causes the membrane to thin and rupture, killing the cell. In the barrel-stave mechanism, the membrane-active compound forms stable trans-membrane pores via self-assembly, which lead to uncontrolled transport of ions and small molecules across the membrane, resulting in cell death.(3, 4) The third mechanism of disruption involves the binding of cationic amphiphilic molecules to the outer layer of the membrane. This binding is highly favored because exposure of hydrophobic segments to the aqueous solution is decreased, resulting in an increase of pressure on the outer leaflet of the bilayer. The unequal pressure between the outer and inner bilayer causes the membrane to rearrange, creating transient holes in the cell membrane that results in cell death.(5)

Peptide concentration is known to have an effect on the mechanism of action. For instance, Hancock and coworkers have shown that virtually all cationic amphiphilic peptides cause severe membrane disruption if high enough concentrations are administered.(6) In order to study the relevant mechanism of action at the MIC, it is important to carry out experiments at or near this concentration. One of the most common and convenient ways to study mechanistic action involves the use of isolated lipid membranes made from pure or mixed lipids. It is important to note that it is difficult to establish whether the effectiveness against model membranes is biologically relevant to living cells, since artificial membranes fail to capture many biological features such as lipid heterogeneity and the presence of membrane proteins. This is further explained in the following section. However, lipid membrane studies provide an important starting point for establishing the mode of action.

5.2 Phospholipid Structure and Membrane Properties

Phospholipids are one of the major constituents that compose cellular membranes. Each phospholipid is composed of a hydrophobic fatty acid tail and a hydrophilic head group. This is shown schematically in Figure 5.1a. The composition of both the phospholipid head group and fatty acid tail can vary widely. Generally, the fatty acid tail made up of a long carbon chain between C_{14} and C_{20}, can either be saturated or unsaturated. Figure 5.1b shows the chemical structure of phosphatidylcholine, a phospholipid with a saturated C_{15} carbon chain and an ethylamine group attached to the phosphate head group. The amphiphilic property of lipids makes them ideal structural components of membranes since in aqueous solution

they aggregate into a bilayer structure with the hydrophobic portions inside the bilayer and the hydrophilic moieties toward the aqueous intra- and extra-cellular environments. The bilayer structure serves as an important permeability barrier to the diffusion of substances into or out of the cell. This membrane is a thin structure, about 8nm thick, which completely surrounds a cell. If this membrane is broken, the integrity of the cell is destroyed, causing uncontrolled leakage of the internal components resulting in cell death.

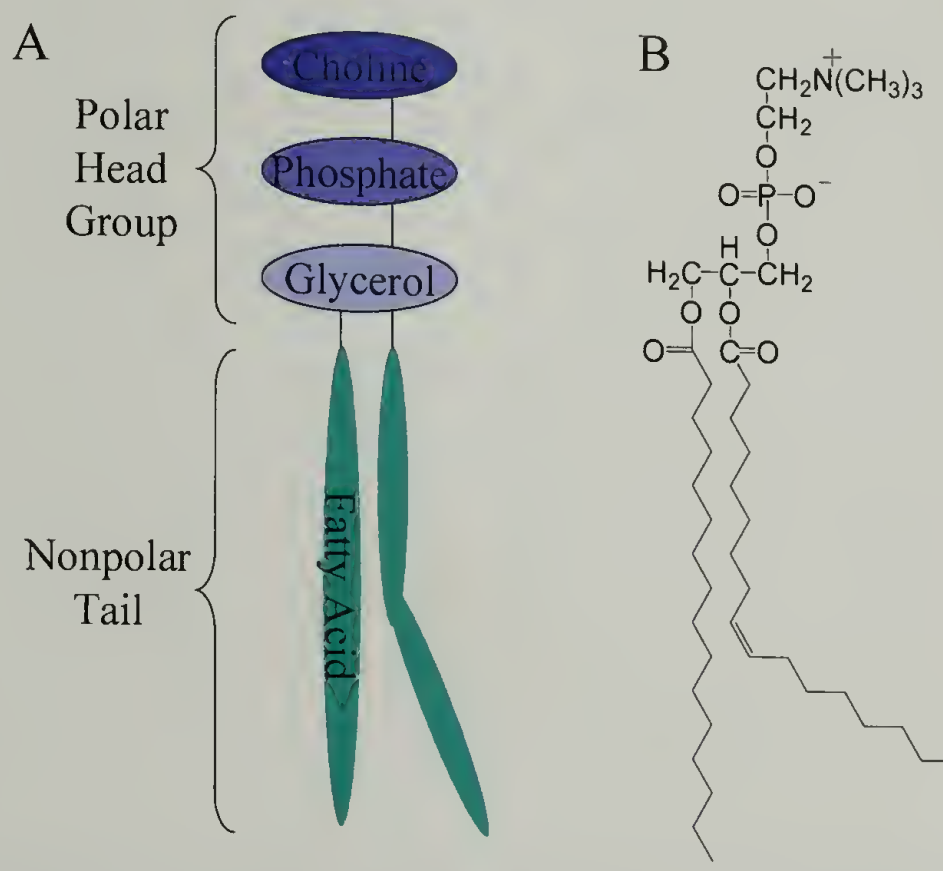

Figure 5.1: a) Schematic representation of a phospholipid. b) Chemical structure of phosphatidylcholine.

An important characteristic of cytoplasmic membranes is their fluidity. The lipid bilayer can be thought of as a two-dimensional fluid in which the lipid molecules are free to move laterally but individual molecules are normally constrained to their own monolayer.(7) The cell does produce enzymes called phospholipid translocators which catalyze the rapid flip-flop of specific phospholipids from one monolayer to the other, but this specialized process does not happen arbitrarily. The fluidity of the bilayer

depends on its composition and temperature. Lipids have a phase transition temperature at which the bilayer changes from a fluid state to a more rigid crystalline state and this temperature depends on the length and saturation of the hydrocarbon tail. Bacterial cells can maintain their fluidity as the environment changes by synthesizing different lipids as necessary.(7)

Another factor influencing membrane fluidity is the presence of membrane stiffening agents such as sterols and hopanoids. These are rigid planar molecules that make up 5-25% of the total lipids in eukaryotic cells, less in prokaryotic cells.(7, 8) In fact, cholesterol can be found in mammalian membranes at concentrations up to one molecule for every phospholipid molecule.(8) The strengthening of the membrane occurs due to the immobilization of the first few CH_2 groups of the hydrocarbon chains. This also makes the bilayer less deformable in the region near the lipid head groups, decreasing the permeability of the bilayer.

In both prokaryotes and eukaryotes the overall structure of the cytoplasmic membrane is similar, although there are some key chemical differences.(8) The chemical differences come from the types of lipids as well as the other membrane components such as proteins and strengthening agents as discussed earlier. In general, there are four major phospholipids found in mammalian membranes (head groups are shown in Figure 5.2): phosphatidylethanolamine (PE), phosphatidylserine (PS), phosphatidylcholine (PC), and sphingomyelin. In addition, phosphatidylglycerol (PG) is another lipid primarily found in bacterial membranes. Notice that both PS and PG carry a negative charge. These lipids are found in varying amounts in both prokaryotes and eukaryotes.

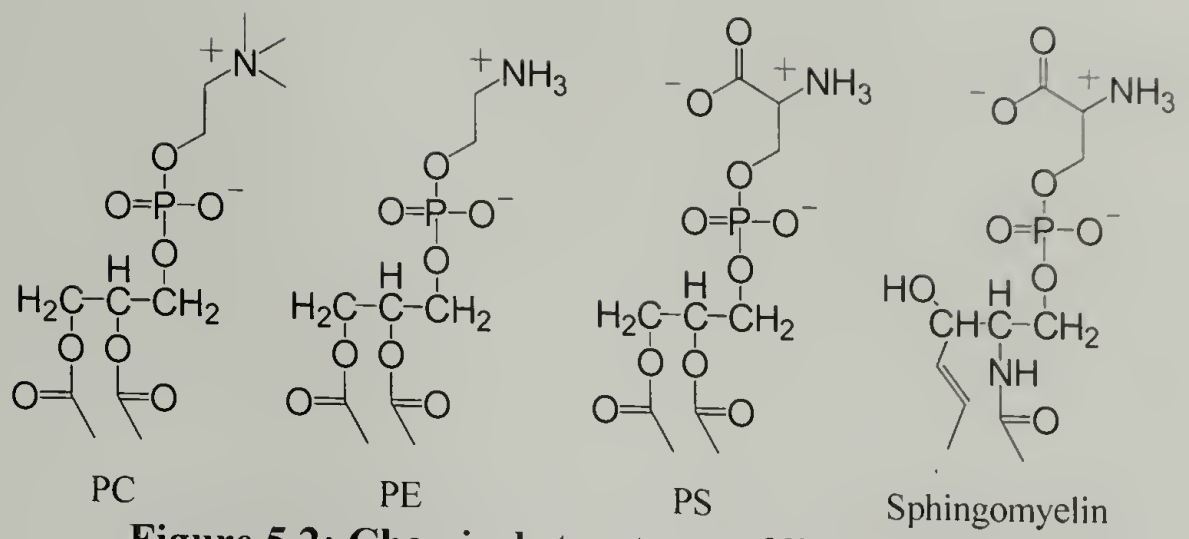

Figure 5.2: Chemical structures of lipid head groups.

Table 5.1: Approximate lipid compositions of different cell membranes. Numbers are percentage of total lipid by weight.

Cell	Cholesterol	PE	PS	PC	PG	Sphingomyelin	Glycolipids	Other
RBC	23	18	7	17	0	18	3	13
E. Coli	0	75	trace	0	20	0	0	5

Table 5.1 shows approximate lipid compositions of the membranes of red blood cells and *E. coli*.(7) The red blood cell, a eukaryotic cell, is made up of similar amounts of PE, PC, and sphingomyelin with some PS while *E. coli* is mostly PE. PG is found at varying concentrations in bacterial cells depending in species and growth conditions, but in general, it is roughly 20%.(9, 10)

An important factor to recall from Chapter 1 is that the lipid bilayer of mammalian cells is asymmetrical while bacterial cell membranes are nearly symmetrical. In the red blood cell membrane, almost all the lipid molecules that have choline in the head group (PC and sphingomyelin) are in the outer leaflet of the membrane while almost all of the phospholipid molecules that contain a terminal primary amino group (PE and PS) are in the inner membrane. Because the negatively charged phospholipid, PS, is only found in the inner leaflet, there is a difference in

charge between the two leaflets of the bilayer resulting in the neutrality of the outer bilayer. This difference between the neutral and negatively charged outer leaflets of red blood cell membranes and bacterial membranes, respectively, can lead to selectivity, as discussed in Chapters 1 and 4.

5.3 Uses of Vesicles in the Literature

Previous studies have described the use of synthetic lipid membranes, or vesicles, to assess the extent of amphiphilic molecule membrane activity.(11-15) The experiments reported suggest that an appropriate lipid composition contains negatively charged lipids mixed with zwitterionic lipids to mimic the charge distribution of bacterial membranes. These lipid vesicles are made via rehydration of lipid films, resulting in unilamellar vesicles which can then be utilized to monitor membrane activity. There are three common experiments established in the literature using vesicles; encapsulation of a fluorescent dye, lipid flip-flop, and peptide translocation.(6)

By incorporating a fluorescent dye inside vesicles, the extent and rate of membrane disruption can be investigated.(16-18) Calcein is commonly used since it self-quenches at high concentrations (inside the vesicle) and fluoresces (λ_{ex}= 490 nm, λ_{em}=515 nm) upon leakage from the vesicular membrane. This is shown schematically in Figure 5.3. In general, an increase in the rate of dye leakage over time due to the addition of antimicrobial peptides is directly related to the increase in the concentration of the peptides. At low concentrations of peptide, less than 100% of the dye is released suggesting that the amount of free peptide available in solution for membrane interaction is decreased.

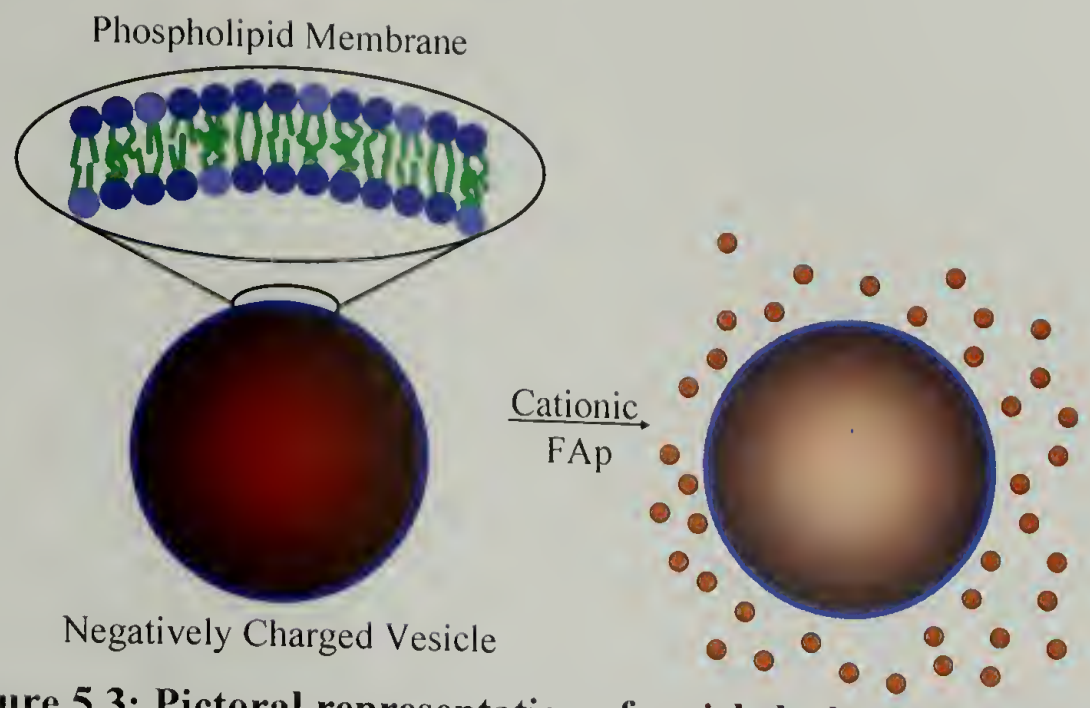

Figure 5.3: Pictoral representation of vesicle leakage experiment.

The above experiment can further probe membrane activity by incorporating two dyes encapsulated within the same vesicle.(19) By using two different size dyes, the selectivity of dye release can be monitored. While calcein is considered to be a relatively small dye (MW = 622), fluorescently tagged polymers up to molecular weights of 70,000 can be used as the larger dye. This experiment is shown schematically in Figure 5.4. The smaller of the two dyes will be released with any membrane permeabilization, as in the experiment above, however, the larger of the two

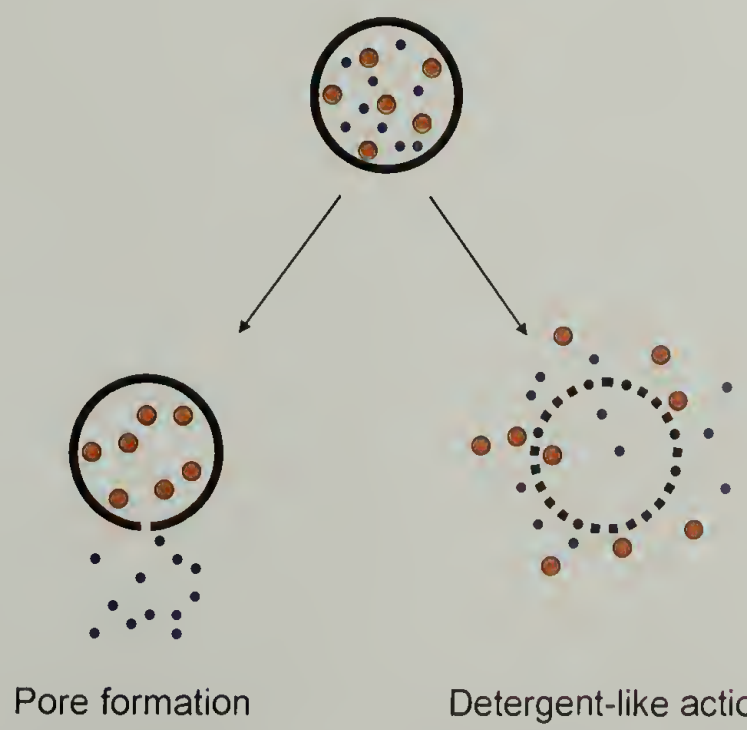

Figure 5.4: Schematic of vesicle pore formation vs. detergent-like action.

dyes will only be released upon complete destruction of the membrane (detergent-like action). This size selective leakage can be used to investigate pore-formation or detergent-like action against the membrane.

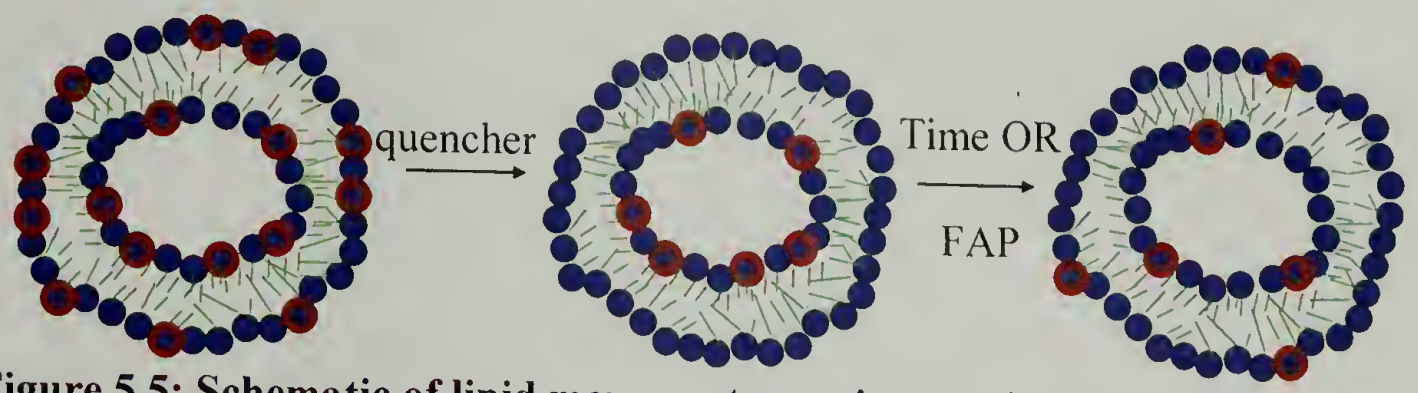

Figure 5.5: Schematic of lipid movement experiments a) symmetrically labeled vesicles, b) asymmetrically, c) symmetrically labeled vesicles.

The second vesicle experiment, pioneered by Matsuzaki and coworkers, monitors lipid flip-flop induced by cationic peptides, shown in Figure 5.5.(20) Vesicles are dynamic systems where the lipids are in motion and have the ability to move within a monolayer leaflet relatively fast. This lateral diffusion occurs with a diffusion coefficient of about 10^{-8} cm^2/sec, which means that the average lipid molecule diffuses the length of a large bacterial cell (~2 μm) in about one second.(7) On the other hand, movement between the membrane bilayers is usually slow, on the time-scale of hours or days, due to the unfavorable passage of a hydrophilic head group across the hydrophobic membrane core.(15) Depending on the lipid, it has been shown that this process occurs less than once a month for any individual molecule.(7) However, the addition of certain antimicrobial peptides has been shown to induce rapid lipid flip-flop across the membrane.(15, 18, 20, 21) One hypothesis is that this lipid movement, or flip-flop, is indicative of pore formation across the bilayer, as in the barrel-stave mechanism.(20) Another hypothesis is that after the peptides reach a sufficient concentration, they insert

into the membrane forming informal aggregates containing both peptides and lipids that span the membrane. The collapse of these channels would permit lipid translocation across the membrane as observed in lipid flip-flop experiments.(15)

A third vesicle experiment, often performed to look at cationic peptide-membrane interactions, is the measurement of peptide translocation.(6, 20) These assays monitor the uptake and enzymatic digestion of peptides in unilamellar vesicles, as shown in Figure 5.6. In these experiments, tryptophan residues on the peptide interact with dansyl groups on the lipid head groups within the membrane, showing an initial increase in fluorescence upon peptide binding. If the peptide is translocated across the membrane, it is digested by an enzyme encapsulated in the vesicle resulting in desorption of the peptide from the bilayer and a decrease in dansyl fluorescence. Since this requires the presence of tryptophan groups on the active compound, it cannot be utilized with our system.

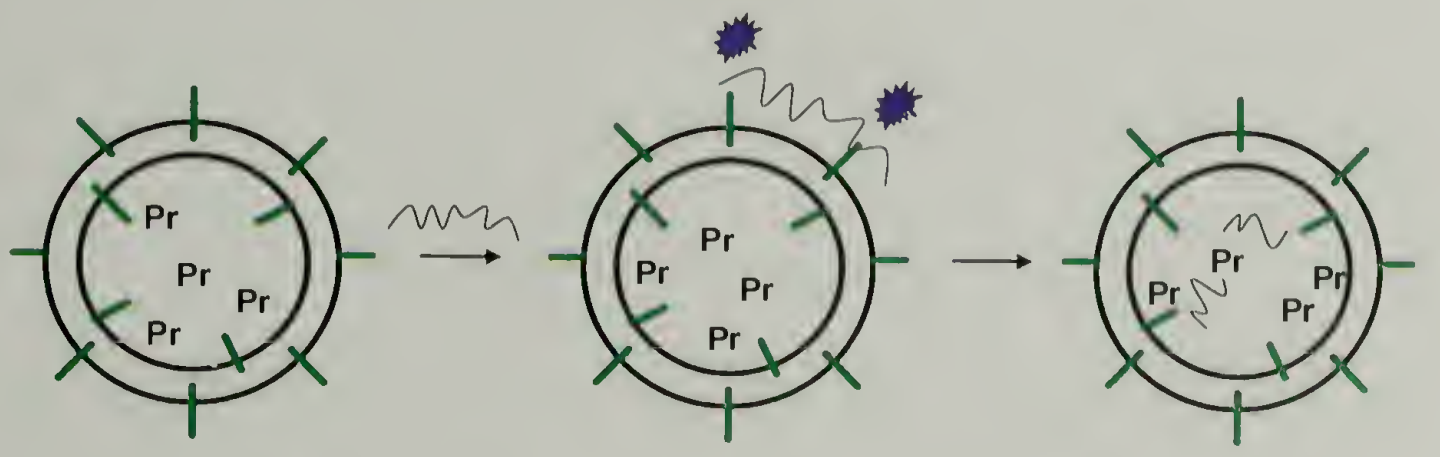

Figure 5.6: Schematic of peptide translocation.

Monitoring the interaction of host defense peptides with vesicle membranes, provides an introduction to the understanding of the mechanism of antibacterial action, but as stated above, the results might not be entirely biologically relevant. Examining

the interactions with intact bacterial cells can provide more realistic insight into the method of cell disruption. This can be accomplished by doing a cytoplasmic membrane permeabilization experiment with living cells.(22-27) Here, cells are induced to uptake a lipophilic dye into the cytoplasmic membrane due to the membrane potential; the dye self-quenches upon aggregation within the membrane. The dye is released from the cell upon addition of membrane active compounds which permeate and disrupt the cytoplasmic membrane. The increase in fluorescence can then be monitored over time.

There are varying degrees of activity of cationic peptides in this type of experiment.(22-24, 28) Hancock and coworkers demonstrated that the α-helical peptide CP-29 permeabilizes the membrane of *E. coli* maximally at the MIC while a close homologue, CP-26, does not cause dye release at the MIC.(24) In general, many peptides require four to ten times the MIC concentration to have a depolarization effect on the membrane and cause dye leakage in this experiment. Polymyxin B, a cationic peptide, is an extreme case: it permeabilizes the *P. aeruginosa* membrane only at 50-fold the MIC.(29)

The previous chapters have discussed a series of *meta*-PE molecules that mimic the FA structure and biological selectivity of host defense peptides. This chapter explores the mechanism of cell membrane disruption that ultimately results in cell death. Vesicles have been a successful tool in investigating membrane activity of many different peptides and several of those experiments have been repeated with the *meta*-PE molecules discussed in Chapter 2. There is left a great deal of work to determine the exact mechanism, and additional future experiments are discussed throughout the chapter.

5.4 Monitoring Membrane Activity of Cationic FA Molecules on Vesicles

As discussed in Section 5.3, vesicles can be used as cell membranes mimics to determine membrane activity of antibacterial compounds. Varying the phospholipid content of vesicle membranes has been used to mimic different types of cells. For instance, mammalian cell membranes are typically composed of PS, PC, and PE while bacterial membranes only contain PE and PG. In all the following experiments, the vesicles have a 10% excess of negatively charged phospholipids (PG or PS) to mimic the charged phospholipids in the outer leaflet of bacterial cytoplasmic membranes. For simplicity, vesicles mimicking mammalian cell membranes only consist of PS and PC.

Vesicles were prepared using a reverse phase evaporation method.(30) A desired amount of lipid solution was transferred to a glass vial and dried using nitrogen to form a thin film on the wall of the vial. Either buffer (90 mM NaCl, 10 mM Na_2PO_4, pH 7) or calcein solution (40 mM calcein, 10 mM Na_2PO_4, pH 7) was added to the lipid film to obtain a final concentration of 10 μmol lipid/mL of solution. The solution was then warmed in water and frozen in acetone/liquid nitrogen for three cycles and then sonicated for 15 minutes. This procedure was repeated for another sonication cycle, ultimately ending with freezing and warming the solution. The vesicles containing calcein were passed through a size exclusion Sephadex G-25 column to remove the excess dye and collect the vesicles. All vesicles were used within two days.

To establish if the molecules were membrane active, vesicle leakage experiments were performed as discussed in Section 5.3. Briefly, calcein self-quenches inside the vesicles and upon release, the fluorescence increases over time. This experiment is only used to determine if the molecules are membrane active since it can

not determine exactly how the dye is released; either leakage through holes in an intact membrane or lysis where the membrane is fully destroyed.

The chemical structures and results for the polymeric molecules, **60d**, **61d**, and **62d**, are shown in Figure 5.7. The polymers tested produced leakage curves similar to those obtained for antimicrobial peptides and biomimetic polymers.(31-33) First, these

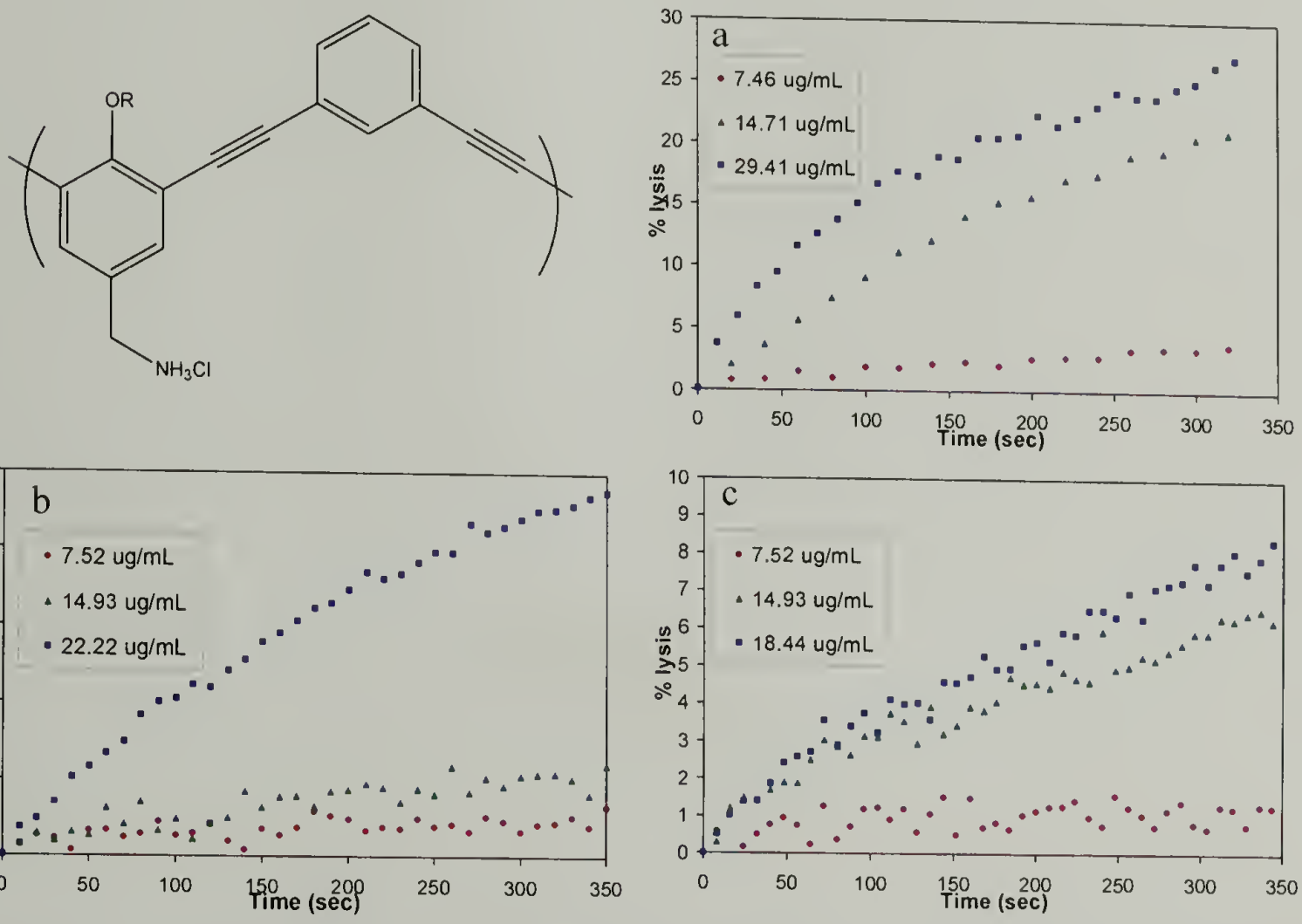

Figure 5.7: Leakage data for polymers a) 60d (R=C_5H_{11}), b) 61d (R=C_8H_{17}), and c) 62d (R=$C_{12}H_{25}$).

curves show that the amount of dye released is dependent not only on time of exposure but also on the polymer concentration. The initial rate of dye release is fast but slows down. It is speculated that this happens due to less free polymer in solution as the experiment proceeds. Second, the amount of dye release appears dependent on polymer structure. This cooperative behavior between leakage and polymer concentration is

consistent with the three mechanisms of membrane disruption proposed for antimicrobial peptides and discussed in Section 5.1.(32, 34)

Table 5.2: Summary of membrane activity at 325 seconds.

Polymer	Concentration (μg/mL)	% Leakage
60d	29.4	27.1
61d	22.2	22.9
62d	18.44	8.1

Table 5.2 summarizes the amount of dye released after 325 seconds. Notably, there is a distinct dependence of dye release on the hydrophobic NP chain length. As the carbon chain length on the antibacterial PE compound increases, the amount of dye released decreases. This is best explained by the solubility of the polymer. The concentrations listed in the table are the highest concentrations of the polymers that are soluble in the aqueous buffered solution. Above those concentrations, the polymer begins to aggregate and precipitation of the polymer is observed, explaining the decrease in membrane activity. As expected, **62d**, the C12 polymer is the most hydrophobic and not soluble at the concentrations needed to induce a high degree of lysis.

This experiment was also performed with **34d**, the C0 discrete oligomer, to determine membrane activity as well as to investigate if selectivity could be demonstrated in vesicle experiments. Figure 5.8 shows the results for two different vesicle compositions as well as different concentrations of the oligomer. The red line shows activity against vesicles made from mammalian lipids, PS-PC, while the rest of

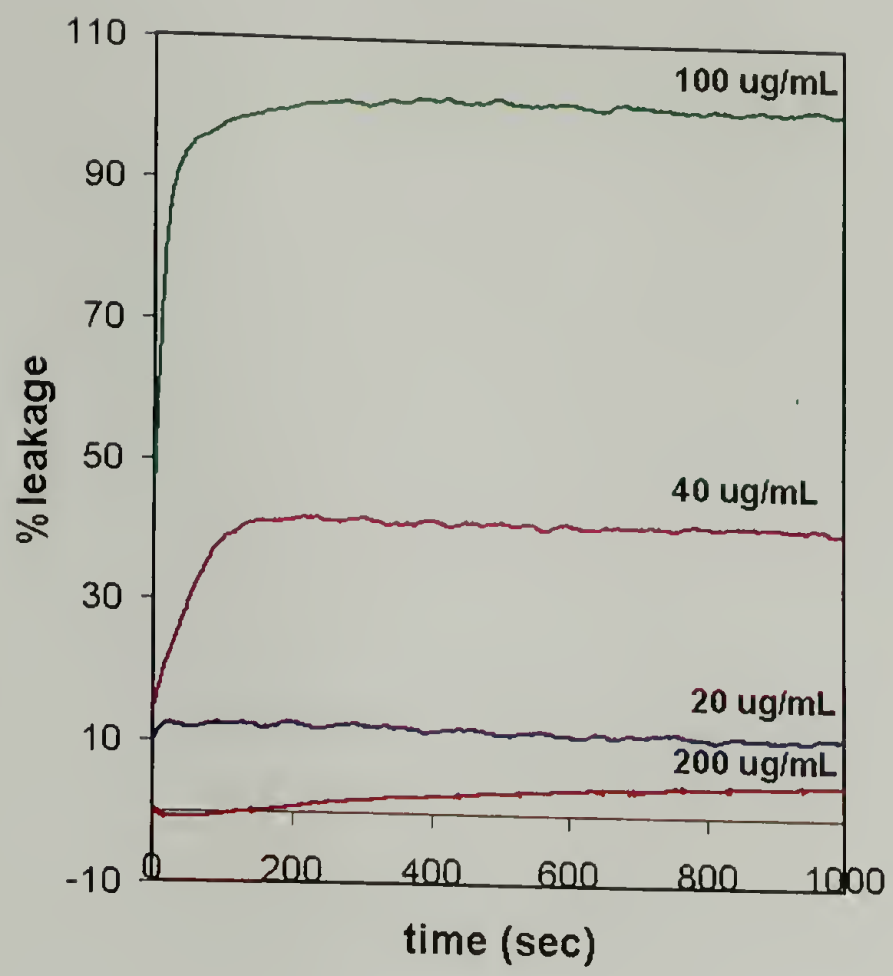

Figure 5.8: Vesicle leakage by 34d, the C0 oligomer. Red line: PS-PC vesicles. Rest are PG-PE vesicles at varing concentrations.

the lines show activity against vesicles made from the bacterial lipids, PG-PE. Both sets of vesicles have 10 mol% excess of negatively charged lipids in their membrane.

Similar observations can be seen for **34d** as for the polymers in which dye release is concentration dependent. The rate is initially fast and becomes slower as the amount of free oligomer in solution is decreased. However, through this experiment another important point is made; this compound shows selectivity towards PG-PE vesicles over PS-PC vesicles. At 20 μg/mL, there is 10% dye release from the PG-PE vesicles while it takes ten times more **34d** (200 μg/mL) to show 5% leakage from the PS-PC vesicles. This result is significant because it suggests that the selectivity seen in

the baeterial experiments is based on the membrane strueture rather than the intereellular organization.

After determining that these moleeules were membrane aetive, lipid movement experiments were performed. Lipid movement can be detected by preparing vesicles as diseussed above using fluoreseently labeled phospholipids to produce symmetrically labeled vesieles. The fluoreseenee of the outer leaflet can be then quenehed by mixing the vesieles with sodium hydrosulfite ($Na_2S_2O_4$) in buffer for 15 minutes yielding asymmetrieally labeled vesieles. These vesicles were incubated in the presence of varying eoneentrations of **34d** for up to 15 minutes while monitoring the fluoreseenee. This short time period was ehosen to avoid errors from the possible slow permeation of the queneher through the membrane. These experimental parameters provide one of the most sensitive teehniques to examine lipid-aetive compound interaction.(15, 20) Here, "lipid movement" is used to denote the outeome of lipid flip-flop experiment deseribed above. This is beeause the experiment determines lipid movement from the inner to the outer bilayer (flop). If the reverse experiment was done (flip; outer to inner bilayer) and matehed data was obtained, then it could be denoted as flip-flop. The literature is confusing in respeet to these experiments beeause several researehers do experiments that are teehnieally "flop" but denote it as "flip-flop."

This experiment was also used to look at the effeet of **34d** on two different vesiele eompositions, PG-PE and PS-PC, and the results are shown in Figure 5.9. The pereent of the lipid movement was determined by monitoring the deerease in fluoreseenee as labeled lipids moved to the outer membrane and quenehed. Similarities

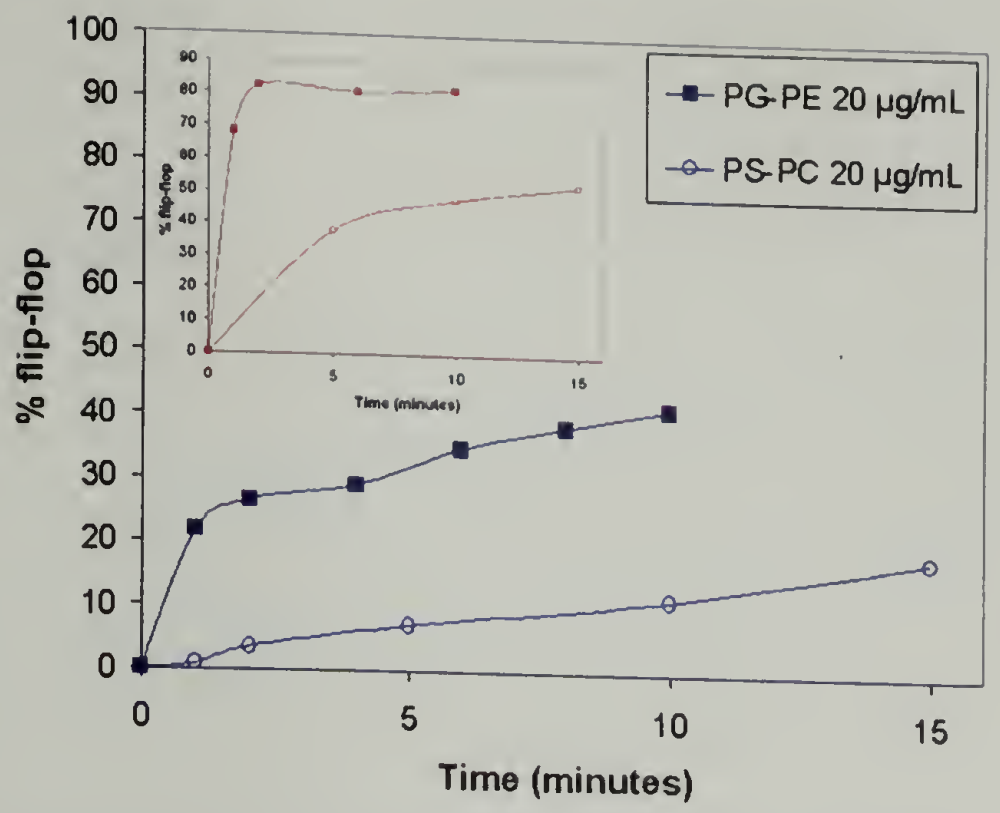

Figure 5.9: Lipid movement experimental data showing movement of bacterial lipids is faster than mammalian lipids when exposed to 34d. (Insert is at 40 µg/mL)

are seen between these curves and those in Figure 5.8. Namely, the lipid movement has a concentration dependence and the kinetics are significantly faster during the first few minutes of incubation and slow down as there is less free oligomer in solution. This result further confirms selectivity between vesicles of different compositions. The main part of the graph shows the same concentration of **34d** (20 µg/mL) incubated with different vesicles for 15 minutes. The change in fluorescence in the vesicles made from bacterial lipids is close to 40% after 10 minutes while the mammalian lipids are closer to 10%. This difference is also seen at higher concentrations (40 µg/mL), shown in the inset of Figure 5.9.

Comparing the amount of lipid movement (Figure 5.9) to the amount of dye released (Figure 5.8) illustrates that there is significantly more lipid movement than dye release in the PG-PE vesicles under the same conditions. After 10 minutes of

incubation with 20 μg/mL of **34d**, almost 40% of the labeled lipids have moved from the inner to the outer leaflet while after the same amount of time only 10% of the dye has been released. At 40 μg/mL, after the same time period there is almost complete fluorescence quenching of the labeled lipids while only about 50% of the dye has been released from the calcein-loaded vesicles.

There are a few possible explanations for the discrepancies in the results. One explanation is that the vesicles prepared are different sizes. Even though the procedures to make the vesicles are identical, there are several parameters that can affect the vesicle size including the buffer and the specific lipids. To determine if the size of the vesicles has an effect on the results, one could use an extruder to control vesicle size. A second explanation is the quantity of vesicles. In previous experiments we saw a relationship between the amount of membrane present and the concentration needed of an active compound to disrupt cells or membranes. For instance, if there is less lipid membrane present in a vesicle experiment then it takes less of the active compound to disrupt the vesicles. There are significantly less vesicles in the lipid movement experiment than the calcein experiment, suggesting discrepancies in the results could be due to the higher ratio of **34d** to lipid in the movement experiment. A third explanation is that the vesicles are not lysed during the lipid movement experiment; rather, vesicles leak while the membranes remain intact. This possibility can be addressed by the experiment shown in Figure 5.4 in which vesicles entrap two different dyes of significantly different sizes so that one will be released during all membrane disruption events (holes or lysis of the vesicle) and the other will be released only during full lysis.(19)

One could also monitor vesicles in the presence of these membrane active compounds under a microscope. This monitoring could either be done with a phase contrast or fluorescence microscope, depending on what issue was being investigated. By using a phase contrast microscope, vesicles in solution can be monitored as long as there is a slight difference in osmotic pressure between the inner solution of the vesicles and the outer aqueous solution. Vesicles encapsulating a fluorescent dye or containing labeled phospholipids can be monitored under a fluorescence microscope to investigate the lysis or the slow leakage of vesicles.

Monitoring vesicles under a microscope also provides insight into membrane budding and vesicle tubulation. Forming vesicles by budding and tubulation is essential in a variety of cellular processes such as transport and signaling of molecules. These processes are promoted by specific proteins assembling at the membrane and proceeds through well-defined pathways. It has been shown that with the addition of amphiphilic molecules, vesicle undergo shape changes and can even begin to interact with each other.(35-37) This is often seen as fusion between vesicle membranes, budding and the appearance of finger-like protrusions from the membranes, or simply a change in shape of the membrane. This is related to the interaction of amphiphiles with cells due to their reliance on signaling pathways as well as formation of vesicles for survival. The detrimental interference of membrane active molecules with these cellular processes could result in cell death.

5.5 Monitoring Membrane Activity of Cationic FA Molecules on Living Cells

After determining that the membrane activity of these compounds was sufficient to disrupt vesieles focus turned to the membrane stability of living cells. Experiments exploited a membrane potential-sensitive cyanine dye such as diSC3-5 (λ_{em}=622) that distributes between eells and the medium depending on the cytoplasmic membrane potential gradient.(24) When a cell membrane is disrupted, the membrane potential dissipates and the dye is released into the medium, causing an increase in fluoreseence. The bacteria used in this experiment were *S. aureus*, and the dye release was monitored over ten minutes, as shown in Figure 5.10. DMSO (1%) was added as a control to demonstrate that solvent alone did not induced dye release from the cells over the time-period of the experiment.

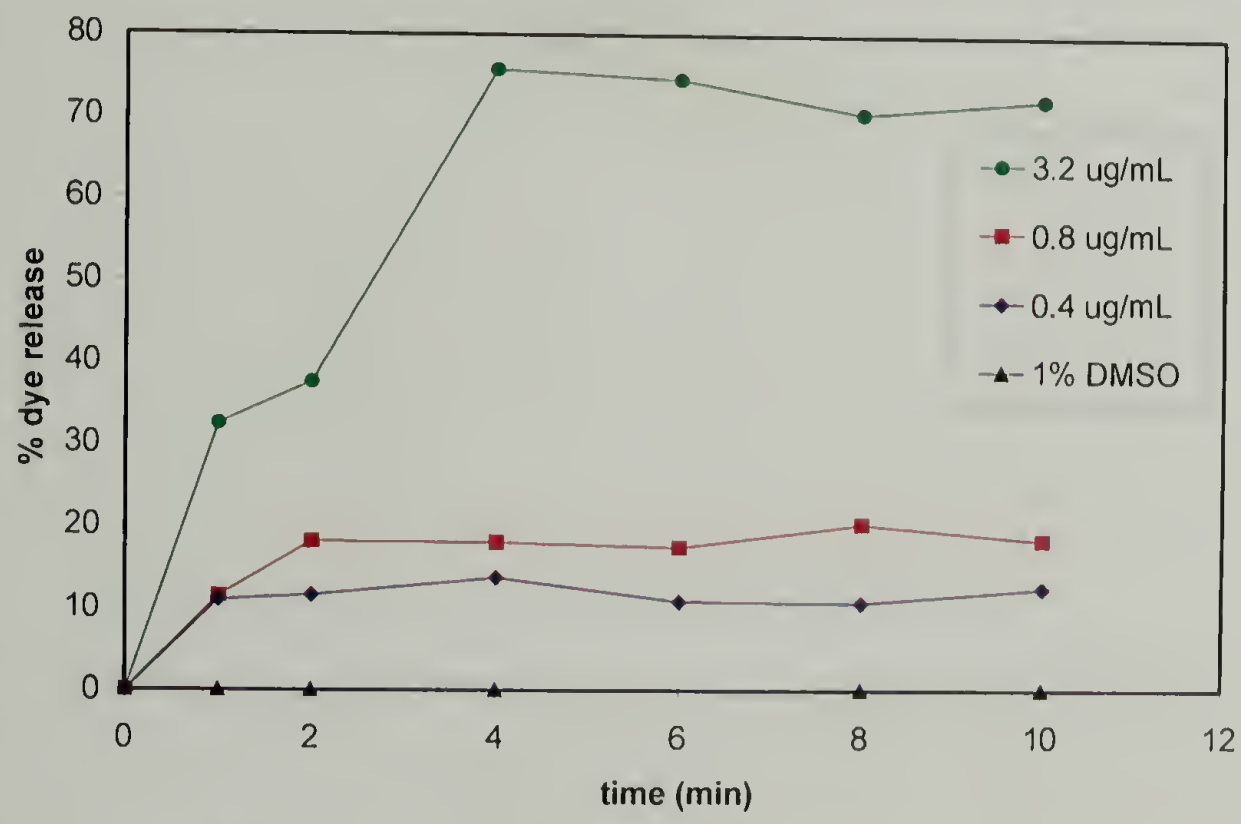

Figure 5.10: Dye Leakage from S. aureus when exposed to 34d.

The curve shape is similar to that of the vesicle experiments in Figure 5.8 and 5.9, indicating dependence on concentration as well as on time. When **34d** is introduced to the cells, the dye leakage is fast until the free **34d** in solution decreases and dye release slows down. At the lowest concentration of **34d** tested, 0.4 μg/mL, (one quarter the MIC) about 10% of the dye is released. The highest concentration tested, 3.2 μg/mL, twice the MIC, affords almost full dye release. These results are substantial for two reasons: some peptides do not depolarize the membrane until four- to ten-fold the MIC and somewhat surprisingly, **34d** starts disrupting the membrane potential below one-quarter the MIC, indicating that **34d** is more effective. Secondly, these results support the antimicrobial data suggesting that, in general, twice the MIC is the MBC.

5.6 Conclusions

From the experiments described in Sections 5.4 and 5.5, it can be concluded that the *meta*-PE molecules do exert their antibacterial action on the cytoplasmic membrane. In some of the vesicle experiments, selectivity between bacterial lipids and mammalian lipids was shown, indicating that the differences in membrane composition likely accounts for the cellular selectivity discussed in Chapter 4. Furthermore, the activity exerted from **34d** at the membrane causes significant leakage, lipid movement, and disruption of the membrane potential, resulting in cellular stress. Exact mechanisms are still unknown but further experiments are underway.

5.7 References

1. Pouny, Y., Rapaport, D., Mor, A., Nicolas, P. & Shai, Y. (1992) *Biochemistry* **31,** 12416-12423.
2. Gazit, E., Boman, H. G. & Shai, Y. (1995) *Biochemistry* **34,** 11479-11488.
3. Merriefield, R., Merriefield, E., Juvvadi, P., Andreu, D. & Boman, H. G. (1994) *Antimicrobial Peptides-Ciba Foundation Symposium No. 186* (John Wiley & Sons: New York.
4. Ehrenstein, G. & Lecar, H. Q. (1977) *Rev. Biophys.* **10,** 1-34.
5. DeGrado, W. F., Musso, G. F., Leiber, M., Kaiser, E. T. & Kezdy, F. J. (1982) *Biophys. J.* **37,** 329-338.
6. Hancock, R. E. & Rozek, A. (2002) *FEMS Microbio. Lett.* **206,** 143-149.
7. Alberts, B., Bray, D., Lewis, J., Raff, M., Roberts, K. & Watson, J. D. (1994) *Molecular Biology of the Cell* (Garland Publishing, Inc., New York).
8. Madigan, M. T., Martinko, J. M. & Parker, J. (2003) *Brock Biology of Microorganisms* (Pearson Education, Inc., Upper Saddle River).
9. Wikstrom, M., Xie, J., Bogdanov, M., Mileykovskaya, E., Heacock, P., Wieslander, A. & Dowhan, W. (2004) *Journal of Biological Chemistry* **279,** 10484-10493.
10. Cronan, J. E. (2003) *Annual Review of Microbiology* **57,** 203-224.
11. Matsukaki, K., Sugishita, K., Fujii, N. & Miyajima, K. (1995) *Biochemistry* **34,** 3423-3429.
12. Oren, Z. & Shai, Y. (1998) *Biopolymers* **47,** 451-463.
13. Matsukaki, K. (1998) *Biochim. Biophys. Acta* **1376,** 391-400.
14. Epand, R. M. & Vogel, H. J. (1999) *Biochim. Biophys. Acta* **1462,** 11-28.
15. Zhang, L., Rozek, A. & Hancock, R. E. (2001) *J. Biol. Chem.* **276,** 35714-35722.
16. Liu, D. & DeGrado, W. F. (2001) *J. Am. Chem. Soc.* **123,** 7553-7559.
17. Gazin, E., Boman, A., Boman, H. G. & Shai, Y. (1995) *Biochemistry* **34,** 11479-11488.
18. Epand, R. F., Umezawa, N., Porter, E. A., Gellman, S. H. & Epand, R. M. (2003) *Eur. J. Biochem.* **270,** 1240-1248.
19. Ladokhin, A. S. & White, S. H. (2001) *Biochemica et Biophysica Acta* **1514,** 253-260.
20. Matsukaki, K., Murase, O., Fujii, N. & Miyajima, K. (1996) *Biochemistry* **35,** 11361-11368.
21. Kol, M. A., van Dalen, A., de Kroon, A. I. P. M. & de Kruijff, B. (2003) *J. Biol. Chem.* **278,** 24586-24593.
22. Zhang, L., Scott, M. G., Yan, H., Mayer, L. D. & Hancock, R. E. (2000) *Biochemistry* **39,** 14504-14514.
23. Friedrich, C. L., Moyles, D., Beveridge, T. J. & Hancock, R. E. (2000) *Antimicrob. Agents Chemother.* **44,** 2086-2092.
24. Wu, M., Maier, E., Benz, R. & Hancock, R. E. (1999) *Biochemistry* **38,** 7235-7242.

25. Ehringer, W. D., Su, S., Chiang, B., Stillwell, W. & Chien, S. (2002) *Lipids* **37,** 885-892.
26. Sims, P. J., Waggoner, A. S., Wang, C.-H. & Hoffman, J. F. (1974) *Biochemistry* **13,** 3315-3330.
27. Ghazi, A., Schechter, E., Letellier, L. & Labedan, B. (1981) *FEBS Letters* **125,** 197-200.
28. Anderson, R. C., Hancock, R. E. & Yu, R.-L. (2004) *Antimicrob. Agents Chemother.* **48,** 673-676.
29. Zhang, L., Dhillon, P., Yan, H., Farmer, S. & Hancock, R. E. (2000) *Antimicrob. Agents Chemother.* **44,** 3317-3321.
30. Wilschut, J., Duzgunes, N., Fraley, R. & Papahadjopoulos, D. (1980) *Biochemistry* **19,** 6011-6021.
31. Tew, G. N., Lui, D., Chen, B., Doerksen, R. J., Kaplan, J., Corroll, P. J., Klein, M. L. & DeGrado, W. F. (2002) *Proc. Natl. Acad. Sci. U.S.A.* **99,** 5110-5114.
32. Liu, D. & DeGrado, W. F. (2001) *J. Am. Chem. Soc.* **123,** 7553-7559.
33. Grant, E. J., Beeler, T. J., Taylor, K. M. P., Gable, K. & Roseman, M. A. (1992) *Biochemistry* **31,** 9912-9918.
34. DeGrado, W. F. (1988) *Adv. Protein Chem* **39,** 51-124.
35. Sackmann, E., Duwe, H.-P. & Engelhardt, H. (1986) *Faraday Discuss. Chem. Soc.* **81,** 281-290.
36. Tsafrir, I., Caspi, Y., Guedeau-Boudeville, M.-A., Arzi, T. & Stavans, J. (2003) *Phys. Rev. Lett.* **91,** 138102-1-138102-4.
37. Tanaka, T., Sano, R., Yamashita, Y. & Yamazaki, M. (2004) *Langmuir* **20,** 9526-9534.

CHAPTER 6

EXPERIMENTAL

6.1 Measurements

^{1}H and ^{13}C NMR spectra were obtained at 300 MHz and 125 MHz, respectively, with a Bruker DPX-300 NMR spectrometer. The gel permeation chromatography (GPC) was performed in THF at room temperature using a PL LC 1120 pump, a Waters R403 differential refractometer, and three PLgel columns (10^5, 10^4, and 10^3 Å). Molecular weights are reported relative to polystyrene standards. Emission and excitation spectra were taken on a Perkin-Elmer LS 50B spectrometer with a xenon lamp light source. The maximum absorptions of the solutions were 0.1 or less. Elemental analysis was carried out in the Microanalysis Laboratory at the University of Massachusetts Amherst. Mass spectral data were obtained at the University of Massachusetts Amherst mass spec facility, which is supported in part by the National Science Foundation.

6.2 Materials

Toluene was either passed sequentially through columns of activated alumina (LaRoche A-2) and Q-5 supported copper redox catalyst (Engelhard CU-0226S) under a purified nitrogen atmosphere or distilled from sodium benzophenone. Reagent grade tetrahydrofuran (THF) was distilled under nitrogen from sodium benzophenone. All other solvents were used as received. 3,5 diiodo-4-hydroxy benzonitrile was purchased from Avocado Research Chemicals Ltd., *m*-diethynylbenzene and propargyl amine from

GFS Chemicals, 3,5-dibromo benzoic acid from Lancaster Chemicals, and propargyl alcohol from TCI chemicals. All other reagents were either purchased from Aldrich Chemical Co. or Alfa Aesar and were used as received. All lipids were purchased from Avanti Polar Lipids.

6.3 Synthesis of Alkylated Compounds

6.3.1 General Procedure for Mitsunobu

A 100 mL round bottom flask equipped with a magnetic stir bar was charged with 50 mL dry THF and purged with nitrogen. The solution was then cooled to 0°C in an ice bath. 2.00 g of 3,5-diiodo 4-cyanophenol (5.39 mmol, 1 mol eq.) was added to the flask and allowed to stir. 0.5694 g of an alcohol (6.47 mmol, 1.2 mol eq.) and 2.1190 g of triphenylphosphine (8.09 mmol, 1.5 mol eq.) were added to the flask. 1.6354 g diisopropylazodicarboxylate (DIAD) (8.09 mmol, 1.5 eq.) was added slowly to the stirring solution. The solution was allowed to warm up to room temperature and stir under nitrogen overnight. After confirmation of the disappearance of the starting diiodobenzene by TLC, the mixture was evaporated under reduced pressure. The residue was chromatographed on a silica gel column using mixed eluent of hexane-dichloromethane (5:1) to give a white solid.

6.3.2 General Procedure for Reduction

A 500 mL three necked round bottom flask was equipped with a stir bar and charged with 100 mL dry THF and purged with nitrogen. The solution was cooled to 0°C in an ice bath. 90 mL 1.0 M $BH_3 \cdot THF$ (88.18 mmol, 17 mol eq.) was added to the

flask and allowed to stir for 10 minutes. 2.2825 g of the benzyl nitrile, **2**, (5.188 mmol, 1 mol eq.) was dissolved in 20 mL of THF and added to the solution over 10 minutes. The ice bath was removed and a heating mantle and condenser were installed. The reaction was allowed to reflux overnight. The heating mantle was removed and the reaction allowed to cool to 0°C for 30 minutes. Methanol was added cautiously, via syringe until bubbling ceased. The mixture was evaporated under reduced pressure and washed three times with methanol. The viscous oil was then taken up in methanol and cooled to zero. HCl gas was bubbled through the solution for five minutes. The solution was removed from the ice bath and ether added until a white precipitate formed. The white precipitated material was collected and dried under vacuum. In the case of the dodecyl side chain, the molecule was chromatographed on a silica gel column to give a white solid. The product was then taken and immediately protected with Boc due to the instability of the amine.

6.3.3 General Procedure for Boc Protection of Free Amine

A 20 mL screw top vial with a magnetic stir bar was charged with 1.600 g of the amine (3.3221 mmol, 1 mol eq.), and 1.0863 g di-*tert*-butyl dicarbonate (4.9831g, 1.5 mol eq.). 12 mL of dimethylformamide was added to the vial and the solution was allowed to stir. After the solution was homogeneous, 0.2923 g sodium hydroxide (7.3086 mmol, 2.2 mol eq.) and 4 mL of distilled water were added. The vial was covered in aluminum foil and allowed to stir overnight. At the end of the reaction, some white precipitate was present. Addition of more water precipitates the product. The solid was filtered, dissolved in ether, and dried over magnesium sulfate. The solvent

was evaporated under reduced pressure. A white solid was collected and dried under vacuum.

6.3.4 Characterization of Alkoxy Molecules (2-10)

2 was made by the mitsonobu procedure in 89% yield. ^{1}H NMR ($CDCl_3$): δ 8.04 (s, 2H, phenyl H), 4.00 (t, 2H, CH_2), 1.94 (m, 2H, CH_2), 1.39-1.56 (m, 4H, $(CH_2)_2$), 0.95 (t, 3H, CH_3) ppm. ^{13}C NMR ($CDCl_3$): δ 1162.7, 143.5, 115.8, 111.7, 91.7, 74.4, 30.1, 28.4, 22.9, 4.5 ppm. MS: *m/z* 440.8 (M^+). Anal. Calcd for $C_{12}H_{13}NOI_2$: C, 32.65: H, 2.95: N, 3.17: I, 57.60. Found: C, 32.76: H, 3.15: N, 3.11: I, 57.7.

3 was made by the mitsonobu procedure in 90% yield. ^{1}H NMR ($CDCl_3$): δ 8.04 (s, 2H, phenyl H), 4.00 (t, 2H, CH_2), 1.94 (m, 2H, CH_2), 1.39-1.56 (m, 12H, $(CH_2)_6$), 0.95 (t, 3H, CH_3) ppm.

4 was made by the mitsonobu procedure in 87% yield. ^{1}H NMR ($CDCl_3$): δ 8.04 (s, 2H, phenyl H), 4.00 (t, 2H, CH_2), 1.93 (m, 2H, CH_2), 1.53 (m, 2H, CH_2), 1.26 (m, 16H, $(CH_2)_6$), 0.88 (t, 3H, CH_3) ppm. ^{13}C NMR ($CDCl_3$): δ 162.7, 143.5, 115.8, 111.7, 91.6, 74.4, 32.4, 30.4, 30.1, 30.0, 29.9, 29.8, 26.3, 23.1, 14.6 ppm. Anal. Calcd for $C_{19}H_{27}NOI_2$: C, 42.28: H, 5.01: N, 2.60: I, 47.07. Found: C, 42.38: H, 4.98: N, 2.57: I, 47.4.

5 was made by the reduction described above and protected immediately. ^{1}H NMR (DMSO-D_6): δ 8.34 (s, 2H, NH_2), 7.97 (s, 2H, phenyl H), 3.91 (s, 2H, CH_2), 3.85 (t, 2H, CH_2), 1.81 (m, 2H, CH_2), 1.33-1.49 (m, 4H, $(CH_2)_2$), 0.90 (t, 3H, CH_3) ppm. MS: *m/z* 445 (M^+).

6 was made by the reduction described above and protected immediately. ^{1}H NMR (DMSO-D_6): δ 8.00 (s, 2H, phenyl H), 3.87 (s, 2H, CH_2), 2.50 (m, 2H, CH_2), 1.22-1.84 (m, 10H, $(CH_2)_5$), 0.86 (t, 3H, CH_3) ppm.

7 was made by the reduction described above and protected immediately. ^{1}H NMR (DMSO-D_6): δ 7.82 (s, 2H, phenyl H), 4.08 (s, 2H, CH_2), 3.93 (t, 2H, CH_2), 1.90 (m, 2H, CH_2), 1.22-1.53 (m, 19H, $(CH_2)_2$), 0.89 (t, 3H, CH_3) ppm.

8 was synthesized by the protection stated above in 62% yield. ^{1}H NMR ($CDCl_3$): δ 7.66 (s, 2H, phenyl H), 4.96 (s, 1H, NH), 4.19 (d, 2H, CH_2), 3.94 (t, 2H, CH_2), 1.90 (m, 2H, CH_2), 1.46 (s, 9H, $3CH_3$), 1.41-1.55 (m, 4H, $(CH_2)_2$), 0.95 (t, 3H, CH_3) ppm. ^{13}C NMR ($CDCl_3$): δ 157.5, 156.1, 139.0, 91.4, 80.3, 73.9, 43.0, 30.1, 28.8, 28.5, 23.0, 14.5 ppm. MS: *m/z* 545.0 (M^+). Anal. Calcd: C, 37.43: H, 4.59: N, 2.57: I, 46.61. Found: C, 37.36: H, 4.73: N, 2.50: I, 46.8.

9 was synthesized by the protection stated above in 63% yield. ^{1}H NMR ($CDCl_3$): δ 7.65 (s, 2H, phenyl H), 4.87 (s, 1H, NH), 4.18 (d, 2H, CH_2), 3.93 (t, 2H, CH_2), 1.87 (m, 2H, CH_2), 1.46 (s, 9H, $3CH_3$), 1.29-1.58 (m, 10H, $(CH_2)_5$), 0.89 (t, 3H, CH_3) ppm.

10 was synthesized by the protection stated above in 64% yield. ^{1}H NMR ($CDCl_3$): δ 7.66 (s, 2H, phenyl H), 4.96 (s, 1H, NH), 4.19 (d, 2H, CH_2), 3.94 (t, 2H, CH_2), 1.91 (m, 2H, CH_2), 1.48 (s, 9H, $3CH_3$), 1.28-1.57 (m, 18H, $(CH_2)_9$), 0.89 (t, 3H, CH_3) ppm. ^{13}C NMR ($CDCl_3$): δ 157.5, 139.0, 91.4, 73.8, 43.0, 32.3, 30.4, 30.1, 30.0, 29.9, 29.7, 28.7, 26.4, 23.1, 14.6 ppm. Anal. Calcd for $C_{12}H_{13}NOI_2$: C, 44.86: H, 5.91: N, 2.18: I, 39.56. Found: C, 45.61: H, 6.14: N, 2.13: I, 39.9.

6.4 Synthesis of C0 Molecules (12-16)

6.4.1 Preparation of Benzyl Alcohol (12)

A round bottom flask equipped with a magnetic stir bar was charged with ether and purged with nitrogen. Dibromobenzoic acid, **11**, (2.00 g, 7.15 mmol,1 equiv) was added to the ether (50 mL) and the solution was cooled to 0°C in an ice bath. A 1 M solution of $LiAlH_4$ (15 mL, 14.33 mmol; 2 equiv.) was added slowly while the reaction was vented. The reaction was allowed to warm up to room temperature and stir overnight in an inert atmosphere. After confirmation by TLC that all the starting material was gone, ice was slowly added to the solution until all the bubbling stopped. Cold HCl was added to the solution until all the solid was dissolved. The product was then extracted with ether, dried over magnesium sulfate and evaporated to dryness. The product, **12**, was purified by column chromatography using dichloromethane as the eluent to give a white solid (yield 90%). ^{1}H NMR ($CDCl_3$): δ 7.58 (t, 1H, phenyl H), 7.45 (d, 2H, phenyl H), 4.67 (s, 2H, CH_2) ppm. *m/z*: [M]: 266, [M-Br]: 185.

6.4.2 Preparation of Benzyl Bromide (13)

A round bottom flask equipped with a magnetic stir bar was charged with dry THF (100 mL) and purged with nitrogen. Benzyl alcohol, **12**, (1.90 g, 7.15 mmol, 1 equiv.) was added to the solvent and allowed to dissolve. N-bromosuccinamide (1.72 g, 9.65 mmol, 1.5 equiv.) was added to the solution. Triphenylphosphine (2.53 g, 9.65 mmol, 1.5 equiv.) was added slowly and the reaction was allowed to stir overnight. After confirmation by TLC that all the starting benzyl alcohol was gone, the solution

was evaporated to dryness. The product was purified by column chromatography using 1:1 dichloromethane:hexane as the eluent. The product, **13**, was a white solid (yield 76%). ^{1}H NMR ($CDCl_3$): δ 7.61 (t, 1H, phenyl H), 7.48 (d, 2H, phenyl H), 4.43 (s, 2H, CH_2) ppm. *m/z*: [M^+]: 327.7, [M^+-Br]: 248.8.

6.4.3 Preparation of Benzyl Cyanide (14)

A round bottom flask equipped with a magnetic stir bar was charged with 3:1 ethanol:water (10 mL) and purged with nitrogen. Benzyl bromide, **13**, (1.00 g, 3.04 mmol, 1 equiv.) and sodium cyanide (0.16 g, 3.35 mmol, 1.1 equiv.) were added to the flask. The reaction was heated to 70°C for 2 hours or until **13** was consumed. The product was extracted with dichloromethane and ethyl acetate and dried with magnesium sulfate. The organic layer was evaporated to dryness and the product was purified by column chromatography using 1:4 dichloromethane to hexane. The product, **14**, was a white solid (yield 90%). ^{1}H NMR ($CDCl_3$): δ 7.66 (t, 1H, phenyl H), 7.44 (d, 2H, phenyl H), 3.72 (s, 2H, CH_2) ppm. *m/z*: [M^+]: 275, [M^+-Br]: 194, [M^+-Br -CN]: 167.

6.4.4 Preparation of the Free Amine (15)

A round bottom flask was equipped with a stir bar and charged with dry THF (75 mL) and purged with nitrogen. The solution was cooled to 0°C in an ice bath. Benzyl cyanide, **14**, (1.06 g, 3.85 mmol, 1 equiv.) was dissolved and 1.0 M BH_3·THF (66 mL, 65.43 mmol, 17 equiv.) was added cautiously to the flask and allowed to stir. The ice bath was removed and a heating mantle and condenser were installed. The

reaction was allowed to reflux overnight. The heating mantle was removed and the reaction was allowed to cool to 0°C for 30 minutes. Methanol was added cautiously, via syringe until bubbling ceased. The mixture was evaporated under reduced pressure and washed three times with methanol. The viscous oil was then taken up in methanol and cooled to 0°C. Concentrated HCl was added to the solution until precipitate formed. The solution was removed from the ice bath and ether added until more white precipitate formed. The white precipitated material was collected and dried under vacuum. The product, **15**, was then immediately protected due to the instability of the amine (yield 78.5%). ^{1}H NMR (DMSO-D_6): δ 7.94 (s, 3H, NH_3Cl), 7.73 (t, 1H, phenyl H), 7.55 (d, 2H, phenyl H), 3.08 (m, 2H, CH_2), 2.88 (t, 2H, CH_2) ppm.

6.4.5 Preparation of Boc Protected Amine (16)

A round bottom flask was charged with a magnetic stir bar, the amine, **15**, (0.95 g, 3.02 mmol, 1 equiv.), and di-*tert*-butyl dicarbonate (0.99 g, 4.54 mmol, 1.5 mol equiv.). Dimethylformamide (8 mL) was added to the vial and the solution was allowed to stir. After the solution was homogeneous, sodium hydroxide (0.27 g, 6.65 mmol, 2.2 equiv.) and distilled water (4 mL) were added. The reaction was covered in aluminum foil and allowed to stir overnight. Some white precipitate was present. Addition of more water precipitates the product. The solid was filtered, dissolved in ether, and dried over magnesium sulfate. The solvent was evaporated under reduced pressure. A white solid, **16**, was collected and dried under vacuum (yield 92%). ^{1}H NMR ($CDCl_3$): δ 7.54 (t, 1H, phenyl H), 7.29 (d, 2H, phenyl H), 4.53 (s, 1H, NH), 3.35 (m, 2H, CH_2), 2.77 (t,

2H, CH_2) ppm. ^{13}C NMR ($CDCl_3$): δ 155.8, 143.1, 132.1, 130.7, 122.9, 79.5, 41.4, 35.5, 28.4, 27.4 ppm. *m/z* [M^+]: 379, [M^+-t-butyl]: 323, [M^+-Boc]: 278.

6.5 Synthesis of Other Monomers

6.5.1 Preparation of 1,3-Dibromo-5-pentyloxymethyl-benzene (17)

A round bottom flask was purged with nitrogen and dry THF (75 mL) was added. Potassium hydride was allowed to stir in the THF before adding pentanol to the mixture slowly as the reaction bubbled. **13** (1.5084 g, 4.587 mmol) was dissolved in dry THF and added to the solution. The reaction turned grey and was allowed to stir overnight. The reaction was rotovapped down and taken up in ether and extracted with water, washed with saturated salt solution and dried over magnesium sulfate. The solution was filtered and rotovaped to a liquid. The product, **17**, was separated by column chromatography in 20% dichloromethane:hexane yielding 69%. ^1H NMR ($CDCl_3$): δ 7.57 (s, 1H, phenyl H), 7.42 (s, 2H, phenyl H), 7.43 (s, 2H, CH_2), 3.63 (t, 2H, CH_2), 3.46 (t, 2H, CH_2), 1.57 (m, 4H, $2CH_2$), 0.93 (t, 3H, CH_3). *m/z*: [M^+]: 334.7, [M^+-O-pentyl]: 248.7.

6.5.2 Preparation of [2-(2,6-Dibromo-4-methyl-phenoxy)-ethyl]-carbamic acid tert-butyl ester (19)

A 100 mL round bottom flask equipped with a magnetic stir bar was charged with 20 mL dry THF and purged with nitrogen. The solution was then cooled to 0°C in an ice bath. 0.500 g of **18** (1.8801 mmol, 1 mol eq.) was added to the flask and allowed to stir. 0.3637 g of (2-Hydroxy-ethyl)-carbamic acid tert-butyl ester (2.2561 mmol, 1.2

mol eq.) and 0.7389 g of triphenylphosphine (2.8202 mmol, 1.5 mol eq.) were added to the flask. 0.5703 g diisopropylazodicarboxylate (DIAD) (2.8202 mmol, 1.5 eq.) was added slowly to the stirring solution. The solution was allowed to warm up to room temperature and stir under nitrogen overnight. After confirmation of the disappearance of **18** by TLC, the mixture was evaporated under reduced pressure. The residue was chromatographed on a silica gel plug using mixed eluent of dichloromethane to give a clear oil in 72% yield. ^{1}H NMR ($CDCl_3$): δ 7.32 (s, 2H, phenyl H), 5.31 (s, 1H, NH), 4.07 (t, 2H, CH_2), 3.57 (m, 2H, CH_2), 2.29 (s, 3H, CH_3), 1.48 (s, 9H, $3CH_3$).

6.5.3 3,5-Diiodo-benzoic acid 2-[2-(2-methoxy-ethoxy)-ethoxy]-ethyl ester (22)

20 was reacted with excess methanol and potassium carbonate (1.5 equiv) under reflux conditions overnight to yield **21**. **21** was reacted with triethyleneglycol monomethyl ether (1.5 eq) and potassium carbonate (1.5 equiv) in acetone under reflux conditions for 12 hours. The crude reaction was extracted with ethyl acetate and rotovapped to dryness. The mixture was then purified using column chromatography in 20% ethyl acetate/hexane to yield **22** in 49%. ^{1}H NMR ($CDCl_3$): δ 8.13 (s, 2H, phenyl H), 7.86 (t, 1H, phenyl H), 4.50 (m, 2H, $2CH_2$), 3.85 (m, 2H, CH_2), 3.73-3.66 (m, 6H, $3CH_2$), 3.56 (m, 2H, CH_2), 3.38 (s, 3H, CH_3). *m/z*: [M^+] 520, [M^+ -peg] 357.

6.5.4 Preparation of 1,3-Dibromo-5-{2-[2-(2-methoxy-ethoxy)-ethoxy]-ethoxymethyl}-benzene (23)

A round bottom flask was purged with nitrogen and dry THF (75 mL) was added. Potassium hydride was allowed to stir in the THF before adding1.4955 g of triethylene glycol monomethyl ether (9.1080 mmol, 2 eq) to the mixture slowly as the

reaction bubbled. 1.4975 g of **13** (4.554 mmol, 1eq) was dissolved in dry THF and added to the solution. The reaction turned grey and was allowed to stir overnight. The reaction was rotovapped down and taken up in ether and extracted with water, washed with saturated salt solution and dried over magnesium sulfate. The solution was filtered and rotovaped to a liquid. The product, **23**, was separated by column chromatography in 20% dichloromethane:hexane yielding 54%. ^{1}H NMR (DMSO): δ 7.73 (s, 1H, phenyl H), 7.53 (s, 2H, phenyl H), 4.49 (s, 3H, CH_2), 3.56-3.32 (m, 12H, $12CH_2$), 3.22 (s, 3H, CH_3). ^{13}C NMR ($CDCl_3$): δ 144.4, 133.0, 129.8, 123.2, 41.2, 40.9, 40.6, 40.4, 40.1, 39.8, 39.5 ppm.

6.6 Polymerization Procedures

6.6.1 General Procedure for Polymerization

A 20 mL airfree schlenk flask was charged with a magnetic stir bar and dried in the oven then cooled under nitrogen. 27.0 mg of *m*-diethynylbenzene (0.2140 mmol, 1.03 mol eq.) was weighed directly into the schlenk flask. 0.1133 g of the dihalogenated monomer (0.2078 mmol, 1 mol eq.), 0.0072 g $Pd(PPh_3)_4$ (0.0062 mmol, 0.03 mol eq.), and 0.0023 g CuI (0.0124 mmol, 0.06 mol eq.) were added to the flask. The flask was then returned to positive nitrogen pressure. 0.6699 mL of distilled diisopropylamine (DIPA) (4.7797 mmol, 23 mol eq.) and 5 mL of dry toluene were added via syringe. The reaction was then placed in an oil bath at 78°C and stirred overnight. The mixture was clear at first and by the next morning it was cloudy. The reaction was poured into methanol to give a yellow solid.

6.6.2 General Procedure for Deprotection of Polymers

A 10 mL round bottom flask was charged with a magnetic stir bar. 25mg of Boc protected polymer was added to the flask. The flask was then cooled to 0°C and 6 mL of 4M HCl in dioxane was added to the polymer. The solution was allowed to warm up to room temperature and stir overnight. The solvent was evaporated under reduced pressure and the solid was washed with ether three times and dried under vacuum to yield a yellow solid.

6.6.3 Characterization of Polymer Structure and Molecular Weight

The polymers have a "p" after the number if they are "protected" polymers. After the deprotection by removal of the Boc group, the polymer numbers have a "d" after them to denote "deprotected."

The polymerization to make **24p** was carried out by the Sonogashira conditions in 52% yield. ^{1}H NMR ($CDCl_3$): δ 7.69 (m, 1H, phenyl H) , 7.49-7.52 (m, 2H, phenyl H), 7.36-7.40 (m, 3H, phenyl H), 4.90 (s, 1H, NH), 4.29 (m, 2H, CH_2), 1.88 (m, 2H, CH_2), 1.47 (s, 9H, $3CH_3$), 1.37-1.59 (m, 4H, $(CH_2)_2$), 0.88 (t, 3H, CH_3) ppm. GPC: Mn 17,800; Mw 40,500; PDI 2.276.

24p was deprotected to make **24d** by the general deprotection stated above. ^{1}H NMR (DMSO-D_6): δ 8.40 (s, 2H, NH_2), 7.79 (s, 2H, phenyl H), 7.62 (m, 4H, phenyl H), 4.32 (m, 1H, NH), 4.03 (m, 2H, CH_2), 1.82 (m, 2H, CH_2), 1.54 (m, 2H, CH_2), 1.32 (m, 2H, CH_2), 0.78 (t, 3H, CH_3) ppm. UV (DMSO): ε=30,000, λ_{max} (297nm), sh (332 nm).

The polymerization to make **25p** was carried out by the Sonogashira conditions in 50% yield. ^{1}H NMR ($CDCl_3$): δ 7.69 (m, 1H, phenyl H) , 7.50 (m, 2H, phenyl H),

7.36-7.40 (m, 3H, phenyl H), 4.89 (s, 1H, NH), 4.29 (m, 2H, CH_2), 1.88 (m, 2H, CH_2), 1.47 (s, 9H, $3CH_3$), 1.37-1.59 (m, 12H, $(CH_2)_6$), 0.87 (t, 3H, CH_3) ppm. GPC: Mn 7,700; Mw 10,300; PDI 1.331.

25p was deprotected to make **25d** by the general deprotection stated above. ^{1}H NMR (DMSO-D_6): δ 8.43 (s, 2H, NH_2), 7.76 (s, 2H, phenyl H), 7.61 (m, 4H, phenyl H), 4.30 (m, 1H, NH), 4.03 (m, 2H, CH_2), 1.82 (m, 2H, CH_2), 1.27-1.00 (m, 8H, CH_2), 0.71 (t, 3H, CH_3) ppm. UV (DMSO): λ_{max} (295nm), sh (337 nm).

The polymerization to make **26p** was carried out by the Sonogashira conditions in 41% yield. ^{1}H NMR ($CDCl_3$): δ 7.70 (m, 1H, phenyl H), 7.51 (m, 2H, phenyl), 7.37-7.42 (m, 3H, phenyl H), 4.87 (s, 1H, NH), 4.31 (m, 2H, CH_2), 1.89 (m, 2H, CH_2), 1.21-1.57 (m, 18H, $(CH_2)_9$), 0.86 (t, 3H, CH_3) ppm. GPC: Mn 10,100; Mw 13,800; PDI 1.369.

26p was deprotected to **26d** by the general deprotection stated above. ^{1}H NMR (DMSO-D_6): δ 8.40 (s, 2H, NH_2), 7.56-7.75 (m, 6H, phenyl H), 4.16 (m, 1H, NH), 4.00 (m, 2H, CH_2), 1.78 (m, 2H, CH_2), 1.48 (m, 2H, CH_2), 1.05 (m, 16H, $(CH_2)_2$), 0.72 (t, 3H, CH_3) ppm. UV (DMSO): λ_{max} (294 nm), sh (337 nm).

The polymerization to make **27p** was carried out by the Sonogashira conditions in 54% yield. ^{1}H NMR ($CDCl_3$): δ 7.69 (m, 1H, phenyl H) , 7.49-7.52 (m, 2H, phenyl H), 7.36-7.40 (m, 3H, phenyl H), 4.90 (s, 1H, NH), 4.29 (m, 2H, CH_2), 1.98 (m, 2H, CH_2), 1.74 (m, 2H, CH_2), 1.49 (s, 9H, $3CH_3$), 1.27-1.40 (m, 3H, CH, CH_2), 1.15 (m, 3H, CH_3), 0.97 (t, 3H, CH_3) ppm. GPC: Mn 10,100; Mw 16,100; PDI 1.6.

27p was deprotected to make **27d** by the general deprotection stated above. ^{1}H NMR (DMSO-D_6): δ 8.47 (s, 2H, NH_2), 7.79 (s, 2H, phenyl H), 7.60 (m, 4H, phenyl H),

4.21 (m, 1H, NH), 4.03 (m, 2H, CH_2), 1.87 (m, 2H, CH_2), 1.65 (m, 2H, CH_2), 1.32 (m, 2H, CH_2), 1.08 (t, 3H, CH_3), 0.90 (t, 3H, CH_3) ppm. UV (DMSO): λ_{max} (299 nm), sh (333 nm).

The polymerization to make **28p** was carried out by the Sonogashira conditions in 57% yield. ^{1}H NMR ($CDCl_3$): δ 7.72 (m, 1H, phenyl H) , 7.50-7.60 (m, 2H, phenyl H), 7.37-7.30 (m, 3H, phenyl H), 4.60 (s, 1H, NH), 3.41 (m, 2H, CH_2), 2.83 (m, 2H, CH_2), 1.47 (s, 9H, $3CH_3$) ppm. GPC: Mn 5,500; Mw 8,100; PDI 1.471.

28p was deprotected to make **28d** by the general deprotection stated above. ^{1}H NMR (DMSO-D_6): δ 8.03 (s, 2H, NH_2), 7.77 (s, 2H, phenyl H), 7.59 (m, 4H, phenyl H), 3.11 (m, 2H, CH_2), 2.96 (m, 2H, CH_2) ppm. UV (DMSO): λ_{max} (308nm), sh (289 nm).

The polymerization to make **30** was carried out by the Sonogashira conditions in 47% yield. I cannot find the NMR and do not have any more sample to retake the spectrum. GPC: Mn 4,800; Mw 10,100; PDI 2.264.

The polymerization to make **31p** was carried out by the Sonogashira conditions in 57% yield. ^{1}H NMR ($CDCl_3$): δ 7.47 (s, 2H, phenyl H), 7.32 (s, 2H, phenyl H), 5.74 (s, 1H, NH), 5.15 (s, 1H, NH), 4.43 (t, 2H, CH_2), 4.30 (m, 4H, $2CH_2$), 3.55 (m, 2H, CH_2), 2.34 (s, 3H, CH_3), 1.89 (m, 2H, CH_2), 1.48 (s, 18H, $3CH_3$), 1.57-1.28 (m, 4H, $2CH_2$), 0.88 (t, 3H, CH_3) ppm. GPC: Mn 23,500; Mw 54,300; PDI 2.312.

31p was never successfully deprotected to make **31d**.

The polymerization to make **32** was carried out by the Sonogashira conditions in 57% yield. ^{1}H NMR ($CDCl_3$): δ 7.62 (s, 1H, phenyl H), 7.52 (s, 2H, phenyl H), 4.60 (s, 2H, CH_2), 3.71 (m, 8H, $4CH_2$), 3.56 (m, 4H, $2CH_2$), 3.37 (s, 3H, CH_3) ppm. GPC: Mn 10,900; Mw 16,700; PDI 1.534.

The polymerization to make **33** was carried out by the Sonogashira conditions in 57% yield. ^{1}H NMR ($CDCl_3$): δ 8.10 (s, 4H, phenyl H), 7.88 (s, 1H, phenyl H), 4.53 (s, 2H, CH_2), 3.99-3.88 (m, 10H, $5CH_2$), 3.80 (s, 3H, CH_3) ppm. GPC: Mn 5,100; Mw 19,600; PDI 3.837.

The polymerization to make **63p** was carried out by the Sonogashira conditions in 52% yield. ^{1}H NMR ($CDCl_3$): δ 7.69 (m, 1H, phenyl H) , 7.49-7.52 (m, 2H, phenyl H), 7.36-7.40 (m, 3H, phenyl H), 4.90 (s, 1H, NH), 4.29 (m, 2H, CH_2), 1.88 (m, 2H, CH_2), 1.47 (s, 9H, $3CH_3$), 1.37-1.59 (m, 4H, $(CH_2)_2$), 0.88 (t, 3H, CH_3) ppm. GPC: Mn 8,500; Mw 11,000; PDI 1.3.

63p was deprotected to make **63d** by the general deprotection stated above. ^{1}H NMR (DMSO-D_6): δ 8.40 (s, 2H, NH_2), 7.79 (s, 2H, phenyl H), 7.62 (m, 4H, phenyl H), 4.32 (m, 1H, NH), 4.03 (m, 2H, CH_2), 1.82 (m, 2H, CH_2), 1.54 (m, 2H, CH_2), 1.32 (m, 2H, CH_2), 0.78 (t, 3H, CH_3) ppm. UV (DMSO): ε=30,000, λ_{max} (297nm), sh (332 nm).

The polymerization to make **64p** was carried out by the Sonogashira conditions in 57% yield. ^{1}H NMR ($CDCl_3$): δ 7.72 (m, 1H, phenyl H), 7.50-7.60 (m, 2H, phenyl H), 7.37-7.30 (m, 3H, phenyl H), 4.60 (s, 1H, NH), 3.41 (m, 2H, CH_2), 2.83 (m, 2H, CH_2), 1.47 (s, 9H, $3CH_3$) ppm. GPC: Mn 1,800; Mw 8,900; PDI 2.873.

64p was deprotected to make **64d** by the general deprotection stated above. ^{1}H NMR (DMSO-D_6): δ 8.03 (s, 2H, NH_2), 7.77 (s, 2H, phenyl H), 7.59 (m, 4H, phenyl H), 3.11 (m, 2H, CH_2), 2.96 (m, 2H, CH_2) ppm. UV (DMSO): λ_{max} (308nm), sh (289 nm).

The polymerization to make **65p** was carried out by the Sonogashira conditions in 52% yield. ^{1}H NMR ($CDCl_3$): δ 11.57 (s, 1H, NH), 8.55 (s, 1H, NH), 7.70 (m, 1H, phenyl H) , 7.53-7.34 (m, 5H, phenyl H), 4.58 (m, 2H, CH_2), 1.89 (m, 2H, CH_2), 1.48 (s,

18H, 6CH_3), 1.52-1.40 (m, 4H, $(CH_2)_2$), 0.89 (t, 3H, CH_3) ppm. GPC: Mn 11,400; Mw 21,000; PDI 1.83.

65p was deprotected to make **65d** by the general deprotection stated above. ^{1}H NMR (DMSO-D_6): δ 9.65 (s, 1H, NH), 9.05 (s, 1H, NH), 8.87 (s, 1H, NH), 8.12 (s, 1H, NH), 7.65 (m, 6H, phenyl H), 4.27 (m, 4H, 2CH_2), 3.97 (m, 2H, CH_2), 1.80 (m, 2H, CH_2), 1.49 (m, 2H, CH_2), 1.21 (m, 2H, CH_2), 0.77 (t, 3H, CH_3) ppm.

The polymerization to make **66p** was carried out by the Sonogashira conditions in 46% yield. ^{1}H NMR ($CDCl_3$): δ 11.57 (s, 1H, NH), 8.55 (s, 1H, NH), 7.70 (m, 1H, phenyl H) , 7.53-7.34 (m, 5H, phenyl H), 4.58 (m, 2H, CH_2), 1.89 (m, 2H, CH_2), 1.48 (s, 18H, 6CH_3), 1.52-1.40 (m, 4H, $(CH_2)_2$), 0.89 (t, 3H, CH_3) ppm. GPC: Mn 9,300; Mw 15,500; PDI 1.67.

66p was deprotected to make **66d** by the general deprotection stated above. ^{1}H NMR (DMSO-D_6): δ 9.65 (s, 1H, NH), 9.05 (s, 1H, NH), 8.87 (s, 1H, NH), 8.12 (s, 1H, NH), 7.65 (m, 6H, phenyl H), 4.27 (m, 4H, 2CH_2), 3.97 (m, 2H, CH_2), 1.80 (m, 2H, CH_2), 1.49 (m, 2H, CH_2), 1.21 (m, 2H, CH_2), 0.77 (t, 3H, CH_3) ppm.

The polymerization to make **67p** was carried out by the Sonogashira conditions in 44% yield. ^{1}H NMR ($CDCl_3$): δ 11.57 (s, 1H, NH), 8.55 (s, 1H, NH), 7.70 (m, 1H, phenyl H) , 7.53-7.34 (m, 5H, phenyl H), 4.58 (m, 2H, CH_2), 1.89 (m, 2H, CH_2), 1.48 (s, 18H, 6CH_3), 1.52-1.40 (m, 4H, $(CH_2)_2$), 0.89 (t, 3H, CH_3) ppm. GPC: Mn 4,300; Mw 6,200; PDI 1.43.

67p was deprotected to make **67d** by the general deprotection stated above. ^{1}H NMR (DMSO-D_6): δ 9.65 (s, 1H, NH), 9.05 (s, 1H, NH), 8.87 (s, 1H, NH), 8.12 (s, 1H,

NH), 7.65 (m, 6H, phenyl H), 4.27 (m, 4H, $2CH_2$), 3.97 (m, 2H, CH_2), 1.80 (m, 2H, CH_2), 1.49 (m, 2H, CH_2), 1.21 (m, 2H, CH_2), 0.77 (t, 3H, CH_3) ppm.

The polymerization to make **68p** was carried out by the Sonogashira conditions in 46% yield. ^{1}H NMR ($CDCl_3$): δ 11.57 (s, 1H, NH), 8.55 (s, 1H, NH), 7.70 (m, 1H, phenyl H), 7.53-7.34 (m, 5H, phenyl H), 3.58 (m, 2H, CH_2), 2.75 (m, 2H, CH_2), 1.48 (s, 18H, $6CH_3$) ppm. GPC: Mn 6,100; Mw 15,300; PDI 2.512.

68p was deprotected to make **68d** by the general deprotection stated above. ^{1}H NMR (DMSO-D_6): δ 9.65 (s, 1H, NH), 9.05 (s, 1H, NH), 8.87 (s, 1H, NH), 8.12 (s, 1H, NH), 7.65 (m, 6H, phenyl H), 4.15 (m, 2H, CH_2), 2.87 (m, 2H, CH_2) ppm.

The polymerization to make **69p** was carried out by the Sonogashira conditions in 46% yield. ^{1}H NMR ($CDCl_3$): δ 11.57 (s, 1H, NH), 8.55 (s, 1H, NH), 7.70 (m, 1H, phenyl H), 7.53-7.34 (m, 5H, phenyl H), 3.58 (m, 2H, CH_2), 2.75 (m, 2H, CH_2), 1.48 (s, 18H, $6CH_3$) ppm. GPC: Mn 5,600; Mw 8,700; PDI 1.538.

69p was deprotected to make **69d** by the general deprotection stated above. ^{1}H NMR (DMSO-D_6): δ 9.65 (s, 1H, NH), 9.05 (s, 1H, NH), 8.87 (s, 1H, NH), 8.12 (s, 1H, NH), 7.65 (m, 6H, phenyl H), 4.15 (m, 2H, CH_2), 2.87 (m, 2H, CH_2) ppm.

6.7 Synthesis of Discrete Trimers

6.7.1 General Procedure for the Preparation of Discrete Oligomers

An airfree schlenk flask was charged with a magnetic stir bar and dried in the oven then cooled under nitrogen. *m*-diethynylbenzene (0.17 g, 1.34 mmol, 0.25 mol equiv.) was weighed directly into the schlenk flask. The halogenated monomer (2.04 g,

5.38 mmol, 1 equiv.), $Pd(PPh_3)_4$ (0.19 g, 0. 16 mmol, 0.03 equiv.), and CuI (0.06 g, 0.32 mmol, 0.06 equiv.) were added to the flask. The flask was then returned to positive nitrogen pressure. Distilled diisopropylamine (DIPA) (17.3 mL, 123.6 mmol, 23 equiv.) and dry toluene (60 mL) were added via syringe. The reaction was then placed in an oil bath at 65°C and stirred overnight. The reaction was evaporated to dryness and the product was purified by column chromatography first using dichloromethane and then 1% acetone/dichloromethane. If the product was still yellow in color after chromatography, the impurity could be removed by titration with methanol to yield a white solid.

6.7.2 General Procedure for the Deprotection of Discrete Oligomers

A round bottom flask was charged with a magnetic stir bar and the boc-protected trimer (50 mg). The flask was then cooled to 0°C and 4M HCl in dioxane (5 mL) was added to the trimer. The solution was allowed to warm up to room temperature and stir overnight. The solvent was evaporated under reduced pressure and the solid was titrated with ether three times and dried under vacuum to produce a white solid (quantitative yield).

6.7.3 Characterization of Discrete Oligomers

34p was prepared as described above in 30% yield. ^{1}H NMR ($CDCl_3$): δ 7.68 (t, 1H, phenyl H), 7.56 (t, 2H, phenyl H), 7.51 (t, 1H, phenyl H), 7.48 (d, 1H, phenyl H), 7.37 (d, 1H, phenyl H), 7.34 (m, 2H, phenyl H), 7.31 (m, 2H, phenyl H), 4.58 (s, 2H, 2NH), 3.38 (m, 4H, $2CH_2$), 2.79 (t, 4H, $2CH_2$), 1.46 (s, 18H, $6CH_3$) ppm. ^{13}C NMR

($CDCl_3$): δ 156.1, 141.7, 135.1, 132.8, 132.5, 132.0, 131.1, 129.0, 125.4, 123.6, 122.7, 90.0, 88.9, 79.9, 41.8, 36.1, 31.3, 28.7 ppm. *m/z* [M^++Na]: 745.3 [M^+-2Boc +2Na]: 567.2. The TLC for the purification of this compound is shown at the end of this section in DCM.

34p was then deprotected to **34d** as described above in quantitative yield. ^1H NMR (DMSO-D_6): δ 7.92 (s, 4H, $2NH_2$), 7.77 (t, 1H, phenyl H), 7.71 (t, 2H, phenyl H), 7.65 (t, 1H, phenyl H), 7.62 (m, 2H, phenyl H), 7.58 (d, 1H, phenyl H), 7.52 (m, 2H, phenyl H), 3.11 (m, 4H, $2CH_2$), 2.92 (t, 4H, $2CH_2$) ppm. ^{13}C NMR ($CDCl_3$): δ 138.7, 134.6, 133.0, 131.8, 131.6, 128.6, 125.3, 122.9, 122.5, 89.8, 87.9, 60.3, 58.2, 48.0, 41.6, 40.4, 32.9 ppm.

35p was prepared as described above in 23% yield. ^1H NMR ($CDCl_3$): δ 7.69 (d, 1H, phenyl H), 7.66 (t, 2H, phenyl H), 7.50 (d, 2H, phenyl H), 7.48 (d, 1H, phenyl H), 7.39 (m, 4H, phenyl H), 4.85 (s, 2H, 2NH), 4.24 (d, 4H, $2CH_2$), 4.15 (t, 4H, $2CH_2$), 1.91 (m, 4H, $2CH_2$), 1.48 (s, 18H, $6CH_3$), 1.60-1.37 (m, 8H, $4CH_2$), 0.92 (t, 6H, $2CH_3$) ppm. *m/z* [M^++Na]: 983.2 [M^+-t-butyl +Na]: 927.2 [M^+-2t-butyl +Na]: 871.2. The TLC for the purification of this compound is shown at the end of this section in 20% DCM/Hexane.

35p was deprotected to **35d** as described above. ^1H NMR (DMSO): δ 8.29 (s, 5H, NH), 8.04 (s, 2H, phenyl H), 7.71 (s, 2H, phenyl H), 7.65-7.56 (m, 6H, phenyl H), 4.12 (t, 4H, $2CH_2$), 3.99 (s, 4H, $2CH_2$), 1.82 (m, 4H, $2CH_2$), 1.47 (m, 4H, $2CH_2$), 1.35 (m, 4H, $2CH_2$), 0.84 (t, 6H, $2CH_3$) ppm.

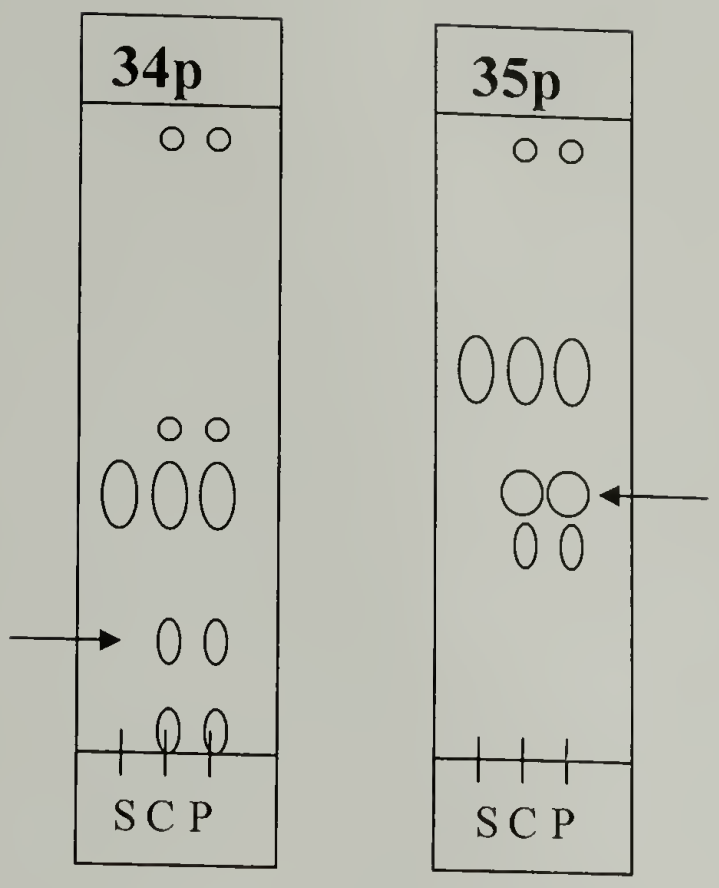

Figure 6.1: TLC of 34p (dichloromethane) and 35p (20%hexane/dichloromethane). Arrows point to product. S=starting dihalogenated material, C = cospot, P= crude reaction mixture.

6.8 Synthesis of Structure-Activity Relationship Monomers and Discrete Oligomers

All oligomers were synthesized according the procedure listed in Section 6.7.1 and deprotected by the procedure in Section 6.7.2 unless otherwise noted. The monomers were functionalized before doing the oligomerization reaction.

6.8.1 Characterization of Discrete Oligomers with Varying End Groups

36p: ^{1}H NMR ($CDCl_3$): δ 7.68 (t, 1H, phenyl H), 7.50-7.46 (m, 4H, phenyl H), 7.38-7.33 (m, 3H, phenyl H), 7.24 (s, 2H, phenyl H), 4.85 (s, 2H, 2NH), 4.55 (s, 2H, 2NH), 4.16 (m, 4H, $2CH_2$), 3.38 (m, 4H, $2CH_2$), 2.80 (t, 4H, $2CH_2$), 1.46 (s, 36H, $12CH_3$) ppm. *m/z* +Na: 893.6.

36d: ^{1}H NMR (DMSO): δ 8.45 (s, 4H, NH), 7.95 (s, 4H, NH), 7.75 (m, 1H, phenyl H), 7.68-7.50 (m, 6H, phenyl H), 7.42 (m, 2H, phenyl H), 4.02 (s, 4H, 4CH_2), 3.15 (m, 4H, 2CH_2), 2.95 (m, 4H, 2CH_2) ppm.

37p: ^{1}H NMR ($CDCl_3$): δ 7.70 (m, 1H, phenyl H), 7.57 (m, 1H, phenyl H), 7.51-7.48 (m, 3H, phenyl H), 7.39-2.33 (m, 4H, phenyl H), 4.58 (s, 2H, 2NH), 4.38 (d, 2H, CH_2), 3.40 (m, 4H, 2CH_2), 2.80 (t, 4H, 2CH_2), 1.47 (s, 18H, 6CH_3) ppm. *m/z*: 673.4.

37d: Not sufficient amount of sample to tell any more than the removal of Boc.

38p: ^{1}H NMR ($CDCl_3$): δ 7.72-7.65 (m, 2H, phenyl H), 7.59-7.46 (m, 4H, phenyl H), 7.38-7.35 (m, 3H, phenyl H), 7.27 (s, 1H, phenyl H), 4.59 (s, 2H, 2NH), 4.50 (d, 4H, 2CH_2), 3.39 (m, 4H, 2CH_2), 2.79 (t, 4H, 2CH_2), 1.46 (s, 18H, 6CH_3) ppm. *m/z*: 673.4.

38d: Not sufficient amount of sample to tell any more than the removal of Boc.

39p: ^{1}H NMR ($CDCl_3$): δ 7.69 (m, 1H, phenyl H), 7.47 (m, 2H, phenyl H), 7.35 (m, 2H, phenyl H), 6.75 (s, 2H, phenyl H), 6.65 (s, 2H, phenyl H), 6.44 (s, 2H, phenyl H), 4.85 (s, 2H, 2NH), 4.62 (s, 2H, 2NH), 3.39 (m, 8H, 4CH_2), 3.28 (m, 4H, NH), 2.72 (t, 4H, 2CH_2), 1.47 (s, 36H, 12CH_3) ppm. *m/z*: [M^++Na] 903.6, [M^+ +2Na -Boc] 825.3, [M^+ +2Na -2Boc] 725.3, [M^+ +2Na -3Boc] 625.4.

39d: ^{1}H NMR ($CDCl_3$): δ 8.15 (m, 4H, 2NH_2), 8.04 (m, 4H, 2NH_2), 7.66 (m, 1H, phenyl H), 7.57-7.45 (m, 4H, phenyl H), 7.26 (m, 1H, phenyl H), 7.00-6.97 (m, 1H, phenyl H), 6.70 (d, 2H, phenyl H), 6.60 (s, 1H, phenyl H), 3.17 (t, 4H, 2CH_2), 2.88 (m, 8H, 4CH_2), 2.80 (t, 4H, 2CH_2) ppm.

40p: ^{1}H NMR ($CDCl_3$): δ 7.72 (t, 1H, phenyl H), 7.51 (t, 2H, phenyl H), 7.49 (d, 1H, phenyl H), 7.43-7.48 (m, 4H, phenyl H), 7.34 (m, 2H, phenyl H), 7.32 (m, 2H,

phenyl H), 7.28 (s, 1H, phenyl H), 7.21 (m, 2H, phenyl H), 4.58 (s, 2H, 2NH), 3.41 (m, 4H, $2CH_2$), 2.82 (t, 4H, $2CH_2$), 1.46 (s, 18H, $6CH_3$) ppm. *m/z*: 587.3.

40d: ^{1}H NMR (DMSO): δ 7.87 (s, 4H, NH), 7.77 (t, 1H, phenyl H), 7.72-7.63 (m, 2H, phenyl H), 7.62-7.58 (m, 2H, phenyl H), 7.55-7.32 (m, 8H, phenyl H), 3.10 (m, 4H, $2CH_2$), 2.90 (t, 4H, $2CH_2$) ppm.

46p: ^{1}H NMR ($CDCl_3$): δ 8.45 (t, 2H, phenyl H), 7.66 (t, 1H, phenyl H), 7.57 (t, 2H, phenyl H), 7.51 (t, 1H, phenyl H), 7.48 (t, 1H, phenyl H), 7.38-7.34 (m, 5H, phenyl H), 3.69 (m, 4H, $2CH_2$), 2.87 (t, 4H, $2CH_2$), 1.49 (s, 36H, $12CH_3$) ppm. *m/z*: 673.4.

46d: Not sufficient amount of sample to tell any more than the removal of Boc.

47p: ^{1}H NMR ($CDCl_3$): δ 7.98 (t, 2H, phenyl H), 7.93 (t, 2H, phenyl H), 7.78 (t, 2H, phenyl H), 7.69 (t, 1H, phenyl H), 7.52-7.50 (m, 4H, phenyl H), 7.38 (t, 1H, phenyl H), 5.05 (t, 2H, 2NH), 3.57 (m, 4H, $2CH_2$), 3.45 (m, 4H, $2CH_2$), 1.49 (s, 18H, $6CH_3$) ppm. *m/z* [M+Cl^-]: 843.5.

47d: ^{1}H NMR (DMSO): δ 7.96 (s, 4H, 2NH), 7.82-7.77 (m, 2H, phenyl H), 7.70 (m, 2H, phenyl H), 7.65-7.52 (m, 6H, phenyl H), 3.10 (s, 4H, $2CH_2$), 2.93 (m, 4H, $2CH_2$) ppm.

48p: ^{1}H NMR ($CDCl_3$): δ 7.70 (t, 1H, phenyl H), 7.65 (t, 2H, phenyl H), 7.52 (m, 3H, phenyl H), 7.49 (m, 3H, phenyl H), 7.40-7.37 (m, 1H, phenyl H), 5.07 (s, 4H, $2CH_2$), 1.52 (s, 18H, $6CH_3$) ppm. *m/z*: [M^+ +Na] 719.2, [M^+ +Na -t-butyl] 663.2, [M^+ +Na -2t-butyl] 607.1.

48d: ^{1}H NMR (DMSO): δ 7.79 (m, 1H, phenyl H), 7.70-7.62 (m, 3H, phenyl H), 7.61 (d, 1H, phenyl H), 7.57 (m, 2H, phenyl H), 7.51 (s, 3H, phenyl H), 5.45 (s, 2H, NH), 4.52 (s, 4H, $2CH_2$) ppm.

49p: ^{1}H NMR ($CDCl_3$): δ 7.69 (t, 1H, phenyl H), 7.53 (m, 2H, phenyl H), 7.49 (m, 1H, phenyl H), 7.37 (d, 1H, phenyl H), 7.33 (m, 1H, phenyl H), 7.30 (m, 2H, phenyl H), 7.28 (s, 1H, phenyl H), 4.57 (s, 2H, 2NH), 3.19 (m, 4H, $2CH_2$), 2.64 (t, 4H, $2CH_2$), 1.84 (m, 4H, $2CH_2$), 1.47 (s, 18H, $6CH_3$) ppm. *m/z*: [M^+ +Na] 773.3, [M^+ +Na -t-butyl] 717.2, [M^+ -Boc] 649.1, [M^+ +Na -2Boc] 572.2.

49d: ^{1}H NMR (DMSO): δ 7.89 (s, 4H, $2NH_2$), 7.77 (m, 1H, phenyl H), 7.65-7.63 (m, 2H, phenyl H), 7.61 (d, 1H, phenyl H), 7.56 (m, 2H, phenyl H), 7.48 (m, 2H, phenyl H), 2.77-2.67 (m, 8H, $4CH_2$), 1.87 (m, 4H, $2CH_2$) ppm.

50p: ^{1}H NMR ($CDCl_3$): δ 7.71-7.66 (m, 5H, phenyl H), 7.55-7.50 (m, 10H, phenyl H), 7.38 (t, 3H, phenyl H), 5.12 (s, 2H, 2NH), 5.07 (s, 4H, $2CH_2$), 1.47 (s, 27H, $9CH_3$) ppm. *m/z*: [M^+ +Na] 1049.2, [M^+ +Na -t-butyl] 993.2, [M^+ +Na -2t-butyl -Boc] 834.3.

50d: ^{1}H NMR (DMSO): δ 7.78-7.52 (m, 17H, phenyl H), 5.45 (s, 3H, 3NH), 4.52 (s, 6H, $3CH_2$) ppm.

51p: ^{1}H NMR ($CDCl_3$): δ 7.75-7.63 (m, 6H, phenyl H), 7.56-7.50 (m, 13H, phenyl H), 7.44-7.37 (m, 4H, phenyl H), 5.12 (s, 4H, 4NH), 5.07 (s, 8H, $4CH_2$), 1.53 (s, 36H, $12CH_3$) ppm.

51d: ^{1}H NMR (DMSO): δ 7.79-7.50 (m, 24H, phenyl H), 5.45 (s, 4H, 4NH), 4.52 (s, 8H, $4CH_2$) ppm. *m/z*: [M^+ +Na] 1379.1.

58p: Missing NMR and no more sample to retake.

58d: ^{1}H NMR (DMSO): δ 8.05 (s, 4H, $2NH_2$), 7.75-7.45 (m, 8H, phenyl H), 6.50 (s, 6H, $2CH_3$) 3.10 (m, 4H, $2CH_2$), 2.95 (m, 4H, $2CH_2$) ppm.

59p: ^{1}H NMR ($CDCl_3$): δ 12.47 (s, 2H, 2NH), 8.56 (t, 1H, NH), 7.73 (d, 2H, phenyl H), 7.67 (t, 1H, phenyl H), 7.52 (m, 2H, phenyl H), 7.43 (d, 2H, phenyl H), 7.38 (t, 1H, phenyl H), 4.54 (d, 2H, 2NH), 4.15 (t, 4H, $2CH_2$), 1.92 (m, 4H, $2CH_2$), 1.52 (s, 36H, $12CH_3$), 1.60-1.42 (m, 4H, $2CH_2$), 1.27 (t, 8H, $4CH_2$), 0.92 (t, 6H, $2CH_3$) ppm. *m/z*: [M+Na] 1321.3, [M^+ -Boc] 1199.3, [M^+ -2Boc] 1098.2, [M^+ -3Boc] 998.2, [M^+ -4Boc] 897.2.

59d: Not sufficient amount of sample to tell any more than the removal of Boc.

6.8.2 Synthesis and Characterization of Monomers for SAR Study

43: An airfree schlenk flask was charged with a magnetic stir bar and dried in the oven then cooled under nitrogen. The halogenated monomer, **16**, (0.050 g, 0.1389 mmol, 1 equiv.), $Pd(PPh_3)_4$ (0.0038 g, 0.0033 mmol, 0.025 equiv.), and CuI (0.0006 g, 0.0032 mmol, 0.025 equiv.) were added to the flask. **41** (0.0077 g, 0.1384 mmol, 1.05 mol equiv.) was added directly into the schlenk flask. The flask was then returned to positive nitrogen pressure. Triethylamine (1.5 mL, from a sure seal bottle) was added. The reaction was then placed in an oil bath at 65°C and stirred overnight. The reaction was orange the next morning and it was evaporated to dryness and the product was purified by column chromatography in 10% ethyl acetate/dichloromethane yielding 52.4%. ^{1}H NMR ($CDCl_3$): δ 7.46 (t, 1H, phenyl H), 7.32 (t, 1H, phenyl H), 7.22 (t, 1H, phenyl H), 4.50 (m, 3H, NH, CH_2), 3.36 (m, 2H, CH_2), 2.76 (m, 2H, CH_2), 1.48 (s, 9H, $3CH_3$) ppm.

44: An airfree schlenk flask was charged with a magnetic stir bar and dried in the oven then cooled under nitrogen. The halogenated monomer, **16**, (0.0613 g, 0.1618

mmol, 1 equiv.), $Pd(PPh_3)_4$ (0.0047 g, 0.0040 mmol, 0.025 equiv.), and CuI (0.0008 g, 0.0040 mmol, 0.025 equiv.) were added to the flask. **42** (0.0276 g, 0.1780 mmol, 1.1 mol equiv.) was added directly into the schlenk flask. The flask was then returned to positive nitrogen pressure. Triethylamine (4mL, from a sure seal bottle) was added. The reaction was then placed in an oil bath at 65°C and stirred overnight. The reaction was orange the next morning and it was evaporated to dryness and the product was purified by column chromatography in 5% ethyl acetate/dichloromethane yielding 47%. ^{1}H NMR ($CDCl_3$): δ 7.43 (t, 1H, phenyl H), 7.30 (t, 1H, phenyl H), 7.19 (t, 1H, phenyl H), 4.80 (s, 1H, NH), 4.57 (s, 1H, NH), 4.16 (m, 2H, CH_2), 3.35 (m, 2H, CH_2), 2.76 (t, 2H, CH_2), 1.48 (s, 18H, $6CH_3$) ppm.

45: An airfree schlenk flask was charged with a magnetic stir bar and dried in the oven then cooled under nitrogen. The halogenated monomer, **16**, (0.05 g, 0.1318 mmol, 1 equiv), potassium phosphate (0.056 g, 0.264 mmol, 2 equiv), salicylamide (0.0051 g, 0.0263 mmol, 0.2 equiv), and copper iodide (0.0013 g, 0.0066 mmol, 0.05 equiv) were added directly into the schlenk flask. The flask was kept under positive pressure of nitrogen and 0.4 mL DMF (sure seal) and ethylene diamine boc (0.023 g, 0.145 mmol, 1.1 equiv.) were added. The reaction was placed in an oil bath at 90°C overnight and was yellowish/red the next morning. The product was extracted with ethyl actetate/5% aqueous sodium hydroxide and rotovapped to dryness. The product was run through a silica plug yielding 52.8%. ^{1}H NMR ($CDCl_3$): δ 6.66 (s, 1H, phenyl H), 6.60 (s, 1H, phenyl H), 6.34 (s, 1H, phenyl H), 4.85 (s, 1H, NH), 4.61 (s, 1H, NH), 3.36 (m, 4H, $2CH_2$), 3.23 (s, 1H, NH), 2.67 (t, 2H, CH_2), 1.46 (s, 18H, $6CH_3$) ppm.

52: A round bottom flask was charged with a magnetic stir bar and flushed with nitrogen. The halogenated monomer, **11**, (49.7 mg, 0.1775 mmol, 1 equiv.), EDC (0.0580 g, 0.195 mmol, 1.1 equiv), HOBt (0.0264 g, 0.195 mmol, 1.1 equiv.), and ethylene diamine boc (0.0313 g, 0.195 mmol, 1.1 equiv.) were added to the flask. Dry DMF (1.5 mL, sure seal) was added and the reaction was allowed to flush with nitrogen and stir over night. The product was extracted with water and dichloromethane and rotovapped to dryness yielding 63%. ^{1}H NMR ($CDCl_3$): δ 7.92 (s, 2H, phenyl H), 7.79 (s, 1H, phenyl H), 5.02 (s, 1H, NH), 3.54 (m, 2H, CH_2), 3.44 (t, 2H, CH_2), 1.48 (s, 9H, $3CH_3$) ppm.

53: A round bottom flask was charged with a magnetic stir bar and flushed with nitrogen. **12** (1.000g, 3.759 mmol, 1 equiv.) and sodium azide (0.2932 g, 4.511 mmol, 1.2 equiv.) were added to the flask and dissolved in 20 mL dry DMF (sure seal). Triphenyl phosphine (2.1693 g, 8.27 mmol, 2.2 equiv.) was added slowly. The reaction was submerged in a 90°C oil bath overnight. The next morning the reaction was quenched with water and extracted with dichloromethane. The product was purified by column chromatography in dichloromethane and then taken up in methanol, cooled to 0°C, and precipitated with HCl. The solid was collected and dried under vacuum yielding 75%. ^{1}H NMR ($CDCl_3$): δ 7.63 (s, 1H, phenyl H), 7.50 (s, 2H, phenyl H), 4.47 (t, 2H, CH_2), 3.15 (t, 2H, NH) ppm.

54: A round bottom flask was charged with a magnetic stir bar, the amine, **53**, (0.7078 g, 2.36 mmol, 1 equiv.), and di-*tert*-butyl dicarbonate (0.7741 g, 3.55 mmol, 1.5 mol equiv.). Dimethylformamide (9 mL) was added to the vial and the solution was allowed to stir. After the solution was homogeneous, sodium hydroxide (0.208 g, 5.207

mmol, 2.2 equiv.) and distilled water (3 mL) were added. The reaction was covered in aluminum foil and allowed to stir overnight. Some white precipitate was present. Addition of more water precipitates the product. The solid was filtered, dissolved in ether, and dried over magnesium sulfate. The solvent was evaporated under reduced pressure. The product was further purified by silica column chromatography in 10% dichloromethane/hexane to yield a white solid, **54**, in 93% yield. ^{1}H NMR ($CDCl_3$): δ 7.63 (s, 1H, phenyl H), 7.47 (s, 2H, phenyl H), 5.03 (s, 2H, CH_2), 1.52 (s, 9H, $3CH_3$) ppm. *m/z*: [M^+] 366, [M^+ -Boc] 266.

55: An airfree schlenk flask was charged with a magnetic stir bar, dried in the oven, and flame dried while cooling under nitrogen. The flask was charged with dry THF (1.0 mL, distilled from sodium) and acetonitrile (0.0312 g, 0.7602 mmol, 2.5 equiv.). The solution was cooled to -78°C before adding 2.87 M *n*-butyl lithium (0.286 mL, 0.8217 mmol, 2.7 equiv.). This solution was allowed to stir for an hour at -78°C and was yellowish in color with some solid. After an hour, a solution of **13** (0.1 g, 0.304 mmol, 1 equiv.) in 0.4 mL THF was added and the solution turned reddish. The solution was allowed to stir for another hour before warming to room temperature and adding water. The product was extracted with dichloromethane and purified by column chromatography on silica in dichloromethane yielding 75%. (Note: This reaction is size dependent. On a larger scale (4 g) the yield was 10 %.) ^{1}H NMR ($CDCl_3$): δ 7.62 (s, 1H, phenyl H), 7.35 (s, 2H, phenyl H), 2.93 (m, 4H, $2CH_2$), 2.65 (t, 2H, CH_2) ppm.

56: A round bottom flask was equipped with a stir bar and charged with dry THF (20 mL) and purged with nitrogen. The solution was cooled to 0°C in an ice bath. **55**, (0.3 g, 1.03 mmol, 1 equiv.) was dissolved and 1.0 M BH_3·THF (17.6 mL, 17.6

mmol, 17 equiv.) was added cautiously to the flask and allowed to stir. The ice bath was removed and a heating mantle and condenser were installed. The reaction was allowed to reflux overnight. The heating mantle was removed and the reaction was allowed to cool to 0°C for 30 minutes. Methanol was added cautiously, via syringe until bubbling ceased. The mixture was evaporated under reduced pressure and washed three times with methanol. The viscous oil was then taken up in methanol and cooled to 0°C. Concentrated HCl was added to the solution until precipitate formed. The solution was removed from the ice bath and rotovapped to a white solid in 43% yield. ^{1}H NMR (MeOD): δ 5.50 (s, 1H, phenyl H), 5.36 (s, 2H, phenyl H), 1.69 (s, 2H, CH_2), 1.50 (t, 2H, CH_2), 1.24 (t, 2H, CH_2) ppm.

57: A round bottom flask was charged with a magnetic stir bar, the amine, **56**, (0.1467 g, 0.445 mmol, 1 equiv.), and di-*tert*-butyl dicarbonate (0.1456 g, 0.667 mmol, 1.5 mol equiv.). Dimethylformamide (2 mL) was added to the vial and the solution was allowed to stir. After the solution was homogeneous, sodium hydroxide (0.0392 g, 0.979 mmol, 2.2 equiv.) and distilled water (0.8 mL) were added. The reaction was covered in aluminum foil and allowed to stir overnight. Some white precipitate was present. Addition of more water precipitates the product. The solid was filtered, dissolved in ether, and dried over magnesium sulfate. The solvent was evaporated under reduced pressure. A white solid, **57**, was collected and dried under vacuum (yield 75%). ^{1}H NMR ($CDCl_3$): δ 7.51 (s, 1H, phenyl H), 7.33 (s, 2H, phenyl H), 4.55 (s, 1H, NH), 3.15 (m, 2H, CH_2), 2.60 (m, 2H, CH_2), 1.79 (m, 2H, CH_2), 1.46 (s, 9H, $3CH_3$) ppm.

6.9 Characterization of Facial Amphiphilicity and Aggregation

6.9.1 Langmuir Data

A Langmuir trough equipped with a Cahn electrobalance was used for monolayer measurements. The surface pressure measurements were obtained using a Wilhelmy plate attached to the Cahn electrobalance. The barriers were compressed at 0.1648 cm/min. The film was made by spreading 50 μL of a solution containing 0.5 mg/mL of polymer in 5% DMSO/$CHCl_3$ on the surface. For the reversibility experiment, the barriers were compressed, allowed to relax, and recompressed. The surface pressure was monitored during the whole experiment.

A program was written in LabView to run barrier compression in the Langmuir trough and determine the surface pressure of the water for each i^{th} data point. This program was written by a previous student in Dr. Hsu's group and is no longer available. The following equations were used to process the raw data into surface pressure-area isotherms.

To determine the starting area per repeat unit (A_o) of the polymer molecule:

$$A_0 = A_{trough}\left(\frac{MW_{repeat}}{N_A CV}\right)$$

Where MW_{repeat} is the molecular weight of the repeat unit, N_A is Avogadro's number, C is the concentration of the polymer solution, and V is the volume of the polymer solution added.

To determine the area per repeat unit during compression (A_i):

$$A_i = \frac{\left[\left(L_o - \Delta L\left(\frac{i}{N_i}\right)\right)W\right]MW_{repeat}}{N_A CV}$$

Where L_o is the starting length between the barriers, ΔL is the final change in length between the barriers, i is the data point number, N_i is the total number of data points, and W is the width of the trough.

To determine the surface pressure during compression (Π_i):

$$\Pi_i = \left[\frac{S_{cal}(\Pi_{water} - \Pi_i)}{2A_{plate}}\right] + I_{cal}$$

Where S_{cal} is the slope of the calibration curve of surface tension, Π_{water} is the surface pressure of pure water, Π_i is the surface pressure of the i^{th} data point, A_{plate} is the area of the Whilhelmy plate, and I_{cal} is the intercept of the surface tension calibration curve.

From these calculated areas and surface pressures, the surface-pressure isotherm can be generated. The steepest part of the slope can be extrapolated to zero surface pressure to determine the area per repeat unit of the molecule. If the area per molecule is desired then, instead of using the molecular weight per repeat unit (MW_{repeat}) in the equations above, the total molecular weight of the polymer could be used.

6.9.2 Emission Studies

The fluorescence of the polymer solutions was initially monitored in several solvents to determine the effect of solvation of the polymer fluorescence. After determining the initial emission, the fluorescence was monitored with increasing percentage of water. A stock solution of polymer was made in DMSO as to keep the

concentration constant throughout the experiment. The samples were at a concentration where the UV absorbance was less that 0.1 so that inner filter effects were minimal. Fluorescence was also monitored with the addition of polymer solution in DMSO to the buffer used for the lysis data. The percentage of water in these experiments ranged from 96% to 98.5%.

6.9.3 Turbidity Data with Varying Polymers

Turbidity experiments were run with polymer dissolved in a DMSO solution at 1mg/mL added in varying concentrations to either water or a buffered solution (90 mM NaCl, 10 mM Na_2PO_4, pH 7). Mixed solutions were then allowed to equilibrate for several minutes before measuring the optical density at 500 nm (OD_{500}). OD_{500} was measured for six consecutive runs, and the numerical values were averaged. Data was then plotted as percent transmission versus concentration.

6.10 Antimicrobial Activity

6.10.1 Antimicrobial Testing

Compounds were dissolved in DMSO to make a stock solution, which was then diluted into 96-well plates and diluted with Mueller Hinton (MH) medium to a constant volume. All bacteria were either taken from stock glycerol solutions or from a frozen stock, diluted into MH medium, and grown overnight at 37°C. Subsamples of these cultures were grown for 3 hours, the OD_{600} was measured, and then the cells were diluted to 0.001 OD_{600}. The diluted cell solutions (approximately 10^5 cells/mL) were then added to the 96-well plate and incubated at 37°C for 20 hours. The MIC values

reported in Table 1 are the minimum concentration necessary to inhibit 90% of the cell growth. This was determined by measuring cell growth at OD_{600} after 20 hours in two-fold serial dilutions of the abiogenic polymer following standard protocols.(1) All reported values represent a minimum of duplicate experiments.

6.10.2 Hemolysis Assay

Hemolysis experiments were performed by incubating a 0.35% (v/v) suspension of fresh human erythrocytes in 10 mM TRIS buffer containing 150 mM NaCl at pH 7.0 with varying amounts of polymer. Hemolysis samples were prepared by combining 80 μL of the washed RBC suspension and 20 μL total of buffer and polymer solution in 96-well plates. After incubation for 30 minutes at 37°C, the suspensions were concentrated at 1000x "g" for 5 minutes. An aliquiot of the supernatant was diluted with buffer and the OD_{414} of the solution was measured to quantitate released hemoglobin. Complete hemolysis was measured by adding 1% Triton X-100 to the RBC's and measuring OD_{414}. Non-linear exponential curve-fitting plots of OD_{414} vs. polymer concentration resulted in HC_{50}, the hemolytic dose required to lyse 50% of the RBCs.

6.10.3 Minimal Bactericidal Concentration

Minimal bactericidal concentrations (MBC) were measured by preparing serial ten-fold dilutions from the growth inhibition assay, and plating them on nutrient agar plates. The plates were incubated overnight at 37°C and the colonies were counted the next morning. The MBC is defined as the minimum concentration at which a 99.9% reduction in the number of colonies of the original inoculums occurred.

6.10.4 MIC in the Presence of Whole Blood

The antibacterial activity in the presence of whole blood was examined in sterile 96-well plates in a final volume of 100 µL per well. Aliquots of 80 µL of a bacterial suspension diluted to an OD_{600} of 0.001 were added to 20 µL of a mixture of 1% whole blood, the compound in DMSO, and medium. The concentration of the active compound decreased in 2-fold serial dilutions while the amount of whole blood remained constant at 1%. Three independent experiments were performed: (a) co-incubation of blood, compound, and the suspension of bacteria; (b) a mixture of blood and compound was preincubated for 30 minutes at 37°C, after which the suspension of bacteria was added; (c) the compound was first mixed with the suspension of bacteria and preincubated for 30 minutes at 37°C, after which the blood was added. Growth inhibition was determined by plating out dilutions of 1:100 of each well after incubation of the completed mixtures at 37°C for 6 hours. Antibacterial activity is expressed as the minimum inhibitory concentration (MIC_{90}) at which 90% inhibition of growth was observed after incubating the spread plates for 18 hours.

6.10.5 Killing Kinetics

Time-kill studies were performed for the Gram-negative *E. coli* D31 and the Gram-positive *B. subtilis* ATCC 8037 to measure the time dependence of bactericidal activity following the guidelines of the NCCLS (NCCLS 1999) with small variations. Generally, cells grown in Mueller-Hinton broth to OD ~0.2 in mid-log phase were adjusted to OD 0.02, and amended with a range of the compound in question at concentrations from 0 to 2 times the MIC_{90} for each strain. Aliquots from the assay

were removed at certain time intervals (0, 5 min, 10 min, and 30 min), immediately diluted 1:100 to remove the effects of the drug, and visualized under the microscope. At each time point, three samples were quantified and averaged to produce the number of bacterial survivors.

6.10.6 Resistance Studies

E.coli and *S.aureus* were used to look for the development of resistance toward the discrete oligomer.(2-4) Control antibiotics used were ciprofloxacin for *E.coli* and penicillin for *S.aureus*. For each compound, the amount needed to achieve one half the MIC_{90} value in 200μL of M-H media was determined and metered out with media to make 10μL. Cultures of the bacteria were grown overnight at 37˚C with agitation and the OD_{600} values determined. The cultures were diluted to an OD_{600} of 0.001 in fresh M-H and 190μL of each was metered out into the well of a 96-well polystyrene plate containing the proper antibiotic. After roughly 24h the OD_{600} was determined using a 96-well plate reader and the cultures were diluted again to an OD_{600} of 0.001, 190μL were then added to new wells containing the proper antibiotic. Every 4 days four tubes are inoculated with *E.coli*/active compound, *E.coli*/ciprofloxacin, *S.aureus*/active compound, and *S.aureus*/penicillin, grown overnight at 37˚C, diluted in the morning and regrown into the log phase (~2.5-3h) in fresh M-H media. These log cells are then used for determining the MIC values and to look for an increase in concentration for the MIC_{90} relative to cells not exposed to the compounds (0d). Cells used for MIC tests are stored at -80˚C.

6.11 Material Applications

6.11.1 Making the Polymer Plugs

Two different polymers, polyurethane (PU, from the Army lot #RLE16133C02) and poly(vinyl chloride) (PVC, Self-Cath® by Mentor, 14Fr Ref 414), were used to test the incorporation of the antibacterial compound into materials. To make the antibacterial incorporated polymer plugs, a solution of the antibacterial compound (2mg/mL) was added to the polymer solution to a final concentration of 5% v/v active compound/polymer substrate (in the case of PVC, the polymer was first dissolved in 1g/5mL THF). Then 0.25 mL of the mixture was placed in the bottom of a glass vial. The plugs were allowed to harden overnight and then were placed in a vacuum oven for 12 hours to remove all residual solvent. To make the control plugs, 0.25 mL of the solution of the polymer was added to the vial and treated the same as the antibacterial samples. The final weight percent of the treated polymer plugs were 0.05% and 0.008% for PVC and PU respectively.

6.11.2 Testing the Materials Antibacterial Properties

Both sets of polymer plugs were tested for their antibacterial properties. Generally, the bacterium were grown overnight and diluted to an OD_{600} of 0.001 in fresh media to use as inoculums. 1 mL of fresh media was added to the vial with the polymer plug and was inoculated with 50 μL of the bacterial solution. The samples were incubated for 24 hours at 37°C with gentle shaking.

For the PU samples, the media was then gently removed and 500 μL of fresh media was added so that the biofilm was not disturbed and the unattached cells were removed. 2.5 μL of 10 mg/mL solution of TTC was added to make a 0.005% v/v solution and the sample was incubated for another ninety minutes. Following incubation, a red color developed indicating metabolism of the dye by the bacteria. 150 μL of the solution was transferred into a 96 well plate and read on the plate reader at 490 nm.

The PVC samples could not be quantified in this way since the plugs often floated off the bottom of the glass vial. After incubating for 24 hours, the media was analyzed under the microscope and no bacteria were observed. The solution above the plug was also visibly clear.

6.11.3 Leaching Experiment

To determine if the active compound was leaching, an HPLC (high performance liquid chromatography) experiment was performed. In this experiment, the prepared PU plugs (treated and untreated samples) were incubated with pure water and 10 μL aliquots were removed at specific time points (0, 1h, 2h, 4h, 6h, 8h, 12h, 27h, 36h, 48h, 72h, 96h, 120h). Each of these samples was diluted to 1mL volumes with pure water and run on the HPLC in pure water. The initial data was collected at all wavelengths; however it was analyzed at 190 nm. This wavelength is where the intensity of the control sample is maximal. The area of the peak was compared to a control sample with the concentration of active compound expected if 100% of it leached out.

6.12 Testing Breast Cancer Cell Activity

Two human breast cancer cell lines, MCF-7 (ATCC HTB-22) and TMX2-28, and one non-cancerous breast cell line, MCF-10A (ATCC CRL-10317), were used in this study. The MCF-7 and TMX2-28 cells were grown in DC_5 cell growth media while the MCF-10A cells were grown in MEGM, both supplemented with 5% bovine growth serum. The cells were grown using standard techniques. In short, the cells were seeded in flasks and allowed to incubate at 37°C with 5% CO_2. When the cells reached 50% confluence they were split into several flasks. After growing again to 50% confluence, the cells were removed from the flasks using trypsin. The trypsin was then removed from solution by centrifugation and the cells were resuspended into fresh medium. Sterile 96 well plates were seeded at a density of 10,000 cells/well and allowed to grow overnight yielding 50% confluence. The molecules were then added to solution and allowed to further incubate for 48 hours. An XTT kit (purchased from Roche) was used to determine the amount of metabolizing cells in each well.

6.13 Lysis Data

6.13.1 Preparation of the Vesicles

Vesicles were prepared using the film rehydration method. The desired amount of lipid solution was transferred to a glass vial and dried using nitrogen to form a thin film on the wall of the vial. Either buffer or calcein solution (40 mM calcein in pH 7 mM Na_2PO_4 buffer) was added to the lipid film to a final concentration of 10 μmol lipid/mL of solution. The solution was then warmed in water and frozen in

acetone/liquid nitrogen for three cycles and then sonicated for 15 minutes making the solution less clear. This procedure was repeated for another sonication cycle, ultimately ending with freezing and warming the solution. In the case of the calcein encapsulated vesicles, the vesicles were then run through a size exclusion Sephadex G-25 column to remove the excess dye and collect the vesicles. The vesicles were used within two days for best results.

6.13.2 Leakage Experiments

Calcein leakage experiments were performed by using vesicles in a pH 7.0 sodium phosphate buffered solution and adding various amounts of polymer in DMSO.(5-7) Emission at 515 nm was monitored over time. The excitation wavelength was 490 nm. The percentage of DMSO in any given experiment was less than 4%. The vesicles were not lysed by the presence of DMSO, as tested by the addition of pure DMSO. After monitoring the fluorescence of the polymer, 50 μL of 0.2% triton X-100 was added to determine the intensity at 100% lysis.

6.13.3 Lipid Movement Experiments

The lipid movement experiments were performed by using asymmetrically labeled vesicles.(8) In this case, the vesicles were prepared using 0.5 mol % head-group NBD-PS lipids to make symmetrically labeled vesicles. The NBD fluorescence of the outer leaflet of the vesicle was quenched by dithionite reduction by adding 75 μL of 1M sodium hydrosulfite/1M Tris to 1 mL of vesicles and allowing incubation for 15

minutes. Only the amount of vesicles to be used was asymmetrically quenched since the quencher in the aqueous solution was not removed.

The fraction of the NBD-lipids that had moved from the inner to the outer leaflet of the vesicles with the addition of the active compound was determined by dithionite quenching. The asymmetric vesicles (25 μL) were added to buffer (1mL). 10 μL of quencher solution was added to the 1.025 μL solution to make a total volume of 1.035 μL. To this solution, varying concentrations of the active compound was added from a stock solution of 2mg/mL keeping the DMSO concentration less than 5%. DMSO did not have an effect on lipid movement as determined by adding pure DMSO. The fluorescence was monitored at 530 nm (exciting at 450). The resulting fluorescence values were normalized to the intensity prior to addition of the active agent.

6.14 Membrane Activity with Living Cells

Cytoplasmic membrane permeability was measured using the membrane potential-sensitive cyanine dye diSC3-5.(9-14) This dye is known to distribute between the cells and the medium depending on the membrane potential gradient. Once the dye is inside the membrane, it aggregates and self-quenches. With the addition of a membrane permeabilizing agent, the dye is released and fluorescence over time can be monitored. In this experiment, *S. aureus* ATCC 25923 was used and grown at 37°C with shaking until mid-logarithmic phase. The cells were collected by centrifugation, washed once with buffer (5mM HEPES, pH 7, 5mM glucose) and resuspended until an optical density (OD_{600}) of 0.05. The cells were incubated with 0.4 μM diSC3-5 for an hour for maximal uptake of the dye after which 100 mM KCl was added to equilibrate

the cytoplasmic and external potassium ion concentration. The cells were mixed with the concentration of active compound desired and the fluorescence was monitored using a Perkin-Elmer Model LS5 spectrophotometer with an excitation wavelength of 622 nm and an emission wavelength of 670 nm. The dye release with the addition of 1% DMSO was monitored as a control.

6.15 References

1. , National Committee for Clinical Laboratory Standards. 2002. Performance Standards for antimicrobial susceptibility testing; 12th informational supplement (aerobic dilution) M100-S12. National Committee for Clinical Laboratory Standards, Wayne, PA.
2. Shelburne, C. E., Coulter, W. A., Olguin, D., Lantz, M. S. & Lopatin, D. E. (2005) *Antimicrobial Agents and Chemotherapy* **49,** 183-187.
3. Cudic, M., Lockatell, C. V., Johnson, D. E. & Otvos, L. (2003) *Peptides* **24,** 807-820.
4. Lui, S. Y., Yeoh, K. G. & Ho, B. (2003) *Journal of Clinical Microbiology* **41,** 5011-5014.
5. Liu, D. & DeGrado, W. F. (2001) *J. Am. Chem. Soc.* **123,** 7553-7559.
6. Gazin, E., Boman, A., Boman, H. G. & Shai, Y. (1995) *Biochemistry* **34,** 11479-11488.
7. Epand, R. F., Umezawa, N., Porter, E. A., Gellman, S. H. & Epand, R. M. (2003) *Eur. J. Biochem.* **270,** 1240-1248.
8. Matsukaki, K., Murase, O., Fujii, N. & Miyajima, K. (1996) *Biochemistry* **35,** 11361-11368.
9. Zhang, L., Scott, M. G., Yan, H., Mayer, L. D. & Hancock, R. E. (2000) *Biochemistry* **39,** 14504-14514.
10. Friedrich, C. L., Moyles, D., Beveridge, T. J. & Hancock, R. E. (2000) *Antimicrob. Agents Chemother.* **44,** 2086-2092.
11. Wu, M., Maier, E., Benz, R. & Hancock, R. E. (1999) *Biochemistry* **38,** 7235-7242.
12. Ehringer, W. D., Su, S., Chiang, B., Stillwell, W. & Chien, S. (2002) *Lipids* **37,** 885-892.
13. Sims, P. J., Waggoner, A. S., Wang, C.-H. & Hoffman, J. F. (1974) *Biochemistry* **13,** 3315-3330.
14. Ghazi, A., Schechter, E., Letellier, L. & Labedan, B. (1981) *FEBS Letters* **125,** 197-200.

APPENDIX

CONFORMATIONAL CHANGES OF FACIALLY AMPHIPHILIC *META*-POLY(PHENYLENE ETHYNYLENE)S IN AQUEOUS SOLUTION

A.1 Introduction

Many natural molecules take on different conformations depending on their environment and sequence. These conformations can be stabilized by noncovalent interactions such as hydrogen bonding, the hydrophobic effect, or van der Waals forces.(1) A challenging but interesting problem is faced when trying to prepare synthetic, non-biological molecules that will react similarly to changes in their environment. Success in this area may provide a simpler model for complex macromolecules and lead to insight on the formation of secondary, tertiary, and quaternary structures of natural molecules. Although folded structures induced by specific metal-ligand and hydrogen bonding have been widely studied,(2-6) there are only a few reports on the use of solvophobic(7-9) or π-π stacking interactions(10, 11) to control conformation. Alternately, it is known that when traditional synthetic macromolecules, such as polymers, are placed in poor solvents, they form collapsed, dense globular structures lacking well-defined order and when placed in a good solvent the molecules assume an expanded, random coil structure but still lack internal order.(12, 13)

There has been recent interest in molecules that form well defined, ordered structures in solution.(14-16) Fleet and co-workers synthesized oligomers of furanose with only four repeat units that adopt secondary structures held together by hydrogen

bonding.(17) β-amino acid oligomers as short as six residues have been reported to form stable helices.(18, 19) Zuckermann and co-workers synthesized oligo-N-substituted-glycines of various lengths and despite the achirality of the backbone and the lack of internal hydrogen bonds, these molecules form helical structures.(20) In addition, aromatic amides adopt well-defined crescent and helical structures.(21-25) A common theme of this research is that the molecules studied are discrete oligomers where the structure can be controlled by changes in temperature or pH.

Moore and co-workers reported aromatic hydrocarbon backbones based on *meta*-phenylene ethynylene (m-PE) in which solvent was used to influence an extended random coil or helical structure.(8, 9, 26) By attaching polar triethylene glycol side chains to the nonpolar m-PE backbone, high dielectric constant solvents induce collapsed (helical) structures which minimize solvent-backbone interactions while maximizing solvent-side chain contacts. Structural investigations into helix stability have included the addition of methyl groups(27) and metal-ligands(6) to the helix interior, aromatic ring electronics,(8) and hydrogen bonding.(28) By manipulating the linker functionality between the ethylene glycol chain and the PE backbone, it is possible to influence the stability of the collapsed, helical structure in solution.(8, 29) The coil-helix folding transition of these oligomers has been conveniently monitored by UV-Vis and fluorescence spectroscopy(8, 29) and confirmed by chiral guest induced circular dichroism.(27) Like other studies on folding oligomers, only discrete chain length m-PEs have been studied so that the influence of molecular weight polydispersity is not known.

We have been interested in the study of facially amphiphilic polymers based on *meta*-poly(phenylene ethynylene)s(30) (m-PPE) and langmuir experiments performed on these molecules confirmed their amphiphilicity at the air-water interface by adopting an extended structure.(31) During this research, we observed a clear difference in properties between facially amphiphilic m-PPEs with and without alkyl side chains. The fact that molecules of m-PPE lacking an alkyl side chain consistently provided different results from those with an alkyl substituent prompted us to investigate the possibility of helix formation in polymeric m-PPEs with cationic, polar side chains. The alkyl side chain would be located in the helix interior upon folding and the absence of this group would allow helix formation.

A.2 Experimental

The synthesis of polymers **70d** and **25d** followed previously reported procedures and polymers **71d** and **32** were synthesized using similar procedures.(30) ^{1}H and ^{13}C NMR spectra were obtained at 300 MHz with a Bruker DPX-300 NMR spectrometer. The gel permeation chromatography (GPC) experiment was performed in THF at room temperature using a PL LC 1120 pump, a Waters R403 differential refractometer, and three PLgel columns (10^5, 10^4, and 10^3 Å). The system was calibrated with polystyrene standards. Absorption spectra were measured on a Hewlett Packard 8453 spectrophotometer. Emission and excitation spectra were taken on a Perkin-Elmer LS 50B spectrometer with a xenon lamp light source.

To determine the corrected $n^{\dagger}$ values listed in Table 1, **25d** was fractionated by the GPC. Refractive index detector was used to monitor peak elution and 0.3 mL

fractions were collected during the elution totaling 20 samples. These fractions were then analyzed by MALDI-ToF. The fraction that included the top of the peak, as determined by GPC, was used to calculate $n^{\dagger}$. This data was obtained at the University of Massachusetts Amherst mass spec facility, which is supported in part by the National Science Foundation.

The fluorescence and UV-vis was monitored with increasing percentage of water. A stock solution of polymer was made in DMSO as to keep the polymer concentration constant throughout the experiment. The concentrations explored ranged from 50 to 5000 μg/mL to test for concentration independence. For fluorescence, the samples were prepared at a concentration where the UV absorbance was less that 0.1 so that inner filter effects were minimal. For UV spectra, the OD values were around 0.75.

Circular Dichroism (CD) was monitored on a JASCO J720 spectrometer at ambient temperature in 0.1 cm rectangular quartz cuvettes using concentrations of 0.100 mg/mL. The concentration of polymer and the number of equivalents (100) of the chiral acid were calculated based on the molecular weight of the monomer unit.

A.3 Results and Discussion

Both helical and extended structures of *meta*-phenylene ethynylene's have been observed confirming the rich conformational flexibility available from this molecular backbone. Helical structures were driven by solvophobic collapse(8, 9) while extended conformations are governed by patterning of polar and nonpolar side chains(31, 32) or the reduction of free volume in the solid state.(33, 34) The four polymers discussed in this paper are shown in Table A.1 along with molecular weight information based on

GPC standards and MALDI-ToF experiments. Polymers **70d**, **25d**, and **71d** contain polar groups with cationic amines while **32** has triethylene glycol side chains. In addition, **70d** and **25d** have nonpolar alkyl side chains in contrast to **71d** and **32**. Polymer **32** was prepared in order to make direct comparisons to Moore's structure; although, **32** is a polydisperse sample while Moore studied discrete oligomers.(8)

Table A.1: Molecules used in this study.

Polymer	Structure	Mn	PDI	n*	corrected n†
70d	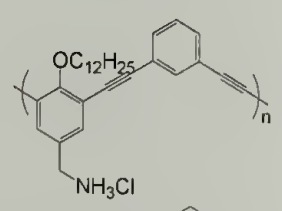	8,420	1.40	16	8
25d	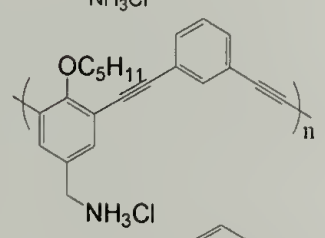	8,450	1.31	20	10
71d	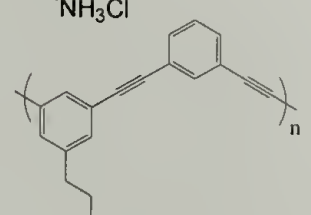	6,760	1.48	20	10
32	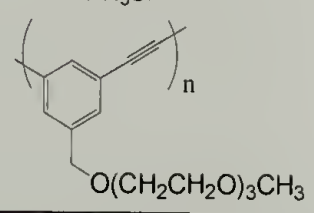	10,900	1.53	31	16

* These values are based on GPC data calibrated to polystyrene standards.
† The corrected n values are based on MALDI-ToF data for polymer **25d**.

When studying the aggregation behavior of facially amphiphilic *m*-PPEs **70d** and **25d**, fluorescence spectroscopy showed small wavelength shifts (~10 nm) upon water addition consistent with intermolecular distances of ~4.9 Å.(35) Much larger red shifts would be expected for a highly collapsed structure with aromatic distances less than 4.9 Å.(29, 35-38) For polymers **70d** and **25d**, DMSO appears to be a good solvent

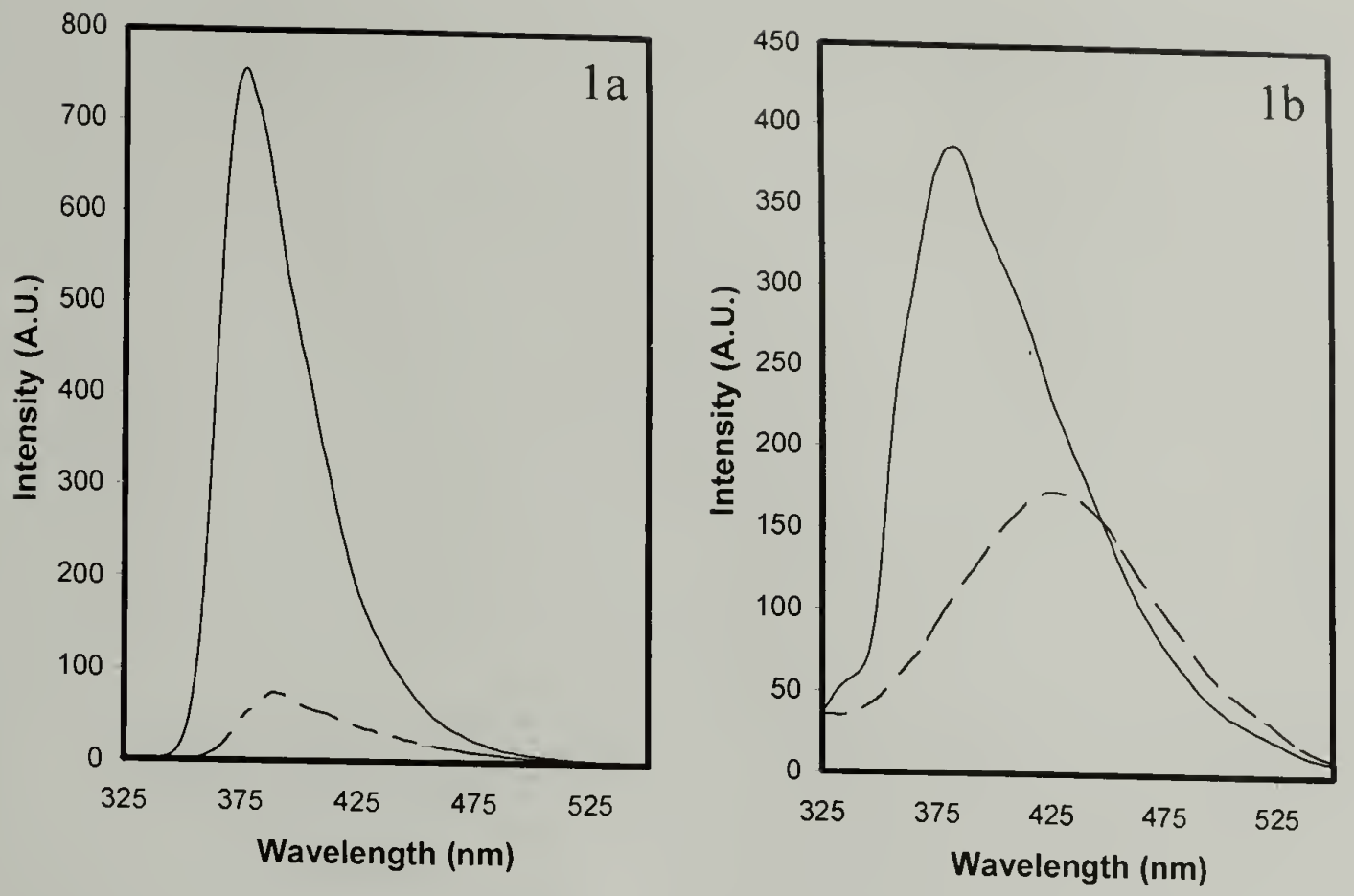

Figure A.1: Fluorescence spectra of polymer 70d (1a) and polymer 71d (1b) in DMSO (solid) and 90% H2O/DMSO (dashed). The concentration of 70d and 71d were held constant in each experiment so direct comparison of intensity was made.

in which the polymer adopts a random coil conformation based on NMR, absorption, and emission spectroscopy, while water is a poor solvent resulting in precipitation of polymers **70d** and **25d** at high water content.

Figure A.1 shows the fluorescence spectra of polymers **70d** and **71d** in two different solvents, DMSO and 90% H_2O/DMSO, while keeping the polymer concentration constant. The spectra for **70d**, Figure 1a, has an intense peak in DMSO, however, as water is added up to 90% H_2O/DMSO, the emission spectra decreases in intensity, broadens, and red shifts slightly by 10 nm. In contrast, when similar experiments were performed with **71d**, very different spectra were obtained in 90% H_2O/DMSO compared to those of polymers **70d** and **25d**.(30) The fluorescence spectra of polymer **71d** has an intense peak in DMSO with λ_{max} of 383 nm compared to **70d** at

377 nm but broader than that observed for **70d** by 40 nm at full width half-height (FWHH). The small differences in λ_{max} can be explained by electron density of the two polymers since **71d** does not have the ether substituent of **70d**. The increase in width at FWHH observed for **71d** may indicate that DMSO is a better solvent for **70d**, which might not be surprising given the absence of the alkyl side chain in **71d**.(39) This is further supported by the spectrum obtained in 95% chloroform/DMSO in which λ_{max} is 381 nm; however, the peak is substantially narrower than those obtained in DMSO.(39) This suggests the DMSO spectrum may be a combination of those observed in 95% $CHCl_3$/DMSO and 90% H_2O/DMSO. Upon changing to 90% H_2O/DMSO, the signal for **71d** decreases intensity and red shifts approximately 50 nm. This broad, featureless red-shifted band can be explained by close π-π stacking of the aromatic rings.(29) Regardless, the changes are consistent with spectra obtained by Moore and co-workers for helical conformations(29); however, random collapse, to provide close aromatic contacts without helix formation, could also give rise to these observations.(40) The differences observed in the emission spectra between **70d** and **71d** in 90% H_2O/DMSO strongly suggest different conformational or aggregational modes are present.

In fact, conformational changes are more likely than aggregation based on the observation that **70d** precipitated from 90% H_2O/DMSO solutions at 50 μg/mL after 2 days while **71d** remains soluble in this solvent at 100 times the concentration (5000 μg/mL) over months. Polymer **25d** is also observed to precipitate from 90% H_2O/DMSO solutions after two days at concentrations of 50 μg/mL. Polymer **70d** is believed to aggregate through an extended amphiphilic structure(31) organized into layers(32) which is likely to give macroscopic precipitation as more molecules are

added to the aggregate. Interestingly, the lack of precipitation from **71d** in 90% H_2O/DMSO would indicate random collapse of the polymer chains is not responsible for the changes observed by fluorescence spectroscopy since this is expected to result in precipitation over time.(41)

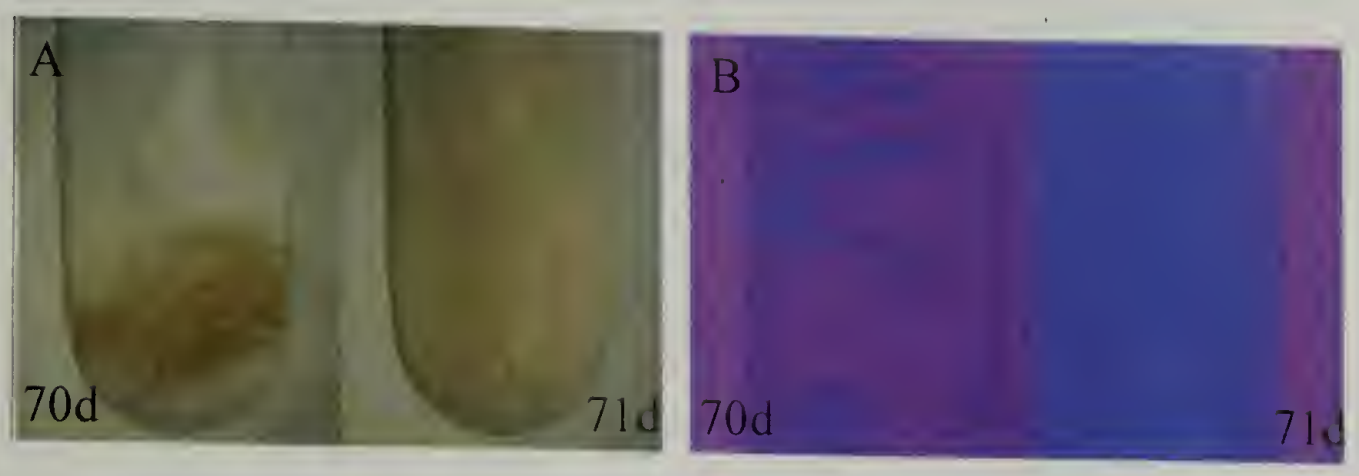

Figure A.2: Pictures of polymer 70d (left) and 71d (right) in (A) natural light and (B) long wave UV light. Notice the differences in the solution. Polymer 70d has a turbid nature with visible aggregates while 71d remains optically clear.

Shown in Figure A.2a are photographs of polymers **70d** and **71d** in 90% H_2O/DMSO solution taken under natural light in which **70d** has precipitated out of solution while polymer **71d** is still optically clear and in solution as observed by the slight yellow color due to the higher concentration of polymer. Figure A.2b was taken under long wavelength UV illumination and shows that only the particles formed by precipitation of **70d** fluoresce while **71d** shows homogeneous emission from the solution. The lack of precipitate from **71d** but dramatic change observed in the emission spectra suggests this polymer adopts a new conformation in 90% H_2O/DMSO which is quite different from **70d** and would be consistent with intramolecular helix formation. It is clear that **70d** cannot adopt helical conformations because three dodecyloxy side chains are much too large for the interior cavity formed by the helix while **71d** does not have this steric problem due to the lack of alkyl side chains. It is

also possible that **71d** adopts some other structure by intermolecular self-assembly which does not lead to macroscopic precipitation. For example, the formation of cylindrical micelle-like structures(42, 43) in which the polymer backbone extends along the cylinder length cannot be ruled out. However, this is not consistent with close π-π stacking suggested by the emission spectrum. Initial ^{1}H-NMR investigations have not provided insight into these changes and vapor pressure osmometry cannot be performed in DMSO(44) to measure an increase in molecular weight due to intermolecular aggregation.

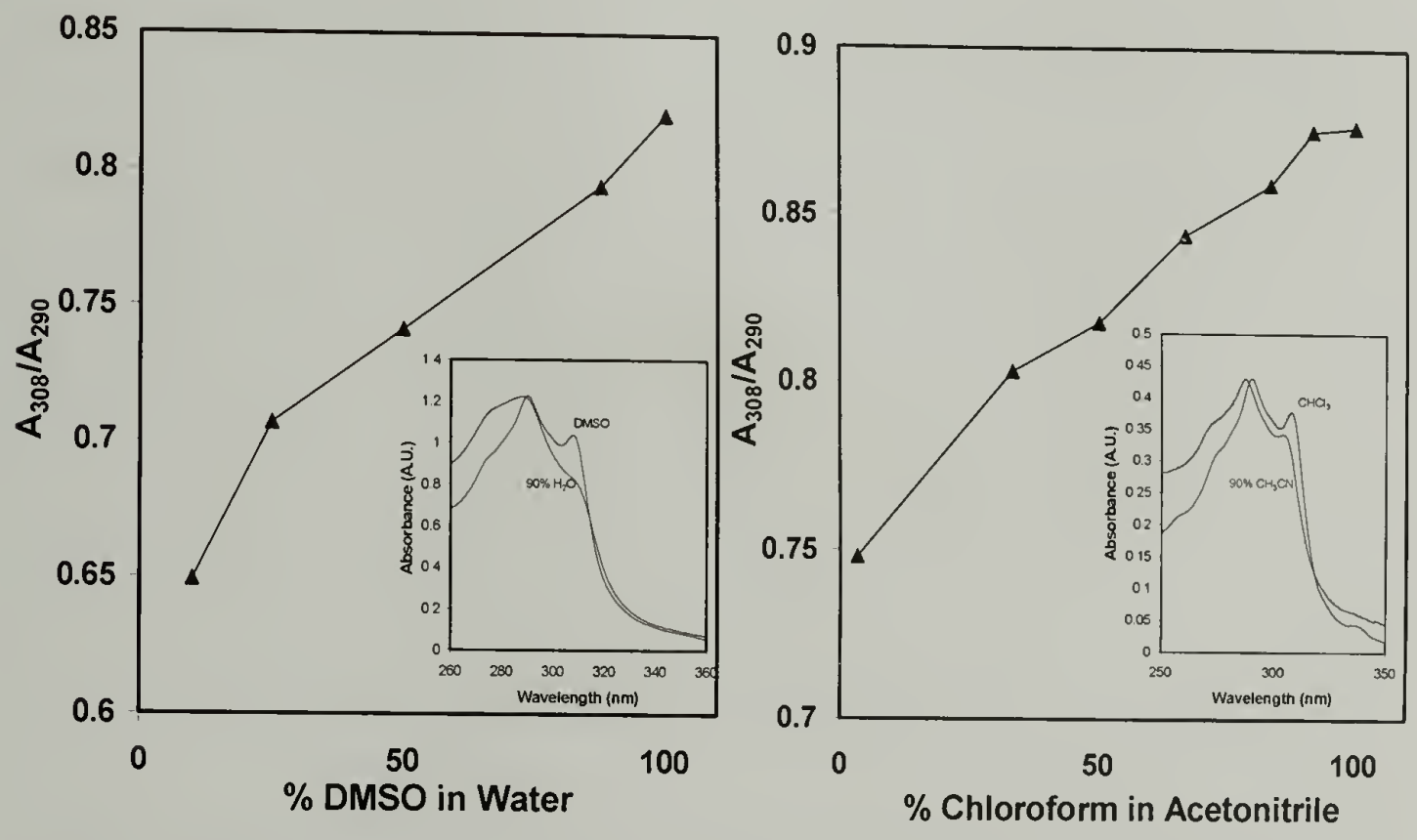

Figure A.3: (a) Titration curve for polymer 71d when changing solvents from DMSO to 90% H_2O/DMSO. The inset shows the absorbance spectra for polymer 71d at the beginning and end points of the curve. (b) Titration curve for polymer 32 when changing solvents from

UV-Vis spectroscopy has proven extremely beneficial for characterizing the random coil to helix folding reaction in m-PEs by monitoring the relative populations of transoid and cisoid confirmations, respectively.(29) Moore and co-workers were able to

produce sigmoidal titration curves from discrete m-PE oligomers with triethylene glycol ester side chains by monitoring the ratio of peaks at 289 nm and 305 nm as the solvent was changed from acetonitrile to chloroform. In their system, strongly cooperative unfolding is seen for oligomers longer than 12 units, while broad non-cooperative transitions are seen for shorter chain lengths. Most of their work has focused on ester m-PE derivatives, although, the influence of aromatic ring electron density was investigated.(29) For benzyl ethers, similar to **32**, UV-Vis and emission spectra were consistent with helix formation but no titration curves were provided. In this regard, we examined UV-Vis titration curves of **71d** in DMSO and water as well as the polymeric analog of Moore's triethylene glycol benzyl ether, **32**, in chloroform and acetonitrile. The insets of Figures A.3a and A.3b show UV-Vis curves for **71d** in DMSO and 90% H_2O/DMSO and **32** in chloroform and 90% acetonitrile/chloroform, respectively. These end points show the characteristic changes observed for the coil to helix transitions of m-PE, which in Moore's work have been confirmed by circular dichroism spectroscopy (CD).(27) However, titration curves shown in Figures A.3a and A.3b for **25d** and **32**, respectively, do not show cooperative unfolding reactions. The lack of a distinct transition may be due to the relatively low molecular weight of these polymers so that large populations of short chains are present. These short chains would contribute significantly to a non-cooperative transition as observed by Moore for discrete oligomers of 8 and 10 repeats. The reported molecular weights are referenced to polystyrene standards, which are known to overestimate the molecular weight of rigid polymers by 1.5 to 2.0.(45-48) In addition, MALDI-ToF spectra were obtained by fractionation of the GPC peak and suggest the molecular weights are between 0.5 and

0.6 the value obtained from GPC. The kind of transitions observed in Figure 3 have also been attributed to multichain interactions,(49) however, it is believed that, in this case, it is intramolecular folding since the results are independent of time and concentration (50-5000 μg/mL). In addition, intermolecular associations, like those to form cylindrical micelles, would not be expected to increase the population of cisoid conformations as observed by the UV-Vis experiments. Also, Moore and co-workers report that the oligomer of polymer **32** needs a more polar solvent (ie. water) in order to undergo a strong transition in UV and fluorescence spectroscopy,(8) however, **32** is not soluble in neat acetonitrile so that addition of water cannot be performed due to the presence of chloroform.

From UV-Vis titration curves, changes in 308/290 ratio, and emission in polar solvents, a helical conformation of **71d** cannot be firmly concluded. As a result, CD experiments were performed; however, **71d** does not contain any chiral centers and so an equal population of right and left handed helical conformations would be expected. Chiral additives have been used previously to induce a preference of one handedness in helical structures.(50) Therefore, we speculated that the addition of chiral carboxylic acids could result in associations with the primary amines of **71d** and influence helical handedness.(50-52) When the chiral carboxylic acid, D-mandelic acid, was added to solutions of **71d** in 90% H_2O/DMSO, a CD spectrum was obtained with a negative ellipticity characteristic of the absorption spectra for this polymer as shown in Figure A.4. In addition, the same experiment performed in DMSO resulted in no observed change in ellipticity. The CD spectrum of D-mandelic acid in 90% H_2O/DMSO without **71d** also resulted in a spectrum with no change in molar ellipticity. The appearance of a

negative molar ellipticity from solutions of **71d** in 90% H_2O/DMSO with D-mandelic acid but no change in molar ellipticity from DMSO solutions is consistent with a helical conformation of **71d** in 90% H_2O/DMSO. Chiral guest experiments were also conducted but no change in ellipticity could be observed.(27)

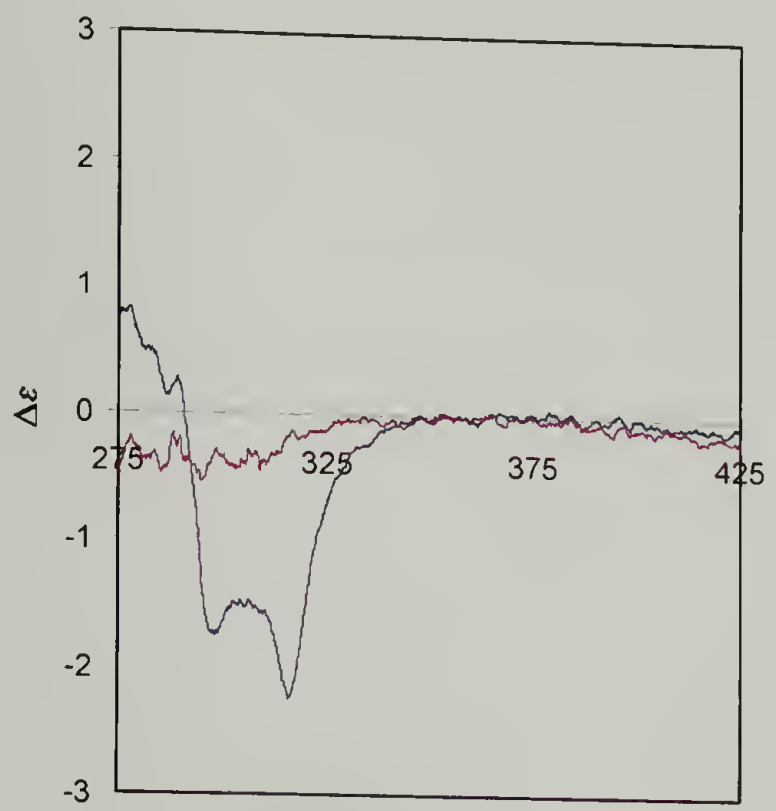

Figure A.4: Circular dichroism spectra of 71d in DMSO (red line) and 90% H_2O/DMSO (blue line) with D-mandelic acid (100 equivalents). The appearance of a signal only in 90% H_2O/DMSO suggests a helical conformation is likely.

A.4 Conclusions

The solution conformations of facially amphiphilic polymers based on m-PPE backbones were studied. Those with alkyl substituents clearly form extended structures even in 90% H_2O/DMSO solution,(31, 32) while polymers without alkyl side chains appear to adopt alternative conformations with spectroscopic features similar to helical structures reported in the literature.(29) CD spectroscopy in the presence of a chiral carboxylic acid additive showed a signal consistent with a helical structure. Although, intermolecular self-assembly into cylindrical or other structures cannot be entirely ruled

out, these other structures are not consistent with the UV-Vis spectra. The benzyl ether function may not produce the most stable helical conformations, according to Moore, and this might also influence the results discussed here. However, it can be safely concluded that m-PPEs without alkyl groups adopt different conformations and structures in solution than those with alkyl groups. Polymers with significantly higher molecular weights should eliminate the influence of small chains on the titration curves and are a future synthetic target. This is the initial report of polydisperse phenylene ethynylenes folding in solution toward helical structures and demonstrates some of the difficulties that will be encountered during these studies. The ability to control molecular conformation by side chain decoration of the backbone with polar and non-polar groups leads to some interesting opportunities.

A.5 References

1. Friedman, R. A. & Honig, B. (1995) *Biophys. J.* **69,** 1528-1535.
2. Delnoye, D. A. P., Sijbesma, R. P., Vekemans, J. & Meijer, E. W. (1996) *J. Am. Chem. Soc.* **118,** 8717-8718.
3. Brunsveld, L., Zhang, H., Glasbeek, M., Vekemans, J. & Meijer, E. W. (2000) *J. Am. Chem. Soc.* **122,** 6175-6182.
4. Bielawski, C., Chen, Y. S., Zhang, P., Prest, P. J. & Moore, J. S. (1998) *Chem. Comm.*, 1313-1314.
5. Yagi, S., Sakai, N., Yamada, R., Takahashi, H., Mizutani, T., Takagishi, T., Kitagawa, S. & Ogoshi, H. (1999) *Chem. Comm.*, 911-912.
6. Prince, R. B., Okada, T. & Moore, J. S. (1999) *Angew., Chem., Int. Ed.* **38,** 233-236.
7. Ben-Naim, A. (1971) *J. Chem. Phys.* **54,** 1387-1404.
8. Lahiri, S., Thompson, J. L. & Moore, J. S. (2000) *J. Am. Chem. Soc.* **122,** 11315-11319.
9. Nelson, J. C., Saven, J. G., Moore, J. S. & Wolynes, P. G. (1997) *Science* **277,** 1793-1796.
10. Cubberley, M. S. & Iverson, B. L. (2001) *J. Am. Chem. Soc.* **123,** 7560-7563.
11. Hunter, C. A. & Sanders, J. K. M. (1990) *J. Am. Chem. Soc.* **112,** 5525-5534.
12. Chan, H. S. & Dill, K. A. (1989) *Macromolecules* **22,** 4559-4573.
13. Flory, P. J. (1953) *Principles of Polymer Chemistry* (Cornell University Press, Ithica).
14. Gellman, S. H. (1998) *Acc. Chem. Res.* **31,** 173-180.
15. Iverson, B. (1997) *Nature* **385,** 114.
16. Hill, D. J., Mio, M. J., Prince, R. B., Hughes, T. S. & Moore, J. S. (2001) *Chem. Rev.* **101,** 3893-4011.
17. Smith, M. D., Claridge, T. D. W., Tranter, G. E., Sansom, M. S. P. & Fleet, G. W. J. (1998) *Chem. Comm.*, 2041-2042.
18. Seebach, D. & Matthers, J. L. (1997) *Chem. Comm.*, 2015-2022.
19. Cheng, R. P., Gellman, S. H. & DeGrado, W. F. (2001) *Chem. Rev.* **101,** 3219-3232.
20. Kirshenbaum, K., Barron, A. E., Goldsmith, R. A., Armand, P., Bradley, E. K., Truong, K. T. V., Dill, K. A., Cohen, F. E. & Zuckermann, R. N. (1998) *Proc. Natl. Acad. Sci.* **95,** 4303-4308.
21. Jiang, H., Leger, J.-M. & Huc, I. (2003) *J. Am. Chem. Soc.* **125,** 3448-3449.
22. Hamuro, Y., Geib, S. J. & Hamilton, A. D. (1997) *J. Am. Chem. Soc.* **119,** 10587-10593.
23. Hamuro, Y., Geib, S. J. & Hamilton, A. D. (1996) *J. Am. Chem. Soc.* **118,** 7529-7541.
24. Berl, V., Huc, I., Khoury, R. G., Krische, M. J. & Lehn, J.-M. (2000) *Nature* **407,** 720-723.
25. Berl, V., Huc, I., Khoury, R. G. & Lehn, J.-M. (2001) *Chem. -Eur. J.* **7,** 2810-2820.
26. Hill, D. J. & Moore, J. S. (2002) *Proc. Natl. Acad. Sci.* **99,** 5053-5057.

27. Prince, R. B., Barnes, S. A. & Moore, J. S. (2000) *J. Am. Chem. Soc.* **122,** 2758-2762.
28. Cary, J. M. & Moore, J. S. (2002) *Org. Lett.* **4,** 4663-4666.
29. Prince, R. B., Saven, J. G., Wolynes, P. G. & Moore, J. S. (1999) *J. Am. Chem. Soc.* **121,** 3114-3121.
30. Arnt, L. & Tew, G. N. (2002) *J. Am. Chem. Soc.* **124,** 7664-7665.
31. Arnt, L. & Tew, G. N. (2003) *Langmuir* **19,** 2404-2408.
32. Arnt, L. & Tew, G. N. (2004) *Macromolecules* **37,** 1283-1288.
33. Kubel, C., Mio, M. J., Moore, J. S. & Martin, D. C. (2002) *J. Am. Chem. Soc.* **124,** 8605-8610.
34. Prest, P.-J., Prince, R. B. & Moore, J. S. (1999) *J. Am. Chem. Soc.* **121,** 5933-5939.
35. McQuade, D. T., Kim, J. & Swager, T. M. (2000) *J. Am. Chem. Soc.* **122,** 5885-5886.
36. Bunz, U. H. F. (2000) *Chem. Rev.* **100,** 1605-1644.
37. Halkyard, C. E., Rampey, M. E., Kloppenburg, L., Studer-Martinez, S. L. & Bunz, U. H. F. (1998) *Macromolecules* **31,** 8655-8659.
38. Kim, J. & Swager, T. M. (2001) *Nature* **411,** 1030-1034.
39. Lu, S. L., Yang, M. J., Luo, J. & Cao, Y. (2004) *Synthetic Metals* **140,** 199-202.
40. Birks, J. B. (1970) *Photophysics of Aromatic Molecules* (Wiley-Interscience, New York).
41. Tompa, H. (1950) *Trans. Faraday Soc.* **46,** 970.
42. Rulkens, R., Wegner, G. & Thurn-Albrecht, T. (1999) *Langmuir* **15,** 4022-4025.
43. Bockstaller, M., Kohler, W., Wegner, G., Vlassopoulos, D. & Fytas, G. (2001) *Macromolecules* **34,** 6359-6366.
44. Mays, J. W. (1991) in *Modern Methods of Polymer Characterizations*, ed. Mays, J. W. (John Wiley and Sons, Inc., New York).
45. Kloppenburg, L., Jones, D., Claridge, J. B., zur Loye, H.-C. & Bunz, U. H. F. (1999) *Macromolecules* **32,** 4460-4463.
46. Kloppenburg, L., Jones, D. & Bunz, U. H. F. (1999) *Macromolecules* **32,** 4194-4203.
47. Vanhee, S., Rulkens, R., Lehmann, U., Rosenauer, C., Schulze, M., Kohler, W. & Wegner, G. (1996) *Macromolecules* **29,** 5136-5142.
48. Choudry, U. H., Marshall, A. R. & Bunz, U. H. F. (2003) *Macromolecules* **36,** 1424-1425.
49. Cornelissen, J., Peeters, E., Janssen, R. A. J. & Meijer, E. W. (1998) *Acta Polym.* **49,** 471-476.
50. Maeda, K., Okada, S., Yashima, E. & Okamoto, Y. (2001) *Jounal of Polymer Science: Part A: Polymer Chemistry* **39,** 3180-3189.
51. Lermo, E. R., Langeveld-Voss, B. M. W., Janssen, R. A. J. & Meijer, E. W. (1999) *Chemical Communications*, 791-792.
52. Green, M. M., Peterson, N. C., Sato, T., Teramoto, A., Cook, R. & Lifson, S. (1995) *Science* **268,** 1860-1866.

BIBLIOGRAPHY

1. Albert, M., Feiertag, P., Hayn, G., Saf, R. & Honig, H. (2003) *Biomacromolecules* **4,** 1811-1817.

2. Alberts, B., Bray, D., Lewis, J., Raff, M., Roberts, K. & Watson, J. D. (1994) *Molecular Biology of the Cell* (Garland Publishing, Inc., New York).

3. Anderson, R. C., Hancock, R. E. & Yu, R.-L. (2004) *Antimicrob. Agents Chemother.* **48,** 673-676.

4. Arias, E., Maillou, T., Moggio, I., Guillon, D., Le Moigne, J. & Geffroy, B. (2002) *Synthetic Metals* **127,** 229-231.

5. Arias-Martin, E., Arnault, J. C., Guillon, D., Maillou, T., Le Moigne, J., Geffroy, B. & Nunzi, J. M. (2000) *Langmuir* **16,** 4309-4318.

6. Arnt, L. & Tew, G. N. (2002) *J. Am. Chem. Soc.* **124,** 7664-7665.

7. Arnt, L. & Tew, G. N. (2003) *Langmuir* **19,** 2404-2408.

8. Arnt, L. & Tew, G. N. (2004) *Macromolecules* **37,** 1283-1288.

9. Arnt, L., Nusslein, K. & Tew, G. N. (2004) *J. Polym. Sci. Part A* **42,** 3860-3864.

10. Arnt, L., Breitenkamp, R. B. & Tew, G. N. (2005) *Polymers for Advanced Technologies*, accepted.

11. Ben-Naim, A. (1971) *J. Chem. Phys.* **54,** 1387-1404.

12. Berl, V., Huc, I., Khoury, R. G., Krische, M. J. & Lehn, J.-M. (2000) *Nature* **407,** 720-723.

13. Berl, V., Huc, I., Khoury, R. G. & Lehn, J.-M. (2001) *Chem. -Eur. J.* **7,** 2810-2820.

14. Bessalle, R., Haas, H., Goria, A., Shalit, I. & Fridkin, M. (1992) *Antimicrob. Agents Chemother.* **36,** 313-317.

15. Bielawski, C., Chen, Y. S., Zhang, P., Prest, P. J. & Moore, J. S. (1998) *Chem. Comm.*, 1313-1314.

16. Birks, J. B. (1970) *Photophysics of Aromatic Molecules* (Wiley-Interscience, New York).

17. Bjørnholm, T., Greve, D. R., Reitzel, N., Hassenkam, T., Kjaer, K., Howes, P. B., Larsen, N. B., Bøgelund, J., Jayaraman, M., Ewbank, P. C. & McCullough, R. D. (1998) *J. Am. Chem. Soc.* **120,** 7634-7644.

18. Blodgett, K. B. (1935) *J. Am. Chem. Soc.* **57,** 1007-1022.

19. Blondelle, S. E. & Houghten, R. A. (1992) *Biochemistry* **31,** 12688-12694.

20. Bo, Z., Rabe, J. P. & Schulter, A. D. (1999) *Angew. Chem., Int. Ed.* **38,** 2370-2372.

21. Bo, Z., Zhang, C., Severin, N., Rabe, J. P. & Schulter, A. D. (2000) *Macromolecules* **33,** 2688-2694.

22. Bockstaller, M., Kohler, W., Wegner, G., Vlassopoulos, D. & Fytas, G. (2001) *Macromolecules* **34,** 6359-6366.

23. Boman, H. G. (2000) *Immunol. Rev.* **173,** 5-16.

24. Brade, L., Bessler, W. G. & Brade, H. (1988) *Infection and Immunity* **56,** 1382-1384.

25. Breen, C. A., Deng, T., Breiner, T., Thomas, E. L. & Swager, T. M. (2003) *Journal of the American Chemical Society* **125,** 9942-9943.

26. Breitenkamp, R. B. & Tew, G. N. (2004) *Macromolecules* **37,** 1163-1165.

27. Bren, L. (2002) *FDA Consumer Magazine* **July-August**.

28. Brizius, G., Pschirer, N. G., Steffen, W., Stitzer, K., zur Loye, H. C. & Bunz, U. H. F. (2000) *Journal of the American Chemical Society* **122,** 12435-12440.

29. Broady, K. W., Rietschel, E. T. & Luderitz, O. (1981) *Eur. J. Biochem.* **115,** 463-468.

30. Brodsky, I. E., Ernst, R. K., Miller, S. I. & Falkow, S. (2002) *Journal of Bacteriology* **184,** 3203-3213.

31. Brodsky, I. E., Ghori, N., Falkow, S. & Monack, D. (2005) *Mol Microbiol* **55,** 954-972.

32. Brogden, K. A., Ackermann, M., McCray Jr., P. B. & Tack, B. F. (2003) *Int. J. of Antimicrobial Agents* **22,** 465-478.

33. Brunsveld, L., Zhang, H., Glasbeek, M., Vekemans, J. & Meijer, E. W. (2000) *J. Am. Chem. Soc.* **122,** 6175-6182.

34. Brustolin, F., Goldoni, F., Meiger, E. W. & Sommerdijk, N. A. J. M. (2002) *Macromolecules* **35,** 1054-1059.

35. Bumm, L. A., Arnold, J. J., Cygan, M. T., Dunbar, T. D., Burgin, T. P., Jones, L., Allara, D. L., Tour, J. M. & Weiss, P. S. (1996) *Science* **271,** 1705-1707.

36. Bunz, U. H. F. (2000) *Chem. Rev.* **100,** 1605-1644.

37. Burkoth, T. S., Beausoleil, E., Kaur, S., Tang, D. Z., Cohen, F. E. & Zuckerman, R. N. (2002) *Chem. Bio.* **9,** 647-654.

38. Cai, L. T., Skulason, H., Kushmerick, J. G., Pollack, S. K., Naciri, J., Shashidhar, R., Allara, D. L., Mallouk, T. E. & Mayer, T. S. (2004) *Journal of Physical Chemistry B* **108,** 2827-2832.

39. Cary, J. M. & Moore, J. S. (2002) *Org. Lett.* **4,** 4663-4666.

40. Chan, H. S. & Dill, K. A. (1989) *Macromolecules* **22,** 4559-4573.

41. Cheng, R. P., Gellman, S. H. & DeGrado, W. F. (2001) *Chem. Rev.* **101,** 3219-3232.

42. Choudry, U. H., Marshall, A. R. & Bunz, U. H. F. (2003) *Macromolecules* **36,** 1424-1425.

43. Cornelissen, J., Peeters, E., Janssen, R. A. J. & Meijer, E. W. (1998) *Acta Polym.* **49,** 471-476.

44. Cronan, J. E. (2003) *Annual Review of Microbiology* **57,** 203-224.

45. Cubberley, M. S. & Iverson, B. L. (2001) *J. Am. Chem. Soc.* **123,** 7560-7563.

46. Cudic, M., Lockatell, C. V., Johnson, D. E. & Otvos, L. (2003) *Peptides* **24,** 807-820.

47. Dathe, M. & Wieprecht, T. (1999) *Biochim. Biophys. Acta* **1462,** 71-87.

48. Dathe, M., Nikolenko, H., Meyer, J., Beyerman, M. & Bienert, M. (2001) *FEBS Letters* **501,** 146-150.

49. DeGrado, W. F. & Lear, J. D. (1985) *J. Am. Chem. Soc.* **107,** 7684-7689.

50. DeGrado, W. F. (1988) *Adv. Protein Chem.*, 51-124.

51. Delnoye, D. A. P., Sijbesma, R. P., Vekemans, J. & Meijer, E. W. (1996) *J. Am. Chem. Soc.* **118,** 8717-8718.

52. Devine, D. A. & Hancock, R. E. (2002) *Current Pharmaceutical Design* **8,** 703-714.

53. Dholakia, G. R., Fan, W., Koehne, J., Han, J. & Meyyappan, M. (2003) *Journal of Nanoscience and Nanotechnology* **3,** 231-234.

54. DiCesare, N., Pinto, M. R., Schanze, K. S. & Lakowicz, J. R. (2002) *Langmuir* **18,** 7785-7787.

55. Donelli, G., Francolini, I., Piozzi, A., Di Rosa, R. & Marconi, W. (2002) *Journal of Chemotherapy* **14,** 501-507.

56. Egbe, D. A. M., Birckner, E. & Klemm, E. (2002) *J Polym Sci Part A: Polym Chem* **40,** 2670-2679.

57. Ehringer, W. D., Su, S., Chiang, B., Stillwell, W. & Chien, S. (2002) *Lipids* **37,** 885-892.

58. Eisenberg, D., Weiss, R. M. & Terwillinger, T. C. (1984) *Proc. Natl. Acad. Sci. U.S.A.* **81,** 140-144.

59. Ellison III, R. T., Boose, D. & LaForce, F. M. (1985) *J. Infect. Dis.* **151,** 1123-1129.

60. Epand, R. M. & Vogel, H. J. (1999) *Biochim. Biophys. Acta* **1462,** 11-28.

61. Epand, R. F., Umezawa, N., Porter, E. A., Gellman, S. H. & Epand, R. M. (2003) *Eur. J. Biochem.* **270,** 1240-1248.

62. Ernst, R. K., Guina, T. & Miller, S. I. (2001) *Microbes and Infection* **3,** 1327-1334.

63. Ernst, J. T., Becerril, J., Park, H. S., Yin, H. & Hamilton, A. D. (2003) *Angew. Chem., Int. Ed.* **42,** 535-539.

64. Fink, J., Merrifield, R. B., Boman, A. & Boman, H. (1989) *J. Biol. Chem.* **264,** 6260-6267.

65. Flory, P. J. (1953) *Principles of Polymer Chemistry* (Cornell University Press, Ithica).

66. Friedman, R. A. & Honig, B. (1995) *Biophys. J.* **69,** 1528-1535.

67. Friedrich, C. L., Scott, M. G., Karunaratne, D. N., Yan, H. & Hancock, R. E. (1999) *Antimicrob. Agents Chemother.* **43,** 1274-1276.

68. Friedrich, C. L., Moyles, D., Beveridge, T. J. & Hancock, R. E. (2000) *Antimicrob. Agents Chemother.* **44,** 2086-2092.

69. Friedrich, C. L., Rozek, A., Patrzykat, A. & Hancock, R. E. (2001) *J. Biol. Chem.* **276,** 24015-24022.

70. Gazit, E., Boman, A., Boman, H. G. & Shai, Y. (1995) *Biochemistry* **34,** 11479-11488.

71. Gellman, S. H. (1998) *Acc. Chem. Res.* **31,** 173-180.

72. Gelman, M. A., Weisblum, B., Lynn, D. M. & Gellman, S. H. (2004) *Org. Lett.* **6,** 557-560.

73. Ghazi, A., Schechter, E., Letellier, L. & Labedan, B. (1981) *FEBS Letters* **125,** 197-200.

74. Gibbons, H. S., Kalb, S. R., Cotter, R. J. & Raetz, C. R. H. (2005) *Mol Microbiol* **55,** 425-440.

75. Giesa, R. (1996) *J. Macromol. Sci., Rev. Macromol. Chem. Phys.* **36,** 631-670.

76. Gotz, H., Harth, E., Schiller, S. M., Frank, C. W., Knoll, W. & Hawker, C. J. (2002) *J Polym Sci Part A: Polym Chem* **40,** 3379-3391.

77. Green, M. M., Peterson, N. C., Sato, T., Teramoto, A., Cook, R. & Lifson, S. (1995) *Science* **268,** 1860-1866.

78. Grubbs, R. H. & Kratz, D. (1993) *Chem. Ber.* **126,** 149-157.

79. Guckian, K. M., Schweitzer, B. A., Ren, X. F., Sheilds, C. J., Paris, P. L., Tahmassebi, D. C. & Kool, E. T. (1996) *J. Am. Chem. Soc.* **118,** 8182-8183.

80. Guina, T., Purvine, S. O., Yi, E. C., Eng, J., Goodlett, D. R., Aebersold, R. & Miller, S. I. (2003) *Proceedings of the National Academy of Sciences of the United States of America* **100,** 2771-2776.

81. Gunn, J. S. & Miller, S. I. (1996) *Journal of Bacteriology* **178,** 6857-6864.

82. Gunn, J. S., Lim, K. B., Krueger, J., Kim, K., Guo, L., Hackett, M. & Miller, S. I. (1998) *Mol Microbiol* **27,** 1171-1182.

83. Gunn, J. S., Ryan, S. S., Van Velkinburgh, J. C., Ernst, R. K. & Miller, S. I. (2000) *Infection and Immunity* **68,** 6139-6146.

84. Guo, L., Lim, K. B., Poduje, C. M., Daniel, M., Gunn, J. S., Hackett, M. & Miller, S. I. (1998) *Cell* **95,** 189-198.

85. Halkyard, C. E., Rampey, M. E., Kloppenburg, L., Studer-Martinez, S. L. & Bunz, U. H. F. (1998) *Macromolecules* **31,** 8655-8659.

86. Hamuro, Y., Geib, S. J. & Hamilton, A. D. (1996) *J. Am. Chem. Soc.* **118,** 7529-7541.

87. Hamuro, Y., Geib, S. J. & Hamilton, A. D. (1997) *J. Am. Chem. Soc.* **119,** 10587-10593.

88. Hamuro, Y., Schneider, J. P. & DeGrado, W. F. (1999) *J. Am. Chem. Soc.* **121,** 12200-12201.

89. Hancock, R. E. (1997) *Lancet* **349,** 418-422.

90. Hancock, R. E. & Lehrer, R. (1998) *Trends Biotechnol.* **16,** 82-88.

91. Hancock, R. E. & Chapple, D. S. (1999) *Antimicrob. Agents Chemother.* **43,** 1317-1323.

92. Hancock, R. E. (1999) *Drugs* **57,** 469-473.

93. Hancock, R. E. & Scott, M. G. (2000) *Proc. Natl. Acad. Sci.* **97,** 8856-8861.

94. Hancock, R. E. (2000) *Expert Opin. Investig. Drugs* **9,** 1723-1729.

95. Hancock, R. E. & Rozek, A. (2002) *FEMS Microbio. Lett.* **206,** 143-149.

96. Hill, D. J., Mio, M. J., Prince, R. B., Hughes, T. S. & Moore, J. S. (2001) *Chem. Rev.* **101,** 3893-4011.

97. Hill, D. J. & Moore, J. S. (2002) *Proc. Natl. Acad. Sci. U.S.A.* **99,** 5053-5057.

98. Hittinger, E., Kokil, A. & Weder, C. (2004) *Macromolecular Rapid Communications* **25,** 710-715.

99. Ho, S. W., Kwei, T. K., Vyprachticky, D. & Okamoto, Y. (2003) *Macromolecules* **36,** 6894-6897.

100. Houston Jr., M. E., Kondejewski, L. H., Karunaratne, D. N., Gough, M., Fidai, S., Hodges, R. S. & Hancock, R. E. W. (1998) *J. Peptide Res.* **52,** 81-88.

101. Huang, H. M., Wang, K. M., Xiao, Y., Zhai, Q. G., An, D. L., Huang, S. S. & Li, D. (2003) *Chinese Science Bulletin* **48,** 1947-1951.

102. Hunter, C. A. & Sanders, J. K. M. (1990) *J. Am. Chem. Soc.* **112,** 5525-5534.

103. Hwang, J. J. & Tour, J. M. (2002) *Tetrahedron* **58,** 10387-10405.

104. Ilker, M. F., Schule, H. & Coughlin, E. B. (2004) *Macromolecules* **37,** 694-700.

105. Iverson, B. (1997) *Nature* **385,** 114.

106. Jiang, H., Leger, J.-M. & Huc, I. (2003) *J. Am. Chem. Soc.* **125,** 3448-3449.

107. Jones, T. V., Blatchly, R. A. & Tew, G. N. (2003) *Organic Letters* **5,** 3297-3299.

108. Juvvadi, P., Vunnam, S., Merrifield, E. L., Boman, H. G. & Merrifield, R. B. (1996) *J. Peptide Res.* **49,** 89-102.

109. Kato, H., Haishima, Y., Iida, T., Tanaka, A. & Ken-Ichi, T. (1998) *J Bacteriol* **180,** 3891-3899.

110. Katz, M., Tsubery, H., Kolusheva, S., Shames, A., Fridkin, M. & Jelinek, R. (2003) *Biochemical Journal* **375,** 405-413.

111. Kenawy, E. R., Abdel-Hay, F. I., El-Shanshoury, A. & El-Newehy, M. H. (2002) *J Polym Sci Part A: Polym Chem* **40,** 2384-2393.

112. Kim, G., Hong, H. W. & Lee, S. H. (1999) *Bull. Korean Chem. Soc.* **20,** 321-324.

113. Kim, J. & Swager, T. M. (2001) *Nature* **411,** 1030-1034.

114. Kim, J., Levitsky, I. A., McQuade, T. & Swager, T. M. (2002) *J. Am. Chem. Soc.* **124,** 7710-7718.

115. Kim, S. K., Kim, S. S., Bang, Y. J., Kim, S. J. & Lee, B. J. (2003) *Peptides* **24,** 945-953.

116. Kim, I. B., Erdogan, B., Wilson, J. N. & Bunz, U. H. F. (2004) *Chemistry-a European Journal* **10,** 6247-6254.

117. Kirshenbaum, K., Barron, A. E., Goldsmith, R. A., Armand, P., Bradley, E. K., Truong, K. T. V., Dill, K. A., Cohen, F. E. & Zuckermann, R. N. (1998) *Proc. Natl. Acad. Sci.* **95,** 4303-4308.

118. Kirshenbaum, K., Zuckermann, R. N. & Dill, K. A. (1999) *Current Opinion in Structural Biology* **9,** 530-535.

119. Klapars, A., Huang, X. & Buchwald, S. L. (2002) *J. Am. Chem. Soc.* **124,** 7421-7428.

120. Kloppenburg, L., Jones, D., Claridge, J. B., zur Loye, H.-C. & Bunz, U. H. F. (1999) *Macromolecules* **32,** 4460-4463.

121. Kloppenburg, L., Jones, D. & Bunz, U. H. F. (1999) *Macromolecules* **32,** 4194-4203.

122. Kol, M. A., van Dalen, A., de Kroon, A. I. P. M. & de Kruijff, B. (2003) *J. Biol. Chem.* **278,** 24586-24593.

123. Kubel, C., Mio, M. J., Moore, J. S. & Martin, D. C. (2002) *J. Am. Chem. Soc.* **124,** 8605-8610.

124. Kuroda, K. & Swager, T. M. (2003) *Macromolecular Symposia* **201,** 127-134.

125. Kutzki, O., Park, H. S., Ernst, J. T., Orner, B. P., Yin, H. & Hamilton, A. D. (2002) *J. Am. Chem. Soc.* **124,** 11838-11839.

126. Kwong, F. Y., Klapars, A. & Buchwald, S. L. (2002) *Organic Letters* **4,** 581-584.

127. Kwong, F. Y. & Buchwald, S. L. (2003) *Organic Letters* **5,** 793-796.

128. Ladokhin, A. S. & White, S. H. (2001) *Biochemica et Biophysica Acta* **1514,** 253-260.

129. Lahiri, S., Thompson, J. L. & Moore, J. S. (2000) *J. Am. Chem. Soc.* **122,** 11315-11319.

130. Lai, J. R., Huck, B. R., Weisblum, B. & Gellman, S. H. (2002) *Biochemistry* **41,** 12835-12842.

131. Langmuir, I. (1917) *J. Am. Chem. Soc.* **39,** 1848.

132. Lee, S., Mihara, H., Aoyagi, H., Kato, T., Izumuya, N. & Yamasaki, N. (1986) *Biochim. Biophys. Acta* **862,** 211-219.

133. Lee, V. J. & Hecker, S. J. (1999) *Medicinal Research Reviews* **19,** 521-542.

134. Lee, H., Hsu, F. F., Turk, J. & Groisman, E. A. (2004) *Journal of Bacteriology* **186,** 4124-4133.

135. Leonard, N. J. (1979) *Acc. Chem. Res.* **12,** 423-429.

136. Lermo, E. R., Langeveld-Voss, B. M. W., Janssen, R. A. J. & Meijer, E. W. (1999) *Chemical Communications*, 791-792.

137. Lewis, R. (1995) *FDA Consumer Magazine*.

138. Lin, J., Huang, S. X. & Zhang, Q. J. (2002) *Microbes and Infection* **4,** 325-331.

139. Liu, D. & DeGrado, W. F. (2001) *J. Am. Chem. Soc.* **123,** 7553-7559.

140. Lockwood, N. A. & Mayo, K. H. (2003) *Drugs of the Future* **28,** 911-923.

141. Lopez-Solanilla, E., Garcia-Olmedo, F. & Rodriguez-Palenzuela, P. (1998) *Plant Cell* **10,** 917-924.

142. Lu, S. L., Yang, M. J., Luo, J. & Cao, Y. (2004) *Synthetic Metals* **140,** 199-202.

143. Lui, S. Y., Yeoh, K. G. & Ho, B. (2003) *Journal of Clinical Microbiology* **41,** 5011-5014.

144. Madigan, M. T., Martinko, J. M. & Parker, J. (2003) *Brock Biology of Microorganisms* (Pearson Education, Inc., Upper Saddle River).

145. Maeda, K., Okada, S., Yashima, E. & Okamoto, Y. (2001) *Jounal of Polymer Science: Part A: Polymer Chemistry* **39,** 3180-3189.

146. Maloy, W. L. & Kari, U. P. (1995) *Biopolymers* **37,** 105-122.

147. Marshall, S. H. & Arenas, G. (2003) *Electronic J. of Biotech* **6,** 271-284.

148. Matsukaki, K., Sugishita, K., Fujii, N. & Miyajima, K. (1995) *Biochemistry* **34,** 3423-3429.

149. Matsukaki, K., Murase, O., Fujii, N. & Miyajima, K. (1996) *Biochemistry* **35,** 11361-11368.

150. Matsukaki, K. (1998) *Biochim. Biophys. Acta* **1376,** 391-400.

151. Matyjaszewski, K. & Xia, J. (2001) *Chem. Rev.* **101,** 2921-2990.

152. Mays, J. W. (1991) in *Modern Methods of Polymer Characterizations*, eds. Barth, H. G. & Mays, J. W. (John Wiley and Sons, Inc., New York).

153. McQuade, T., Kim, J. & Swager, T. M. (2000) *J. Am. Chem. Soc.* **122,** 5885-5886.

154. Miller, S. M., Simon, R. J., Ng, S., Zuckerman, R. N., Kerr, J. M. & Moos, W. H. (1995) *Drug Dev. Res.* **35,** 20-32.

155. Miwa, J. H., Pallivathucal, L., Gowda, S. & Lee, K. E. (2002) *Org. Lett.* **4,** 4655-4657.

156. Moore, J. S. (1997) *Acc. Chem. Res.* **30,** 402-413.

157. Mor, A. & Nicolas, P. (1994) *J. Biol. Chem.* **269,** 1934-1939.

158. Nelson, J. C., Saven, J. G., Moore, J. S. & Wolynes, P. G. (1997) *Science* **277,** 1793-1796.

159. Newcomb, L. F. & Gellman, S. H. (1994) *J. Am. Chem. Soc.* **116,** 4993-4994.

160. Nielsen, M., Thomsen, A. H., Clo, E., Kirpekar, F. & Gothelf, K. V. (2004) *Journal of Organic Chemistry* **69,** 2240-2250.

161. Nordenberg, T. (1998) *FDA Consumer Magazine.*

162. Nummila, K., Kilpelainen, I., Zahringer, U., Vaara, M. & Helander, I. M. (1995) *Mol Microbiol* **16,** 271-278.

163. Nusslein, K., Arnt, L., Rennie, J., Owens, C. & Tew, G. N. (2005) *Nature - Chemistry and Biology*, submitted.

164. Oh, S. T., Han, S. H., Ha, C. S. & Cho, W. J. (1996) *J. Appl. Polym. Sci.* **59,** 1871-1878.

165. Oren, Z. & Shai, Y. (1998) *Biopolymers* **47,** 451-463.

166. Oren, Z., Lerman, J. C., Gudmundsson, G. H., Agerberth, B. & Shai, Y. (1999) *Biochem. J.* **341,** 501-513.

167. Papo, N. & Shai, Y. (2003) *Biochem. J.* **42,** 9346-9354.

168. Papo, N., Braunstein, A., Eshhar, Z. & Shai, Y. (2004) *Cancer Research* **64,** 5779-5786.

169. Patch, J. A. & Barron, A. E. (2003) *J. Am. Chem. Soc.* **125,** 12092-12093.

170. Patel, M. B., Patel, S. A., Ray, A. & Patel, R. M. (2003) *J Appl Polym Sci* **89,** 895-900.

171. Patel, S. A., Patel, M. V., Ray, A. & Patel, R. M. (2003) *J Polym Sci Part A: Polym Chem* **41,** 2335-2344.

172. Patten, T. E. & Matyjaszewski, K. (1999) *Acc. Chem. Res.* **32,** 895-903.

173. Percec, S., Getty, R., Marshall, W., Skidd, G. & French, R. (2004) *Journal of Polymer Science Part a-Polymer Chemistry* **42,** 541-550.

174. Peschel, A., Otto, M., Jack, R. W., Kalbacher, H., Jung, G. & Gotz, F. (1999) *Journal of Biological Chemistry* **274,** 8405-8410.

175. Pinto, M. R. & Schanze, K. S. (2002) *Synthesis-Stuttgart*, 1293-1309.

176. Pinto, M. R., Kristal, B. M. & Schanze, K. S. (2003) *Langmuir* **19,** 6523-6533.

177. Piozzi, A., Francolini, I., Occhiaperti, L., Di Rosa, R., Ruggeri, V. & Donelli, G. (2004) *Journal of Chemotherapy* **16,** 446-452.

178. Popa, A., Davidescu, C. M., Trif, R., Ilia, G., Iliescu, S. & Dehelean, G. (2003) *Reactive and Functional Polmyers* **55,** 151-158.

179. Porter, E. A., Wang, X., Lee, H. S., Weisblum, B. & Gellman, S. H. (2000) *Nature (London)* **404,** 565.

180. Porter, E. A., Weisblum, B. & Gellman, S. H. (2002) *J. Am. Chem. Soc.* **124,** 7324-7330.

181. Powers, J.-P. S. & Hancock, R. E. (2003) *Peptides* **24,** 1681-1691.

182. Prest, P.-J., Prince, R. B. & Moore, J. S. (1999) *J. Am. Chem. Soc.* **121,** 5933-5939.

183. Prince, R. B., Saven, J. G., Wolynes, P. G. & Moore, J. S. (1999) *J. Am. Chem. Soc.* **121,** 3114-3121.

184. Prince, R. B., Okada, T. & Moore, J. S. (1999) *Angew., Chem., Int. Ed.* **38,** 233-236.

185. Prince, R. B., Barnes, S. A. & Moore, J. S. (2000) *J. Am. Chem. Soc.* **122,** 2758-2762.

186. Prosa, T. J., Winokur, M. J. & McCullough, R. D. (1996) *Macromolecules* **29,** 3654-3656.

187. Raguse, T. L., Porter, E. A., Weisblum, B. & Gellman, S. H. (2002) *J. Am. Chem. Soc.* **124,** 12774-12785.

188. Rappaport, H., Kjaer, K., Jensen, T. R., Leiserowitz, L. & Tirrell, D. A. (2000) *J. Am. Chem. Soc.* **122,** 12523-12529.

189. Reitzel, N., Greve, D. R., Kjaer, K., Howes, P. B., Jayaraman, M., Savoy, S., McCullough, R. D., McDevitt, J. T. & Bjørnholm, T. (2000) *J. Am. Chem. Soc.* **122,** 5788-5800.

190. Rennie, J., Arnt, L., Tang, H., Nusslein, K. & Tew, G. N. (2005) *Soc. Indust. Microbiol.*, accepted.

191. Rivas, B. L., Pereira, E. D., Mondaca, M. A., Rivas, R. J. & Saavedra, M. A. (2003) *J. Appl. Polym. Sci.* **87,** 452-457.

192. Rulkens, R., Wegner, G. & Thurn-Albrecht, T. (1999) *Langmuir* **15,** 4022-4025.

193. Sackmann, E., Duwe, H.-P. & Engelhardt, H. (1986) *Faraday Discuss. Chem. Soc.* **81,** 281-290.

194. Sanborn, T. J., Wu, C. W., Zuckerman, R. N. & Barron, A. E. (2002) *Biopolymers* **63,** 12-20.

195. Sanford, A. R. & Gong, B. (2003) *Current Organic Chemistry* **7,** 1649-1659.

196. Sauvet, G., Fortuniak, W., Kazmierski, K. & Chojnowski, J. (2003) *J Polym Sci Part A: Polym Chem* **41,** 2939-2948.

197. Savage, P. B., Li, C. H., Taotafa, U., Ding, B. W. & Guan, Q. Y. (2002) *FEMS Microbio. Lett.* **217,** 1-7.

198. Schiedel, M. S., Briehn, C. A. & Bauerle, P. (2002) *Journal of Organometallic Chemistry* **653,** 200-208.

199. Schierholz, J. M., Steinhauser, H., Rump, A. F. E., Berkels, R. & Pulverer, G. (1997) *Biomaterials* **18,** 839-844.

200. Schierholz, J. M., Rump, A. & Pulverer, G. (1997) *Arzneimittel-Forschung/Drug Research* **47,** 70-74.

201. Schlievert, P., Johnson, W. & Galask, R. P. (1976) *Am. J. Obstet. Gynecol.* **125,** 906-910.

202. Schmidt, F. R. (2004) *Applied Microbiology and Biotechnology* **63,** 335-343.

203. Scott, M. G., Yan, H. & Hancock, R. E. (1999) *Infection and Immunity* **67,** 2005-2009.

204. Seebach, D. & Matthers, J. L. (1997) *Chem. Comm.*, 2015-2022.

205. Seebach, D., Schaeffer, L., Brenner, M. & Hoyer, D. (2003) *Angew. Chem., Int. Ed.* **42,** 776-778.

206. Seurynck, S. L., Patch, J. A., Wu, C. W., Brown, N. J. & Barron, A. E. (2003) *Biophysical Journal* **84,** 298A-298A.

207. Shelburne, C. E., Coulter, W. A., Olguin, D., Lantz, M. S. & Lopatin, D. E. (2005) *Antimicrobial Agents and Chemotherapy* **49,** 183-187.

208. Sheppard, S. E. & Geddes, A. L. (1944) *J. Am. Chem. Soc.* **66,** 1995-2009.

209. Shi, Y. X., Cromie, M. J., Hsu, F. F., Turk, J. & Groisman, E. A. (2004) *Mol Microbiol* **53,** 229-241.

210. Shima, S., Matsuoka, H. & Iwamoto, S. (1984) *J. Antibiotics* **37,** 1449-1455.

211. Shotwell, S., Windscheif, P. M., Smith, M. D. & Bunz, U. H. F. (2004) *Organic Letters* **6,** 4151-4154.

212. Sima, P., Trebichavsky, I. & Sigler, K. (2003) *Folia Microbiologica* **48,** 123-137.

213. Simmaco, M., Mignogna, G. & Barra, D. (1998) *Biopolymers* **47,** 435-450.

214. Sims, P. J., Waggoner, A. S., Wang, C.-H. & Hoffman, J. F. (1974) *Biochemistry* **13,** 3315-3330.

215. Sindkhedkar, M. D., Mulla, H. R. & Cammers-Goodwin, A. (2000) *J. Am. Chem. Soc.* **122,** 9271-9277.

216. Smith, M. D., Claridge, T. D. W., Tranter, G. E., Sansom, M. S. P. & Fleet, G. W. J. (1998) *Chem. Comm.*, 2041-2042.

217. Spiliopoulos, I. K. & Mikroyannidis, J. A. (2002) *J Polym Sci Part A: Polym Chem* **40,** 2591-2600.

218. Stigers, K. D., Soth, M. J. & Nowick, J. S. (1999) *Current Opinion in Structural Biology* **3,** 714-723.

219. Stone, M. T. & Moore, J. S. (2004) *Organic Letters* **6,** 469-472.

220. Subbalakshmi, C., Nagaraj, R. & Sitaram, N. (1999) *FEBS Letters* **448,** 62-66.

221. Subbalakshmi, C., Nagaraj, R. & Sitaram, N. (2001) *J. Peptide Res.* **57,** 59-67.

222. Sun, Y. Y., Chen, T. Y., Worley, S. D. & Sun, G. (2001) *J Polym Sci Part A: Polym Chem* **39,** 3073-3084.

223. Sun, Y. Y. & Sun, G. (2001) *J Polym Sci Part A: Polym Chem* **39,** 3348-3355.

224. Tan, C. Y., Pinto, M. R., Kose, M. E., Ghiviriga, I. & Schanze, K. S. (2004) *Advanced Materials* **16,** 1208-+.

225. Tanaka, T., Sano, R., Yamashita, Y. & Yamazaki, M. (2004) *Langmuir* **20,** 9526-9534.

226. Tashiro, T. (2001) *Macromolecular Mater. Eng.* **286,** 63-87.

227. Taylor, P. N., Hagan, A. J. & Anderson, H. L. (2003) *Organic & Biomolecular Chemistry* **1,** 3851-3856.

228. Tew, G. N., Lui, D., Chen, B., Doerksen, R. J., Kaplan, J., Corroll, P. J., Klein, M. L. & DeGrado, W. F. (2002) *Proc. Natl. Acad. Sci. U.S.A.* **99,** 5110-5114.

229. Tiller, J. C., Liao, C. J., Lewis, K. & Klibanov, A. M. (2001) *Proc. Natl. Acad. Sci. U.S.A.* **98,** 5981-5985.

230. Tomasinsig, L., Scocchi, M., Mettulio, R. & Zanetti, M. (2004) *Antimicrobial Agents and Chemotherapy* **48,** 3260-3267.

231. Tompa, H. (1950) *Trans. Faraday Soc.* **46,** 970.

232. Tossi, A., Scocchi, M., Skerlavaj, B. & Gennaro, R. (1994) *FEBS Letters* **339,** 108-112.

233. Tossi, A., Sandri, L. & Giangaspero, A. (2000) *Biopolymers* **55,** 4-30.

234. Tsafrir, I., Caspi, Y., Guedeau-Boudeville, M.-A., Arzi, T. & Stavans, J. (2003) *Phys. Rev. Lett.* **91,** 138102-1-138102-4.

235. Vanhee, S., Rulkens, R., Lehmann, U., Rosenauer, C., Schulze, M., Kohler, W. & Wegner, G. (1996) *Macromolecules* **29,** 5136-5142.

236. Wang, L. & Li, P. H. (2003) *Chinese Journal of Chemistry* **21,** 474-476.

237. Watanabe, Y., Mihara, T. & Koide, N. (1998) *Macromol. Chem. Phys.* **199,** 977-983.

238. Wikstrom, M., Xie, J., Bogdanov, M., Mileykovskaya, E., Heacock, P., Wieslander, A. & Dowhan, W. (2004) *Journal of Biological Chemistry* **279,** 10484-10493.

239. Wilschut, J., Duzgunes, N., Fraley, R. & Papahadjopoulos, D. (1980) *Biochemistry* **19,** 6011-6021.

240. Wilson, J. N., Josowicz, M., Wang, Y. Q. & Bunz, U. H. F. (2003) *Chemical Communications*, 2962-2963.

241. Wong, M. S. & Nicoud, J. F. (1994) *Tetrahedron Lett.* **35,** 6113-6116.

242. Woo, G. L. Y., Mittelman, M. W. & Santerre, J. P. (2000) *Biomaterials* **21,** 1235-1246.

243. Worley, S. D. & Sun, G. (1996) *Trends Polym. Sci.* **4,** 364-370.

244. Wosnick, J. H. & Swager, T. M. (2003) *Abstracts of Papers of the American Chemical Society* **226,** U171-U171.

245. Wosnick, J. H. & Swager, T. M. (2004) *Chemical Communications*, 2744-2745.

246. Wu, M., Maier, E., Benz, R. & Hancock, R. E. (1999) *Biochemistry* **38,** 7235-7242.

247. Wu, M. & Hancock, R. E. (1999) *Antimicrob. Agents Chemother.* **43,** 1274-1276.

248. Wu, C. W., Sanborn, T. J., Huang, K., Zuckerman, R. N. & Barron, A. E. (2001) *J. Am. Chem. Soc.* **123,** 6778-6784.

249. Wu, C. W., Sanborn, T. J., Zuckerman, R. N. & Barron, A. E. (2001) *J. Am. Chem. Soc.* **123,** 2958-2963.

250. Wu, C. W., Seurynck, S. L., Lee, K. Y. C. & Barron, A. E. (2003) *Chemistry & Biology* **10,** 1057-1063.

251. Xue, C. H. & Luo, F. T. (2004) *Tetrahedron* **60,** 6285-6294.

252. Yagi, S., Sakai, N., Yamada, R., Takahashi, H., Mizutani, T., Takagishi, T., Kitagawa, S. & Ogoshi, H. (1999) *Chem. Comm.*, 911-912.

253. Yagi, S., Morinaga, T., Nomura, T., Takagishi, T., Mizutani, T., Kitagawa, S. & Ogoshi, H. (2001) *J. Org. Chem* **66,** 3848-3853.

254. Zasloff, M. (1992) *Curr. Opin. Immunol.* **4,** 3-7.

255. Zasloff, M. (2002) *Nature (London)* **415,** 389-395.

256. Zhang, L., Dhillon, P., Yan, H., Farmer, S. & Hancock, R. E. (2000) *Antimicrob. Agents Chemother.* **44,** 3317-3321.

257. Zhang, L., Scott, M. G., Yan, H., Mayer, L. D. & Hancock, R. E. (2000) *Biochemistry* **39,** 14504-14514.

258. Zhang, L., Rozek, A. & Hancock, R. E. (2001) *J. Biol. Chem.* **276,** 35714-35722.

259. Zhang, C. M., Schlaad, H. & Schluter, A. D. (2003) *J Polym Sci Part A: Polym Chem* **41,** 2879-2889.

260. Zhang, L. & Falla, T. J. (2004) *Expert Opin. Investig. Drugs* **13,** 97-106.

261. Zhao, D. H. & Moore, J. S. (2003) *Macromolecules* **36,** 2712-2720.

262. Zheng, J. & Swager, T. M. (2004) *Chemical Communications*, 2798-2799.